Systematics of the parasitoid wasp subfamily Banchinae (Hymenoptera; Ichneumonidae) in the Afrotropical region

by

Terry Reynolds Berry

Submitted in partial fulfillment for the degree

PhD Zoology

Supervisor: Simon van Noort

Co-supervisor: Conrad Matthee

Department of Botany and Zoology

University of Stellenbosch

Research and Exhibitions Department

Iziko South Africa Museum

December 2019

DECLARATION

By submitting this thesis/dissertation electronically, I declare that the entirety of the work contained herein is my own, original work, and that I have not previously in its entirety or in part submitted it for obtaining any qualification.

VERKLARING

Deur hierdie verhandeling elektronies in te lewer, verklaar ek dat die geheel van die werk hierin vervat, my eie, oorspronklike werk is, en dat ek dit nie vantevore, in die geheel of gedeeltelik, ter verkryging van enige kwalifisasie aangebied het nie.

Date: December 2019

ABSTRACT

Parasitoid wasps play an important ecological role as natural controllers of insect populations and, as a result, are increasingly used in agricultural biological control of insect pests. They are an economically important group as they render an ecosystem service to society. The parasitoid wasp family Ichneumonidae (Hymenoptera) is arguably the largest animal family on earth. However, relatively little is known about the diversity of this group within the Afrotropical region. The present study contributes to the growing body of systematic studies of ichneumonids by providing a comprehensive systematic revision of the subfamily Banchinae occurring in the region. This study includes an investigation of evolutionary relationships, historical biogeography of Afrotropical species, description of new species, and the development of updated generic and species identification keys.

A key to Banchinae genera within the Afrotropical region was last created over 40 years ago. Since then, recent advances have been made through the development of good quality high definition images which accompany dichotomous keys and allow for reliable identification of genera/species by taxonomists. The Afrotropical banchine fauna currently comprises 12 genera: *Apophua* Morley, *Atropha* Kriechbaumer, *Cryptopimpla* Taschenberg, *Exetastes* Gravenhorst, *Glyptopimpla* Morley, *Himertosoma* Schmiedeknecht, *Lissonota* Gravenhorst, *Sjostedtiella* Szépligeti, *Spilopimpla* Cameron, *Syzeuctus* Förster, *Tetractenion* Seyrig, and *Tossinola* Viktorov. One of these, *Cryptopimpla* is a predominately northern hemisphere genus represented by 47 described species of which only one is known from the Afrotropical region. Another genus, *Tetractenion*, which is restricted to the Afrotropical region, is only represented by two described species. This study provides the first species-level identification key to these two rare genera, including description of nine and four new species respectively. All Afrotropical species of *Cryptopimpla* are, to this date, only known from South Africa. Studies (prior and current) suggest that both genera are restricted to temperate areas, with a prediction through morphological investigation that the genus *Tetractenion* is possibly nocturnal. In addition, the generic key to Banchinae in the Afrotropical region is updated. Online interactive Lucid Phoenix and Lucid matrix keys are available at: http://www.waspweb.org/Ichneumonoidea/Ichneumonidae/Keys/index.htm.

To investigate the phylogeny of Banchinae in the Afrotropical region, morphological data were combined with molecular sequence data obtained from two nuclear genes, 18S and 28S, and one mitochondrial gene, COI, for 76 taxa, representing all three tribes and 10 of the 12

currently recognized genera. Divergence dates and historical biogeography were estimated on the inferred phylogeny. The most important results of the study suggest that (1) the *Banchus* group of the tribe Banchini does not form part of the subfamily Banchinae, (2) the endemic genus *Sjostedtiella*, along with other "forest-associated" lineages, was found to be the oldest banchine genus within the Afrotropical region, and (3) the dating of the temperate-associated genus *Cryptopimpla* refutes the hypothesis that banchine lineages found within the Cape region are more derived because of their association with the Cape Floristic Region. There is some inference to suggest that Malagasy taxa show strong affinities to East African taxa, due to the close proximity of the island to the East African coast, and some inference indicating the connectedness between East and tropical West and Central Africa. However, it is important to bear in mind that molecular specimens from West and East Africa available for DNA extraction were limited and likewise suitable samples from India, which was historically connected to Madagascar, were also lacking. While many of the genera were found to be monophyletic, paraphyly was established for *Himertosoma* and *Lissonota*. There was an unresolved placement of a clade comprising two Malagasy species, which share both typical and unique morphological characteristics with the genus *Himertosoma*. However, this clade falls outside of the well-supported clade comprising the remaining *Himertosoma* species. Although genetically divergent, a lack of a true synapomorphy suggests that these two species are, for now, better placed within the genus *Himertosoma*. Their inclusion does, however, render *Himertosoma* a paraphyletic group, but analyses of further taxa is required to achieve a robustly supported decision on the affinities of the species within this genus. Paraphyly for the genus *Lissonota* was found both within the Afrotropical region and on a global scale, which was not surprising given the uncertainty on the validity and circumscription, as well as the worldwide distribution of species, of this very large genus.

OPSOMMING

Parasitoïede wespe speel 'n belangrike ekologiese rol as natuurlike beheerders van insekbevolkings en word gevolglik toenemend gebruik in die biologiese beheer van landbou plae. Hulle is ekonomies 'n belangrike groep aangesien hulle 'n ekosisteemdiens aan die gemeenskap lewer. Die parasitoïede wespfamilie Ichneumonidae (Hymenoptera) is waarskynlik die grootste dierfamilie op aarde. Relatief min is egter bekend oor die diversiteit van hierdie groep binne die Afrotropiese streek. Die huidige studie dra by tot die groeiende basis van sistematiese studies van ichneumoniede deur 'n omvattende sistematiese hersiening van die subfamilie Banchinae wat in die streek voorkom te verskaf. Die studie sluit in die evolusionêre verhoudings, historiese biogeografie van Afrotropiese spesies, beskrywing van nuwe spesies en die ontwikkeling van opgedateerde generiese en spesies identifikasie sleutels.

'n Taksonomiese sleutel tot Banchinae genus in die Afrotropiese streek is 40 jaar gelede geskep. Sedertdien is onlangse vordering gemaak deur die ontwikkeling van hoë kwaliteit definisie beelde wat digotome sleutels vergesel en toelaat dat betroubare identifikasie van genera / spesies deur taksonome toegepas kan word. Die Afrotropiese banchine fauna bestaan tans uit 12 genera: *Apophua* Morley, *Atropha* Kriechbaumer, *Cryptopimpla* Taschenberg, *Exetastes* Gravenhorst, *Glyptopimpla* Morley, *Himertosoma* Schmiedeknecht, *Lissonota* Gravenhorst, *Sjostedtiella* Szepaleti, *Spilopimpla* Cameron, *Syzeuctus* Förster, *Tetractenion* Seyrig en *Tossinola* Viktorov. Een van hierdie, *Cryptopimpla* is 'n oorheersende noordelike halfrond genus verteenwoordig deur 47 beskryfde spesies waarvan slegs een van die Afrotropiese streek bekend is. Nog 'n genus, *Tetractenion*, wat beperk is tot die Afrotropiese streek, word slegs verteenwoordig deur twee beskryfte spesies. Hierdie studie bied die eerste spesievlak-identifikasietoets van hierdie twee skaars genera, met onderskeidelik nege en vier nuwe spesies wat beskryf is. Alle Afrotropiese spesies wat tot die genus *Cryptopimpla* behoort is tot op hierdie stadium slegs van Suid-Afrika bekend. Studies (vorige en huidige) dui daarop dat beide genera beperk is tot gematigde gebiede, met 'n voorspelling deur morfologie dat die genus *Tetractenion* moontlik naglewend is. Daarbenewens is die generiese sleutel tot Banchinae in die Afrotropiese streek opgedateer. Aanlyn interaktiewe Lucid Phoenix en Lucid matriks sleutels is beskikbaar by: http://www.waspweb.org/Ichneumonoidea/Ichneumonidae/Keys/index.htm.

Om die filogenie van Banchinae in die Afrotropiese streek te ondersoek, is morfologiese data asook molekulêre volgorde data verkry vanaf twee nukluêre fragmente, 18S en 28S, en een mitochondriale geen, COI, vir 76 taxa, wat al drie stamme verteenwoordig en 10 van die 12 huidige erkende genera. Divergensiedatums en historiese biogeografie is op die afgeleide filogenie bereken. Die belangrikste resultate van die studie dui aan dat (1) die *Banchus*-groep van die stam Banchini nie deel uitmaak van die subfamilie Banchinae nie, (2) die endemiese genus *Sjostedtiella*, saam met ander "woudverwante" afstammelinge, is die oudste banchine-genus in die Afrotropiese streek, en (3) die datering van die gematigde-verwante genus *Cryptopimpla* verwerp die hipotese dat banchine afstammelinge in die Kaapse streek meer divergent is as gevolg van hul assosiasie met die Kaapse Floristiese Streek. Daar is 'n mate van bewyse wat voorstel dat die Malagasiese taxa sterk affiniteite met Oos-Afrikaanse taxa toon, waarskynlik weens die nabyheid van die eiland aan die Oos-Afrikaanse kus en daar is voorts ook 'n mate van aanduidings dat daar 'n verband is tussen Oos-en Tropiese Wes- en Sentraal-Afrika. Dit is egter belangrik om in gedagte te hou dat molekulêre monsters uit Wes- en Oos-Afrika beskikbaar vir DNA-ekstraksie beperk was en geskikte monsters uit Indië (wat histories aan Madagaskar gekoppel was) ontbreek ook. Terwyl baie van die genera monofieleties is, is parafiletiese groepe aangetoon vir *Himertosoma* en *Lissonota*. 'n Onopgeloste plasing van 'n groep wat uit twee spesies van Madagaskar bestaan, wat morfologiese eienskappe (beide atipies en unieke) deel met die genus *Himertosoma*, val buite die goed geondersteunde groep van die oorbylwende *Himertosoma* spesies. Hoewel geneties uiteenlopend, 'n gebrek aan 'n ware sinapomorfie stelvoor dat die twee spesies tans beter ooreenstem met die genus *Himertosoma*. Hul insluiting egter verander *Himertosoma* in 'n parafiletiese groep, maar analise van meer taxa is nodig om 'n sterk ondersteunde besluit aangaande op die verwantskappe van die spesies binne die genus te maak. Die genus *Lissonota* was parafileties gevind beide binne die Afrotropiese streek en op wêreldwye skaal. Dit was nie verbasend nie, gegee die onsekerheid oor die geldigheid en omskrywing, sowel as die wêreldwye verspreiding van spesies, van die baie groot genus.

ACKNOWLEDGEMENTS

This study would not have been made possible without the support and encouragement of several people I would like to give thanks to. First and foremost, thanks be to God for protecting my brain and keeping my sanity intact, for the wisdom and guidance in times of despair and confusion, and for giving me the inner strength and perseverance to complete, finally. I also thank those who constantly prayed for and with me and fed me words of encouragement when I doubted myself, which was very often. I thank my supervisors, Dr. Simon van Noort and Prof. Conrad A. Matthee for all their expertise in the field and sharing that knowledge with me. I will forever be a proud Matie and proud of the top-notch education I received at this university.

My gratitude also goes out to my colleagues in the Entomology Department at the Iziko South Africa Museum for their words of encouragement and spiritual upliftment, particularly to Dr. Pascal Rousse, Aisha Mayekiso Rayners, Tiyisani Chavala and Victor Mutavhatsindi in assisting me with a variety of issues involving curating. I would also like to thank members of the Evolutionary Genomics Group at Stellenbosch University for their support and useful discussions, particularly to Dr. Nina du Toit and Francis Sands for all their contributions to advancing my knowledge in genomics and the statistical programs used in this study. Carel van Heerden and his team at the Central Sequencing Facility of Stellenbosch University are thanked for their services.

This study also benefited from generous contributions of banchine material from the following sources: The Natural History Museum in London and California Academy of Sciences loaned specimens used in this study; additional specimens were donated to the Iziko South African Museum by Drs. Mike Mostovski and Alec Gumovsky; and the bulk of specimens were collected by Dr. Simon van Noort.

This project would not have been made possible without the financial assistance provided by the South African National Research Foundation (NRF) through the Professional Development Program (PDP), a Merit bursary from Stellenbosch University and funding from the City of Cape Town. Lastly I would like to give special thanks to my mother Jean Reynolds, who is my pillar of strength, my constant motivator, my biggest supporter. Thank you for your faith, your belief in me and for being the only one who truly understood what I was going through.

TABLE OF CONTENTS

LIST OF FIGURES

LIST OF TABLES

Chapter 1

General Introduction:

Rationale for investigating the systematics of banchine ichneumonid parasitoid wasps in the Afrotropical region

The taxonomy and evolution of the Afrotropical banchine genera are not well understood in both an African and a global context. This study investigates the evolutionary relationships and historical biogeography of parasitoid wasp species of the subfamily Banchinae and specifically those present in the Afrotropical region. Morphological and molecular data were utilized to examine the historical processes which have shaped the evolution of Banchinae and to test (1) the monophyly of the subfamily (2) the validity of the tribes and (3) whether the species in different localities within the Afrotropical region are linked either geographically and/or ecologically. The study also addresses the taxonomic revisions of two rare genera, *Cryptopimpla* Taschenberg and *Tetractenion* Seyrig and includes an updated generic key for Afrotropical Banchinae. The overarching aim is to provide a systematic revision of the subfamily for the Afrotropical region.

1.1 The role of parasitoid wasps in natural ecosystems

Approximately one out of ten insect species is a parasitoid, that is, their larvae develop by feeding on or in a host organism, which they eventually kill. Most parasitoid insects are Hymenoptera (wasps, bees & ants) and in turn they are important bioindicators. Parasitoid wasps are regarded as representative of the diversity and the taxon richness of the hosts they attack (Sharkey 2007, Anderson et al. 2011). They play an essential ecological role as natural controllers of insect populations. Almost every pest insect species has at least one associated wasp species. As a result, parasitoids are increasingly used in agriculture as biological control agents and in particular to control agricultural pests and invasive phytophagous (plant-feeding) insects (Shaw & Hochberg 2001, Gauld et al. 2002).

Photograph by: David Marquina Reyes (used with permission)

Figure 1.1: Oviposition of a larva hidden inside a dried flower by the Palearctic banchine species, *Syzeuctus tigris* Seyrig, which the wasp located using it's antennae.

Apart from reducing the population density of hosts causing injury to crops and forest products (Sharkey 2007), parasitoids also play an important role in trophic interactions, particularly food web dynamics, as they influence or regulate the population densities of their hosts (Veijalainen et al. 2012a). Therefore, it is important to have a clear understanding of their diversity and species richness. The importance of investigating the biodiversity of beneficial arthropods, such as parasitoid wasps, can also be justified based on the value of the services they provide to society, i.e. ecosystem service. For example, the annual value of beneficial arthropods in the biological control of insect pests (as opposed to investing in pesticides) in agricultural landscapes was estimated at 4.5 billion dollars in the US alone (Losey & Vaughan 2006). Apart from their bio-control function, it is also noteworthy that tropical diversity in general is disappearing at an alarming rate, owing largely to human-induced climate change (emission of green-house gases) resulting in aridification. In addition, the transformation of land for agricultural use and urbanization, further results in habitat destruction. Since parasitoids form a critical component of biodiversity there is again a need for an accurate systematic assessment of biodiversity.

1.2 Problem identification

Despite the fact that the Ichneumonidae are estimated to possibly be the largest animal family on earth (over 100 000 species, Yu et al. 2018), the fauna of the Afrotropical region is poorly known. In addition, species accumulation curves and proportions of undescribed species per sample suggest that the majority of tropical lowland ichneumonid species are still to be discovered (Sääksjärvi et al. 2004, van Noort 2004, Veijalainen et al. 2012a). With only an estimated 15% of ichneumonid species in the Afrotropical region known to science, existing species level identification keys are of little use (van Noort 2004). For many taxa, identification keys do not exist and where they do, they are outdated and poorly backed up with applicable illustrations (van Noort 2004). Taxonomists often need to examine type specimens for reliable identification and recent advances in the development of good quality, high definition images, have enabled the opportunity of virtual examination of type specimens through online digital resources such as WaspWeb (van Noort 2018). This has reduced the need to loan type specimens and the associated risk of voucher damage or loss. A comprehensive taxonomic revision of the Banchinae will address the lack of systematic knowledge of this economically important group of wasps and this taxonomic revision aimed to include the description of new species and the development of user-friendly identification keys accessible to taxonomists, conservationists and ecologists.

1.3 Study species

The family Ichneumonidae is monophyletic and is currently divided into 48 extant subfamilies of which 27 have been recorded from the Afrotropical region (van Noort 2018, Yu et al. 2018). Globally more than 34 000 species have been described (Yu et al. 2018). Within the Afrotropical region (continental Africa south of the Sahara, southern part of the Arabian Peninsula, Madagascar and offshore islands), (Crosskey & White 1977), 12 100 ichneumonid species are estimated to occur, of which only 20% in the 360 genera have been described (Yu et al. 2018). The major groupings of ichneumonid subfamilies include the ichneumoniformes, pimpliformes, and ophioniformes which, based on the species included thus far, were recovered as three monophyletic entities

(Quicke et al. 2009). Ophioniformes consists of several subfamilies including Banchinae, the focus of this study.

Most ichneumonids are parasitoids and are divided into two major groups according to their life-history characteristics: the koinobionts and the idiobionts. Koinobiont species lay their eggs in their host (egg or larva) and allow the host to continue its development (through growth and/or feeding) after oviposition. The host remains alive until the parasitoid larvae are mature and the host invariably dies, either when the parasitoids pupate or when they emerge as adults. As a result, the parasitoids have become specialized to tolerate the host's immunological and chemical defenses. In addition, there is evidence that koinobionts utilize fewer host families than idiobionts, which suggests they may be more host specific (Althoff 2003). Idiobionts are more generalist in that they paralyze the host permanently after oviposition, thus preventing it from developing further after attack and to dodge its immune system (Santos & Quicke 2011). By paralyzing or killing the host, female wasps also restrict the food available for their larvae to the resources already present in the host's body at the moment of oviposition.

1.3.1 Banchinae: the subfamily

Banchinae is a large cosmopolitan group of medium-sized to large-sized ichneumonids (Gauld et al. 2002, Broad et al. 2011). Where known, all species are koinobiont endoparasitoids of Lepidoptera larvae, which makes the subfamily of considerable interest as a source of biological control agents (Gauld & Mitchell 1978, Gauld et al. 2002, Fernandes et al. 2010, Broad et al. 2011, Tschopp et al. 2013). For example, *Syzeuctus* includes species that are important endemic parasitoids of various graminaceous borers, particularly in Africa (Quicke 2015). There are roughly 1800 described species and 66 genera of Banchinae currently recognized (Watanabe & Maeto 2012, 2014, Broad 2014, Choi et al. 2015, Reynolds Berry & van Noort 2016, Herrera-Florez 2017, Vas 2017, Watanabe 2017, 2018, Kasparyan & Kulitzky 2018, Li et al. 2018, Sheng 2018, Yu et al. 2018, Kang et al. 2018, 2019).

With the banchine fauna of many areas of the world poorly known, and a number of undescribed genera from tropical regions in museum collections, the number of species is certainly far greater (Broad et al. 2011). Most Banchinae can be readily diagnosed by the following characters: 1) a submetapleural carina anteriorly generally expanded into a lobe; 2) an arched posterior transverse carina of the propodeum; and 3) a dorsal apical notch on the ovipositor (Wahl & Sharkey 1993, Broad et al. 2011). However, some or all of these characters do not apply to aberrant genera and species and therefore these morphological characters cannot be classified as synapomorphies for the Banchinae (Broad et al. 2011). An additional two further apomoporphies were proposed: firstly, the subapical flagellomeres of female antennae possess elongate placoid sensilla only on the dorsal surface, with smaller, rounded sensilla on the ventral surface; and secondly, the posterior corner of the pronotum is rounded, slightly twisted and flattened (Gauld & Wahl 2000a, Broad et al. 2011). While within the Ophioniformes group (Ophioninae, Ctenopelmatinae, Banchinae, Mesochorinae, Nesomesochorinae, Motopiinae, Campopleginae, Tatogastrinae, Cremastinae, Tersilochinae, Anomaloninae, Neorhacodinae, Oxytorinae, Stilbopinae, Sisyrostolinae and Lycorinae; Gauld 1985, Wahl 1991, 1993, Quicke et al. 2009) these two characters are phylogenetically informative, it has been established that they are not synapomorphic for the subfamily Banchinae (Broad et al. 2011).

Banchinae is mostly solitary with gregarious behaviour known in three species at present (Shaw 1999, Gauld et al. 2002, Quicke 2015). Members of the Banchini have very short ovipositors and utilize exposed caterpillars (Fitton 1985, 1987), compared to Glyptini and Atrophini which have ovipositors about as long or longer than the metasoma and exploit semi-concealed hosts such as leaf rollers (Quicke 2015). Atrophini utilize a considerably large range of hosts, including hosts in concealed situations (Quicke 2015). This is also apparent in the variation of the ovipositor length in this tribe. For example, some Atrophini genera such as *Cryptopimpla* and *Spilopimpla* have short ovipositors and utilize exposed hosts (Townes 1969, Gauld et al. 2002), whereas genera with long ovipositors, such as *Syzeuctus*, exploit larvae in tunnels, leaf rolls, buds, etc. (Townes 1969, Fig. 1.1).

1.3.2 Banchinae: the genera within the Afrotropical region

The most comprehensive identification key to Banchinae genera in the Afrotropical region was produced by Townes and Townes (1973). Since then *Glyptopimpla* Morley was removed from synonymy with *Teleutaea* Förster, and was established as a senior synonym of *Zygoglypta* Momoi and *Orientoglypta* Kuslitzky (i.e. *Glyptopimpla* is now the accepted name, Gupta 2002). At present, Banchinae comprises 12 genera within the Afrotropical region. *Sjostedtiella* Szépligeti, *Tetractenion* Seyrig and *Atropha* are all restricted to the Afrotropical region. Both *Sjostedtiella* and *Atropha* Kriechbaumer are moderately-speciose genera, whereas *Tetractenion* is a very rare genus and include only two described species (Townes 1969, van Noort 2018, Yu et al. 2018). *Glyptopimpla* is a moderately small genus containing 15 species mostly distributed in the Eastern Palearctic region (Yu et al. 2018). *Apophua* Morley is a rather speciose genus occurring in the Afrotropical; Australasian; Palearctic; Nearctic; and Oriental regions (Townes 1969, Yu et al. 2018).

Banchinae generally lack carinae, with the exception of the posterior transverse carina, on the propodeum. However, a few species of *Apophua* possess complete propodeal carination (Broad et al. 2011, Watanabe & Maeto 2014). *Lissonota* Gravenhorst is a very speciose genus with an almost worldwide distribution, occurring in the Afrotropical, Australasian, Palearctic, Nearctic, Neotropical, Oceanic and Oriental regions (Townes 1969, Yu et al. 2018). It is very species-rich in the northern temperate areas (e.g. Aubert 1978). There is a fair range of morphological diversity among the species within this genus, which has led to the proposal of a number of generic names for various species groups (Townes 1969). *Cryptopimpla* Taschenberg, was considered to be a moderately speciose genus by Townes (Townes 1969), but it is actually extremely rare in the Afrotropical region with the presence of a single currently recognized species (Yu et al. 2018). The genus has a wide distribution, and is present in the Afrotropical, Palearctic, Nearctic, Neotropical and Oriental regions (Yu et al. 2018). *Himertosoma* Schmiedeknecht and *Tossinola* Viktorov are found in the Afrotropical, Palearctic, Oceanic, and Oriental regions (Yu et al. 2018). While *Himertosoma* is considered to be a moderately speciose genus, widespread in the Old World tropics and subtropics and with

the greatest concentration of species in the Afrotropical region, *Tossinola* is a rare genus with only five described species (Townes 1969, Yu et al. 2018). *Syzeuctus* Förster is a very speciose genus of worldwide distribution: Afrotropical, Australasian, Palearctic, Nearctic, Neotropical and Oriental regions (Townes 1969, Yu et al. 2018). Most *Syzeuctus* species occur in tropical or subtropical areas, while the remaining species in this genus seem adapted to relatively dry habitats (Townes 1969). *Exetastes* Gravenhorst has an almost worldwide distribution, found in the Afrotropical, Palearctic, Nearctic, Neotropical and Oriental regions and occur mostly in open country: grassland, meadows, shrubby and semi-desert areas, and on almost bare ground (Townes 1969, Yu et al. 2018).

1.3.3 Phylogenetics of ichneumonid wasps

Belshaw et al. (1998) investigated evolutionary relationships in the Ichneumonidae using the D2 variable region of the 28S rRNA and included 40 species and 22 subfamilies, as part of the phylogenetic reconstruction of the superfamily Ichneumonoidea. Laurenne et al. (2006) used the 28S rRNA D2 + D3 fragment to investigate relationships within the largest subfamily, Cryptinae, and between Cryptinae and other related subfamilies. Santos (2017) further provided a comprehensive phylogenetic study focusing on the tribe Cryptini utilizing both morphological (109 characters) and molecular (seven loci) data. The results of his study highlight the ubiquity of morphological homoplasy within the group as has been documented for ichneumonids as a whole (Spasojevic et al. 2017). Klopfstein (2011) investigated the evolutionary relationships with the subfamily Diplazontinae using molecular (four genes) and morphological data. The most comprehensive study to date was done by Quicke et al. (2009), which included a data set of 630 genera representing all currently recognized subfamilies, 1001 partial 28S rRNA (D2 or D2 + D3 region) sequences and a morphological data set of 162 characters scored variously at subfamily, tribe, genus group and genus levels. The most significant result was establishing monophyly of the major groupings of subfamilies (ichneumoniformes, pimpliformes, and ophioniformes). Quicke (2012) constructed a molecular phylogeny on the superfamily Ichneumonoidea, as part of a study of the potential of the CO1 mtDNA gene fragment to improve the accuracy of phylogenetic reconstructions. A total of 3278 sequences representing 84

currently recognized subfamilies, 2500 genera and 41 000 described species were included. The results suggest that the barcoding gene region has the potential to place many hard to recognize taxa correctly to subfamily and in many cases also to genus level.

A number of morphological phylogenetic analyses within and across subfamilies have been undertaken, as well as on the generic level (Sääksjärvi et al. 2004, Broad 2010, Santos & Aguiar 2013, Tedesco & Aguiar 2013). With a focus on Afrotropical ichneumonid species, Townes and Townes (1973) produced the most comprehensive taxonomic classification to date, followed by Gauld and Mitchell (1978) focusing on the subfamily Ophioninae whose revision was further updated by Rousse and van Noort (2014). A diversity survey in Gabon added a further 45 genera to the country's previously poorly known ichneumonid checklist (van Noort 2004) and most recently Rousse and Villemant (2012) produced a taxonomic revision of the ichneumonid fauna of Reunion Island yielding one new genus and 14 newly described species. Within Banchinae, taxonomic revisions have been undertaken on a few genera, but these were restricted to the Neotropical region (Khalaim & Ruíz-Cancino 2008, Broad 2010, Broad et al. 2011, Herrera & Penteado-Dias 2011, Takasuka et al. 2011, Khalaim & Ruíz-Cancino 2012) and Oriental region (Watanabe & Maeto 2012, 2014, Watanabe 2017, Kang et al. 2018, 2019, Li et al. 2018). In addition, a significant contribution by Brock (2017) includes a full taxonomic revision, covering 138 bachine species of the British Isles.

Use of morphological characteristics to establish species delimitation can be problematic, particularly for species where the morphological differences are subtle and also for cryptic species where differentiation can only be seen on the genetic level. Molecular techniques are a necessary additional tool that can help to delimit species. However, it has been found that both morphological evidence and molecular techniques were needed in combination to acquire better resolved phylogenies. Nylander et al. (2004) found that the utility of morphological data influenced the combined-data tree in multigene analyses. Quicke et al. (2009) found that the *Banchus* group of genera was never recovered as monophyletic using DNA alone. They attributed this to the considerable sequence length variation among the component genera. Only when alignment gaps were treated as missing, the tribe Banchini was recovered as monophyletic. In addition, Banchinae was only recovered as monophyletic when

morphology was included (i.e. not only using DNA data), and in the combined morphology-molecular trees, only when alignment gaps were coded as informative. Therefore the integration of both DNA sequences and morphological identification methods provide a powerful tool in the analyses of wasp evolution, and has proven to be an efficient method for separating cryptic ichneumonid species complexes (Butcher et al. 2011, Veijalainen et al. 2011).

Although combining data sets (i.e. total evidence) often result in more robust phylogenies (Eernisse & Kluge 1993, Wahlberg et al. 2005) the outcome is not always robust since analyses of individual data sets can support conflicting topologies. The latter can happen due to the fact that different data sets have different evolutionary histories (gene trees can deviate from species trees). Different combinations of taxonomic characters may be necessary to propose or support species/clades. The major advantage of the multi data set approach is that it promotes taxonomic stability, as most systematists will agree on the validity of a species/clade/monophyly supported by several independent character sets (Miyamoto & Fitch 1995, Padial et al. 2010).

1.4 Historical Biogeography

Biogeography is the study of the distribution of species through geological time and geographic space. Historical (phylogeny-based) biogeography centers on the use of phylogenies to infer the history of geological connections among regions, the climatic and ecological conditions and how these have influenced the current distribution of species. This approach takes into account several evolutionary processes (dispersal, vicariance), which occur over extended temporal and often large spatial scales (Crisci 2001). In addition, dating assessment using e.g. fossil data and molecular clocks can be incorporated with molecular phylogenies to correlate geological and phylogenetic events (origin, evolution, distribution of species) (Weins & Donoghue 2004). One of the key principles of historical biogeography centers on the principle that if different monophyletic groups show the same biogeographical pattern, then they probably share the same biogeographic history (Morrone & Crisci 1995). Biogeography plays an important role in biodiversity conservation, because, if focused on the appropriate taxa, it can lead to the identification of areas of endemism as well as processes central to the

origin and maintenance of that biological diversity (Liu et al. 2012, Fang et al. 2013). Historical biogeography can also contribute to large-scale patterns of species richness, which is fundamentally one of the main areas of ecology. For example, increases in species richness within a region can only occur through dispersal of a species into a region and/or *in situ* speciation, processes that are best identified using historical biogeography (Wiens & Donoghue 2004).

The fossil history of Ichneumonidae dates back to Lower Cretaceous, 99 to 145 million years ago (mya) (Kopylov 2010). The first banchine fossil was found in Ukraine and dates back to the Eocene epoch (Khalaim 2011), 56 to 34 mya.

1.5 Research objectives

The aim of the PhD was to clarify the taxonomy and to elucidate the underlying mechanisms driving the evolution of the subfamily Banchinae within the Afrotropical region. Taxonomic revisions using morphological and molecular evidence were implemented to explain the genetic variation and diversification in the different ecological guilds of banchine wasps. In addition, phylogenetic interpretation allowed inferences on the biogeographical history and evolution of the banchine species related to their geographic distribution (Hewitt 1996). For this, three main topics were addressed:

1) *Phylogenetic assessment of the parasitoid wasp subfamily Banchinae (Hymenoptera; Ichneumonidae) in the Afrotropical region using molecular and morphological techniques.* Partial sequences of the mitochondrial gene cytochrome oxidase subunit 1 (COI) and nuclear genes 28S (D2 + D3 expansion segments), and 18S were compared among 76 banchine species found in the Afrotropical region to estimate the extent of genetic diversity among these species as well as to infer historical biogeography. Not only are these genes informative (see below) but the taxonomic sampling can be expanded based on published data. The slower evolving 28S and 18S genes were chosen to resolve deeper nodes, whilst the faster evolving COI gene was used to resolve terminal nodes. Morphological and molecular phylogenies were constructed to investigate the evolutionary relationships amongst genera/species. The significance of the resulting phylogenetic reconstruction

with biogeography was also examined. Because the rRNA structure is highly conserved throughout evolution the comparison of rRNA sequences is considered to be a powerful tool for deducing phylogenetic and evolutionary relationships among distantly related organisms. The expansion segments of the 28S rRNA are less constrained structurally than core regions of the large subunit, making them ideal as phylogenetic markers (Gillespie et al. 2005). The D2 and D3 expansion regions of the 28S rRNA were chosen for the study and have been successfully used in understanding interspecific patterns in wasps (Zaldívar-Riverón et al. 2008a, b) particularly within ichneumonids (Belshaw et al. 1998, Laurenne et al. 2003, 2006, Quicke et al. 2009, Broad 2010, Klopfstein et al. 2011, Rousse et al. 2016). The nuclear 18S gene has been successfully used in the phylogenetic reconstructions at subfamily level for parasitoid wasps (Sharanowski et al. 2011). To facilitate the need to identify species, the mtDNA protein-coding gene COI has become the genetic marker for the International Barcode of Life Project. In addition, the gene has been useful in elucidating the evolutionary relationships within parasitoid wasp subfamilies and genera (Wagener et al. 2006, Zaldívar-Riverón et al. 2008a, b, Klopfstein et al. 2011, Rousse et al. 2016) and it has been used for the phylogenetic reconstruction of the superfamily Ichneumonoidea (Quicke 2012).

2) *Review of Afrotropical Cryptopimpla Taschenberg (Ichneumonidae: Banchinae), with description of nine new species*. The wing venation and microsculpture of the integument were used as principle characters for species diagnoses while assessment of relative length ratios of various morphological structures to each other and qualitative morphological characters were informative for species delimitation. The species identification key was produced using high quality annotated images, highlighting diagnostic characters of each species. When this work was published as an outcome of this PhD study, a user-friendly electronic output was also produced in Lucid which made the key readily accessible to a wide range of users with diverse expertise (Reynolds Berry & van Noort 2016). This key format avoids the

requirement of familiarity with morphological terminology associated with this group because the characters are visually illustrated making the keys usable by non-specialists. *Cryptopimpla* in the Afrotropical region was previously represented by a single species. This chapter includes the description of an additional nine new species.

3) *Identification key to genera of Banchinae (Hymenoptera; Ichneumonidae) occurring in the Afrotropical region with a review of the endemic genus Tetractenion.* The wing venation and microsculpture of the integument were used as principle characters for taxonomic classification of the subfamily Banchinae and the genus *Tetractenion*, and assessment of relative length ratios of various morphological structures and qualitative morphological characters were applied for the description of new *Tetractenion* species. The generic and species identification keys were produced using high quality annotated images, highlighting diagnostic characters of each genus/species within the subfamily/genus. A visual illustration of diagnostic morphological characters made for a more user-friendly dichotomous key. This chapter updates Townes and Townes (1973) identification key to banchine genera within the Afrotropical region and includes applicable illustrations. *Tetractenion* in the Afrotropical region was previously represented by two species. This chapter includes the description of an additional four new species.

Chapter 2

Phylogenetic assessment of the parasitoid wasp subfamily Banchinae (Hymenoptera; Ichneumonidae) in the Afrotropical region using molecular and morphological techniques.

2.1. Introduction

The parasitoid wasp subfamily Banchinae is amongst the most commonly collected of all ichneumonids, and as a consequence usually well-represented in faunal collections (Zong et al. 2012, Brown et al. 2013, Quicke 2015). Despite concerted efforts to clarify the evolution and taxonomy of the group (Pampel 1913, Seyrig 1935, Benoit 1959, Townes 1969, Townes & Townes 1973, Gauld & Wahl 2000a, Gauld et al. 2002, Quicke et al. 2009, Broad et al. 2011), their systematics remain poorly understood. The fossil history of Ichneumonidae in Africa dates back to the Late Cretaceous, 99 to 145 million years ago (mya, Kopylov et al. 2010) with the oldest known fossil (though from an extant genus) for Banchinae found in the Ukraine, dating back to the Eocene epoch (Khalaim 2011), 56 to 34 mya.

Morphologically, Banchinae can be subdivided into three tribes namely Banchini, Glyptini, and Atrophini (Townes & Townes 1973, Yu et al. 2018), but little evidence can be put forward to show that these entities represent reciprocally monophyletic assemblages (Quicke et al. 2009). Based on 28S rDNA data, Atrophini and Glyptini appear to form a monophyletic group (Quicke et al. 2009). While the two tribes are biologically similar, Atrophini contains more than half of the species in the subfamily, consisting of 41 currently recognized genera (Quicke 2015, Sheng 2018, Yu et al. 2018). Although readily diagnosable by the adult apomorphy represented by diagonal grooves on some metasomal tergites, the Glyptini is not well characterized by apomorphies in the larval form relative to the other tribes (Wahl 1988). Therefore, characters within this tribe probably represent the groundplan state for the subfamily, whereas the Atrophini possess the derived state of having a reduced hypostoma (Quicke 2015). Based on a

morphological investigation of a new genus of Glyptini in the Neotropical region, the tribe was hypothesized to be paraphyletic (Broad et al. 2011). Banchini is made up of two main evolutionary lineages, the *Exetastes* and the *Banchus* groups, with the latter not occurring in the Afrotropical region. The relationships among species within these two assemblages are uncertain and probably best illustrated by the lack of monophyly for the *Banchus* group using gene trees (Quicke et al. 2009). Considerable sequence length variation of the 28S nuclear gene is present among the genera belonging to the *Banchus* group. The tribe Banchini to which this group belongs, however, was recovered as monophyletic when morphology was combined with the molecular data, but also only when alignment gaps were treated as uninformative (i.e. missing) characters (Quicke et al. 2009). The latter is most likely a reflection of weakly supported internal nodes due to a rapid speciation history (incomplete lineage sorting). The combination of morphological and molecular techniques are thus arguably a more effective and informative way to unravel the species tree of members belonging to the subfamily Banchinae (also see Nylander et al. 2004, Butcher et al. 2011, Veijalainen et al. 2012a).

The mitochondrial gene COI and nuclear genes 18S and 28S have been mostly used in the phylogenetic reconstructions of parasitoid wasps to help elucidate evolutionary relationships at different hierarchical levels (Belshaw et al. 1998, Laurenne et al. 2003, 2006, Quicke et al. 2009, Broad 2010, Klopfstein et al. 2011, Sharanowski et al. 2011, Quicke 2012). Using these genes in the present study will assist in broadening the amount of data available for analyses and will also allow for the inclusion of additional data available on GenBank. It should be noted, however, that although combining data sets (i.e. total evidence) often result in more robust phylogenies (Wahlberg et al. 2005, Quicke et al. 2009) the independent outcomes are not always reliable. Multiple independent data sets can for example support conflicting trees since the markers may have different coalescent histories resulting from different lineage-sorting events (gene trees deviate from species trees, Szöllősi et al. 2015, Bossert et al. 2017). Irrespective of this, the major advantage of a congruence approach is that it promotes taxonomic stability, as most taxonomists will agree on the validity of a

species/clade/monophyly supported by several independent character sets (Miyamoto & Fitch 1995, Padial et al. 2010).

Banchinae has a cosmopolitan distribution (Yu et al. 2018). Given their wide distribution, it is possible that their evolution could have been shaped by vicariance events such as the proposed Gondwanan separation of Southern America from Africa which occurred 95-110 mya (eucnemid beetles, Sanmartín & Ronquist 2004) and the K/T event 65 mya (wasp & butterfly subfamilies, Wahlberg 2006, Zaldívar-Riverón 2008a). In Africa, the early Eocene was dominated by tropical rainforests that formed a continuous belt (the ancient Pan-African forest) that stretched across the continent (Burgess et al. 1998, Jacobs 2004). At present, West and Central Africaare geographically separated from the East African regions by a ~1000 km North-South wide arid corridor creating an effective barrier to dispersal for rain forest-restricted taxa (Couvreur et al. 2008). There is also strong floristic evidence suggesting repeated reconnections (expansions) and break-ups (contractions) of savannas and forests between West and Central and East Africa spanning the Oligocene and Miocene, allowing for opportunities for both biotic exchange during warm wet climates and speciation during cool dry climates, respectively (Feakins et al. 2005, Cowling et al. 2008, Couvreur et al. 2008, Dupont 2011). Endemic East African floristic and faunistic taxa, are however thought to be closely related to West and Central African lineages and these affinities are generally explained by the fact that these forests were once connected (White 1981, Couvreur et al. 2008). Evidence for this has been found for several taxa (Burgess et al. 1998, Clausnitzer 2003, Mausfield-Lafdhiya et al. 2004, Tolley et al. 2011). Ecological shifts associated with Pleistocene climate change have also shaped the taxonomic diversity in bovids (Matthee et al. 2001) and their associated arthropod parasites (Sands et al. 2017). During interglacials (warm wet climate), forests displaced savannas, isolating populations of arid-adapted species, while during glacials (cool dry climate) savannas expanded enabling secondary contact among diverged lineages (Lorenzen et al. 2012).

It is also generally accepted that continental drift could have played a major role in vicariance of taxa. In this case India and Madagascar split from Africa in the late

Jurassic/early Cretaceous (~ 160 mya) period, followed by the splitting of Madagascar from India in the mid- to late Cretaceous (~ 90 mya, Karanth 2006, Yoder & Nowak 2006). Although Madagascar has been separated from Africa for 160 million years, its proximity to the East African coast is thought to have facilitated faunal interchange (Yoder & Nowak 2006). Evidence for this has been found in previous studies where Malagasy taxa showed stronger affinities to the Afrotropical region, particularly east Africa, than to India (ants, Fisher 1996; freshwater crabs, Daniels et al. 2006, various fauna and flora, Yoder & Nowak 2006).

Afromontane forests occur along the Cape Fold Mountains (the oldest mountains in Africa) of South Africa and the escarpment in KwaZulu-Natal and Mpumalanga. These Afromontane forests also contain high levels of species diversity and endemism. The Indian Ocean Coastal Belt forests of East Africa also extend to the coast of the Eastern Cape and the KwaZulu-Natal provinces of South Africa. The current distribution of these coastal forests formed after the Last Glacial Maximum (Lawes 1990), which is relatively recent in origin, compared to the Afromontane forests which are thought to represent ancient habitats (White 1981). The Cape Floral Kingdom of southern Africa occurs in two diverse Biomes: Fynbos and Succulent Karoo. The Fynbos is shrubland vegetation that is fire-adapted and is found in the Western, Northern and Eastern Cape Provinces of South Africa. The Succulent Karoo Biome is restricted to the Northern and Western Cape of South Africa and the south-western coastal region of Namibia. The remarkable floristic richness and endemism (fauna and flora) of these Biomes has identified them as global biodiversity hotspots. One of the most important historic events in the origin of the Cape Floristic Region (CFR) is the development of the Benguela Current (which runs northwards along the southwestern coast of Africa), a result of the formation of a permanent ice sheet in Antarctica in the late Miocene (Heinrich et al. 2011). It has resulted in the long-term aridification of south-western Africa and Botswana (van Zinderen Bakker 1975). This climatic deterioration has resulted in habitat fragmentation and subsequent lineage diversification and radiation of several southern African taxa (Tolley et al. 2011, Engelbrecht et al. 2011, du Toit et al. 2012). The further strengthening and cooling of the Benguela Current during the Pliocene led to the

formation of the Mediterranean-type climate in the greater CFR (Datson et al. 2008). A recent origin and rapid radiation of the CFR has been hypothesized (Linder 2003). While studies have shown Succulent Karoo floral endemic lineages to be fairly young (majority < 10 my old), Fynbos endemic lineages displayed a broader age distribution (Verboom et al. 2009). The Succulent Karoo is thought to be a product of a more recent radiation triggered by the aridification process as are some Cape clades, but many other Fynbos endemic lineages are the product of prolonged diversification that began before the onset of winter-rainfall conditions (Linder 2008, Verboom et al. 2009).

The present study aims to address the taxonomic uncertainties in the Banchinae by employing a phylogenetic approach. Sequence data of three molecular markers that vary in overall rates of evolution (COI, 28S, 18S) and morphological data (external characters) were used, with the inclusion of dating analyses, to elucidate some of the evolutionary mechanisms that may have played a role in shaping the present-day diversity within banchine wasps in the Afrotropical region. It is hypothesized that (1) despite increased taxonomic sampling the three tribes within Banchinae are monophyletic; (2) central African taxa are closely-related to East African taxa due to the ancient connection of the two regions when they were both part of the historically extensive pan-African forest; (3) the Banchinae taxa found in Madagascar (although high levels of endemism are also expected) will be closely-related to East African taxa given the islands close proximity to the East African coast; (4) eastern South African taxa will show stronger affinities with West and Central African taxa than with taxa from the nearby Cape region, because of similar climatic conditions; and (5) forest-associated lineages will be more basally positioned, while lineages found in the Cape region of South Africa will be more derived, because of their association with the unique and far younger Cape Floristic Region, which has a very different climate and habitat to the rest of Africa.

Alternatively, (1) based on phylogenetic evidence (Quicke et al. 2009) and morphological investigation (Wahl 1988, Broad et al. 2011), Banchini and Glyptini may possibly be paraphyletic; (2) central African and East African taxa, (3) Madagascan and East African taxa, and (4) eastern South African taxa and West and Central African taxa,

could be more distantly related as a result of geographic isolation and time spent in allopatry; and (5) a high level of divergence between lineages can also be expected in forests because wasps in forests occupy small niches, and the assumed narrow host range for koinobiont parasitoids because of an assumed close parasitoid-host relationship (Gauld & Fitton 1984). Therefore, with the break-up of forests, new niches become available for occupancy, offering opportunity for divergence.

2.2. Materials and Methods

2.2.1 Collection of materials

Taxapad, containing the Ichneumonoidea database, states that there are 13 genera and 183 described banchine species in the Afrotropical region, with the most recent descriptions of a new genus, *Atropatopsis* Sudheer et al. (2007) (Yu et al. 2018). However, the current recorded distribution of the constituent species of *Atropatopsis* in the Middle East falls outside the Afrotropical region, making the total number of banchine genera in the region 12. To obtain as much diversity as possible a subset of 76 ingroup taxa, representing 10 of the 12 Afrotropical genera, was sampled. Aside from *Cryptopimpla rubrithorax*, known to occur in the Afrotropical region, sequence data was obtained from only two of the nine recently described *Cryptopimpla* species (Reynolds Berry & van Noort 2016) as many of the species are only represented by a single specimen and DNA extraction would compromise the integrity of the types. Specimens could not be obtained from the rare genera *Glyptopimpla* (represented by one species from Kenya) and *Tossinola* (represented by one species in the Democratic Republic of Congo), though sequence data was obtained for the latter genus from GenBank. The subfamily Pimplinae (two species) was chosen as an outgroup because of its distant relatedness with the ingroup while the subfamily Ophioninae (two species) was selected as an additional outgroup based on the close sister taxon relatedness with the ingroup (Pampel 1913, Wahl 1991, 1993, Quicke et al. 2009). The list of species and collection sites is given in Table 2.1.

Table 2.1: List of ingroup (Banchinae) and outgroup (Pimplinae & Ophioninae) taxa included in this study. Category A-L refers to the primers used to sequence the genes. The sequences of these primers are listed in Table 2.2. "Abr." refers to the abbreviation code given to distinguish taxa by country and locality (when multiple specimens of the same species are included).

Subfamily/Family	*Species*	Gene	Locality Code	Location	Abr.	Vegetation	Reference
HYMENOPTERA							
Ichneumonoidea							
Ichneumonidae							
Pimplinae	*Echtromorpha*	COI (A, D, E), 28S (H, J), 18S (K, L)	MG-56-5-09	Madagascar	MG	Uapaca forest	CASENT2166050
	Campotypus	COI (A, B, D, E), 28S (H, J), 18S (K, L)	UG08-KEN-S09	Kenya	KEN	Savanna Woodland	SAM-HYM-P044518
Ophioninae	*Dicamptus braunsii*	COI (A, F), 28S (H, I)	HUN10-ACA1-L01	South Africa	SA	Great Fish Thicket	SAM-HYM-P049470
	Enicospillus breviceps	COI (A, F), 28S (H, I)	GB09-SUC2-L01	South Africa	SA	Gamka Thicket	SAM-HYM-P049504
Banchinae	*Apophua sp.* 1	COI (A, B, D, E), 28S (G, I), 18S (K, L)		South Africa	SA		SAM-HYM-P047470
	Apophua hispida	COI (B, C, D, E), 28S (G, I), 18S (K, L)	UG05-M19	Uganda	UG1	Secondary mid-altitude rainforest	SAM-HYM-P044484
	Apophua hispida	COI (A, B, D, E), 28S (H, J), 18S (K, L)	CAR01-S230	Central African Republic	CAR	Lowland rainforest	SAM-HYM-P047430
	Apophua hispida	COI (A, B, D, E), 28S (H, J), 18S (K, L)	UG08-KF3-M13	Uganda	UG2	Primary mid-altitude rainforest	SAM-HYM-P047421
	Apophua sp. 2	COI (A, B, D, E), 28S (G, I), 18S (K, L)	UG08-KF3-Y04	Uganda	UG	Primary mid-altitude rainforest	SAM-HYM-P047422
	Apophua sp. 3	COI (B, D, E), 28S (H, J), 18S (K, L)	KZN03	South Africa	SA	Garden	SAM-HYM-P044559
	Apophua sp. 3	COI (A, B, D, E), 28S (G, I), 18S (K, L)	UG08-KF7-M07	Uganda	UG	Primary mid-altitude rainforest	SAM-HYM-P047423
	Apophua bipunctoria	28S		United Kingdom	UK		Belshaw & Quicke (2002)
	Apophua	COI		Papua New Guinea	PNG		Hrcek *et al.* (2011)
	Lissonota sp. 1	COI (A, F), 28S (H, J), 18S (K, L)	KO97-M02	South Africa	SA	West Coast Strandveld	SAM-HYM-P044497
	Lissonota sp. 2	COI (A, F), 28S (G, I), 18S (K, L)	KO97-M05	South Africa	SA	West Coast Strandveld	SAM-HYM-P044480
	Lissonota sp. 3	COI (A, F), 28S (G,I), 18S (K, L)	NKA03	South Africa	SA	Northern Zululand Sourveld	SAM-HYM-P047417
	Lissonota sp. 4	COI (A, D), 18S (K, L)	KO98-M22	South Africa	SA	Mesic Mountain Fynbos	SAM-HYM-P044517
	Lissonota sp. 5	COI (A, D)	KO98-M22	South Africa	SA	Mesic Mountain Fynbos	SAM-HYM-P044536
	Lissonota sp. 6	COI (A, B, D, E), 28S (G, I), 18S (K, L)	WTB09-GRA1-M02	South Africa	SA	Amathole Mistbelt Grassland	SAM-HYM-P044505
	Lissonota sp. 7	COI (A, D)	KZN03-Nov	South Africa	SA	Garden	SAM-HYM-P047428
	Lissonota	28S		Chile	CH1		Quicke *et al.* (2009)
	Lissonota	28S		Chile	CH2		Quicke *et al.* (2009)
	Lissonota	28S		United States of America	USA		Quicke *et al.* (2009)
	Lissonota	28S		Australia	AUS		Quicke *et al.* (2009)
	Lissonota	28S					Belshaw *et al.* (1998)
	Lissonota	28S		Turkey	TU		Belshaw *et al.* (1998)
	Lissonota lineolaris	COI		Canada	CA		Hebert *et al.* (2016)
	Lissonota recurvariae	COI		Canada	CA		Hebert *et al.* (2016)
	Lissonota	COI		Canada	CA		Hebert *et al.* (unpubl.)
	Lissonota coracina	COI		Canada	CA		Smith *et al.* (2009)
	Lissonota acrobasidis	COI		Canada	CA		Smith *et al.* (2011)
	Spilopimpla leleupi	COI (A, C, D, E), 28S (G, I), 18S (K, L)	UG05-M15	Uganda	UG	Secondary Mid-altitude Rainforest	SAM-HYM-P044467
	Spilopimpla sp. 1	COI (B, C, D, E), 28S (G, I), 18S (K, L)	UG05-Y04	Uganda	UG	Secondary Mid-altitude Rainforest	SAM-HYM-P044471
	Spilopimpla sp. 2	COI (B, C, D, E), 28S (H, J), 18S (K, L)	UG05-Y07	Uganda	UG	Secondary Mid-altitude Rainforest	SAM-HYM-P044473
	Spilopimpla sp. 3	COI (A, B, D, E), 28S (H, J), 18S (K, L)	WTB09-GRA1-M03	South Africa	SA2	Amathole Mistbelt Grassland	SAM-HYM-P044550
	Spilopimpla sp. 3	COI (A, B, D, E), 28S (G, I), 18S (K, L)	WB97-M09	South Africa	SA1	South Coast Strandveld	SAM-HYM-P044549
	Spilopimpla sp. 3	COI (A, D, E), 28S (H, J), 18S (K, L)	ASA09-WOO1-M18	South Africa	SA3	Riverine Woodland	SAM-HYM-P044554
	Spilopimpla sp. 4	COI (B, C, D, E), 28S (G, I), 18S (K, L)	UG05-M15	Uganda	UG	Secondary Mid-altitude Rainforest	SAM-HYM-P044470
	Spilopimpla sp. 5	COI (A, B, D, E), 28S (H, J), 18S (K, L)	CAR01-S252	Central African Republic	CAR	Lowland Rainforest	SAM-HYM-P044511
	Spilopimpla sp. 6	COI (A, B, D, E), 28S (H, J), 18S (K, L)	UG08-KEN-S09	Kenya	KEN	Savanna Woodland	SAM-HYM-P044535
	Spilopimpla sp. 7	28S (G, I)	CAR01-S27	Central African Republic	CAR	Lowland Rainforest, marsh clearing	SAM-HYM-P047455
	Spilopimpla sp. 8	COI (A, B, D, E), 28S (G, I), 18S (K, L)	PCD09-ACA1-M02	South Africa	SA	Camdeboo Escarpement Thicket	SAM-HYM-P044548
	Spilopimpla sp. 9	COI (A, C, D, E), 28S (G, I), 18S (K, L)	UG05-M09	Uganda	UG1	Degraded Mid-altitude Rainforest	SAM-HYM-P044472
	Spilopimpla sp. 9	COI (A, C, D, E), 28S (G, I), 18S (K, L)	UG05-M23	Uganda	UG2	Secondary Mid-altitude Rainforest	SAM-HYM-P044469
	Spilopimpla	28S	BMNH(E) 2005-205	Madagascar	MG	Rainforest	Quicke *et al.* (2009)
	Spilopimpla	28S		Cameroon	CAM		Quicke *et al.* (2009)

Table 2.1: (continued)

Subfamily/Family	*Species*	Gene	Locality Code	Location	Abr.	Vegetation	Reference
	Spilopimpla	28S					Quicke *et al.* (2009)
	Himertosoma sp. 1	COI (A, D)	MG-42B-14-09	Madagascar	MG	Palm trees on sand	CASENT2222649
	Himertosoma sp. 2	COI (A, D, E), 28S (G, I), 18S (K, L)	MG-56-5-08	Madagascar	MG	Uapaca forest	CASENT2222699
	Himertosoma sp. 3	COI (A, D), 28S (H, J), 18S (K, L)	MG-56-2 04	Madagascar	MG	Uapaca forest	CASENT2187027
	Himertosoma sp. 4	COI (A, D), 18S (K, L)	KO97-M09	South Africa	SA	West Coast Strandveld	SAM-HYM-P044542
	Himertosoma sp. 5	COI (A, D), 28S (G, I), 18S (K, L)	CAR01-S87	Central African Republic	CAR	Lowland Rainforest, Marsh Clearing	SAM_HYM_P047454
	Himertosoma sp. 6	COI (A, D), 28S (G, I), 18S (K, L)	KO97-M32	South Africa	SA	West Coast Strandveld	SAM-HYM-P044512
	Himertosoma sp. 7	COI (A, D)	DRA04	South Africa	SA	Lesotho Highland Basalt Grassland	SAM-HYM-P047431
	Himertosoma sp. 8	COI (A, D)	CAR01-S11	Central African Republic	CAR	Lowland Rainforest, Marsh Clearing	SAM-HYM-P047466
	Himertosoma sp. 9	28S (H, J)	KO98-M22	South Africa	SA	Mountain Fynbos, last burnt c. 1978	SAM-HYM-P044525
	Himertosoma sp. 10	COI (A, D), 28S (H, J), 18S (K, L)	MG-45B-15	Madagascar	MG	Gallery forest	CASENT2187026
	Himertosoma sp. 11	COI (A, D), 28S (H, J), 18S (K, L)	MG-54B-31	Madagascar	MG	Dry forest	CASENT2222749
	Syzeuctus sp. 1	COI (B, C, D, E), 28S (G, I), 18S (K, L)	UG05-M02	Uganda	UG	Secondary Mid-altitude Rainforest	SAM-HYM-P044465
	Syzeuctus sp. 1	COI (A, D, E), 28S (G, I), 18S (K, L)	UG08-KEN-S09	Kenya	KEN	Savanna Woodland	SAM-HYM-P044533
	Syzeuctus sp. 2	18S (K, L)	CAR01-M48	Central African Republic	CAR	Lowland Rainforest, Marsh Clearing	SAM-HYM-P044509
	Syzeuctus sp. 3	COI (A, D), 28S (G, I), 18S (K, L)	MG-56-10-03	Madagascar	MG	Uapaca forest	CASENT2222799
	Syzeuctus sp. 4	COI (A, B, D, E), 18S, 28S (G, I)	WTB09-GRA1-M02	South Africa	SA	Amathole Mistbelt Grassland	SAM-HYM-P044539
	Syzeuctus sp. 5	COI (A, D), 18S (K, L)	MG-56-5-09	Madagascar	MG	Upaca forest	CASENT2187033
	Syzeuctus sp. 6	COI (A, B, D, E), 18S, 28S (G, I)	WTB09-GRA1-M03	South Africa	SA2	Amathole Mistbelt Grassland	SAM-HYM-P044541
	Syzeuctus sp. 8	COI (A, B, D, E), 18S, 28S (G, I)	CAR01-M183	Central African Republic	CAR	Lowland Rainforest	SAM-HYM-P047449
	Syzeuctus	28S	BMNH(E) 2005-205	Madagascar	MG	Rainforest	Quicke *et al.* (2009)
	Syzeuctus	28S		Costa Rica	CR		Quicke *et al.* (2009)
	Syzeuctus	28S		Belize	BE		Quicke *et al.* (2009)
	Atropha sp. 1	COI (A, B, E, F), 18S, 28S (G, I)	UG08-KF6-M16	Uganda	UG	Secondary Mid-altitude Rainforest, Marshy Area	SAM-HYM-P044500
	Atropha sp. 2	COI (A, D), 18S, 28S (G, I)	UG08-KF7-M17	Uganda	UG	Primary Mid-altitude Rainforest	SAM-HYM-P047457
	Atropha sp. 3	COI (A, D), 18S, 28S (G, I)	UG08-KF6-M06	Uganda	UG	Secondary Mid-altitude Rainforest, Marshy Area	SAM-HYM-P047453
	Atropha sp. 4	COI (A, B, D, E), 18S, 28S (G, I)	CAR01-S86	Central African Republic	CAR	Lowland Rainforest, Marsh Clearing	SAM-HYM-P044521
	Atropha sp. 5	COI (A, F), 18S, 28S (G, I)	UG08-KF9-M19	Uganda	UG	Primary Mid-altitude Rainforest, Near Stream	SAM-HYM-P044501
	Atropha sp. 5	COI (A, D), 18S (K, L)	CAR01-S74	Central African Republic	CAR	Lowland Rainforest, Marsh Clearing	SAM-HYM-P044522
	Atropha sp. 6	COI (A, B, D, E), 28S (G, I), 18S (K, L)	KZN03	South Africa	SA	Garden	SAM-HYM-P047426
	Atropha	COI, 28S	CAR01-S36	Central African Republic	CAR	Lowland Rainforest, Marsh Clearing	SAM-HYM-P086236
	Atropha	28S		Togo	TO		Quicke *et al.* (2009)
	Cryptopimpla kogelbergensis	COI (A, D, E), 28S (G, I), 18S (K, L)	GB09-SUC4-M38	South Africa	SA1	Gamka Thicket	SAM-HYM-P044551
	Cryptopimpla kogelbergensis	COI (A, E), 18S (K, L)	GL07-REN3-M38	South Africa	SA2	Shale Renosterveld	SAM-HYM-P047463
	Cryptopimpla onyxi	COI (A, D)	WB97-M09	South Africa	SA1	South Coast Strandveld	SAM-HYM-P044545
	Cryptopimpla onyxi	COI (A, D)	WB97-M09	South Africa	SA2	South Coast Strandveld	SAM-HYM-P044545
	Cryptopimpla rubrithorax	COI (A, B, D, E), 28S (G, I), 18S (K, L)	KO98-M40	South Africa	SA	Mesic Mountain Fynbos	SAM-HYM-P044558
	Cryptopimpla	28S		Germany	GE1		Laurenne *et al.* (2006)
	Cryptopimpla	COI		Germany	GE2		Quicke *et al.* (2012)
	Tetractenion sp. 1	COI (A, B, D, E), 28S (G, I), 18S (K, L)	GUM-NAM01	Namibia	NA		SAM-HYM-P047471
	Tetractenion sp. 1	COI (A, B, D, E), 28S (G, I), 18S (K, L)	ASA09-WOO1-M06	South Africa	SA	Southern Karoo Riverine Woodland	SAM-HYM-P044553
	Tetractenion	28S		Togo	TO		Quicke *et al.* (2009)
	Exetastes annulator	28S (H, J), 18S (K, L)	K098-M22	South Africa	SA1	Mesic Mountain Fynbos, last burnt c. 1978	SAM-HYM-P044552
	Exetastes annulator	COI (A, B, D, E), 28S (G, I), 18S (K, L)	STE09-SUC1-M04	South Africa	SA2	Succulent Karoo	SAM-HYM-P047448
	Exetastes personatus	COI (A, B, D, E), 28S (G, I), 18S (K, L)	GL07-REN1-M36	South Africa	SA	Shale Renosterveld	SAM-HYM-P047459
	Exetastes	28S		Austria	AU		Quicke *et al.* (2009)
	Exetastes mexicanus	28S		Costa Rica	CR		Quicke *et al.* (2009)
	Exetastes	28S					Belshaw *et al.* (1998)
	Sjostedtiella sp. 1	COI (A, F), 28S (G, I), 18S (K, L)	UG05-M11	Uganda	UG	Secondary Mid-altitude Rainforest	SAM-HYM-P044474
	Sjostedtiella sp. 2	COI (A, B, D, E), 28S (G, I), 18S (K, L)	GUM-GOI01	Guinea	GU	Gallery forest	SAM-HYM-P047472
	Sjostedtiella sp. 3	COI (B, C, D, E), 28S (G, I), 18S (K, L)	UG08-KF12-S03	Uganda	UG	Primary Mid-altitude Rainforest, Near Stream	SAM-HYM-P044492
	Sjostedtiella sp. 4	COI (A, B, D, E), 28S (G, I), 18S (K, L)	UG08-KF1-M01	Uganda	UG	Secondary Mid-altitude Rainforest	SAM-HYM-P047444
	Sjostedtiella	COI		Togo	TO		Quicke *et al.* (2012)
	Sjostedtiella	28S					Laurenne *et al.* (2006)
	Sjostedtiella sp. 5	COI (A, B, D, E), 28S (G, I), 18S (K, L)	RP12-STR1-S14	South Africa	SA	West Coast Strandveld	SAM-HYM-P047447
	Sjostedtiella sp. 6	COI (A, B, D, E), 28S (H, J), 18S (K, L)	GL07-KOP2-M56	South Africa	SA	Dolerite Koppie Renosterveld	SAM-HYM-P044524
	Sjostedtiella sp. 7	COI (A, D, E), 28S (G, I), 18S (K, L)	ASA09-WOO1-Y14	South Africa	SA	Riverine Woodland	SAM-HYM-P044546
	Tossinola	COI	MUBFS	Uganda	UG	Mesic Montane Forest	Quicke *et al.* (2012)
	Tossinola	28S		Fiji	FJ		Quicke *et al.* (2009)
	Banchopsis	28S		Greece	GRE		Quicke *et al.* (2009)
	Geraldus	28S					Quicke *et al.* (2009)
	Philogalleria bobbyi	28S		Australia	AUS		Quicke *et al.* (2009)
	Banchus volututorias	28S					Quicke *et al.* (2005)
	Banchus	COI		Canada	CA		Hebert *et al.* (unpubl.)
	Rhynchobanchus bicolor	28S		Austria	AU		Quicke *et al.* (2009)
	Agathilla bradleyi	28S		United States of America	USA		Quicke *et al.* (2009)

Thirty four previously used external morphological characters, which were shown to be informative for banchine species (Quicke et al. 2009) were used and the data set was extended by including 33 additional characters specific to the subfamily. This resulted in a data set comprising a total of 67 parsimony informative discrete morphological characters which were scored for all the taxa used in the phylogeny. The presumed plesiomorphic condition is denoted by a '0' and derived states are subsequently denoted by sequential integers.

Adult external morphology

1. *Flagellomeres in females*: (0) visibly narrower distally; (1) not narrowed distally
2. *Ocellus*: (0) not enlarged; (1) enlarged
3. *Horned structures behind ocelli*: (0) absent; (1) present
4. *Mandible*: (0) equal length, (1) upper tooth longer than lower, (2) upper tooth shorter than lower
5. *Clypeus profile(lateral view)*: (0) convex; (1) concave
6. *Clypeus shape*: (0) rounded; (1) with declivity; (2) with transverse ridge
7. *Clypeus edge*: (0) straight or convex; (1) with a median notch
8. *Clypeus*: (0) with fringe; (1) with some setae (2) without setae
9. *Inner margins of compound eye*: (0) not convergent; (1) convergent ventrally
10. *Cheek*: (0) 0.5 to 0.8 as long as basal width of mandible (1) 1.4 to 2.5 as long as basal width of mandible (2) less than 0.5 as long
11. *Hypostomal carina with strong sinuation that extends onto the cheek*: (0) absent; (1) present
12. *Occipital carina*: (0) complete; (1) mid-dorsally absent; (2) interrupted laterally and medially
13. *Intersection of occipital and hypostomal carinae*: (0) intersection distant from base of mandible; (1) intersection at base of mandible (2) do not intersect
14. *Pronotal epomia*: (0) present; (1) absent
15. *Pronotal collar*: (0) not swollen; (1) swollen
16. *Pronotal transverse carina*: (0) absent;(1) present

17. *Pronotal medial furrow*: (0) indistinct; (1) distinct
18. *Posterior corner of the pronotum*: (0) rounded or flattened; (1) rounded, slightly twisted and flattened
19. *Epicnemial carina when present dorsally*: (0) ending at or at least converging toward anterior edge of mesopleuron (1) ending distant from the anterior edge of the mesopleuron, not converging towards it
20. *Mesopleuron*: (0) not compressed; (1) compressed
21. *Propodeum*: (0) short with narrow, shallow, anterior trough; (1) elongated, but not subcylindrical, with shallow groove; (2) long, subcylindrical with deep trough
22. *Propodeum*: (0) not reticulated; (1) reticulated
23. *Median horn on anterior edge of propodeum*: (0) absent; (1) present
24. *Propodeal spiracle*: (0) round or oval (not more than 1.2 times as long as wide); (1) elliptical or elongate (at least 1.3 times as long as wide)
25. *Position of propodeal spiracle*: (0) medially; (1) anteriorly
26. *Medial wrinkling of propodeum*: (0) present (1) absent
27. *Pleural carinae of propodeum*: (0) present (1) reduced or absent
28. *Anterior edge of propodeum*: (0) complete; (1) present medially only
29. *Posterior transverse carina of propodeum*: (0) present but not strongly arched; (1) present and strongly arched; (2) absent
30. *Anterior transverse carina on propodeum*: (0) absent; (1) present
31. *Medial longitudinal groove on propodeum*: (0) absent; (1) present
32. *Postero-lateral indentations on propodeum*: (0) absent; (1) present
33. *Two medial indentations on propodeum*: (0) absent; (1) present
34. *Propodeum*: (0) lateral longitudinal carina in line with spiracle; (1) transverse carina connects lateral longitudinal carina with spiracle; (2) short transverse carina absent
35. *Cell 1M + R1 on fore wing with glabrous fenestra and alar sclerites*: (0) absent; (1) present
36. *Fore wing areolet presence*: (0) closed, not stalked; (1) closed, stalked; (2) open

37. *Fore wing areolet shape*: (0) quadrate; (1) triangular; (2) petiolate; (3) truncate
38. *Ramellus on 1m-cu of fore wing*: (0) absent; (1) present
39. *Fore wing, vein 2m-cu*: (0) with two bullae separate; (1) with two bullae close together; (2) one bulla
40. *Bullae on fore wing when both are closely situated and appearing as one*: (0) 0.5 length of 2m-cu after bullae; (1) 1 times length of 2m-cu after bullae
41. *Fore wing 2m-cu*: (0) curved; (1) sinuate; (2) straight
42. *Length of "bulla" on rs-m vein*: (0) less than 1/3 rs-m vein toward anterior end; (1) more than 1/3 rs-m vein toward anterior
43. *Lengths of fore wing, vein 2cu-aa relative to immediately basal abscissa of Cu*: (0) shorter than; (1) about the same length as; (2) longer than
44. *Number of basal hamuli of hind wing*: (0) two or more; (1) one; (2) none
45. *Number of distal hamuli of hind wing*: (0) 10; (1) 9; (2) 8; (3) 7; (4) 6; (5) 5
46. *Hind wing, intercept of Cu and cu-a (when present)*: (0) posterior to midpoint of *Cu* and *cu-a* (that is, closer to vein *A*); (1) at mid-point; (2) anterior to mid-point (that is, closer to vein *M*); (3) not intercepted
47. *Tarsal claws*: (0) simple; (1) pectinate (with pecten of at least two teeth); (2) densely pectinate
48. *Inner margin of hind tibial apex*: (0) without comb; (1) with comb
49. *Submetapleural lobe*: (0) not extended; (1) extended into a broad flange
50. *Submetapleural lobe shape*: (0) round or triangular; (1) rhombic or rectangular
51. *Metasoma*: (0) dorso-ventrally depressed; (1) laterally depressed
52. *Shape of metasomal tergite 1*: (0) basal half stout; (1) moderately slender;(2) slender
53. *Metasomal tergite 1*: (0) glossy; (1) subpolished
54. *Glymma of first metasomal tergite*: (0) present; (1) absent
55. *Metasomal tergite 1*: (0) without longitudinal striae; (1) with longitudinal striae
56. *Spiracle position on metasomal tergite 1*: (0) anterior to middle; (1) at middle; (2) posterior to middle

57. *Two ridges on metasomal tergite 1(dorsal view)*: (0) extends entire length of tergite; (1) extends to middle of tergite; (2) absent
58. *Metasomal tergite 2*: (0) without grooves; (1) with anterolateral grooves that do not connect at the midpoint; (2) with anterolateral grooves that extend from midpoint
59. *Metasomal segment 3 of female*: (0) at least as wide as high; (1) wider than high
60. *Laterotergites of metasomal segments 3 and 4 of male*: (0) both at least partly separated by a crease; (1) only laterotergite 3 at least partly separated by a crease; (2) neither separated (even partly) by a crease
61. *Female hypopygium*: (0) large and roundly triangular (1) large and sharply triangular
62. *Hypopygium*: (0) without notch; (1) with notch
63. *Ovipositor sheath striations*: (0) occupying at least basal 0.5; (1) present but occupying less than basal 0.5; (2) absent
64. *Ovipositor sheaths strongly sclerotized, covered in hairs*: (0) absent; (1) present
65. *Ovipositor, portion protruding beyond apex of metasoma*: (0) very long (> length of metasoma); (1) long (< 1.0, > 0.3 length of metasoma); (2) short (< 0.3 length of metasoma)
66. *Exposed portion of metasomal tergite 8 of female*: (0) at least as wide as tergite 7 (1) half to less than half the width of tergite 7
67. *Gonocoxite 9*: (0) indistinctly exposed; (1) distinctly exposed

2.2.2 DNA extraction, PCR amplification and sequencing

Genomic DNA was extracted from the whole specimen for 74 taxa using non-destructive techniques and the CTAB (Saghai-Maroof et al. 1984) and Nucleospin® (Macherey-Nagel) DNA extraction protocols. An overnight Proteinase K (10 mg/mL) digestion at 56°C was followed. DNA was eluted in 70µl-100 µl of elution buffer and stored at -20°C. PCR reactions were carried out in an AB GeneAmp 2700 automated thermocycler and PCR products were gel purified using the Nucleospin® Gel and PCR

Clean-Up Kit (Macherey-Nagel). Purified products were cycle-sequenced using a BigDye® Terminator v3.1 Cycle Sequencing kit (Applied Biosystems [ABI]) and run on an ABI 3100 automated sequencer at the Central Analytical Facility at the University of Stellenbosch.

The primer sets that were successful for PCR amplification of the nuclear 28S (D2 + D3) and 18S and mitochondrial COI gene fragments of each taxon are listed in Table 2.2 and a variety of PCR protocols were employed to accommodate the different primer sets and/or species, which are listed in appendix 1.

Table 2.2: Primer sequences used to amplify the COI, 28S and 18S gene fragments

Gene	Designation		Sequence	Reference
COI	LCO 1490	(A)	5'-GGT CAA CAA ATC ATA AAG ATA TTG G-3'	Folmer et al. (1994)
	HCO 2198	(B)	5' TAA ACT TCA GGG TGA CCA AAA AAT CA-3'	Folmer et al. (1994)
	CI-J-1718	(C)	5'-GGA GGA TTT GGA AAT TGA TTA GTT CC-3'	Simon et al. (1994)
	CI-N-2329	(D)	5'-ACT GTA AAT ATA TGA TGT GCT CA-3'	Simon et al. (1994)
	L6625	(E)	5'-GGA GGA TTT GGA AAT TGA TTA GTT CC-3'	Hafner et al. (1994)
	H7005	(F)	5'-ACT GTA AAT ATA TGA TGA GCT CA-3'	Hafner et al. (1994)
28S	Forward	(G)	5'-AGA GAG AGA GTT CAA GAG TAC GTG-3'	Belshaw & Quicke (1997)
		(H)	5'-GCG AAC AAG TAC CGT GAG GG-3'	Laurenne et al. (2006)
	Reverse	(I)	5'-TAG TTC ACC ATC TTT CGG GTC-3'	Laurenne et al. (2006)
		(J)	5'-CGC TAC GGA CCT CCA TCA GG-3'	Laurenne et al. (2006)
18S	H17F	(K)	5'-AAA TTA CCC ACT CCC GGC A-3'	Heraty et al. 2004
	H35R	(L)	5'-TGG TGA GGT TTC CCG TGT T-3'	Heraty et al. 2004

2.2.3 Sequence alignment and phylogenetic reconstructions

Alignment

Sequences were manually inspected and edited using the BioEdit Sequence Alignment Editor software (Hall 1999). COI mtDNA data were translated into protein codons to test for functionality (http://www.ebi.ac.uk/Tools/emboss/transeq/index.html). The 28S fragments were multiply aligned using the Clustal W alogorithm and to accommodate the large insertions and deletions in the data it was further aligned by eye in BioEdit. The 18S fragments were also aligned by eye in BioEdit. All the sequences were blasted in GenBank with published records of 18S, 28S and COI sequences to

ensure sequence integrity and submitted onto the Afrotropical Hymenoptera Initiative project on iBOL (AHI001-18.COI-5P -AHI075-18.COI-5P, AHI001-18.28S-D2 - AHI075-18.28S-D2, AHI001-18 - AHI075-18).

Bayesian inference

The most likely model of sequence evolution for each data partition was determined with the program jModelTest 2 (Darriba et al. 2012). For the choice in model selection, the Akaike Information Criteria (AIC) was used. The COI mtDNA data was (1) unpartitioned and (2) divided into three partitions reflecting each codon position and the gamma shape parameter was unlinked across all partitions of the data. For the morphological matrix the Markov-k model, under the assumption that variable characters where sampled was applied accounting for the fact that only parsimony informative characters were scored.

Bayesian Markov Chain Monte Carlo (BMCMC) analysis on the genetic and morphological data sets was run, and stability and burn-in was determined using the sump and sumt commands in in MrBayes v3.04b. For each data set, two different runs were conducted to test for convergence, each with four chains and sampled every 100 generations, ensuring that the standard deviation of the split frequencies of each run had at least reached 0.01 (Ronquist et al. 2012). The sequence and morphological data sets ran for 2 million and 3 million generations, respectively. Convergence and stationarity was assessed with the chain inspector software Tracer v.1.5. Thereafter, a 50% majority-rule consensus tree was visualised in FigTree 1.3.1. Nodal support was assessed using posterior probabilities for the Bayesian tree, and only values ≥ 0.95 were regarded as significant.

Maximum parsimony

Maximum parsimony (MP) heuristic searches were incorporated into the analyses in PAUP* 4.0 (Swofford 2002), with 1000 and 100 random sequence addition replicates, for the separate data sets and combined data set analyses, respectively. TBR branch swapping was used and nodal support was assessed using 100 nonparametric bootstraps.

Visualization of the data using both methods of phylogenetic inference

Data were analyzed using both methods of phylogenetic inference using the following partitions: (a) each gene separately, (b) a total evidence including all the morphological and molecular data. Gene conflict was visually inspected by comparing the topologies obtained from the partitioned analyses of each data set to that of the total evidence tree.

Prior to data combination in a total evidence tree, the statistical test CADM (Congruence Among Distance Matrices, Legendre & Lapointe 2004, Campbell et al. 2011) was used to test for topological congruence among all the data sets. BMCMC analysis on the combined data ran for 10 million generations, with the standard deviation between the runs reaching 0.01. Thereafter, a 50% majority-rule consensus tree of Banchinae of the combined data set was constructed which was used to infer biogeography.

Divergence time estimation

The divergence times of clades was estimated under a Bayesian framework using BEAST v.1.8.0 by employing an uncorrelated log-normal relaxed molecular clock approach on the combined data set. The fossils that were used for divergence time estimates were of the extant genera *Lissonota* and *Exetastes*, 38-33.9 and 23.8-7.1 mya respectively (Zhang et al. 1989, Khalaim 2011). The *Exetastes* fossil was found in the Shanwang formation in China (Zhang et al. 1989). The same nucleotide-partitioning scheme and substitution models were used as those used for the MrBayes analyses above. A Birth-Death speciation process with a random starting tree was used for the tree prior. MCMC searches were run for 150 million generations with a sampling frequency of 1/ 10,000 generations. Convergence and stationarity was assessed with the chain inspector software Tracer v.1.5. The results from two independent runs were combined using LogCombiner v1.8.0 and node ages were calculated using TreeAnnotator v1.8.0 with a burn-in of 7500 generations. The final tree was visualized using FIGTREE v.1.3.1. The fossil age estimates were depicted on the tree as a point of reference.

2.3 Results

The COI mtDNA, 28S and 18S rDNA data analyses were based on a final alignment of 843 bp, 800 bp, and 800 bp, respectively, for 74 (70 ingroup, 4 outgroup) taxa sampled across the Afrotropical region. Sequences for 37 additional taxa were obtained from GenBank and Andrew Bennett (Canadian National Collection of Insects, Ottawa) (references shown in Table 2.1). A morphological matrix was constructed for 72/74 taxa (68 ingroup and 4 outgroup, Table 2.3). The evolutionary model selected for the 28S and 18S data sets was GTR + G (α =0.26) and TIM3 + G (α = 0.016), respectively. For the unpartitioned COI data set, the evolutionary model selected was GTR + I (0.124) + G (0.323). For the partitioned COI data set, the evolutionary models selected was TPM2uf + G (0.632) (1^{st} codon), GTR + I (0.206) + G (0.201) (2^{nd} codon), and TIM3 + G (0.224).

Further partitioning of the COI data resulted in decreased support for nodes that were well supported when data were unpartitioned (Table 2.4). Hereafter, the unpartitioned COI data set is used in all combined data analyses.

2.3.1 Summary of individual trees with respect to the total evidence tree.

The program CADM tests for the null hypothesis that there is incongruence among the data sets. A significant probability ($P < 0.01$) was found across all the data sets, rejecting the null hypothesis. Thus, the data sets are not significantly incongruent with one another and can be placed in a combined data tree. Kendall's coefficient of concordance (Kendall's *W*) tests the level of strength of that congruence. Kendall's W range between 0 (no agreement) and 1 (complete agreement). A value of 0.58438 (Friedman's Chi-square 3218.77289) suggests an above average degree of agreement among the different data sets.

Table 2.3: A morphological matrix using 67 parsimony informative and discrete morphological characters. The presumed plesiomorphic condition is denoted by a '0' and derived states by other integers in an ordered fashion. Missing data is denoted by a "?" while a "-" denotes where the character state does not apply to that specimen.

	10	20	30	40	50	60
Apophua sp. 3	0 0 0 0 0 0 0 1 0 0 1 1 1 0 0 0 1 1 0 0 0 0 0 0 0 0 0 1 0 0 0 0 1 0 2 - 0 ? 0 2 0 0 1 4 0 1 0 1 1 0 0 1 0 0 0 0 0 1 1 0 0 1 0 0 0 0 0
Apophua sp. 4 SA	0 0 0 0 0 0 0 1 0 0 1 1 1 1 0 0 1 1 0 0 0 0 0 0 0 0 0 1 0 0 0 0 1 0 2 - 0 ? 0 2 0 0 1 4 0 1 0 1 0 0 0 1 0 0 0 0 1 1 0 0 1 0 0 0 0 0
Apophua sp. 4 UG	0 0 0 0 0 0 0 1 0 0 1 1 1 1 0 0 1 1 1 0 0 0 0 0 0 0 0 0 1 0 0 0 0 1 0 2 - 0 1 0 2 0 0 1 4 0 1 0 1 0 0 0 1 0 0 0 0 1 1 0 0 1 0 0 0 0 0
Apophua hispida UG1	0 0 0 0 0 0 0 1 0 0 1 1 1 0 1 0 0 1 1 0 0 0 0 0 0 0 0 0 1 0 0 0 0 1 0 2 - 0 1 0 2 0 0 1 4 0 1 0 1 1 0 0 1 0 0 0 0 1 1 1 0 0 1 0 0 0 0 0
Apophua hispida CAR	0 0 0 0 0 0 0 2 0 0 1 1 1 0 1 0 0 1 1 0 0 0 0 0 0 0 0 0 1 1 0 0 0 0 1 0 2 - 0 1 0 2 0 0 1 4 0 1 0 1 1 0 0 1 0 0 0 0 1 1 1 0 0 1 0 0 0 0 0
Apophua hispida UG2	? 0 0 0 0 0 0 0 1 0 0 1 1 1 0 1 0 0 1 1 0 0 0 0 0 0 0 0 0 1 0 0 0 0 1 0 2 - 0 1 0 2 0 0 1 3 0 1 0 1 1 0 0 1 0 0 0 0 1 1 1 0 0 1 0 0 0 0 0
Lissonota sp. 1	- 0 0 ? ? ? ? ? ? ? 0 ? ? 1 0 0 0 1 1 0 1 0 0 0 0 1 1 1 1 0 0 0 0 0 2 0 1 3 0 1 1 2 0 0 1 4 0 0 0 1 0 0 0 1 0 0 0 2 2 - - - 1 - 0 - - 0
Lissonota sp. 2	- 0 0 0 0 1 0 2 0 0 0 0 0 1 0 0 0 1 1 0 1 0 0 0 0 1 0 1 0 0 0 0 0 1 0 0 3 0 1 1 2 0 0 1 4 0 0 0 1 0 0 0 1 0 1 0 2 2 - - - 1 - 0 - - 0
Lissonota sp. 3	- 0 0 0 0 0 0 1 0 0 0 0 0 1 0 0 0 1 1 1 0 1 0 0 0 0 1 0 1 0 0 0 0 0 1 0 2 - 0 1 1 2 0 0 1 4 0 0 0 1 0 0 0 1 0 0 0 2 2 - - - 1 - 0 - - 0
Lissonota sp. 4	- 0 0 0 0 0 0 1 0 0 0 0 0 1 0 0 0 1 1 0 1 0 0 0 0 1 1 1 2 0 0 0 0 2 0 0 2 0 1 1 1 0 0 1 1 0 0 1 1 0 0 1 1 0 0 0 1 0 1 0 2 2 1 - - 1 - 0 - - 0
Lissonota sp. 5	0 0 0 0 0 1 0 1 0 1 0 0 0 1 0 0 0 1 0 0 1 0 0 0 0 1 1 1 2 0 0 0 0 2 0 0 2 0 1 0 2 0 0 1 2 0 1 0 1 0 0 0 1 0 0 0 2 2 0 0 0 1 0 0 0 0 0 1
Lissonota sp. 6	0 0 0 0 0 1 0 1 0 0 0 0 0 1 0 0 0 1 1 0 1 0 0 0 0 1 0 1 0 0 0 0 0 1 0 1 3 0 0 1 1 ? 0 1 4 0 1 1 1 0 0 0 1 0 0 0 2 2 0 0 0 1 0 0 0 0 0 1
Lissonota sp. 7	- 0 0 0 0 0 0 1 0 0 0 0 0 1 0 0 0 1 1 0 0 1 0 0 0 0 1 0 1 0 0 0 0 0 1 0 1 3 0 1 1 2 0 0 1 5 0 0 0 1 0 0 0 1 0 0 0 2 2 - - - 1 - 0 - - 0
Spilopimpla leleupi	0 0 0 0 0 0 0 2 0 0 0 0 0 1 0 0 0 1 1 0 0 0 0 0 0 1 0 1 0 0 0 0 0 0 2 0 2 - 0 1 1 2 0 1 1 4 0 1 0 1 0 0 0 0 1 0 0 0 2 2 0 0 0 1 0 0 1 1 1
Spilopimpla sp. 1	0 0 0 0 0 1 0 2 0 0 0 0 0 1 0 0 0 1 0 0 0 0 0 0 1 0 1 0 0 0 0 0 0 2 0 2 - 0 1 1 2 0 0 1 5 0 1 0 1 0 0 0 0 1 0 0 0 2 2 1 0 0 1 0 0 1 1 1
Spilopimpla sp. 2	? 0 0 0 0 1 0 1 0 0 0 0 0 1 0 0 0 1 0 0 0 0 0 0 0 1 0 1 0 0 0 0 0 0 2 0 2 - 0 1 0 2 0 0 1 4 0 1 0 1 0 0 0 1 0 0 0 2 2 1 0 0 1 0 0 1 1 1
Spilopimpla sp. 3 UG2	- 0 0 0 0 0 0 1 0 0 0 0 0 1 0 0 0 1 1 0 0 0 0 0 0 1 0 1 0 0 0 0 0 1 0 2 - 0 1 1 2 0 0 1 5 0 1 0 1 0 0 0 1 0 0 0 2 2 - - - 1 - 0 - - 0
Spilopimpla sp. 3 UG1	- 0 0 0 0 0 0 2 0 0 0 0 0 1 0 0 0 1 1 0 0 0 0 0 0 1 0 1 0 0 0 0 0 1 0 2 - 0 1 1 2 0 0 1 5 0 1 0 1 0 0 0 1 0 0 0 2 2 1 - - 1 - 0 - - 0
Spilopimpla sp. 3 UG3	0 0 0 0 0 0 0 1 0 0 0 0 0 1 0 0 0 1 1 0 0 0 0 0 0 1 0 1 1 0 0 0 0 1 0 2 - 0 1 1 2 0 0 1 4 0 1 0 1 0 0 0 1 0 0 0 2 2 0 0 0 1 0 0 1 0 0 1
Spilopimpla sp. 4	0 0 0 1 0 0 0 1 0 0 0 0 0 1 0 0 0 1 1 0 0 0 0 0 0 1 0 1 1 0 0 0 0 2 0 2 - 0 1 0 2 0 0 1 4 0 1 0 1 0 0 0 1 0 0 0 2 2 1 0 0 1 0 0 1 1 1
Spilopimpla sp. 5	- 0 0 0 0 1 0 1 0 0 0 0 0 1 0 0 0 1 0 0 0 0 0 0 0 1 0 1 0 0 0 0 0 0 2 0 2 - 0 1 1 2 0 1 1 5 0 1 0 1 0 0 0 1 0 0 0 2 2 - - - 1 - 0 - - 1
Spilopimpla sp. 6	? 0 0 0 0 1 0 1 0 0 0 0 0 1 0 0 0 1 1 0 0 0 0 0 0 1 0 1 0 0 0 0 0 0 2 0 2 - 0 1 1 2 0 1 1 5 0 1 0 1 0 0 0 1 0 0 0 2 2 0 0 0 1 0 0 1 0 1
Spilopimpla sp. 7	- 0 0 0 0 0 0 0 1 0 0 0 0 0 1 0 0 0 1 1 0 0 0 0 0 0 1 0 1 0 0 0 0 0 1 0 2 - 0 1 0 2 0 0 1 5 0 1 1 1 0 0 0 1 0 0 0 2 2 - - - 1 - 0 - - 0
Spilopimpla sp. 8	0 0 0 0 0 0 0 1 0 0 0 0 0 1 0 0 0 1 1 0 0 0 0 0 0 1 0 1 0 0 0 0 0 1 0 2 - 0 1 1 2 0 0 1 4 0 1 0 1 0 0 0 1 0 0 0 2 2 0 0 0 1 0 0 1 0 1
Spilopimpla sp. 9 UG1	- 0 0 0 0 0 0 1 0 0 0 0 0 1 0 0 0 1 1 0 0 0 0 0 0 1 0 1 0 0 0 0 0 0 1 0 2 - 0 1 0 2 0 1 1 4 0 1 0 1 0 0 0 1 0 0 0 2 2 - - - 1 - 0 - - 1
Spilopimpla sp. 9 UG2	0 0 0 0 0 0 0 1 0 0 0 0 0 1 0 0 0 1 1 0 0 0 0 0 0 1 0 1 0 0 0 0 0 2 0 2 - 0 1 0 2 0 1 1 4 0 1 0 1 0 0 0 1 0 0 0 2 2 0 0 0 1 0 0 1 1 1
Himertosoma sp. 1	- 0 0 0 0 0 0 1 0 0 0 0 0 1 0 0 0 1 0 0 0 ? 0 0 1 0 1 0 0 0 0 0 0 1 0 2 - 0 1 1 2 0 0 1 4 0 1 0 1 0 0 0 0 0 1 0 2 2 - - - 1 - 0 - - 0
Himertosoma sp. 3	0 0 0 0 0 1 0 1 0 0 0 0 0 1 0 0 1 1 1 0 0 0 0 0 0 1 0 1 0 0 0 0 0 2 0 2 - 0 1 0 2 0 0 0 3 0 1 0 1 0 0 0 1 0 0 0 2 2 1 0 0 1 0 0 0 0 1
Himertosoma sp. 4	- 0 0 0 0 1 0 1 0 0 0 0 0 1 0 0 0 1 1 0 0 0 0 0 0 1 0 1 0 0 0 0 0 0 1 0 2 - 0 1 0 2 0 0 1 4 0 1 0 1 0 0 0 0 1 0 1 0 2 2 - - - 1 - 0 - - 1
Himertosoma sp. 5	- 0 0 0 0 1 0 1 0 0 0 0 0 1 0 0 0 1 1 1 0 0 1 0 0 0 1 0 1 0 0 0 0 0 1 0 2 - 0 1 0 2 0 0 1 3 0 1 0 1 1 0 0 0 0 1 0 2 2 - - - 1 - 0 - - 1
Himertosoma sp. 6	? 0 0 0 0 1 0 1 0 0 0 0 0 1 0 0 0 1 1 0 0 0 0 0 0 1 0 1 0 0 0 0 0 0 1 0 2 - 0 1 0 2 0 0 1 4 0 1 0 1 0 0 0 0 1 0 1 0 2 2 1 0 0 1 0 0 0 1 1
Himertosoma sp. 7	- 0 0 0 0 1 0 1 0 0 0 0 0 1 0 0 0 1 1 0 0 0 0 0 0 1 0 1 0 0 0 0 0 0 2 0 2 - 0 1 1 2 0 0 1 4 0 1 1 1 0 0 0 1 0 1 0 2 2 - - - 1 - 0 - - 1
Himertosoma sp. 8	0 0 0 0 0 0 0 1 0 0 0 0 0 1 0 0 0 1 1 0 0 0 0 0 0 1 0 1 0 0 0 0 0 1 0 2 - 0 1 0 2 0 0 1 5 0 1 0 1 0 0 0 0 0 1 0 2 2 0 0 0 1 0 0 1 0 0 0 0 1
Himertosoma sp. 9	- 0 0 0 0 1 0 1 0 0 0 0 0 1 0 0 0 1 0 0 0 0 0 0 0 1 0 1 0 0 0 0 0 0 1 0 2 - 0 1 1 2 0 0 1 5 0 1 1 1 0 0 0 1 0 1 0 2 2 - - - 1 - 0 - - 1
Himertosoma sp. 10	0 0 0 1 0 1 0 1 0 0 0 0 0 1 0 0 0 1 1 0 0 0 0 1 0 1 0 1 2 0 0 0 0 2 0 2 - 1 1 1 2 - 0 0 1 0 1 1 1 1 1 0 0 1 0 0 0 2 2 1 0 1 1 ? 0 0 0 1
Himertosoma sp. 11	0 0 0 1 0 1 0 1 0 0 0 0 0 1 0 0 0 1 1 0 0 0 0 0 0 0 0 1 1 0 0 0 0 1 0 2 - 0 1 1 2 0 0 1 4 0 ? 0 1 0 0 0 0 0 0 0 2 2 1 0 0 1 0 0 0 0 1
Syzeuctus sp. 1 UG	0 0 1 1 0 0 0 1 0 0 0 0 1 0 0 0 0 1 1 0 0 0 0 1 0 0 0 1 1 0 0 0 1 2 0 1 1 0 1 0 2 1 1 1 2 1 1 0 1 0 0 0 1 0 0 0 2 2 1 0 1 1 0 0 0 1 1
Syzeuctus sp. 1 KEN	0 0 1 1 0 0 0 1 0 0 0 0 1 0 0 0 0 1 1 1 0 0 0 0 1 0 1 0 1 0 1 0 0 0 0 1 2 0 1 1 0 1 0 2 1 1 1 3 0 1 0 1 0 0 0 1 0 0 0 2 2 1 0 1 1 0 0 0 1 1
Syzeuctus sp. 2	0 0 1 0 0 0 0 1 0 0 0 0 1 0 0 0 0 1 1 0 0 0 0 1 0 1 0 1 1 0 0 0 1 2 0 1 1 0 ? 0 2 1 1 1 3 1 1 0 1 1 0 0 1 0 0 0 2 2 1 0 1 1 0 0 0 1 1
Syzeuctus sp. 3	0 0 0 0 0 2 0 1 0 0 0 0 1 0 0 0 0 1 1 0 0 0 0 1 0 1 1 1 2 0 0 0 1 2 0 1 1 0 1 0 2 1 1 1 3 0 1 0 1 1 0 0 0 0 0 0 2 2 1 0 1 1 0 0 0 1 1
Syzeuctus sp. 4	0 0 0 0 0 1 0 1 0 0 0 0 1 0 0 0 0 1 1 0 0 0 0 1 0 1 1 1 2 0 0 0 1 2 0 1 1 0 1 0 2 1 1 1 0 0 1 0 1 1 0 0 0 0 0 0 2 2 1 0 1 1 0 0 0 0 1
Syzeuctus sp. 5	0 0 0 1 0 0 0 1 0 0 0 0 1 0 0 0 0 1 1 0 0 0 0 1 0 1 1 1 3 0 0 0 1 2 0 1 1 0 1 0 2 1 1 1 2 1 1 0 1 1 0 0 0 0 0 0 2 2 1 0 1 1 0 0 0 1 1
Syzeuctus sp. 6 SA1	? 0 1 1 0 1 0 1 0 0 0 0 1 0 0 0 0 1 1 1 0 0 0 1 0 1 0 1 1 0 0 0 1 2 0 1 1 0 1 0 2 1 1 1 3 0 1 0 1 1 0 0 1 0 0 0 2 2 1 0 1 1 0 0 0 1 1
Syzeuctus sp. 6 SA2	- 0 1 1 0 1 0 1 0 0 0 0 1 0 0 0 0 1 1 1 0 0 0 1 0 1 0 1 1 0 0 0 1 2 0 1 1 0 1 0 2 1 1 0 1 3 0 1 0 1 1 0 0 1 0 0 0 2 2 - - - 1 - 0 - - 1
Syzeuctus sp. 8	- 0 1 0 0 1 0 2 0 0 0 0 0 1 0 0 0 0 0 1 - 1 0 0 0 1 0 1 1 1 1 1 0 0 0 1 2 0 1 1 0 1 0 2 1 0 1 1 0 0 0 1 1 0 0 0 0 0 0 2 2 - - - 1 - 0 - - 1
Atropha sp. 1	0 0 0 0 0 0 0 1 0 0 0 1 0 1 0 1 0 1 1 1 1 0 0 0 1 0 1 1 1 1 2 0 1 1 0 2 0 1 1 0 1 0 2 0 1 1 3 0 1 0 1 0 1 2 0 1 0 1 0 1 2 2 1 0 0 1 0 0 0 0 1
Atropha sp. 2	0 0 0 0 0 0 0 1 0 0 0 1 0 1 0 0 0 0 1 1 0 1 0 0 0 1 0 1 1 1 1 2 0 1 0 0 2 0 1 1 0 1 0 2 0 1 1 4 1 1 1 1 0 1 2 0 1 0 1 0 1 2 2 1 0 0 1 0 0 0 0 1
Atropha sp. 3	- 0 0 0 0 0 0 0 1 0 0 0 1 0 0 0 1 0 1 1 1 1 0 0 1 0 1 1 1 2 0 1 0 0 2 0 1 1 0 1 0 2 0 1 1 5 0 1 0 1 0 1 2 0 1 0 1 0 1 2 2 - - - 1 - 0 ? - 1
Atropha sp. 4	0 0 0 0 0 0 0 1 0 0 0 1 0 0 0 0 0 1 1 1 1 0 0 1 0 0 1 1 1 2 0 1 0 0 2 0 1 1 0 1 0 2 0 1 1 3 0 1 0 1 0 1 2 0 1 0 1 0 1 2 2 1 0 0 1 0 0 0 0 1
Atropha sp. 5	- 0 0 0 0 0 0 1 0 0 0 1 0 0 0 1 0 1 1 0 1 0 0 1 0 1 1 1 2 0 1 0 0 2 0 1 1 0 1 0 2 0 1 1 5 0 1 1 1 0 1 2 0 1 0 1 0 1 2 2 - - - 1 - 0 - - 1
Atropha sp. 6	- ? 0 ? ? ? ? ? ? ? ? 0 ? ? 0 0 1 0 1 1 0 1 0 0 1 0 1 1 1 2 0 1 0 0 2 0 1 1 0 1 0 2 0 1 1 5 1 1 0 1 0 1 2 0 1 0 1 2 2 - - - 1 - 0 - - 1
Atropha sp. 7	0 0 0 0 0 0 0 1 0 0 0 1 0 1 0 0 0 1 1 1 1 1 0 0 1 0 1 1 1 1 2 0 1 0 0 2 0 1 1 0 1 0 2 0 1 0 4 1 1 1 1 0 1 2 0 1 0 1 0 1 2 2 1 0 0 1 0 0 0 0 1
Cryptopimpla sp. 1 SA1	? 0 0 1 0 0 0 1 0 0 0 0 0 1 0 0 0 1 1 0 0 0 0 0 0 1 0 1 0 0 0 0 0 1 0 0 2 0 1 0 2 0 0 1 4 0 1 1 1 0 0 1 1 0 0 0 2 2 0 0 0 1 0 0 1 1 1
Cryptopimpla sp. 1 SA2	0 0 0 1 0 0 0 1 0 0 0 0 0 1 0 0 0 1 1 0 0 0 0 0 0 1 0 1 0 0 0 0 0 1 0 0 2 0 1 1 1 0 0 1 3 0 1 1 1 0 0 1 1 0 1 0 2 2 1 0 0 1 0 0 0 1 1
Cryptopimpla sp. 2 SA1	- 0 0 1 1 1 0 1 0 1 0 0 0 1 0 0 0 1 1 0 0 0 0 0 0 1 1 1 2 0 0 0 2 0 0 2 0 1 1 1 0 0 0 4 0 1 0 1 0 0 1 1 0 0 0 2 2 - - - 1 - 0 - - 1
Cryptopimpla sp. 2 SA2	- 0 0 1 1 1 0 2 0 0 0 0 0 1 0 0 0 1 1 0 0 0 0 0 0 1 1 1 2 0 0 0 2 0 0 2 0 1 1 1 0 0 1 3 0 1 0 1 0 0 1 1 0 0 0 2 2 - - - 1 - 0 - - 1
Cryptopimpla rubrithorax	? 0 0 1 1 1 0 1 0 0 0 0 0 1 0 0 0 1 1 0 0 0 0 0 0 1 1 1 2 0 0 0 2 0 0 2 0 2 0 1 0 0 1 4 0 1 0 1 0 0 0 1 1 0 0 0 2 2 1 0 0 1 0 0 1 0 1
Tetractenion sp. 1 NA	1 0 0 2 0 1 1 2 0 0 0 0 1 1 0 0 0 1 0 0 0 0 0 0 0 1 1 1 1 0 0 0 0 2 0 1 0 0 2 1 2 0 1 1 2 2 1 0 1 0 1 1 0 0 0 0 2 2 1 1 0 1 2 1 2 0 1
Tetractenion sp. 1 SA	- 0 0 2 0 1 1 1 0 0 0 0 1 1 0 0 0 1 0 0 0 0 0 0 0 1 1 1 0 0 0 0 2 0 1 0 1 2 1 1 - 1 1 2 2 1 0 1 0 1 1 0 0 0 1 1 0 0 2 2 1 - - 1 - 1 - - 0
Exetastes annulator SA1	- 0 0 0 1 1 1 1 0 0 0 0 0 1 0 0 0 1 1 1 0 1 1 1 0 1 1 1 2 0 0 1 0 2 0 0 0 1 1 1 1 - 0 1 2 2 0 0 1 0 0 0 0 0 0 0 2 2 - - - 1 - 1 - - 0
Exetastes annulator SA2	1 0 0 0 1 1 0 1 0 0 0 0 0 1 0 0 0 1 1 1 0 1 1 1 0 1 1 1 2 0 0 1 0 2 0 0 0 1 1 1 1 - 0 1 0 2 0 0 1 0 0 0 0 0 0 0 2 2 1 1 0 1 1 1 2 0 1
Exetastes personatus	1 0 0 0 0 1 1 1 0 0 0 0 0 1 0 0 0 1 1 1 0 0 1 1 0 1 1 1 2 0 0 1 0 2 0 0 0 1 1 1 1 - 0 1 0 2 0 0 1 0 0 0 0 0 0 0 2 2 1 1 0 1 1 1 2 0 1
Sjostedtiella sp. 1	? 0 0 0 0 0 0 0 1 0 1 0 1 0 0 0 0 0 1 0 0 0 0 0 0 1 0 0 0 0 0 0 0 1 0 ? ? ? ? ? ? - ? ? ? ? 1 1 1 1 0 0 1 0 0 0 2 1 0 0 0 1 ? 0 0 0 1
Sjostedtiella sp. 2	0 0 0 0 0 0 1 1 0 1 0 1 0 0 1 1 0 1 1 1 0 0 0 0 0 1 1 1 1 0 0 0 0 1 0 1 0 1 0 1 0 2 0 0 1 5 0 1 1 1 1 0 0 1 0 0 0 0 1 1 0 1 0 0 0 1 1
Sjostedtiella sp. 3	- 0 0 0 0 1 0 1 0 1 0 1 0 0 0 1 0 1 0 0 0 0 0 0 0 0 1 0 0 0 0 1 0 1 3 0 1 0 2 0 0 1 3 0 1 1 1 1 0 0 1 1 - - - 1 - 0 - - 1
Sjostedtiella sp. 4	0 0 0 1 0 1 0 2 0 1 0 1 0 1 0 0 0 1 0 0 0 0 0 0 0 0 1 1 0 0 0 0 1 0 1 0 1 0 1 0 2 0 0 1 1 0 1 0 1 1 0 0 1 0 0 0 1 1 0 0 0 1 ? 0 0 0 1
Sjostedtiella sp. 5	- 0 1 0 0 0 0 1 0 1 0 1 0 0 0 0 0 1 1 0 0 0 0 0 0 1 1 1 1 0 0 0 2 0 1 0 0 1 1 1 0 0 1 2 0 1 0 1 0 0 0 0 0 0 0 2 1 - - - 1 - 0 - - 1
Sjostedtiella sp. 6	0 0 1 0 0 1 0 1 0 1 0 1 2 1 1 0 0 1 1 0 0 0 0 0 0 1 1 1 2 0 0 0 0 2 0 1 0 0 1 0 2 0 0 1 3 0 1 0 1 0 0 0 0 0 0 0 2 2 1 1 0 0 1 0 0 0 1 1
Sjostedtiella sp. 7	- 0 1 0 0 0 1 1 0 1 0 2 0 1 0 0 0 1 0 0 0 0 0 0 0 1 0 1 1 0 0 0 2 0 1 0 0 1 1 1 0 0 1 3 0 1 0 1 1 0 0 1 0 0 0 2 1 - - - 1 - 0 - - 1
Echtromorpha	- 0 0 0 1 1 0 0 0 0 0 0 0 0 0 0 1 0 - 1 1 0 0 0 1 0 1 1 1 2 0 0 1 1 2 0 0 0 0 0 ? 0 0 0 1 0 3 0 0 1 0 0 0 1 0 0 0 0 0 0 - - - 0 - 0 - - 0
Campotypus	- 0 0 0 1 2 1 1 0 2 0 0 0 0 0 0 0 - 1 0 0 0 0 0 0 1 0 1 2 0 0 0 0 0 0 0 0 0 0 ? 0 0 0 1 0 0 0 0 0 0 0 0 0 0 0 0 0 0 0 - - - 0 - 0 - - 1
Dicamptus braunsii	0 1 0 0 0 1 0 1 1 0 0 0 2 1 1 0 0 0 0 0 2 1 0 1 1 1 1 1 0 2 1 0 0 0 2 1 2 - 0 1 0 2 0 0 0 4 0 2 0 1 0 1 2 0 1 0 2 2 2 1 2 0 0 2 0 2 0 1
Enicospillus breviceps	0 1 0 0 0 1 0 1 1 0 0 0 0 1 0 0 0 0 1 0 2 1 0 1 1 1 1 1 0 2 1 0 0 0 2 1 2 - 0 1 0 2 0 0 2 3 0 2 0 1 0 1 2 1 1 0 2 2 2 1 2 0 0 2 0 2 0 1

All the genetic data sets support the monophyly of Banchinae in the Afrotropical region (Clade A, Fig. 2.1), though weakly supported for the partitioned COI data set, and with the exception of the morphological phylogeny which places the Ophioninae representatives within Banchinae (Fig 2.2, Table 2.4). The 28S and morphological phylogenies grouped (1) *Tetractenion* and *Exetastes* (Clade B) into a single clade, representing the *Exetastes* group of the tribe Banchini, and (2) *Apophua* and *Sjostedtiella* (Clade C) into a single clade, representing the tribe Glyptini (Fig 2.2, Table 2.4).

Table 2.4: Summary of Bayesian Inference (BI) and Maximum Parsimony (MP) phylogenetic analyses based on each individual data set, with respect to the phylogenetic analysis representing the total evidence. Categories A-K refers to the clades in the combined data tree in Fig. 2.1. Where strong nodal support was found, pp values above 0.95 and bs values above 75% were indicated; where the node was present but lacking strong support, "WEAK" was indicated; "??" refer to missing data in that respective clade; and "XX" was when the clade was not recovered.

Data	Analysis	A	B	C	D	E	F	G	H	I	J	K
COI	BI (unpartitioned)	0.99	XX	XX	0.99	XX	??	1.0	1.0	??	??	XX
	BI (partitioned)	WEAK	XX	XX	WEAK	XX	??	WEAK	WEAK	??	??	XX
	MP	WEAK	XX	XX	XX	XX	??	XX	XX	??	??	XX
28S	BI	WEAK	0.98	1.0	??	??	??	1.0	??	??	1.0	1.0
	MP	79	WEAK	97	??	??	??	100	??	??	99	100
18S	BI	1.0	XX	XX	XX	XX	XX	XX	XX	XX	??	WEAK
	MP	91	XX	XX	XX	XX	XX	XX	XX	XX	??	XX
Morph	BI	XX	WEAK	WEAK	XX	XX	XX	XX	XX	0.96	??	??
	MP	XX	WEAK	XX	XX	XX	XX	XX	XX	82	??	??

With the exception of *Lissonota* sp. 7 SA which is placed basally to the genus *Spilopimpla* with weak support, all other representative *Lissonota* species form a single clade (Clade D), which is well and weakly supported by the unpartitioned and partitioned COI data sets, respectively; the 28S gene also provides strong nodal support for the *Lissonota* clade (pp = 0.95), but with some missing data (Table 2.4).

Both the COI and 28S genes suggest paraphyly for the genus *Himertosoma*, with weak (COI) to strong support (28S, pp = 0.98, bs = 77) for Clade F (but with missing data), as well as weak (COI partitioned) and strong support (COI unpartitioned, pp = 1; 28S, pp = 1, bs = 100) for Clade G (Table 2.4). Both the 28S and COI genes placed the

genus *Sjostedtiella* into a single clade (Clade H) with weak (28S, *Sjostedtiella* TO absent; COI partitioned) to strong nodal support (COI unpartitioned, pp = 1; Table 2.4). The COI (pp = 1) and 28S (pp = 1, bs = 100) molecular phylogenies and the morphological phylogeny (pp = 0.96, bs = 82) provide robust support for the monophyly of the genus *Syzeuctus* (Clade I), although both the COI and 28S data sets have missing data (Fig. 2.2, Table 2.4). Monophyly of the genus *Atropha* (Clade J) is found for the 28S gene (Table 2.4). This was also the case for the morphological (pp = 1, bs = 78), 18S (pp = 1, bs = 92) and COI (partitioned: pp = 1, bs = 88); unpartitioned: weak support) data sets but with *Atropha* TO absent (Fig. 2.2, Table 2.4). Both the 28S (pp = 1, bs = 94) and morphological (*Apophua* sp. 1 SA absent, Fig. 2.2) phylogenies provide robust support for the monophyly of the genus *Apophua* (Clade K, Table 2.4).

2.3.2 Phylogenetic analyses based on the combined data

Monophyly was resolved for the subfamily Banchinae (posterior probability (pp) = 1, bootstrap support (bs) = 93), for the tribes Glyptini (pp = 0.99, bs = 75) and Banchini (pp = 1) with robust support, and the tribe Atrophini with weak support (Fig 2.1). The genera *Apophua* (pp = 1, bs = 100), *Sjostedtiella* (pp = 0.99, bs = 93), *Cryptopimpla* (pp = 1), *Syzeuctus* (pp = 1, bs = 96), *Atropha* (pp = 1, bs = 78), *Tetractenion* (pp = 1, bs = 99) and *Exetastes* (pp = 1, bs = 100) was found to be monophyletic with robust support for at least one of the analyses (parsimony or Bayesian), and *Spilopimpla* with weak support (Fig. 2.1). All *Lissonota* species (with the exception of *Lissonota* sp. 7 SA) formed a single clade with robust support (pp = 1 Fig. 2.1). *Lissonota* sp. 7 SA was found to be basally situated to

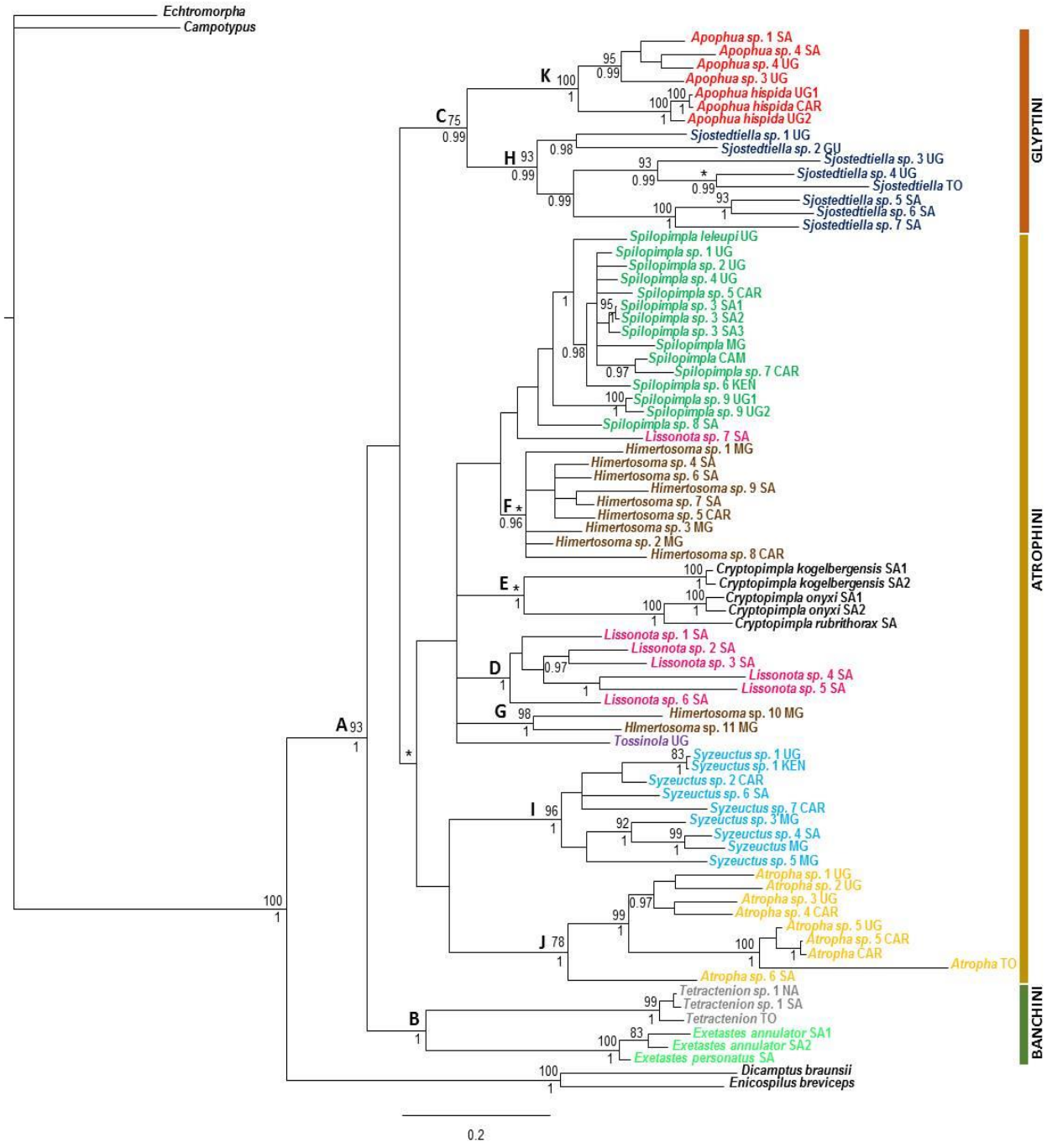

Figure 2.1: The consensus likelihood Bayesian Markov-chain Monte Carlo estimate of Banchinae within the Afrotropical region based on the combined data analysis of COI mtDNA, 28S and 18S rDNA, and morphological data. Clade posterior probabilities are shown above the node, bootstrap support of the maximum parsimony (MP) analysis shown below the node, and an asterix is indicated where nodes were not congruent with the MP analysis. Categories A-K refers to clades as summarized in Table 2.4.

the *Spilopimpla* clade with weak support, making the genus *Lissonota* paraphyletic (Fig. 2.1). Similarly, most of the *Himertosoma* species formed a single well-supported clade (pp = 0.96) with the exception of two *Himertosoma* species sampled from Madagascar that together formed a separate clade with robust support, but the precise phylogenetic position of this clade remains unresolved (Fig. 2.1).

A single *Tetractenion* species from West Africa (Togo, sequence retrieved from GenBank), represented by the 28S gene, was included in the analysis. Results based on the 28S sequence data for the genus *Tetractenion*, showed that species sampled from southern Africa (South Africa and Namibia) were closely-related to the *Tetractenion* species from Togo, with a sequence divergence of 0.24%. Polyphyly within the genera *Spilopimpla* and *Himertosoma* is largely as a result of the morphological phylogeny (Fig. 2.2) and can be attributed to the morphological characters that were used were often shared among the genera (Table 2.3). A long-branch length of *Atropha* TO (Fig. 2.1) was found; a 70bp gap of missing data was found in the middle of the sequence (obtained from GenBank), which was treated as uninformative.

2.3.3 Species connectedness to geography and ecology

The same phylogenetic tree on the combined analysis was used to explain geographic and ecological patterns of banchine species within the Afrotropical region (Fig. 2.3). Within the genus *Apophua*, *Apophua* sp. 4 was sampled from both Uganda and South Africa. Within the genus *Syzeuctus*, two major clades were delimited, but with weak nodal support (Fig. 2.1). All the *Syzeuctus* species, sampled from Madagascar, group in a single clade together with one additional species collected in the Eastern Cape, South Africa (Fig. 2.1). The second clade contains all *Syzeuctus* species sampled from Central and East Africa and a single species from the Eastern Cape, South Africa (Fig. 2.1).

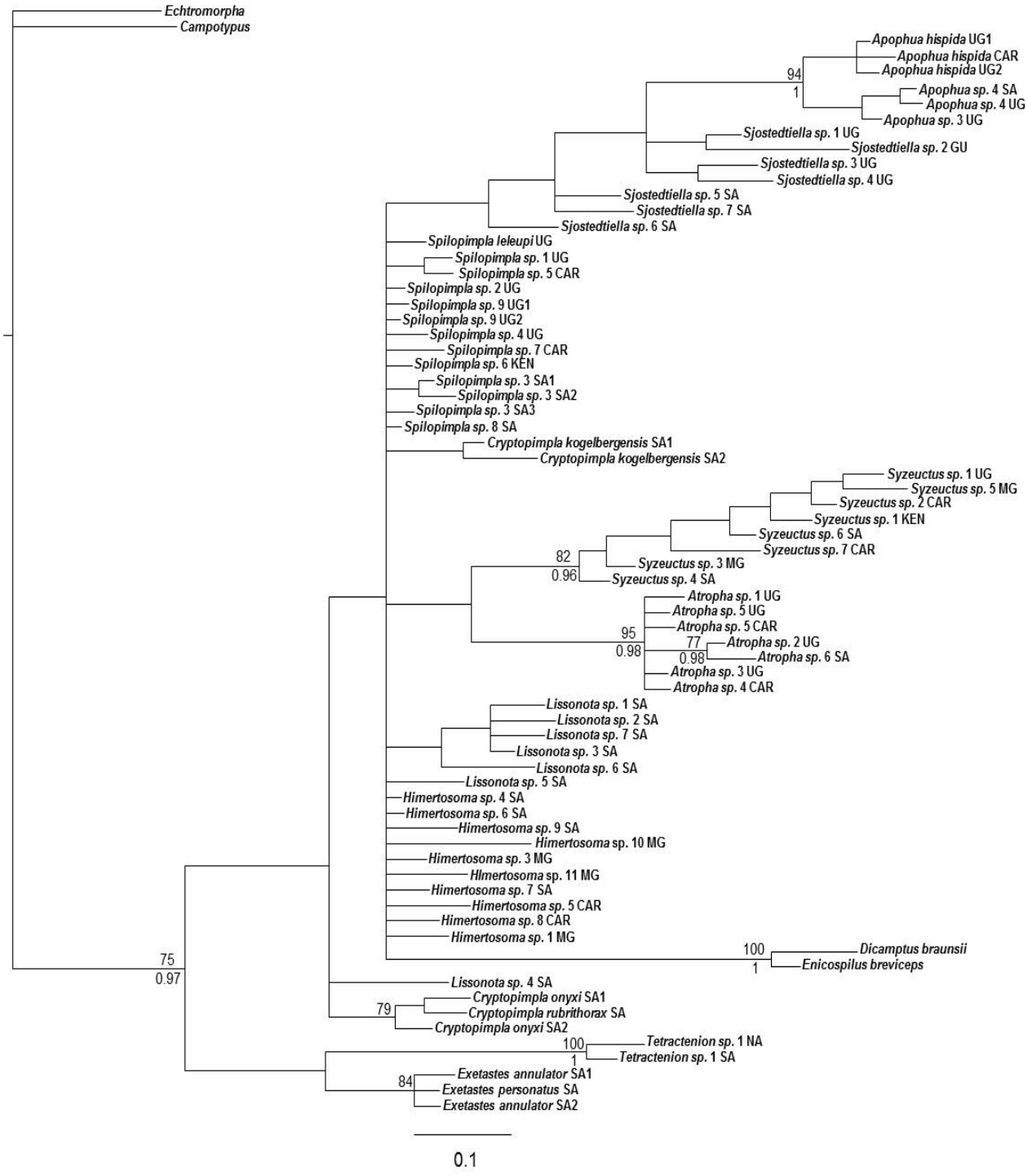

Figure 2.2: The consensus likelihood Bayesian Markov-chain Monte Carlo estimate of Banchinae within the Afrotropical region based on morphological data. Clade posterior probabilities are shown above the node, and bootstrap support of the maximum parsimony analysis shown below the node.

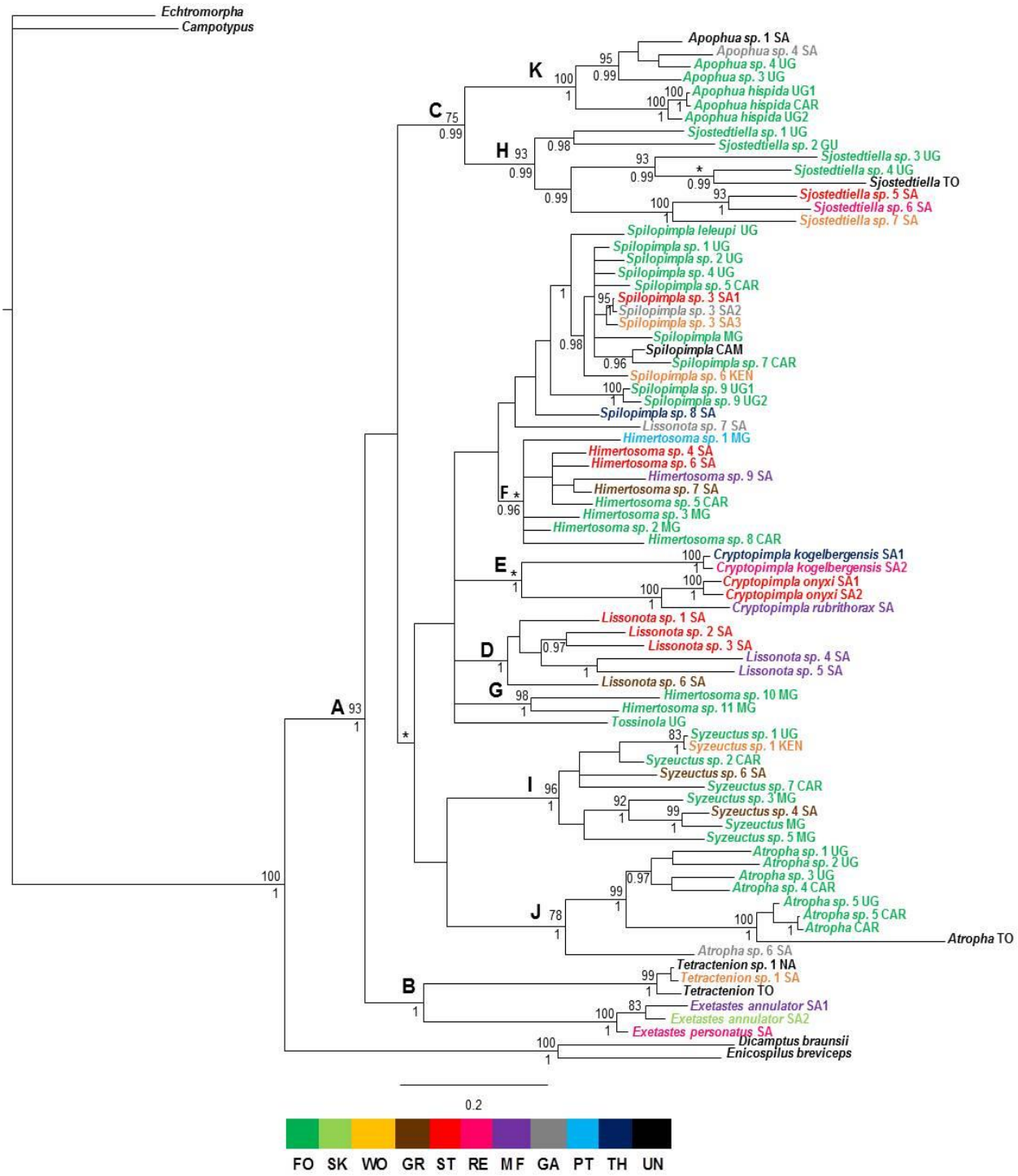

Figure 2.3: Total evidence tree for Banchinae within the Afrotropical region. Taxa are colour-coded according to vegetation type: Forest (FO), Succulent Karoo (SK), Woodland (WO), Grassland (GR), Strandveld (ST), Renosterveld (RE), Mountain Fynbos (MF), Garden (GA), Palm Trees (PT), and Thicket (TH), vegetation data missing and marked as Unknown (UN).

For the genus *Sjostedtiella*, the two more basal clades contain species sampled from savanna (although no vegetation data was available on GenBank, Togo is a West African country where savanna is dominant) and forest in West and Central Africa, respectively (Fig. 2.3). The more divergent South African clade consisted of species sampled from the Cape Floristic Region (Strandveld and Renosterveld) and Savanna Biome (Fig. 2.3).

Within the genus *Atropha*, all species collected from West and Central African countries group in a clade, while the only *Atropha* species collected from South Africa is placed outside of this main clade (Fig. 2.1). The long-branch length found for the *Atropha* specimen collected from Togo is indicative of an accumulation of nucleotide substitutions per site that exist between *Atropha* TO and its closest represented relative within the clade (Figs. 2.1, 2.4). This species is the only representative from the West Africa, while the remaining *Atropha* species in that clade were sampled from Central Africa. The long branch length is thus caused, not by a 70 bp gap in the sequence, but as a result of deficiency of closely related taxa from West Africa (Rannala et al. 1998).

Interestingly, for *Apophua*, *Syzeuctus* and *Atropha*, despite extensive sampling efforts in the temperate areas of southern Africa (van Noort 2018), the majority of taxa were collected from tropical savanna or forested regions (Fig. 2.3). Similarly, despite sampling effort also conducted north of southern Africa in tropical areas of central and eastern Africa, *Lissonota* and *Cryptopimpla* were only ever collected from South Africa (Fig. 2.3), supporting relative affinities of these genera to specific biogeographical areas defined by habitat and climate.

2.3.4 Banchinae on a global scale

With the inclusion of members of the *Banchus* group and members of the *Exetastes* group found outside of the Afrotropical region, the bayesian analysis showed that, with the exception of *Agathilla bradleyi* and *Banchus* CA, the remaining taxa representing the *Banchus* group formed a clade together with the Ophioninae representatives (outgroup) outside of the Banchinae clade, but with weak support (Fig. 2.4). In Quicke et al. (2009), the position of *Agathilla bradleyi* was always associated basal to the *Banchus* group, which they attributed to be in agreement with its lack of

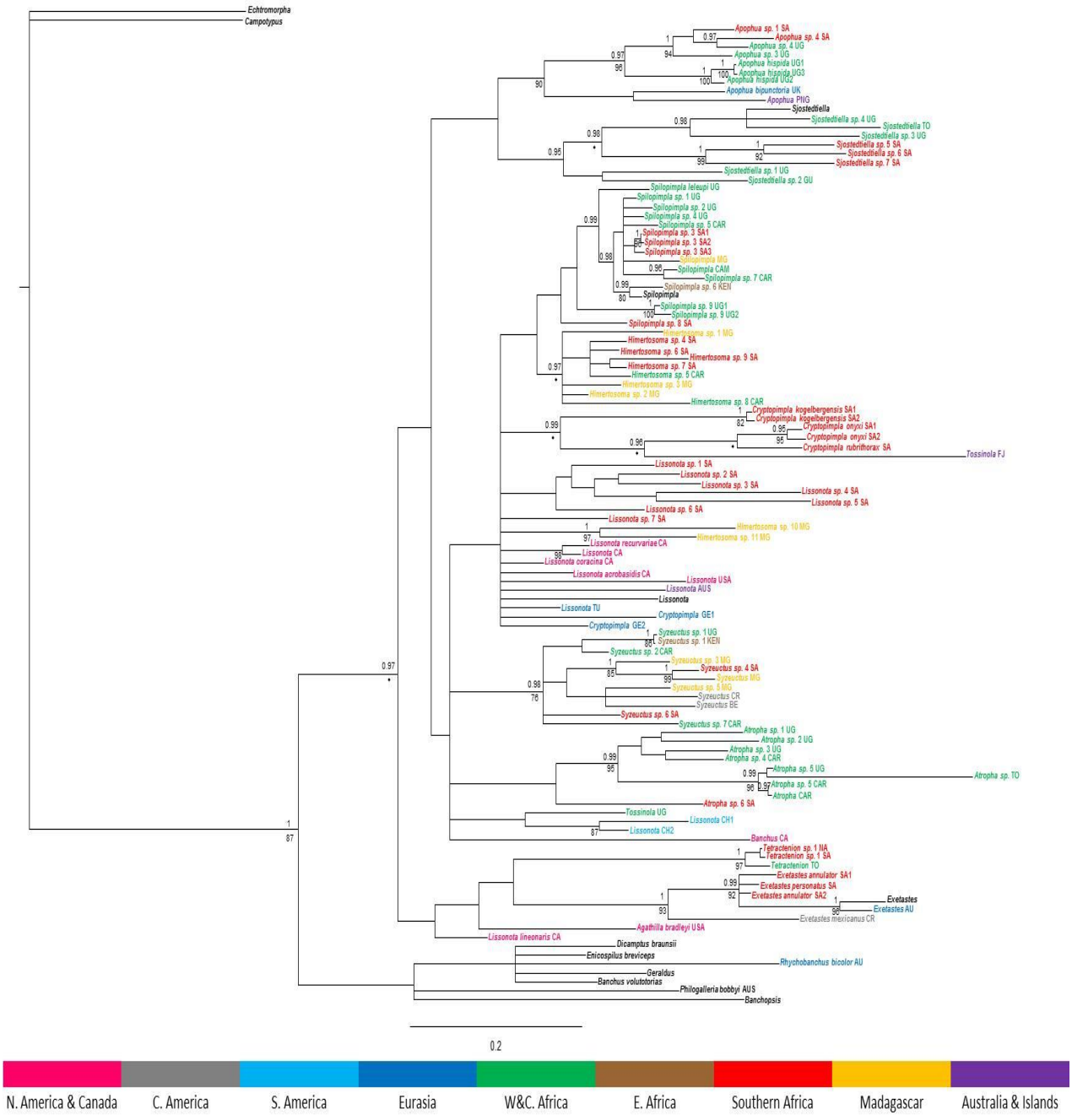

Figure 2.4: The consensus likelihood Bayesian Markov-chain Monte Carlo estimate of Banchinae found globally based on the combined data analysis of COI mtDNA, 28S and 18S rDNA, and morphological data. Clade posterior probabilities are shown above the node, bootstrap support of the maximum parsimony (MP) analysis are shown below the node, and an asterix is indicated where nodes were not congruent with the MP analysis. Taxa are colour coded according to their location.

larval synapomorphies. However, in this study the species is positioned basal to the *Exetastes* group as proposed by Wahl (1985). *Cryptopimpla* appears to be paraphyletic with the position of two species from Germany unresolved within the tribe Atrophini (Fig. 2.4). Similarly, with two species represented, *Tossinola* appears to be paraphyletic and interestingly the *Tossinola* species from Fiji groups with the *Cryptopimpla* clade from South Africa with strong support (pp = 0.96, Fig. 2.4).

The addition of *Lissonota* species from America, Turkey and Australia clearly reveals that the genus is paraphyletic (Fig. 2.4). *Syzeuctus* (pp = 0.98, bs = 76) and *Apophua* (bs = 90) remain monophyletic with robust support (Fig. 2.4).

Two clades make up the genus *Apophua*, the first well supported clade containing species sampled in Africa and the other containing species sampled from Europe and Australasia with weak support (Fig. 2.4). Within the well supported clade that makes up the genus *Exetastes*, one clade contains species sampled from South Africa, and the other clade contains species from Europe and Central America (Fig. 2.4).

2.3.5 Divergence time estimations using fossil calibrations

The divergence tree (Fig. 2.5) is largely in concordance with the total evidence tree (Fig. 2.1), except where it groups *Lissonota* with *Tossinola* and *Cryptopimpla* with *Himertosoma* species from Madagascar. The position of these genera was not resolved in the total evidence tree, while BEAST forces the creation of a completely bifurcating tree. Therefore, the clustering of these genera in the divergence tree is most likely a mis-representation of the evolution of these clades. Furthermore, the divergence tree suggests monophyly for the genus *Lissonota*, which the total evidence tree rejects (Fig. 2.1). The ages of nodes that are well-supported in the total evidence tree are shown together with 95% confidence intervals (CI) in Figure 2.5.

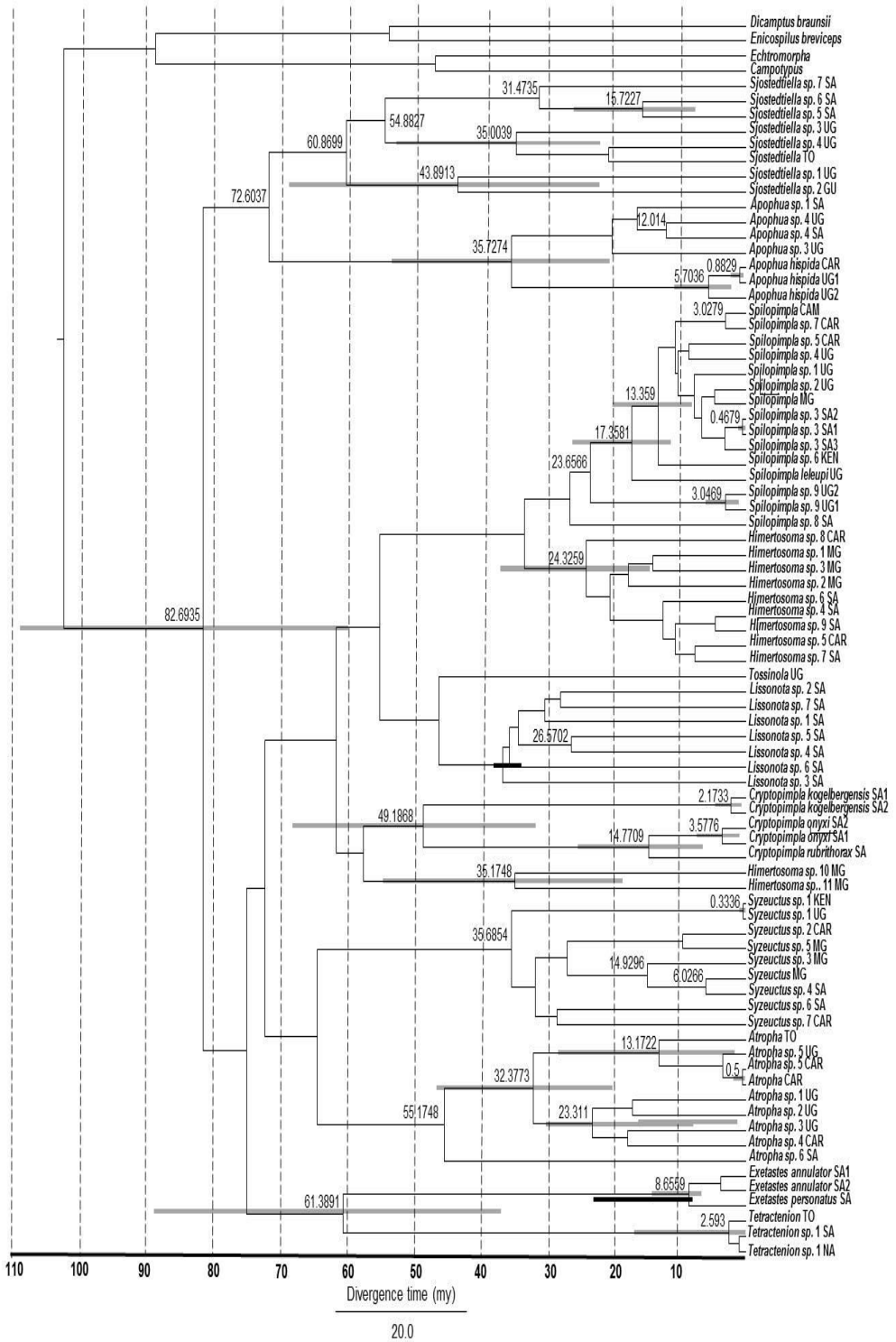

Figure 2.5: Divergence estimation of the subfamily Banchinae. Ages are indicated for nodes that are well-supported in the total evidence tree. HPD 95% confidence intervals and fossil age estimates are indicated using grey and black bars, respectively.

2.4 Discussion

2.4.1 The validity of the tribe Banchini

The combined data phylogenetic representation for Banchinae within the Afrotropical region supports the hypothesis that the tribes of the subfamily are monophyletic, albeit that the tribe Atrophini is only weakly supported (Fig. 2.3). However, this needs to be treated with some caution as the tribe Banchini is only represented by the *Exetastes* group within the Afrotropical region. With the inclusion of the *Banchus* group in a global phylogenetic representation of the subfamily, the tribe is found to be paraphyletic (Fig 2.4). All members of the *Banchus* group (with the exception of *Agathilla bradleyi*) grouped with outgroup members of the subfamily Ophioninae with weak support (Fig. 2.4). In addition to having very short ovipositors, the tribe Banchini differs from the other tribes by having eight or more sensilla on the larval prelabium (Quicke 2015). However, it does not explain the placement of the *Exetastes* group within the subfamily Banchinae. Though it has been clearly demonstrated by Wahl (1988) and Quicke et al. (2009) that the *Exetastes* group belongs within the tribe Banchini, our data suggests otherwise. In addition to the considerable sequence length variation of the 28S nuclear gene that was found to be present among the genera belonging to the *Banchus* group, the morphological character state, presence of tridentate mandibles, is found only within the *Banchus* group, while all other Banchinae including the *Exetastes* group have bidentate mandibles (Quicke et al. 2009). One reason for the lack of monophyletic support for the tribe Banchini may be due to missing data. Only 28S rDNA data was available on GenBank for the *Banchus* group and no supplementary data was available for the COI and 18S genes. In addition, the present study used at least 37 discrete adult morphological characters that appeared to be informative for genera within the subfamily Banchinae from the Quicke et al. 2009 study, and did not make use of all the available morphological data (for e.g. larval morphology) that have contributed to the monophyletic status of the tribe. Results suggest that the tribe Banchini, namely the *Exetastes* group, is the most derived of the three tribes (Fig. 2.5). This tribe is only represented by two genera (three species in total, Table 2.1), and Banchini as a whole does not appear to be monophyletic, so the time since divergence is based solely on the

Exetastes group. The species within the *Exetastes* group differ from members of the tribes Glyptini and Atrophini by having very short ovipositors, whereas members of the other tribes typically have ovipositors about as long as or longer than the metasoma. They attack caterpillars, reliable records all being associated with Noctuidae (nocturnal moths, Fitton 1985, 1987) while Glyptini and Atrophini attack semi-concealed hosts such as leaf rollers (Momoi et al. 1975, Quicke 2015). Therefore their morphological adaptations and host preference does appear to be derived, in support of the relatively young age of the group (Fig. 2.5).

Divergence estimation suggests the tribe Glyptini to be the oldest of three tribes (Fig. 2.5). Glyptini share similar modifications on the metasoma with some Pimplinae and *Lycorina* Holmgren, in that taxa within Glyptini typically possess triangular areas on tergites 2-4, delimited by paired, lateromedian grooves. Though, the precise pattern of grooves differs in the former taxa. Given that Pimplinae is a distantly related subfamily to Banchinae, the similarity of these structures is likely to be the result of analogous structures that appear similar as a result of convergence. This morphological character has been lost in the more derived banchine tribes.

Phylogenetic interpretation enables the determination of which genera are older (plesiomorphic) and which genera are more derived. Morphology can either weaken or strengthen the phylogenetic signal, depending on the morphological characters that are used, i.e. shared derived characters (synapomorphies) strengthen the phylogenetic signal, and plesiomorphies drown out the phylogenetic signal (Kamilar & Cooper 2013). Therefore, the key to obtaining a robust morphological phylogenetic tree is to use as many synapomorphies as possible. However, a plesiomorphic character inherited from a common ancestor can appear anywhere in a phylogenetic tree as the morphological character can be expressed in any/many species, even across genera, and as a result cannot reveal anything about the relationships among the taxa concerned (McLennan 2010). In the morphological phylogeny (Fig 2.2), a number of genera were retrieved as polyphyletic clades including *Spilopimpla* and *Himertosoma*, and this phylogenetic signal was also reflected in the combined analysis (Fig. 2.1). This is probably as a result of symplesiomorphies (21/67) that members within each genus share (Table 2.3). Some of

these symplesiomorphies include: a complete occipital carina with the intersection of the occipital and hypostomal carinae distant from the mandibular base; a short propodeum with a narrow, shallow, anterior trough and the spiracle medially positioned; and a metasoma that is dorsally-ventrally flattened with the basal half of the first metasomal tergite (spiracle positioned anterior to middle) stout, with glymma present (Quicke et al. 2009). Another interesting observation, based on the morphological phylogeny alone, is the placement of the outgroup members of the subfamily Ophioninae within the subfamily Banchinae (Table 2.2). It has already been mentioned that Ophioninae and Banchinae are members of the Ophioniformes with a number of synapomorphies that both subfamilies share (Pampel 1913, Wahl 1991, 1993). The ophionine clade is retrieved as a highly derived banchine clade, but the grouping is likely to be the result of long-branch attraction (Fig. 2.2). The absence of glymma on the first metasomal tergite is noted in both ophionine genera. Based on deviation from the plesiomorphic condition, they are the only genera represented in the morphological matrix that has a slender metasomal tergite 1 with the spiracle positioned at or behind the middle (Table 2.3). Taking total evidence into account, the two genera are not closely-related (Fig. 2.1). Therefore, the long-branch attraction observed in the morphological phylogeny is probably due to convergence of these character states. These results highlight the importance of using genetic data in phylogenetic representation, but it is also important to include morphological data to help explain the observed patterns of convergence.

2.4.2 Linking the combined phylogeny with morphology

At the generic level, this study reveals evolutionary patterns that emphasize the need for taxonomic revision. Most notably, the observations made here reside solely within the largest tribe Atrophini, for which there is weak monophyletic support (Fig. 2.3).

Total evidence suggests a close evolutionary relationship between the genera *Syzeuctus* and *Atropha*. The well supported monophyletic *Syzeuctus* and *Atropha* clades form a combined clade with weak support (Fig. 2.1). This may be due to the inclusion of insufficient taxa to resolve the deeper nodes in the phylogeny. These genera share morphological similarity in that both clades have the presence of a stalked triangular-

shaped areolet through anterior fusion of 2rs-m and 3rs-m (Quicke et al. 2009, Table 2.3), a character state not found in any of the other Afrotropical banchine genera. In addition, both genera are strongly associated with forest regions (Fig. 2.3). *Atropha* is endemic to the Afrotropical region while *Syzeuctus* has a world-wide distribution (Yu et al. 2018). Globally, *Syzeuctus* species occur in tropical or subtropical areas, while the remaining species in this genus seem adapted to relatively dry habitats (Townes 1969). Divergence estimation suggests that the *Atropha* lineage (~55 my, 8-30 my 95% CI) is older than the *Syzeuctus* lineage (~36 my, without 95% CI, Fig. 2.5). Among the several morphological characters that distinguish the two, the most apparent difference is the presence of an arched posterior transverse carina on the propodeum (including pleural carinae) in *Syzeuctus*, as is found in most Banchinae (Wahl and Sharkey 1993), and the complete lack of propodeal carinae in *Atropha* (Townes 1969, Chapter 4). It is more likely that a gradual loss of a character will occur through the evolutionary diversification process, especially if the character is common within the subfamily (plesiomorphic condition), as opposed to complete loss and thereafter evolution of the same character again, i.e. reversal (Cronk 2009). Gauld and Wahl (2000b) listed the presence of propodeal carina in the evolution of the ichneumonid subfamily Labeninae as ancestral if complete and derived if absent. Similarly, complete carination in the genus *Apophua*, within the tribe Glyptini (shown to represent the oldest tribe, Fig. 2.5) represents the ancestral state of that morphological character. It is suggested that the common ancestor of *Atropha* and *Syzeuctus* genera possessed this triangular-shaped areolet and, post-K/T event (~65 mya) given the divergence estimates of these two genera, radiated through the (1) restriction and diversification within the forest regions of the Afrotropical region (*Atropha*) and (2) increase in distribution range and adaptability to different habitats (*Syzeuctus*).

Phylogenetic analyses reveal two clades within the genus *Cryptopimpla*, namely one representing *Cryptopimpla kogelbergensis* and another containing *Cryptopimpla onyxi* and *Cryptopimpla rubrithorax* (Fig. 2.1). This is not surprising as *C. kogelbergensis* is morphologically distinct from the latter group. *Cryptopimpla kogelbergensis* possesses a posterior transverse carina on the propodeum and a bulbous clypeus while in the latter group the posterior transverse carina is absent and the clypeus is slightly concave (see also Chapter 3). There are several genera that do not form

monophyletic lineages based on the combined data analyses. In the global phylogeny (Fig. 2.4) a *Tossinola* species from Fiji groups within the *Cryptopimpla* genus. This may be as a result of long-branch attraction as well as insufficient data (only a 432bp fragment of the 28S gene was available for the *Tossinola* Fiji species to be added to the data set). While both *Cryptopimpla* and *Tossinola* are relatively small genera, there is no morphological evidence to suggest that they are closely-related. In addition, without morphological data, it is unclear why the position of two *Cryptopimpla* species from Germany (sequences obtained from GenBank) was found to be unresolved within the tribe Atrophini (Fig. 2.4).

Within the genus *Himertosoma*, the two Madagascan species *Himertosoma* sp. 10 MG and *Himertosoma* sp. 11 MG form a monophyletic clade within the tribe Atrophini, with strong support (pp = 1, bs = 98, Fig. 2.1). However, the morphological phylogeny suggests that these two species are morphologically divergent from each other (Fig. 2.2). A critical morphological assessment revealed that, apart from the plesiomorphic characters the two species share which are typical of *Himertosoma*, there were some morphological differences that were not typical of the genus. In addition, no true shared derived (synapomorphic) character was found (Table 2.3). The relative phylogenetic position of this clade, representing these two Madagascan species, was unresolved (Fig. 2.1). Therefore, the possibility that these two species represent a new genus endemic to Madagascar can be dismissed. The slightly longer upper tooth of the mandible is a character both species share, but one that is not unique as it is found in other members of the Banchinae. For instance, the banchine genera *Cryptopimpla* and *Alloplasta* also possess this character (Townes 1969, Khalaim & Ruíz-Cancino 2008). In addition, although *Himertosoma* species typically have equally sized mandibular teeth (Townes 1969), *H. kuslitzkii* from Japan has been described as having a lower tooth slightly shorter than the upper tooth (Watanabe & Maeto 2012). Especially since the length of the upper tooth is only slightly longer, this character state is not strong enough to distinguish these two species from the generic delimitation of *Himertosoma*. *Himertosoma* is also characterized by having longitudinal striae on the first tergite (Townes 1969, Chandra & Gupta 1977). However, *Himertosoma* sp. 3, which was sampled from Madagascar, did not possess striation on the metasomal tergite 1 and grouped inside the main

Himertosoma clade with strong support (Fig. 2.1). This suggests that although it may be true for most *Himertosoma* species, there are exceptions, and this additional character state needs to be added to the diagnoses of the genus, broadening the generic concept. Similarly the species from Madagascar that grouped outside of the main *Himertosoma* clade do not possess longitudinal striae on the metasomal tergite 1. The single defining character that separates the genus *Himertosoma* from the morphologically most similar genus *Lissonota* is the absence of a crease separating the laterotergite of the fifth metasomal tergite (Watanabe & Maeto 2012). Given that this is the single main character that separates *Himertosoma* from *Lissonota*, including the absence of the areolet in *Himertosoma* compared to the areolet sometimes lacking in *Lissonota* (Townes & Townes 1973), this then questions the validity of the two genera as some *Himertosoma* species also have the crease present. The crease separating the laterotergite of the fifth metasomal tergite is absent in *Himertosoma* sp. 10 MG, whereas the crease is present in *Himertosoma* sp. 11 MG. This additional evidence presented here supports the current uncertainty regarding delimitation of *Lissonota* and *Himertosoma* (Watanabe & Maeto 2012) that their generic status does need to be reassessed. *Himertosoma* sp. 3, 10 and 11 were all sampled from Madagascar. Though it may be premature to assume that the absence of longitudinal striae on the metasomal tergite 1 is a derived character state, this condition appears to be characteristic of Malagasy *Himertosoma* species and may have evolved subsequently to the 160 my isolation of the island from mainland Africa. However, *Himertosoma* is a relatively large genus with highest species richness in the Afrotropical region and only four species known from the Palaearctic and Oriental regions (Watanabe & Maeto 2012). Based on genetic evidence, the sequence divergence of the mitochondrial COI gene between *Himertosoma* sp. 10 MG and *Himertosoma* sp. 11 MG was ~15.2%. When compared with the remaining *Himertosoma* species included in the study (which formed a single clade), the sequence divergences were similar, ranging from ~13.9-15.8%. For the 28S gene tree, the two species had a sequence divergence of ~1.3%, and had higher sequence divergences (~4.1-5.5%) when compared to the remaining *Himertosoma* species. Therefore, the possibility that these two species represent a new genus endemic to Madagascar is unlikely, but cannot be dismissed. The current evidence, in addition to the lack of a true synapomorphy, suggests that

Himertosoma sp. 10 MG and *Himertosoma* sp. 11 MG, although genetically divergent, are for now better placed within the genus *Himertosoma*. Their inclusion does, however, render *Himertosoma* a paraphyletic group, but analyses of further taxa and resolution at the deeper nodes is required to achieve a robustly supported decision on the affinities of the species within this genus.

Lissonota was also found to be paraphyletic (Figs. 2.1, 2.4). The genus is described as having the presence or absence of an areolet on the fore-wing, whereas all other Afrotropical banchine genera are described as having one or the other. These character states are, among others, used to delimit the genus from other banchine genera (Townes 1969, Townes & Townes 1973). Assessment of these character states present in *Lissonota* species showed that a single specimen could have the areolet closed on one wing and open on another. The areolet in this genus is characteristically very small (Townes 1969) and when very reduced it is indistinct and appears to be absent, risking misinterpretation of the character state. *Lissonota* sp. 7 SA was recovered as basal to the monophyletic genus *Spilopimpla* (Fig. 2.1) but this species possesses an areolet hence this character state does not explain its placement with the *Spilopimpla* clade (Fig. 2.1). Its placement between the *Spilopimpla* and *Himertosoma* clades (both genera lack an areolet) is more likely as a result of insufficient morphological and molecular data (only represented by a 843bp fragment of COI mtDNA) to correctly place *Lissonota* sp. 7 SA within its respective clade (Fig. 2.1). Based on morphological data, this species groups with and thus morphologically more closely resembles *Lissonota* sp. 1, 2, and 3 than any other species in the phylogeny (Fig. 2.2). BEAST analysis suggests monophyly for *Lissonota* (including *Lissonota* sp. 7 SA, Fig. 2.5). However, this result needs to be treated with circumspection since divergence trees in BEAST are strictly bifurcating and thus do not indicate polyphyly if present. By comparing the Afrotropical *Lissonota* with global *Lissonota* species (Fig. 2.4), paraphyly within the genus becomes more apparent. This is not surprising given the uncertainty on the validity and circumscription of the genus. The range of morphological diversity among species within this very large cosmopolitan genus has historically led to the proposal of a number of generic names for various species groups (Broad, pers. comm., Townes 1969, Watanabe & Maeto 2012, Yu et al. 2018).

2.4.3 Historical biogeography

The divergence estimate of Banchinae in the Afrotropical region of ~82 mya (60-109 my 95% CI, Fig. 2.5) implies that the subfamily is a relatively recently evolved lineage within the Ichneumonidae, whose earliest fossil records date from the lowermost Early Cretaceous ~133-145 mya (Kopylov 2011). The specialized life-history of Banchinae also provides some support for this estimate. Banchines are koinobionts and these species lay their eggs inside their host. Hence, banchines would have needed to evolve physiological adaptations in order to tolerate the host's immunological and chemical defenses, whereas the generalist life-history strategy of idiobionts allows wasps to bypass the defenses of the host by paralyzing it (Santos & Quicke 2011). It is for this reason that idiobiont parasitoids are regarded as the hypothesized ancestral condition, which is displayed by various basal ichneumonids, whereas the koinobiont life-history strategy evolved later in the evolution of the family (Gauld 1988). Very few Cretaceous ichneumonids can be assigned to modern subfamilies (Santos 2017). Divergence estimation suggests that Banchinae in the Afrotropical region originated during the Late Cretaceous (Fig. 2.5) preceding the age of the oldest known Banchinae fossil by at least 30 million years (Khalaim 2011). This is not surprising as the fossil is that of the extant genus *Lissonota,* which is a more derived genus within the subfamily (Fig. 2.5). While there is at present no fossil evidence for Banchinae in Africa, there are other ichneumonid fossils (*Labenopimpla* Kopylov and *Rugopimpla* Kopylov) recorded from Botswana, representing the extinct subfamily Labenopimplinae, which also date back to the Late Cretaceous (Kopylov et al. 2010). Labenopimplinae are also known from the Russian Far East (Kopylov 2010). The divergence estimation for Banchinae, including the 95% confidence interval, does seem to suggest that the Gondwanan separation of Southern America from Africa played a role in shaping the evolution of the subfamily. In addition, all splits between genera are estimated at less than 62 my, which post-dates major continental divergence events (Fig. 2.5, Sanmartín & Ronquist 2004, Kopylov et al. 2010). Nonetheless, inferences on the origin of banchine diversity are impeded by the lack of divergence estimates of banchine genera elsewhere in the world, including the fact that the fossil record of the subfamily is limited to an extant genus (Khalaim 2011).

The tribe Glyptini (represented by *Apophua* and *Sjostedtiella*) is hypothesized to be the oldest of the three tribes, diverging ~72 mya (without 95% CI, Fig. 2.5) This is in support of the hypothesis that characters within this tribe probably represent the groundplan state for the subfamily, whereas the Atrophini possess the derived state of having a reduced hypostoma (Quicke 2015). While monophyly was established for the tribe within the Afrotropical region, supporting results by Quicke et al. (2009), no genetic data was available on GenBank to determine whether the Glyptini is paraphyletic based on the descriptions of a new genus of Glyptini in the Neotropical region (Broad et al. 2011). The monophyly of Atrophini was not well-supported and as a result the time since divergence will not be discussed, but the BEAST analysis does seem to suggest that the tribe Banchini, specifically the *Exetastes* group, is the more derived of the three tribes with a divergence of ~61 my (43-89 my 95% CI). Moreover, divergence estimation suggests that the *Exetastes* group and the majority of Afrotropical banchine genera originated during the mid Paleocene-late Eocene (Fig. 2.5) which is comparable with other parasitoid wasp subfamilies. For example, the braconid subfamilies Doryctinae and Rogadinae are suggested to have originated during the early Paleocene-late Eocene and mid-late Eocene, respectively (Zaldívar-Riverón et al. 2008a, b).

It is noteworthy that the results presented here suggest *Sjostedtiella* to be the oldest represented banchine genus in the Afrotropical region as it is endemic to the region, while Afrotropical representatives of the cosmopolitan genus *Syzeuctus* have a much younger divergence estimation (Fig. 2.5). The cosmopolitan distribution of a group implies that either diversification took place before the occurrence of past vicariance events or that rampant dispersal has taken place (Santos 2017). The global distribution of *Syzeuctus*, coupled with a recent divergence estimation (~36 my, without 95% CI), relative to other representatives of banchine genera within the Afrotropical region (Fig. 2.5), implies that dispersal has led to the current distribution patterns because divergence took place long after the major continents split apart, and after the mass extinction (K/T event) of approximately three-quarters of the faunal and floral species on earth (Sanmartín & Ronquist 2004, Renne et al. 2013, Longrich et al. 2011, Rehan et al. 2013, Nichols & Johnson 2008, Yu et al. 2018).

The divergence estimate of both the *Exetastes* group and the genus *Sjostedtiella* (~61 mya without 95% CI) suggest that the K/T event allowed for the diversification of these lineages, as has been found for other hymenopteran and lepidopteran subfamilies (Wahlberg 2006, Zaldívar-Riverón 2008a). The endemicity of *Sjostedtiella* and *Atropha* implies that these genera diversified after this vicariance event followed by restriction to the Afrotropical region, with no subsequent dispersal events. *Sachtlebenia* and *Townesion* are restricted to Eastern Asia and share morphological characters with *Sjostedtiella* (Broad 2014). These genera were proposed by Kasparyan (1993) to comprise a separate subfamily Townesioninae. However, Gauld and Wahl (2000a) proposed that these genera comprised a highly apomorphic lineage of the tribe Glyptini. The inclusion of *Townesion* in a phylogenetic study failed to recover the taxon within the Banchinae where only a single gene was sequenced and did not support the hypothesis of a close relationship between Townesioninae and *Sjostedtiella* (Quicke et al. 2009). Nevertheless, the morphological similarity between Townesioninae and the oldest Afrotropical banchine genus *Sjostedtiella* might suggest a non-African origin, but a more robust molecular phylogenetic analysis is needed to support the placement of Townesioninae within Banchinae.

The species *Apophua* sp.4 was collected from both Uganda and South Africa (Table 2.1, Fig. 2.1). The Kwazulu-Natal locality in which the species was collected in South Africa is situated in the eastern subtropical region of the country. No habitat data is available for this specimen as it was collected from a garden, but the locality falls with the Savanna Biome that extends up to East Africa (Mucina & Rutherford 2006). The mesic component of the Savanna Biome extends from Kwazulu-Natal up the eastern side of Africa to East Africa and a large proportion of this geographical area share floral and faunal affinities (Mucina & Rutherford 2006). Therefore, there is some evidence to suggest a connectedness between subtropical southern Africa and East Africa.

The biogeographical connectedness of West Africa with Central Africa is supported with the grouping of *Spilopimpla* CAM with *Spilopimpla* sp. 7 CAR with strong support (pp = 0.96, Fig. 2.1). The current distribution of *Apophua* sp. 4 and phylogenetic evidence (pp = 0.99) provide some support for a close relatedness between the tropical taxa from Central and East Africa (Fig. 2.1). Similarly, within the genus

Syzeuctus, species sampled from Uganda, Kenya and the eastern subtropical region of South Africa formed a single clade, though the clade was not well supported (Fig. 2.1). This also provides some evidence for the connectedness between tropical (Central and East) and southern African taxa. *Syzeuctus* sp. 1 was sampled from both Uganda and Kenya, which are geographically adjacent to each other from different vegetation types (forest vs. savanna, Fig. 2.4). The Indian Ocean Coastal Belt exists as fragmented patches of forests that are relatively young in origin compared to the Afromontane forests that occur inland in West Africa, hypothesized to represent ancient habitats (White 1981). The current fragmented distribution of these coastal forests was driven by the Last Glacial Maximum (Lawes 1990). Studies have indeed shown that there have been multiple expansions and contractions of forests and savannas in the past that would have facilitated range expansions of species across the two habitats (Couvreur et al. 2008, Lorenzen et al. 2012).

The two *Himertosoma* species that were found in Madagascar diverged ~35 mya (19-55 my 95% CI). The age of the clade supports its endemicity to Madagascar, as the island is suggested to have been isolated from continental Africa for the last 160 my (Yoder & Nowak 2006). The only evidence that may suggest a close relatedness between Malagasy taxa and East African taxa is the grouping of a single species sampled from the Eastern Cape of South Africa with other Malagasy species in a single clade within the genus *Syzeuctus* (Fig. 2.1). Divergence estimation (Fig. 2.5) shows that *Syzeuctus* MG and *Syzeuctus* sp. 4 SA shared a common ancestor ~6 mya (without 95% CI); and *Syzeuctus* MG, *Syzeuctus* sp. 4 SA and *Syzeuctus* sp. 3 MG shared a common ancestor ~15 mya (without 95% CI). It has been suggested that the close proximity of Madagascar with the East coast of Africa allowed faunal interchange for approximately 20 million years (Yoder & Nowak 2006), and these divergence times seem to be in alignment with that suggestion. Similarly, the only evidence that may suggest that the forest taxa are amongst the older taxa within Banchinae in the Afrotropical region is found within the genus *Sjostedtiella* (a genus endemic to the region) with divergence estimation supporting that it is the oldest banchine genus in the region (Figs. 2.3, 2.5). Although *Sjostedtiella* is the oldest genus within the Afrotropical region, it occurs in a variety of habitats with the two clades associated with forest being more basal (Fig. 2.3). In

addition, some genera are more speciose and are strongly associated with forest regions (*Apophua*, *Syzeuctus* and *Atropha*, Fig. 2.3).

The Banchinae collection at the Iziko South Africa Museum is largely the result of recent collecting events over the last 28 years. Bearing in mind that no species richness analyses was conducted, an assessment of the collection suggests that the subfamily is mostly confined to the wetter tropical habitat of Central Africa (Fig. 2.3). This in contrast to the dogma that ichneumonid species richness is hypothesized to be highest in the temperate regions rather than in the tropics; although there is increasing evidence that this latitudinal gradient is simply an artifact of under sampling in the tropics (Veijalainen et al. 2012a, b, Hopkins et al. 2018). There is also evidence to suggest, particularly for the genus *Sjostedtiella*, that the older clades are most strongly represented in forested regions (Fig. 2.3). During the early Eocene Africa was dominated by tropical rainforests (Burgess et al. 1998, Jacobs 2004). *Apophua, Syzeuctus* and *Atropha* species that have been collected in forests have divergence estimates dating to the late Eocene (Fig. 2.5). The opposite pattern is seen in the genera *Cryptopimpla* and *Lissonota* which were only ever collected from South Africa. While the clustering of *Lissonota* as monophyletic in the divergence tree is most likely a mis-interpretation of the evolution of the clade, *Cryptopimpla* dates back to the early Eocene (Figs. 2.1, 2.5). Although *Cryptopimpla* has a worldwide distribution the greatest species richness within the genus is found in the temperate regions (Sheng & Zheng 2005, Kuslitzky 2007, Yu et al. 2018). *Lissonota* is a very large genus which is best represented in the Holarctic region (non-tropical parts of Europe, Asia, Africa (north of the Sahara), and America (south to the Mexican desert region); Townes 1969, Yu et al. 2018). This genus has been noted to be species-rich in the northern temperate regions (e.g. Aubert 1978). Despite an almost worldwide distribution (Yu et. al. 2018), within the Afrotropical region, the prevalence of *Lissonota* in South Africa and exclusion from the forested regions, with the exception of one species in the Democratic Republic of Congo (Lowland forest), does seem to suggest it's a genus associated with temperate habitats (Fig. 2.3).

2.5 Concluding remarks

Based on the Afrotropical banchine genera represented in this study, each of the three tribes form separate clades, with monophyly well-supported for Glyptini and Banchini. Within the Afrotropical region, Banchini is only represented by the *Exetastes* group. By including the *Banchus* group in the global phylogeny, the validity of the Banchini tribe is questionable as the *Exetastes* group and *Agathilla bradleyi* (*Banchus* group) is placed within Banchinae and the remaining representatives of the *Banchus* group are positioned outside of the subfamily. Not only do these results suggest paraphyly within the *Banchus* group, which shows strong morphological (tridentate mandibles) and molecular differentiation (particularly 28S rRNA sequence length variation) with the remaining representatives of the subfamily, but it also warrants a revision of the Banchini tribe. There is some evidence to suggest a connection between Central Africa and eastern regions of South Africa, with the discovery of the same *Apophua* species in both Uganda and eastern regions of South Africa. Species within this genus sampled from Uganda and eastern region of South Africa formed a single clade, which is well supported. Similarly, within the genus *Syzeuctus*, species sampled from Uganda, Kenya and the eastern subtropical region of South Africa formed a single clade, though the clade was not well supported. The only evidence that may suggest a close relatedness between Malagasy taxa and East Africa taxa is the grouping of a single species sampled from the Eastern Cape of South Africa with other Malagasy species in a single clade within the genus *Syzeuctus*. While divergence times seem to be in alignment with the proposed time that dispersal could have still taken place after the island split from mainland Africa, the evidence proves to be insufficient to suggest a close relatedness between the Madagascan and East African banchine taxa. Future assessments will need to include an increased taxonomic representation, particularly from India. The temperate-associated genera, *Cryptopimpla* and *Lissonota*, were found to be older in relation to *Apophua* and *Syzeuctus*, with the majority of species of the latter genera having been collected in forested regions. There is evidence, however, to support the hypothesis that forest-associated lineages are more basally positioned as the genus *Sjostedtiella* dates back to the Paleocene and was most strongly represented in forested

regions. The dating of *Cryptopimpla* (~49 mya, 32-68 my 95% CI) does seem to refute the hypothesis that lineages found within the Cape region are more derived. This is probably owing to the worldwide distribution of this genus and not as an association with the unique Cape Floristic Region. It suggests that *Cryptopimpla* species may have been more widespread in Africa during drier epochs and subsequently retracted to the greater CFR, rather than diversifying along with the more recent species radiation (3-5 million years) of the fynbos.

Appendix 1

PCR reactions were carried out in a ABI GeneAmp 2700 thermocycler with the following conditions: (1) Standard protocol of an initial denaturation step at 94˚C for 3 min, followed by 35 cycles of denaturing at 94˚C for 30 s, annealing (for 30 s) and an extension at 72˚C for 45 s, ending with a final extension at 75˚C for 5 min; or (2) Cold-start protocol of an initial denaturation step at 95˚C for 1 min, followed by 35 cycles of denaturing at 95˚C for 1 min, annealing (for 1 min), an extension at 93˚C for 1 min, a second extension 59˚C for 1 min, a third extension at 72˚C, ending with a final extension at 75˚C for 5 min.

The Standard PCR protocol was applied for the mtDNA COI primer sets HCO2198 and LCO1490; CI-J-1718 and CI-N-2329; CI-J-1718 and H7005; and CI-J-1718 and HCO2198 at the annealing temperatures of 45˚C - 50˚C; 48˚C - 51˚C; 55˚C; and 47˚C - 48˚C respectively. The Cold-Start PCR protocol was applied for mtDNA primer sets CI-J-1718 and H7005; and L6625 and H7005 at the annealing temperatures of 45˚C - 55˚C and 56˚C - 58˚C respectively.

The Standard PCR protocol was applied with the annealing temperature set between 50˚C - 56˚C and 50˚C - 57˚C for the nDNA 18S and 28S loci respectively, and the Cold-Start PCR protocol was applied for the 28S loci at the annealing temperatures of 50˚C - 58˚C.

Chapter 3

Review of Afrotropical *Cryptopimpla* Taschenberg (Ichneumonidae: Banchinae), with description of nine new species

Reynolds Berry TV, van Noort S (2016). Review of Afrotropical *Cryptopimpla Taschenberg* (Hymenoptera, Ichneumonidae, Banchinae), with description of nine new species. Zookeys, 640, 103–137.

3.1 Introduction

The Afrotropical Banchinae is represented by 12 genera: *Apophua* Morley, *Atropha* Kriechbaumer, *Cryptopimpla* Taschenberg, *Exetastes* Gravenhorst, *Glyptopimpla* Morley, *Himertosoma* Schmiedeknecht, *Lissonota* Gravenhorst, *Sjostedtiella* Szépligeti, *Spilopimpla* Cameron, *Syzeuctus* Förster, *Tetractenion* Seyrig and *Tossinola* Viktorov (van Noort 2018, Yu et al. 2018). *Cryptopimpla* belongs to the tribe Atrophini and is a predominately northern hemisphere genus represented by 47 described species, with highest species richness in the temperate regions (Sheng & Zheng 2005, Kuslitzky 2007, Sheng 2011, Takasuka et al. 2011, Yu et al. 2018). A single South African species, *Cryptopimpla rubrithorax* Morley is known from the Afrotropical region (van Noort 2018, Yu et al. 2018). The genus *Cryptopimpla* was defined by Townes (1969) and by Chandra and Gupta (1977).

Over the last 25 years, the temperate winter rainfall region of South Africa encompassing the Cape Floral Kingdom has been fairly extensively sampled by the second author, and large numbers of ichneumonids, including new species of *Cryptopimpla*, have been collected from previously poorly sampled habitats. Sampling inventories have also been conducted in the summer rainfall region of South Africa as well as in other African countries including Central African Republic, Gabon, Kenya, Namibia, Tanzania and Uganda. However, no *Cryptopimpla* species were recorded from these surveys. To our knowledge there are no additional specimens present in historical world collections. In this chapter, we describe nine new species from South Africa and

provide interactive Lucid identification keys that are available online at www.waspweb.org (van Noort 2018).

3.2 Materials and methods

The new species were compared and analysed in the context of the Afrotropical fauna. Where possible species delimitation was assessed in a world context, but many of the descriptions of species from other regions is not comprehensive in their character assessment. These types were not examined and hence strict comparison to species from other regions was not performed, but this should not compromise the taxonomic results since almost all species of *Cryptopimpla* are exclusive of a single biogeographic region (Yu et al. 2018).

3.2.1 Photographs

Specimens were point mounted on black, acid-free cards for examination (using a Leica M205C stereomicroscope with LED light source), photography and long-term preservation. Images were acquired using either the EntoVision® multiple-focus imaging system or the Leica LAS 4.4 imaging system. The EntoVision® system comprised a Leica® M16 microscope with a JVC® KY–75U 3–CCD digital video camera attached that fed image data to a notebook computer. The program Cartograph® 5.6.0 was used to manage image acquisition using an automated Z-stepper and merging of the image series into a single in-focus image. The Leica LAS 4.4 system comprised a Leica® Z16 microscope with a Leica DFC450 Camera with a 0.63× video objective attached. Leica Application Suite V 4.4 software was installed on a desk top computer. Lighting was achieved using techniques summarized in Buffington et al. (2005), Kerr et al. (2008) and Buffington and Gates (2009). All images presented in this paper are available at www.waspweb.org (van Noort 2018).

3.2.2 Depositories

BMNH: The Natural History Museum, London, England (Gavin Broad)

SAMC: Iziko South African Museum, Cape Town, South Africa (Simon van Noort).

3.2.3 Nomenclature and abbreviations

The morphological terminology mainly follows Wahl and Sharkey (1993) and the wing venation nomenclature follows Gauld (1991). Most morphological terms are also defined on the HymAToL website (http://www.hymatol.org) and HAO website (http://portal.hymao.org/projects/32/public/ontology/). The following morphometric abbreviations are used (in order of appearance in the descriptions):

Body length: from toruli to metasomal apex (mm).
Antenna length: from base of scape to flagellar apex (mm).
Fore wing length: from anterior end of tegula to wing apex (mm).
CT (clypeal transversality index): maximum width of clypeus : length between base of tentorial pit to apex of clypeal edge.
ML (malar line index): shortest distance between eye and mandible : basal width of mandible.
IO (inter-ocellar index): shortest distance between posterior ocelli : ocellus diameter.
OO (oculo-ocellar index): shortest distance between eye and posterior ocellus : ocellus diameter.
Fl_1 (length index of flagellomere 1): length : width of flagellomere 1.
OT (ovipositor sheath-hind tibia index): length of ovipositor sheath : length of hind tibia.

The first three measurements (an absolute measure) were measured on all specimens in the type series, with measurements from the primary type reported separately in brackets if necessary.

3.3 Results

3.3.1 *Cryptopimpla* Taschenberg, 1863

Cryptopimpla Taschenberg, 1893. Zeitschrift für die Gesammten Naturwissenschaften, 21:292. Type-species *Phytodietus blandus* Gravenhorst, 1914.

Diagnosis (updated from Townes 1969, Sheng 2011 and Takasuka et al. 2011). Clypeus small, convex and may have a curved lip on the ventral margin. Occipital carina

complete; joining hypostomal carina above base of mandible. Upper tooth of mandible longer than lower tooth. Apical 0.3-0.4 of flagellum tapered to a slender apex. Pronotum without epomia. Lower half of mesopleuron weakly convex or flat. Hind edge of metanotum with projection absent to well-defined. Posterior transverse carina of propodeum present or absent; pleural carina present or absent; propodeal spiracle round or almost so. Fore wing with areolet present, anteriorly truncate or with short petiole; vein 2m-cu with two closely spaced bullae, or with a single bulla 0.5 to 1.0 times as long as the section of 2m-cu below the bulla. Hind wing with first abscissa of Cu1 weakly reclivous; distal abscissa of Cu1 meeting cu-a distinctly closer to M than to 1A. First tergum evenly and strongly tapered toward base, with a glymma, spiracle anterior to middle of tergum, surface matt to subpolished, with sparse or irregular medium-sized punctures and often some wrinkling; dorsal profile of tergum 1 moderately to strongly convex near base and weakly convex near apex; median dorsal carina absent. Apical portion of metasoma weakly to strongly compressed. Ovipositor sheath approximately 0.6 times as long as hind tibia. Ovipositor straight, sometimes upcurved, its subapical portion with a dorsal notch.

3.3.2 Species-groups

The Afrotropical species cluster in two morphological species-groups:

rubrithorax species-group (*C. elongatus*, *C. fernkloofensis*, *C. hantami*, *C. neili*, *C. onyxi*, *C. parslactis*, *C. rubrithorax* and *C. zwarti*) is defined by the presence of a weakly convex clypeus with a curved lip on the ventral margin, small tentorial pits, absence of the pleural carinae, and absence of the posterior transverse carina on the propodeum.

goci species-group (*C. goci* and *C. kogelbergensis*) is defined by the presence of a convex and bulbous clypeus with large tentorial pits, pleural carinae and distinct and well-defined posterior transverse carina on propodeum.

3.3.3 Key to Afrotropical species of the genus *Cryptopimpla*

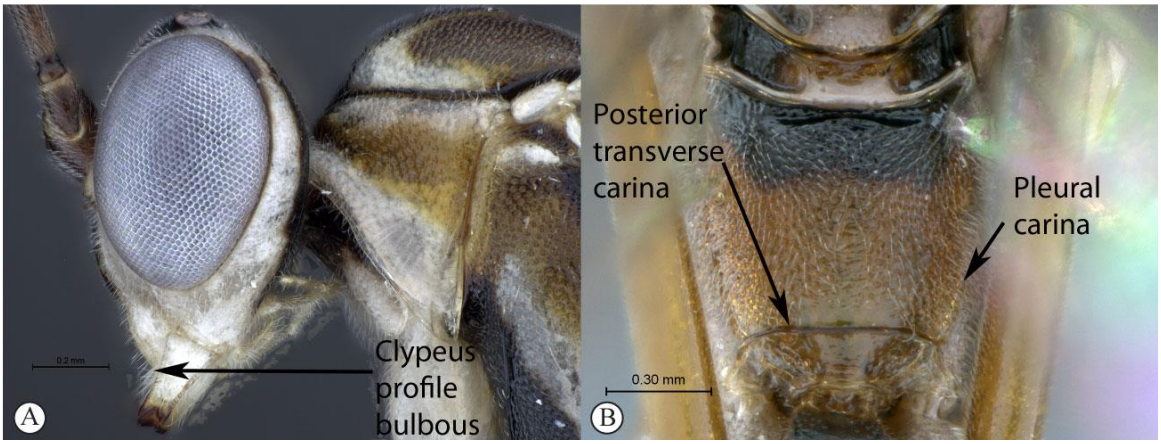

1. Clypeal profile distinctly convex and bulbous (A). Pleural carinae of propodeum present, but may be weak; posterior transverse carina present and well-defined (B)..**2**

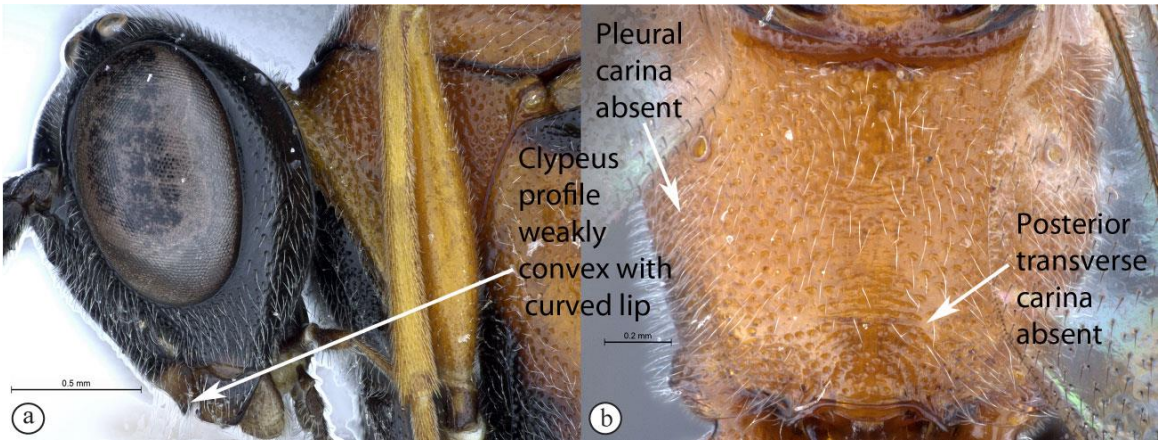

– Clypeal profile weakly convex with a curved lip on ventral margin (a). Pleural carinae and posterior transverse carina of propodeum absent (b) ……...**3**

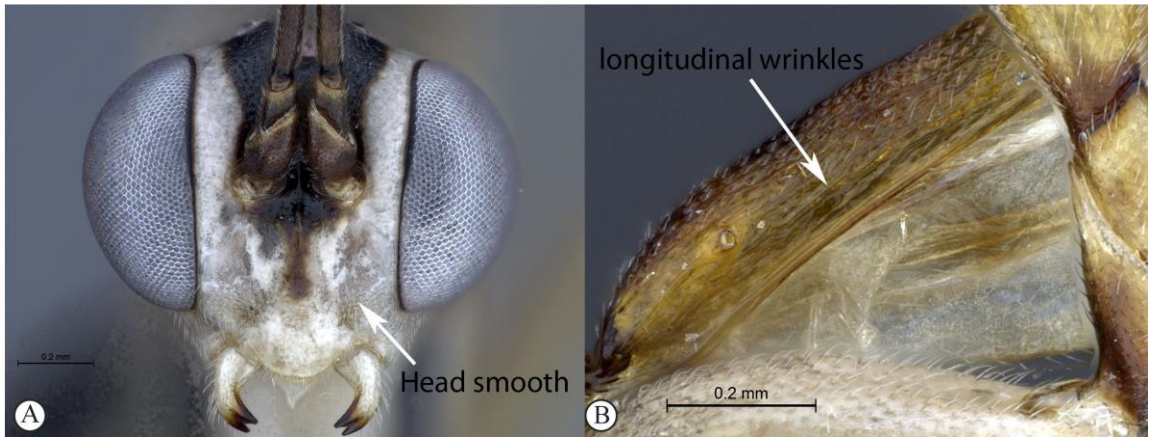

2. Head smooth, impunctate (A). Dorsolateral carinae on tergum 1 substituted with longitudinal wrinkles (B) .....***C. kogelbergensis*** **2016**

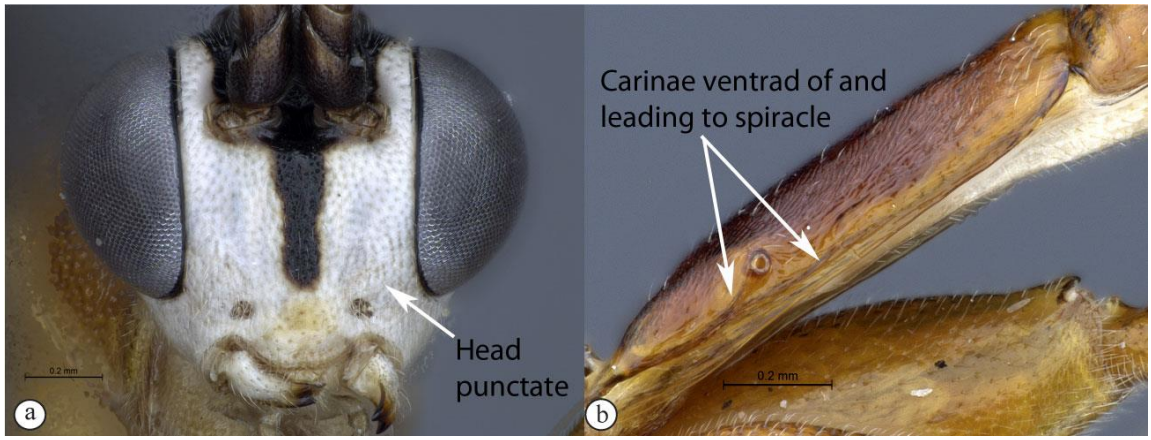

– Head finely punctate (a). Dorsolateral carinae on tergum 1 present as a carina ventrad of spiracle, with a secondary carina leading from the ventral carina to the spiracle (b)……..***C. goci*** **2016**

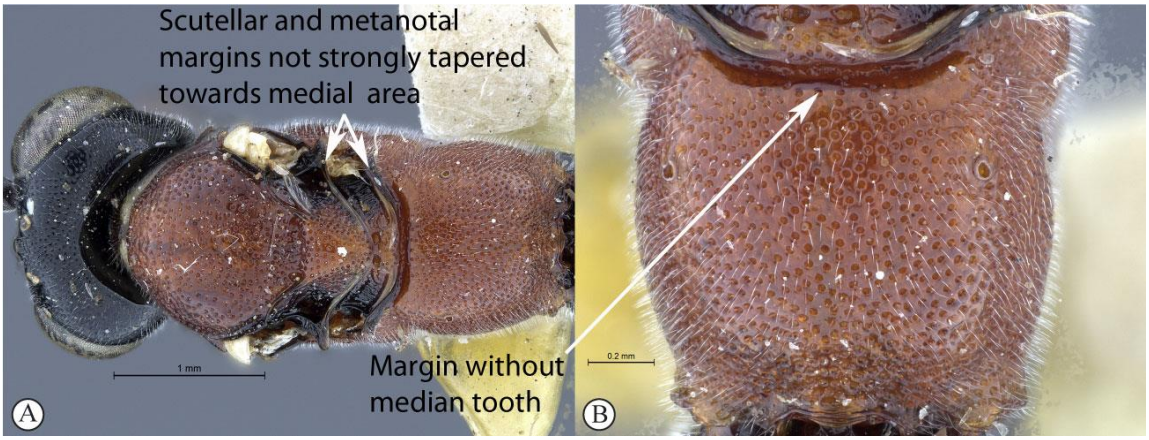

3. Mesosoma with scutellar and metanotal margins not strongly tapered towards medial area (A). Propodeal anterior margin without defined medial tooth, but may have a blunt medial projection (B) ……...**4**

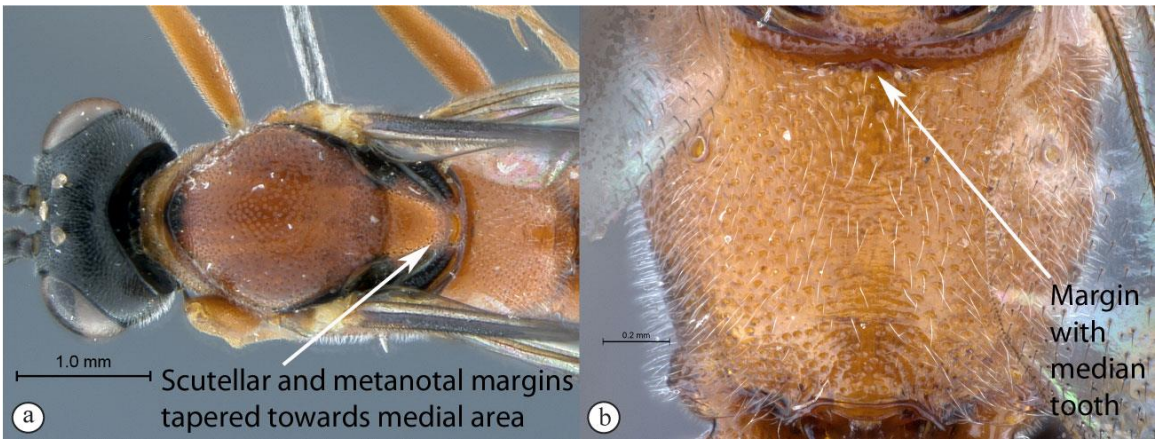

– Metanotum with scutellar margin and metonotal margin tapered towards medial area (a). Propodeal anterior margin with medial tooth (b) ……***C. fernkloofensis*** **2016**

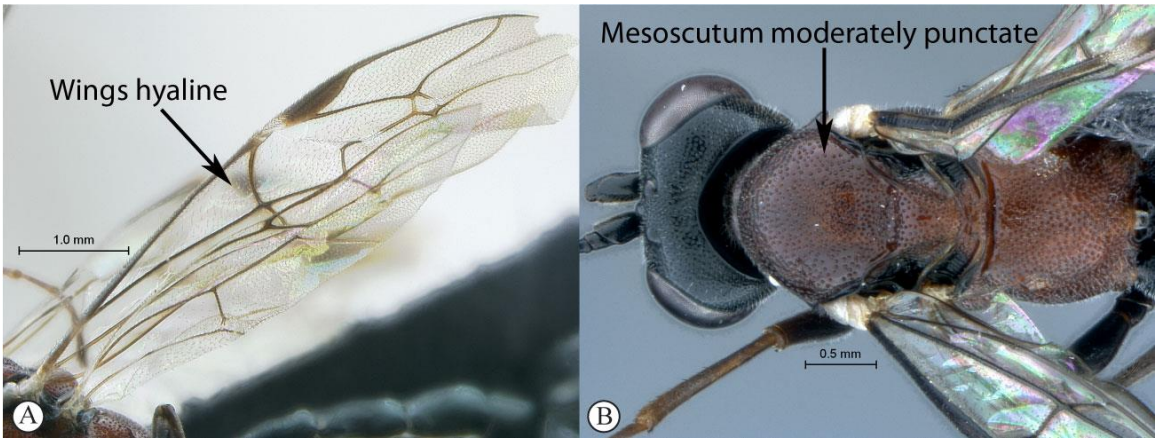

4. Wings hyaline (A). Mesoscutum moderately punctate (B) ……..**5**

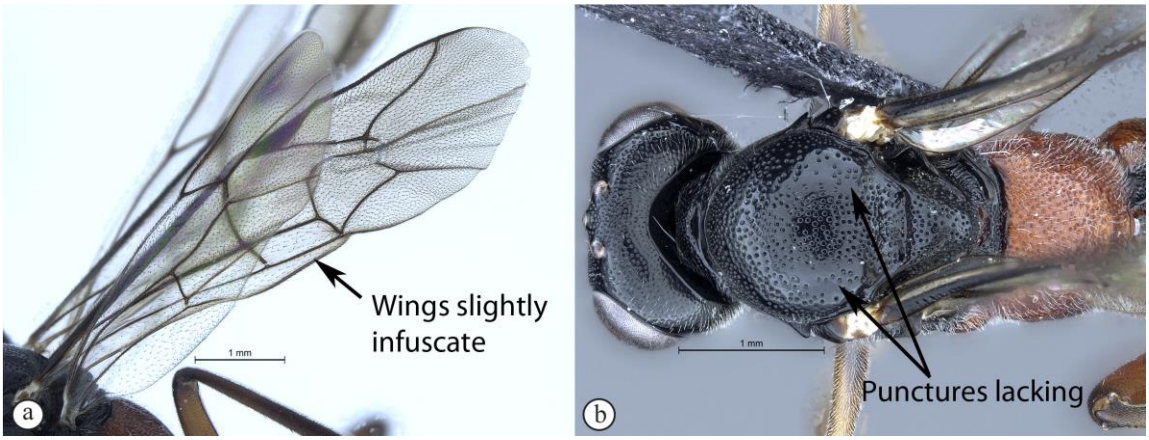

– Wings slightly infuscate, venation darker (a). Mesoscutum with fewer punctures inward of wing bases (b) .....***C. parslactis* 2016**

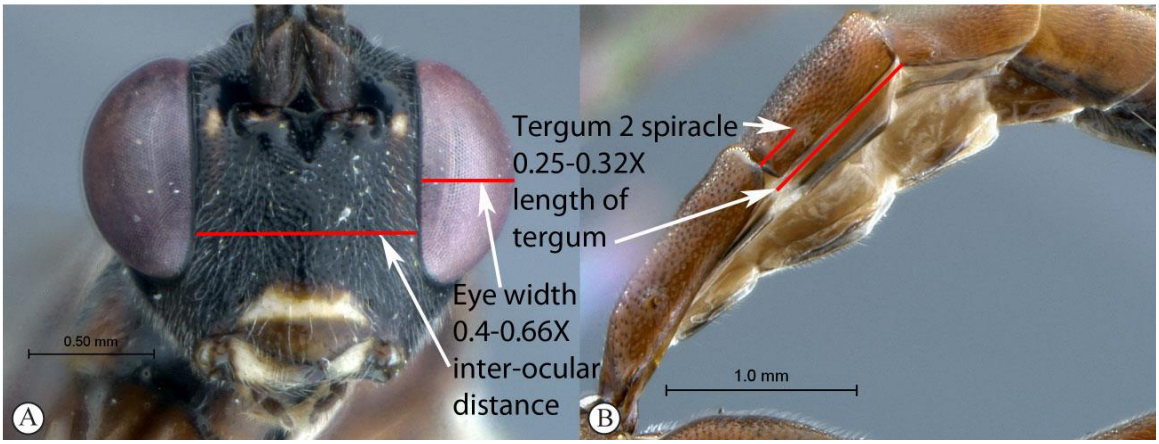

5. Eye in anterior view narrow to moderately-sized: eye maximum width in anterior view 0.4-0.66 times shortest inter-ocular distance (A). Spiracle of tergum 2 situated at basal 0.25-0.32 of tergum (B) ……**6**

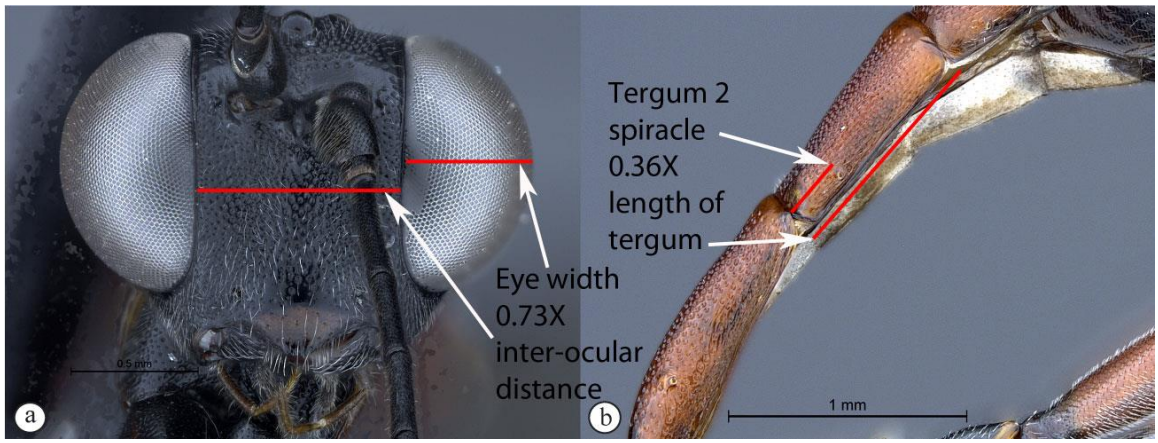

– Eye in anterior view larger, bulbous: eye maximum width in anterior view 0.73 times shortest inter-ocular distance (a). Spiracle of tergum 2 situated at basal 0.36 of tergum (b) .....***C. elongatus* 2016**

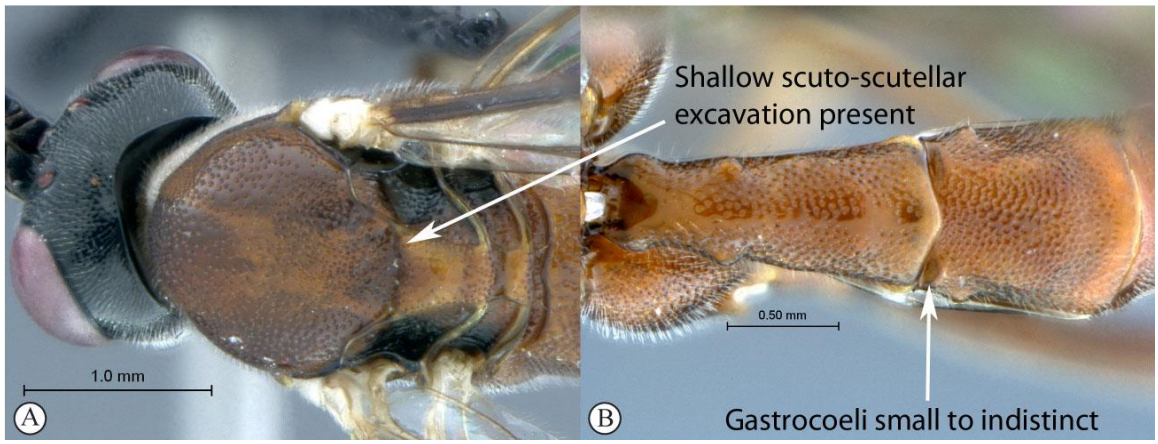

6. Scuto-scutellar excavation shallow, without deep indentations laterally (a). Metasomal tergum 2 with gastrocoeli small to indistinct (b) **7**

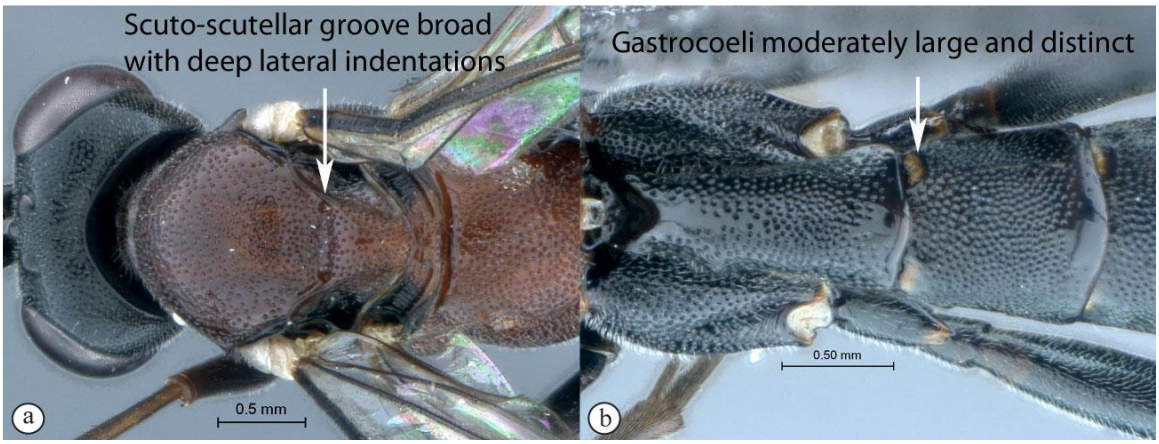

– Scuto-scutellar groove broad with deep lateral indentations (A). Metasomal tergum 1 with gastrocoeli moderately large and distinct (B) ……..**8**

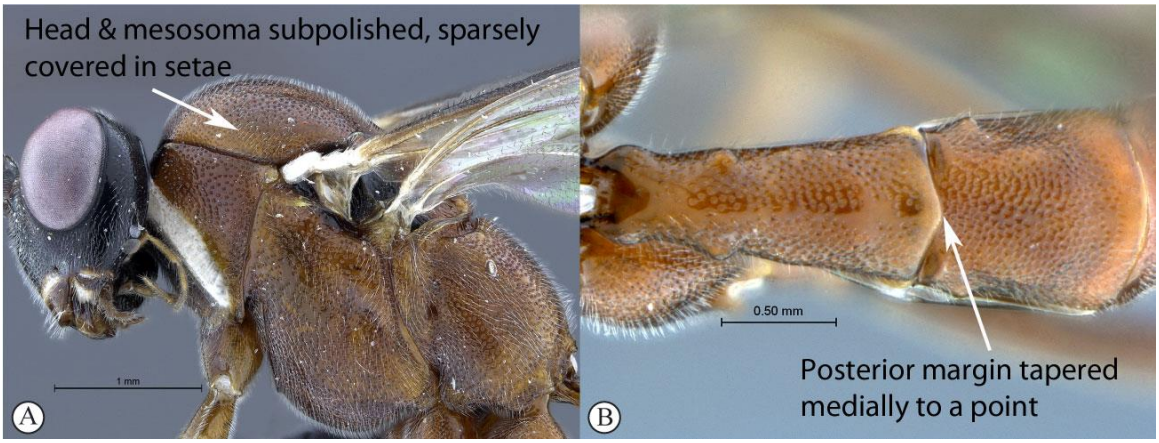

7. Head and mesosoma subpolished, sparsely covered in short setae (A). Metasomal tergum 1 with posterior margin medially tapered to a point (B) …….***C. neili*** **2016**

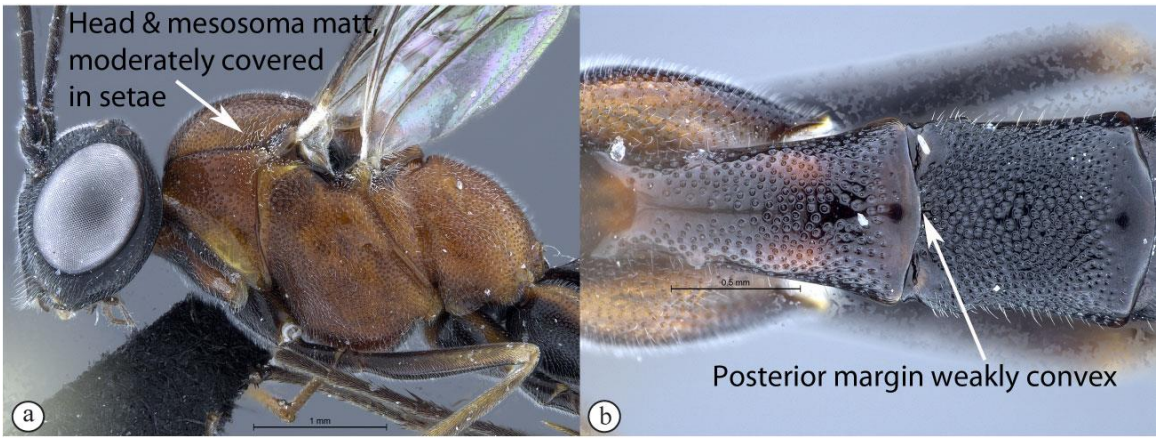

– Head and mesosoma matt, moderately covered in short setae (a). Metasomal tergum 1 with posterior margin weakly convex (b) .....***C. hantami*** **2016**

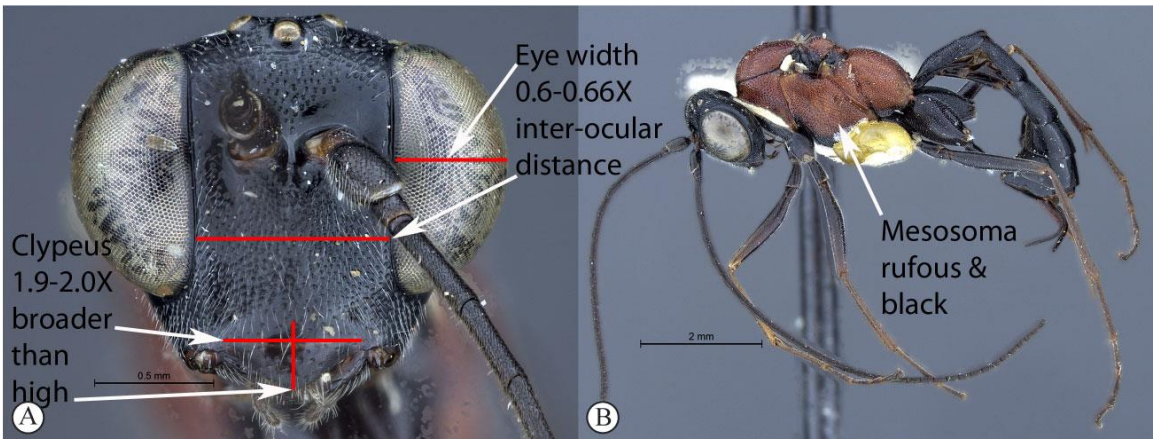

8. Eye maximum width in anterior view 0.6-0.66 times shortest inter-ocular distance (B). Clypeus 1.9-2 times broader than high. Mesosoma predominantly rufous with black markings (C) …….**9**

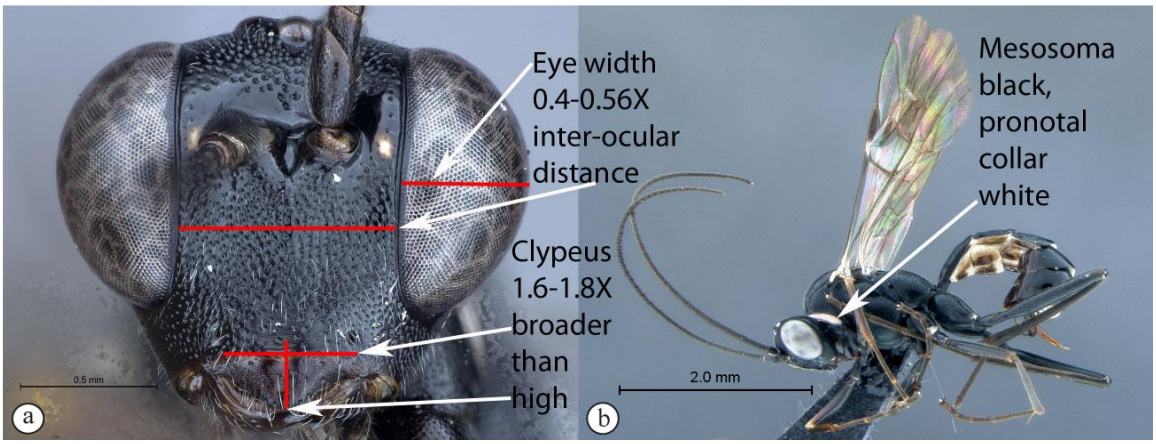

– Eye narrower, its maximum width in anterior view 0.4-0.56 times shortest inter-ocular distance (B). Clypeus 1.6-1.8 times broader than high. Mesosoma black with white pronotal collar (C) ...……..***C. onyxi*** **2016**

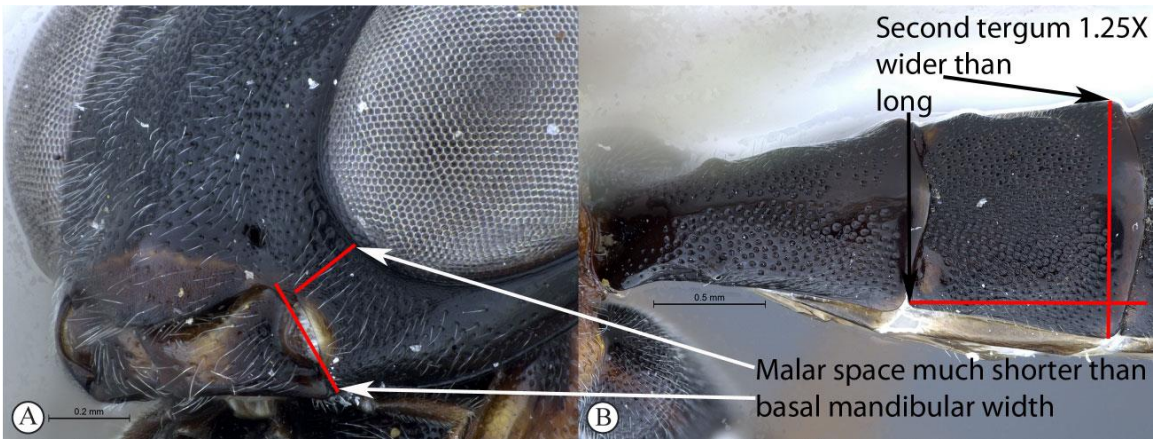

9. Malar space 0.6 times as long as basal mandibular width (A). Second tergum posteriorly 1.25 times broader than long (B) ……..*C. zwarti* **2016**

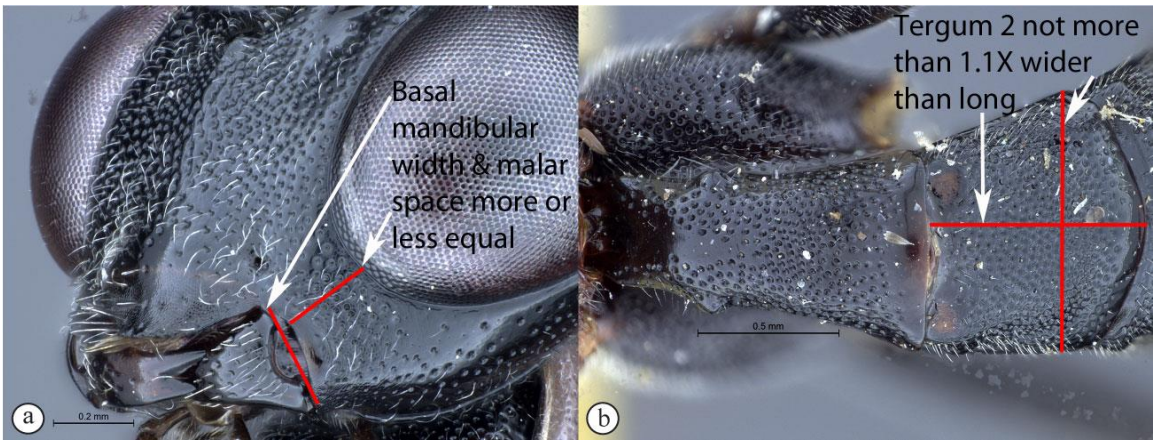

– Malar space 0.9-1.3 times as long as basal mandibular width (a). Tergum 2 posteriorly no more than 1.1 times broader than long (b) ……..*C. rubrithorax* **Morley**

3.3.4 Species descriptions

***Cryptopimpla elongatus* Reynolds Berry & van Noort, 2016.** (Fig. 3.1)

Type material. HOLOTYPE ♀: South Africa, Northern Cape, Hantam National Botanical Garden, 31°24.274'S, 19°09.164'E, 755m, 22 May–12 June 2008, S. van Noort, GL07-DOL1-M39, Malaise trap, Nieuwoudtville-Roggeveld Dolerite Renosterveld, SAM-HYM-P047468 (SAMC).

Description. Body subpolished. Colour. Head black, clypeus and mouthparts dark brown. Body mostly rufescent apart from the mesonotum, black at the wing bases,

mesopleuron ventrally black, submetapleural lobe black, fore and mid coxae black (remaining parts of front leg missing), trochanters and trochantellus of mid and hind legs black and terga 5-8 black.

Head. Densely punctate. Frons unarmed. Clypeus profile weakly convex with a curved lip on the ventral margin. Clypeus edge convex. Upper tooth of mandible longer than the lower. Setae on head and clypeus short and sparse. Eye large and bulbous, maximum width in anterior view 0.73 times shortest inter-ocular distance, maximum width in lateral view 0.79 times maximum length. Tentorial pits small and indistinct. Flagellum tapered to a slender apex.

Mesosoma. Abdomen not compressed. Mesoscutum moderately punctate. Scuto-scutellar groove broad, with deep lateral indentations. Epicnemial carinae present ventrally and dorsally, dorsally converging toward anterior edge of mesopleuron. Propodeum without carinae, its anterior margin with a blunt median projection. Mid coxa posteriorly glossy and smooth. Wings hyaline, base of stigma brown. Fore wing with two bullae close together appearing as one; vein 2m-cu sinuate; areolet anteriorly truncate-shaped. Hind wing with one basal hamulus and six distal hamuli.

Metasoma. Tergum 1 longer than the hind coxae, terga 2 and 3 longer than wide; tergum 1 with dorsolateral carinae substituted by longitudinal wrinkles, densely punctate and with posterior margin weakly convex; second tergum 1.26 times longer than wide posteriorly, spiracle situated at basal 0.36 of tergum (measured in lateral view), gastrocoeli moderately large and circular; terga 4-8 slightly compressed; tergum 6 half as wide as tergum 5. Hypopygium strongly sclerotized. Ovipositor upcurved; sheath striations present.

CT 2.1; ML 0.9; IO 1.9; OO 1.7; Fl_1 5; OT 0.5; body length 6.7 mm; antenna length 8.4 mm; fore wing length 7.0 mm.

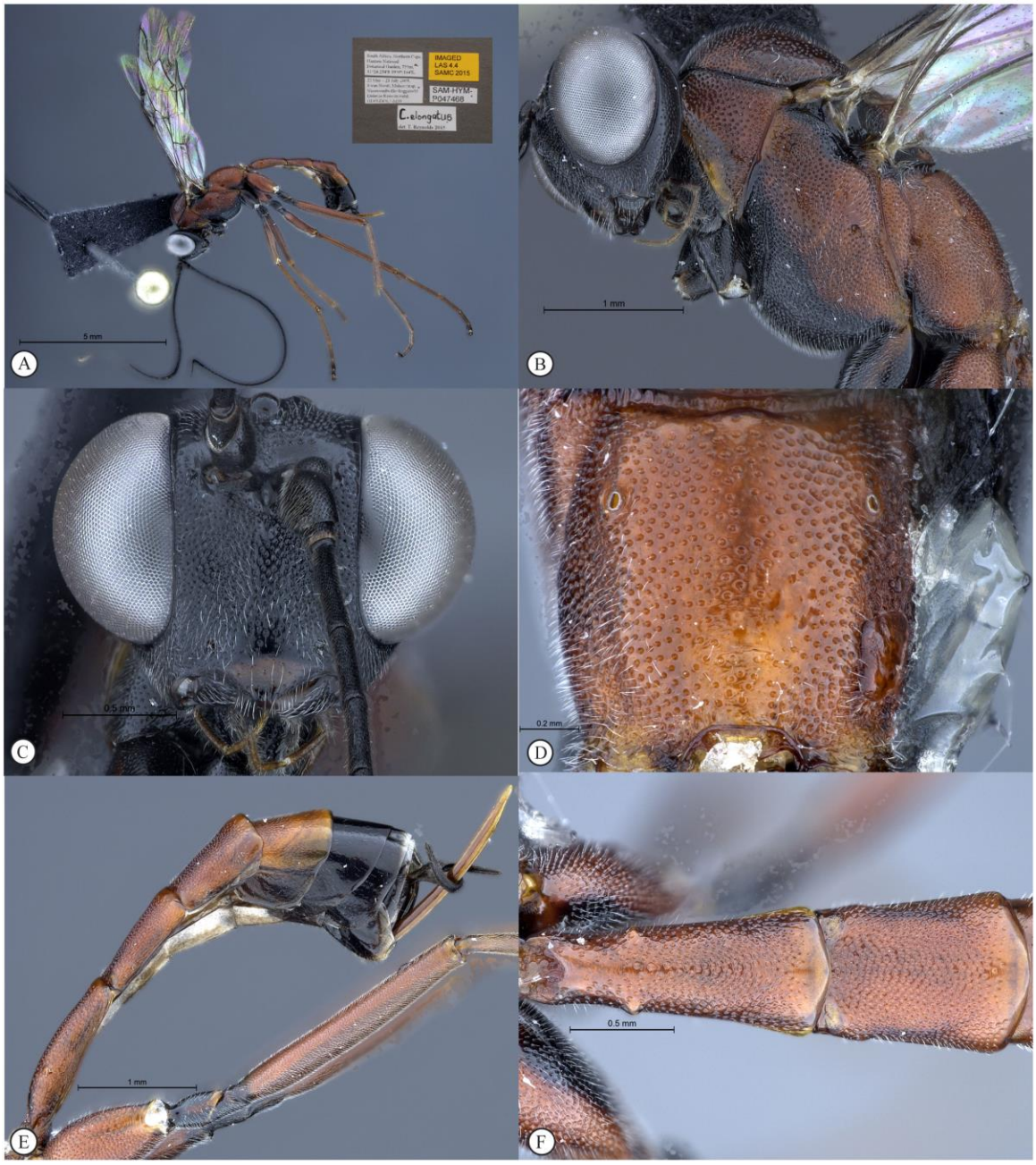

Figure 3.1: *Cryptopimpla elongatus* Holotype (A) Habitus, lateral view (inset: data labels) (B) Head and mesosoma, lateral view (C) Head, anterior view (D) Propodeum, dorsal view (E) Metasoma, lateral view (F) Metasomal terga 1 and 2, dorsal view.

Differential diagnosis. *Cryptopimpla elongatus* can be distinguished from all other Afrotropical *Cryptopimpla* by having a more elongated metasoma, where terga 1-3 are longer than wide with the spiracle on tergum 2 situated at basal 0.36 of tergum (measured

in lateral view). There are a few species with a rufescent/black colour combination, but *C. elongatus* is the only species to have rufescent legs (trochanters black) and a mostly rufescent metasoma (terga 5-8 black). The eye in anterior view is large, its maximum length 0.73 times the shortest inter-ocular distance, separating the species from all other Afrotropical *Cryptopimpla* whose eye length in anterior view is 0.38-0.66 times the shortest inter-ocular distance. A broad scuto-scutellar groove with deep lateral indentations distinguishes *C. elongatus* from closely-related species *C. fernkloofensis*, *C. hantami*, *C. neili* and *C. parslactis*. The metasomal tergum 1 with dorsolateral carinae substituted with longitudinal wrinkles distinguishes *C. elongatus* from closely-related species *C. fernkloofensis* and *C. neili*. Gastrocoeli on tergum 2 are moderately large and circular, separating *C. elongatus* (and *C. fernkloofensis*) from the remaining closely-related species in the *rubrithorax* species-group.

Etymology. The name refers to the rather elongated metasoma of this species. Noun in apposition.

Distribution. South Africa (Northern Cape).

Comments. This is a rare species known only from one female specimen collected in Nieuwoudtville-Roggeveld Dolerite Renosterveld. Intensive sampling in other areas of the Cape Floral Kingdom has produced no further specimens. The female metasoma is depressed (not slightly compressed) distinguishing *C. elongatus* from closely-related species *C. onyxi*, *C. zwarti*, *C. hantami* and *C. rubrithorax*. However, no female specimens are available for closely-related species *C. fernkloofensis*, *C. parslactis* and *C. neili*, so no comparisons could be made with these species.

***Cryptopimpla fernkloofensis* Reynolds Berry & van Noort, 2016.** (Fig. 3.2)

Type material. HOLOTYPE ♂: South Africa, Western Cape, Fernkloof Nature Reserve, 33°39.941'S, 21°53.505'E, 300–340m, 13 May 1995, S. van Noort, Sweep, Mesic Mountain Fynbos, SAM-HYM-P008237 (SAMC).

Description. Body subpolished. Colour. Body mostly fulvous, mesosoma ventrally black. Head black. Clypeus fulvous. Mandibles fulvous to black at apex. Mesoscutum and mesonotum dorso-laterally black. Submetapleural lobe black with various dark markings on legs. Metasomal terga 6-8 and male genitalia brown.

Head. Densely punctate. Frons unarmed. Setae on head and clypeus short and sparse. Clypeus profile weakly convex with a curved lip on the ventral margin. Clypeus edge convex. Flagellum tapered to a slender apex. Tentorial pits small and indistinct. Eye in lateral view 0.67 times as wide as long, moderately sized in anterior view with maximum width 0.54 times the shortest inter-ocular distance. Upper tooth of mandible longer than the lower.

Mesosoma. Abdomen not compressed. Mesoscutum moderately punctate. Scutellar and metanotal margins tapered towards medial area. Epicnemial carinae present ventrally and dorsally, dorsally converging toward anterior edge of mesopleuron. Propodeum with carination reduced to medial area, its anterior margin with medial tooth. Wings hyaline. Fore wing with two bullae closely situated appearing as one; vein 2m-cu sinuate; areolet anteriorly truncate-shaped. Hind wing with one basal hamulus and six (left wing) to seven (right wing) distal hamuli.

Metasoma. Depressed; tergum 1 with a single carina ventrad of spiracle, densely punctate with posterior margin weakly convex; tergum 2 as long as it is broad posteriorly, spiracle situated at basal 0.24 of tergum (measured in lateral view), gastrocoeli moderately large and circular.

CT 2.0; ML 0.9; IO 1.7; OO 1.4; Fl_1 3.5; body length 9.4 mm; antenna length 9.9 mm; fore wing length 7.2 mm.

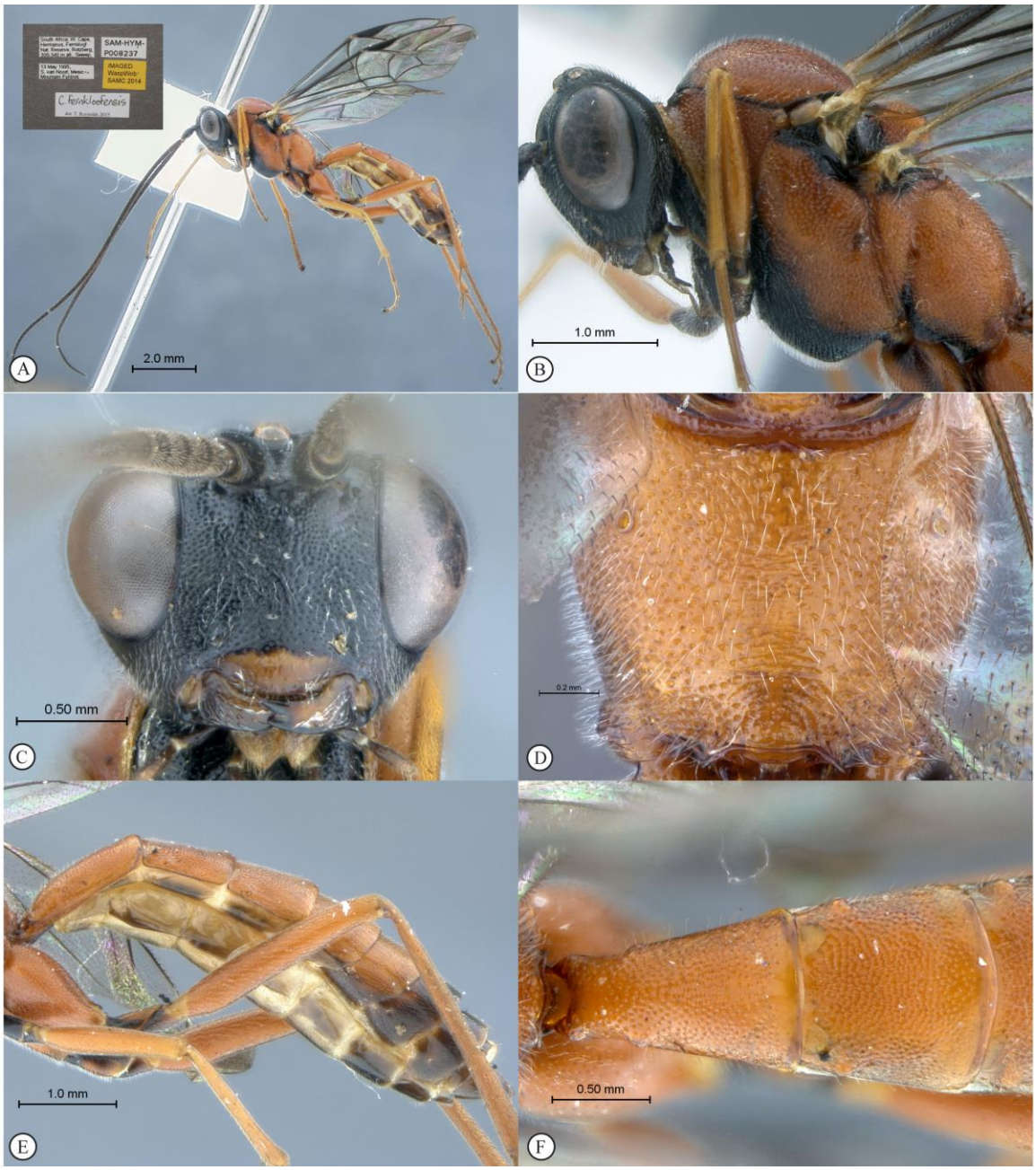

Figure 3.2: *Cryptopimpla fernkloofensis* Holotype (A) Habitus, lateral view (inset: data labels) (B) Head and mesosoma, lateral view (C) Head, anterior view (D) Propodeum, dorsal view (E) Metasoma, lateral view (F) Metasomal terga 1 and 2, dorsal view.

Differential diagnosis. *Cryptopimpla fernkloofensis* can be distinguished from all other Afrotropical *Cryptopimpla* species by having a mostly fulvous body with the mesosoma black ventrally, the head is black and the clypeus and mouthparts are fulvous in colour;

the species is the largest of the *Cryptopimpla* species in the Afrotropical region with a body length of 9.4 mm, compared to other species that have body sizes less than 8.7 mm; the anterior propodeal margin of the species has a medial tooth; the scuto-scutellar groove is narrow, without deep lateral indentations; and the scutellar and metanotal margins distinctly taper towards the medial area. The gastrocoeli on the metasomal tergum 2 are moderately large and circular, which distinguishes *C. fernkloofensis* (and *C. elongatus*) from all other closely-related species in the *rubrithorax* species-group. The presence of a single carina ventrad of the spiracle on the metasomal tergum 1, without wrinkles, separates *C. fernkloofensis* from closely-related species in the *rubrithorax* species-group.

Etymology. Named after the type locality. Noun in apposition.

Distribution. South Africa (Western Cape).

Comments. This is a rare species known only from one male specimen collected in Mesic Mountain Fynbos. Intensive sampling in other areas of the Cape Floral Kingdom, including Mesic Mountain Fynbos at various other localities, has produced no further specimens.

***Cryptopimpla goci* Reynolds Berry & van Noort, 2016** (Fig. 3.3)

Type material. HOLOTYPE ♂: South Africa, Western Cape, Koeberg Nature Reserve, 33°37.622'S, 18°24.259'E, 741m, 3 - 31 October 1997, S. van Noort, KO97-M12, Malaise trap, West Coast Strandveld, SAM-HYM-P0474345 (SAMC).

Description. Body subpolished. Colour. Head white with a median black band on the face, frons, reaching around ocelli and occiput black, not reaching the eyes. Body mostly fulvous, mesoscutum black anteromedially, extending about 0.8 length of mesoscutum.

Head. Finely punctate. Frons unarmed. Setae on head and clypeus short and sparse. Flagellum tapered to a slender apex. Clypeus profile convex, bulbous. Clypeus edge convex. Upper tooth of mandible longer than the lower. Tentorial pits large and distinct.

Eye in lateral view 0.69 times as long as wide, narrow in anterior view with maximum width 0.4 times shortest inter-ocular distance.

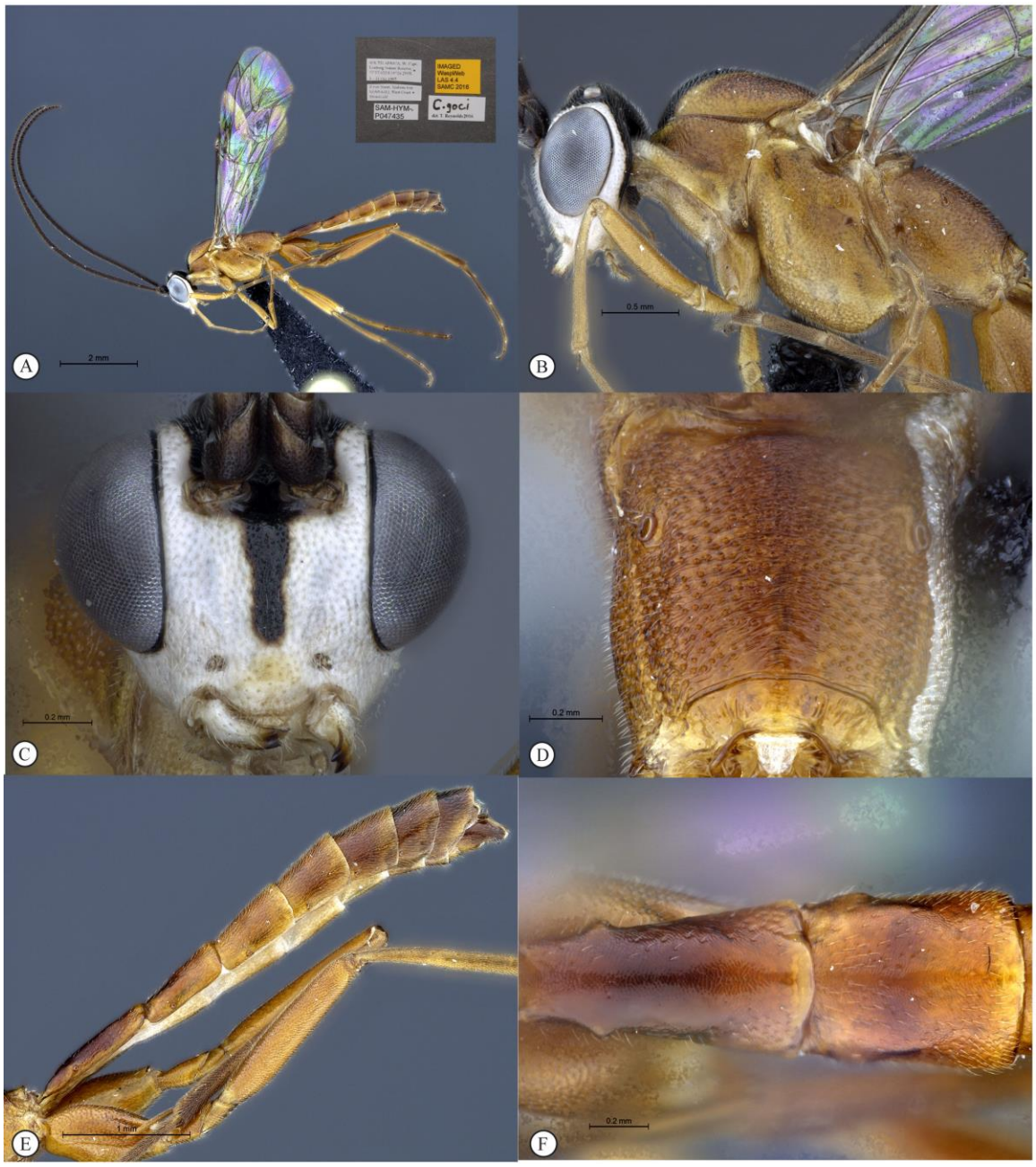

Figure 3.3: *Cryptopimpla goci* Holotype (A) Habitus, lateral view (inset: data labels) (B) Head and mesosoma, lateral view (C) Head, anterior view (D) Propodeum, dorsal view (E) Metasoma, lateral view (F) Metasomal terga 1 and 2, dorsal view.

Mesosoma. Abdomen not compressed. Mesosocutum moderately punctate. Scuto-scutellar groove broad. Epicnemial carinae present ventrally and dorsally, dorsally converging toward anterior edge of mesopleuron. Propodeum with anterior margin medially straight, carination include pleural carinae and a well-defined posterior transverse carina. Wings hyaline; fore wing with two bullae closely situated appearing as one; vein 2m-cu sinuate; areolet anteriorly truncate-shaped. Hind wing with one basal hamulus and seven distal hamuli.

Metasoma. Depressed; tergum 1 impunctate with distinct dorsolateral carinae present as a carina ventrad of spiracle, with a secondary carina leading from the ventral carina to the spiracle, posterior margin weakly convex; second tergum 1.21 times longer than broad, spiracle situated at basal 0.35 of tergum (measured in lateral view), gastrocoeli elongate.

CT 1.8; ML 0.75; IO 1.6; OO 1.1; Fl_1 3.9; body length 7.5 mm; antenna length 7.2 mm; fore wing length 5.3 mm.

Differential diagnosis. *Cryptopimpla goci* is immediately distinguishable from all other Afrotropical *Cryptopimpla* species by having a colour combination of a largely fulvous body, with a white head. A short distinct carina leads to the spiracle from the base of a single carina ventrad of the spiracle which is unique in this species. *Cryptopimpla goci* is closely-related to *C. kogelbergensis* as both species (*goci* species-group) share a truly distinctive and well-defined posterior transverse carina, possess pleural carinae, a convex and bulbous clypeus without a curved lip on the ventral margin, and large tentorial pits distinguishing them from all other Afrotropical *Cryptopimpla* species in the *rubrithorax* species-group. The head is finely punctate, the maximum width of the eye in anterior view 0.38 times the shortest inter-ocular distance; the malar space 0.75 times the basal mandibular width; the length of the first flagellomere 3.9 times longer than wide; 2m-cu on the fore wing is sinuate; metasomal tergum 1 with a short distinct carina that leads to the spiracle from the base of a single carina ventrad of the spiracle; the second tergum 1.21 times longer than wide with elongate gastrocoeli separates *C. goci* from *C. kogelbergensis* where the head is smooth, the maximum width of the eye is much broader at 0.6-0.63 times the shortest inter-ocular distance; the malar space is 1.2 times the basal

mandibular width; the length of the first flagellomere is 6.1-6.8 times longer than wide; vein 2m-cu on the fore wing is straight; dorsolateral carinae on the metasomal tergum 1 are substituted with longitudinal wrinkles and the second tergum is 1.0-1.04 times as long as wide with the gastrocoeli small and indistinct.

Etymology. Named after the late Nosiphiwo Goci who worked as a research assistant in the Natural History Department of the Iziko South African Museum for over 17 years and whose immense contribution to the curation and digitization of the SAMC Hymenoptera collection warrants recognition. Noun in genitive case.

Distribution. South Africa (Western Cape).

Comments. A rare species known only from one specimen collected in West Coast Strandveld in the Koeberg Nature Reserve as part of a continuous 13 month sampling inventory of the reserve using a variety of methods including Malaise traps, yellow pan traps and sweeping. Similar intensive sampling in other areas of the Cape Floral Kingdom, including sampling West Coast Strandveld at numerous other localities, produced no further specimens.

***Cryptopimpla hantami* Reynolds Berry & van Noort, 2016** (Fig. 3.4)

Type material. HOLOTYPE ♀: South Africa, Northern Cape, Hantam National Botanical Garden, 31°24.182'S, 19°08.587'E, 741m, 17 March - 21 April 2008, S. van Noort, GL07-REN3-M24, Malaise trap, Nieuwoudtville Shale Renosterveld, SAM-HYM-P047467 (SAMC). ♂ South Africa, Northern Cape, Hantam National Botanical Garden, 31°24.182'S, 19°08.587'E, 741m, 21 April – 22 May 2008, S. van Noort, GL07 REN3-M31, Malaise trap, Nieuwoudtville Shale Renosterveld, SAMHYM- P047469 (SAMC).

Description. Body moderately covered in short setae. Colour. Head black, clypeus testaceous; mesosoma dark fulvous; pronotal collar and anterior corner of mesopleuron slightly lighter, propleuron ventrally black, metanotum black at the wing bases, sternum of mesothorax with small black spot; metasoma black, terga 6-8 white at the posterior

margins; middle and hind legs black to dark brown with medial dark fulvous longitudinal bands on the coxae, front leg black to testaceous toward apex.

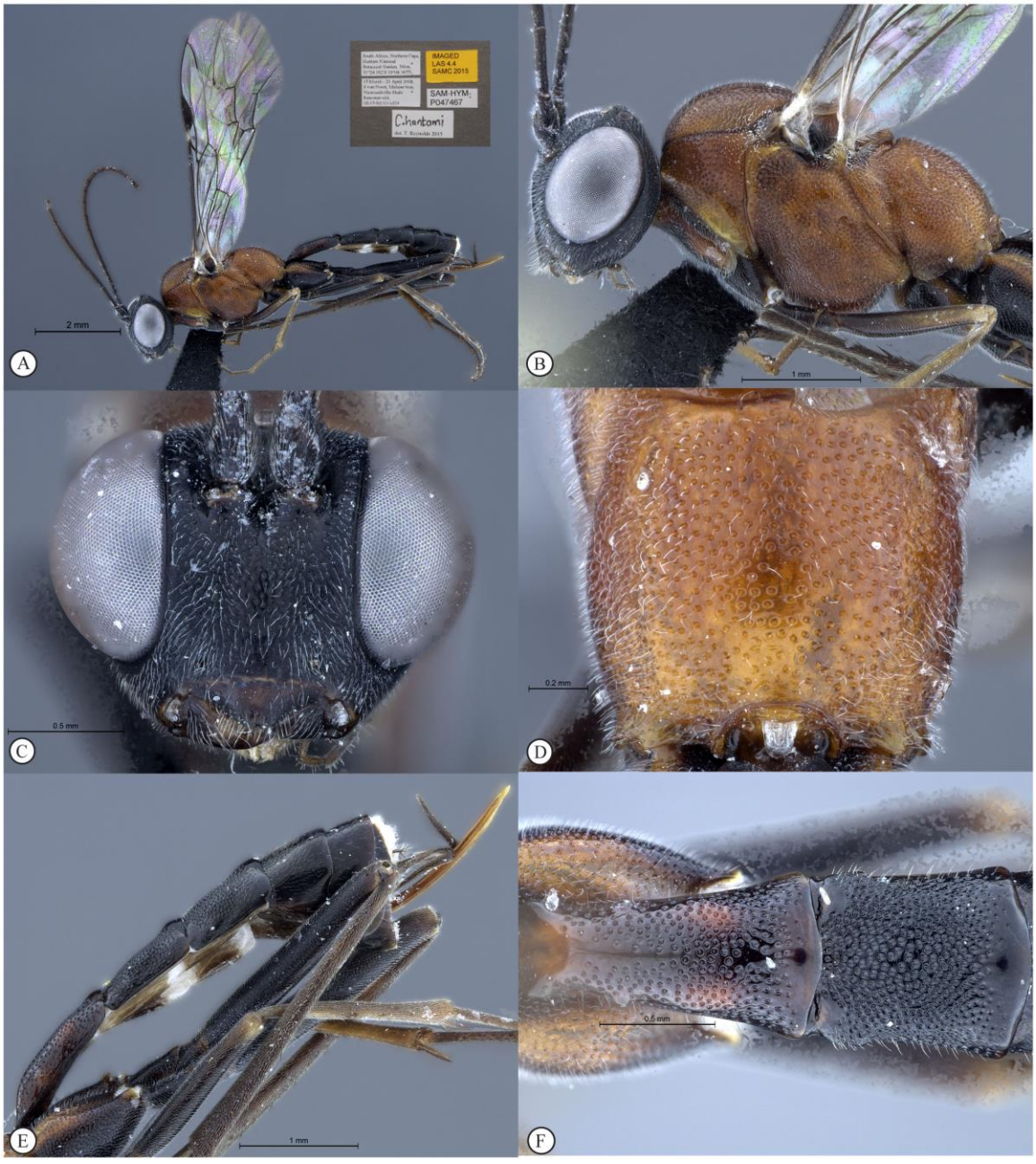

Figure 3.4: *Cryptopimpla hantami* Holotype (A) Habitus, lateral view (inset: data labels) (B) Head and mesosoma, lateral view (C) Head, anterior view (D) Propodeum, dorsal view (E) Metasoma, lateral view (F) Metasomal terga 1 and 2, dorsal view.

Head. Matt. Frons unarmed. Clypeus profile weakly convex with a curved lip on the ventral margin. Clypeus edge convex. Upper tooth of mandible longer than the lower. Head densely punctate. Eye in lateral view 0.73 times as broad as long, maximum width in anterior view half the shortest inter-ocular distance. Tentorial pits small and indistinct. Malar space 0.8-1.0 times basal mandibular width. Flagellum tapered to a slender apex.

Mesosoma. Matt. Abdomen not compressed. Mesosocutum moderately punctate. Scuto-scutellar excavation shallow. Epicnemial carinae present ventrally and dorsally, dorsally converging toward anterior edge of mesopleuron. Propodeum without carinae, its anterior margin with a blunt median projection. Wings hyaline. Fore wing with two bullae close together appearing as one; vein 2m-cu sinuate; areolet anteriorly truncate-shaped. Hind wing with one basal hamulus and six distal hamuli.

Metasoma. Subpolished. Terga 4-8 slightly compressed in female; tergum 1 with dorsolateral carinae substituted with longitudinal wrinkles, densely punctate, posterior margin weakly convex; second tergum 1.06-1.32 times longer than wide, spiracle situated at basal 0.27 of tergum (measured in lateral view), gastrocoeli small and indistinct; tergum 6 half as wide as tergum 5; hypopygium in female strongly sclerotized. Ovipositor upcurved; sheath striations present.

CT 2-2.1; ML 0.8-1; IO 2.3-2.4; OO 1.8-2.1; OT 0.5 (single female); Fl_1 3.7-5.6; body length 8.1-8.9 mm; antenna length 7.9 mm (males antennae intact); fore wing length 5.8-6.2 mm.

Male: Propleuron and pronotum completely black, clypeus testaceous rather than dark brown; colouration of the legs as in female except fulvous bands on mid and hind coxae are lacking and terga 6-8 not white at the posterior margins. Males are more setose; metasoma depressed, tergum 6 half as wide as 5.

Differential diagnosis. *Cryptopimpla hantami* is distinguishable from all species in the *rubrithorax* species-group by having a matt head and mesosoma, with the body moderately covered in short setae, rather than possessing a subpolished body sparsely covered in setae. The presence of a shallow scuto-scutellar excavation and small and

indistinct gastrocoeli on the metasomal tergum 2 distinguishes *C. hantami* (and *C. neili*) from other species in the *rubrithorax* species-group where a broad groove with or without deep lateral indentations may be present and the gastrocoeli are moderately large and distinct. The metasomal tergum 1 with dorsolateral carinae substituted with longitudinal wrinkles distinguishes *C. hantami* from closely-related species *C. fernkloofensis* and *C. neili.*

Distribution. South Africa (Northern Cape).

Etymology. Named after the type locality. Hantam National Botanical Garden. Noun in apposition.

***Cryptopimpla kogelbergensis* Reynolds Berry & van Noort, 2016** (Fig. 3.5)

Type material. HOLOTYPE ♀: South Africa, Western Cape, Kogelberg Nature Reserve, 34°16.481'S, 19°01.033'E, 16 May – 16 June 1999, S. van Noort, KO98- M23, Malaise trap, Mesic Mountain Fynbos, last burnt c. 1988, SAM-HYM-P047475 (SAMC). **Paratypes**: ♀: South Africa, Western Cape, Gamkaberg Nature Reserve, 33°39.504'S, 21°54.947'E, 322m, 30 March 2010 - 24 July 2010, S. van Noort, GB09-SUC04-M38, Malaise trap, Gamka thicket, SAM-HYM-P044551 (SAMC). 2♀: South Africa, Northern Cape, Hantam National Botanical Garden, 31°24.182'S, 19°08.587'E, 22 May – 23 July 2008, S. van Noort, GL07-REN3-M38, 741m, Malaise trap, Nieuwoudtville Shale Renosterveld, SAM-HYM-P047463 (SAMC, BMNH). ♂ South Africa, Western Cape, Gamkaberg Nature Reserve, 33°43.745'S, 21°56.922'E, 1000m, 10 Sept – 4 Nov 2009, S. van Noort, GB09-REN1-Y38, Yellow pan trap, Renosterveld, SAM-HYM-P061546 (SAMC).

Description. Body subpolished. Colour. Head white with a median brown band on the face and brown spots at tentorial pits. Mesoscutum brown dorso-laterally and anteromedially; medially fulvous basad of black colouration; grey or cream stripes medially, extending about 0.8 length of mesoscutum. Mesosoma colour combination brown, white and black; dorsally mostly brown, ventrally black, laterally white. Scutellum and mesonotum black dorso-laterally, testaceous medially. Propodeum mostly

brown to yellowish testaceous, black anteriorly. Legs, antennae and metasoma yellowish testaceous with variable dark markings on terga.

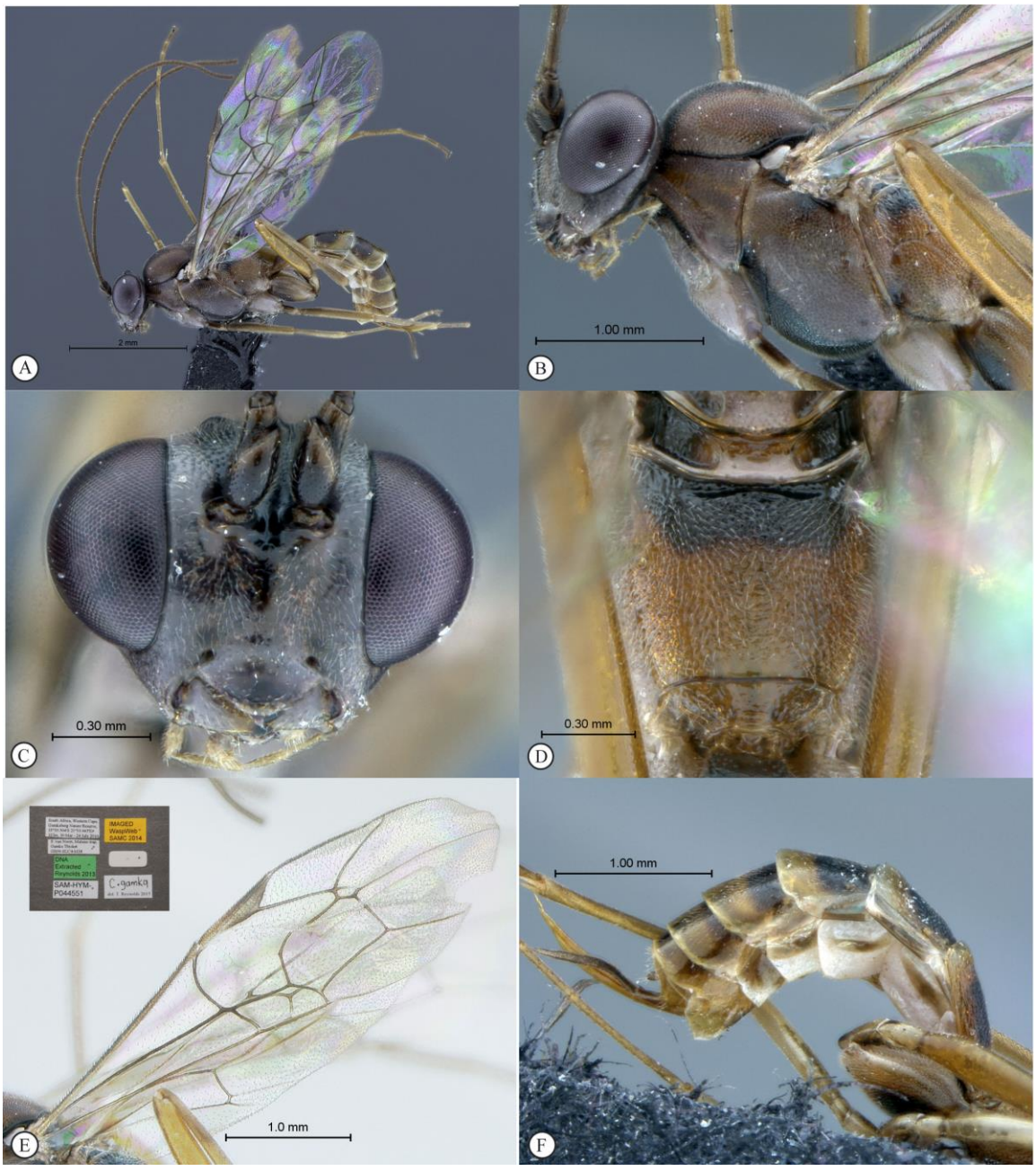

Figure 3.5: *Cryptopimpla kogelbergensis* Holotype (A) Habitus, lateral view (B) Head and mesosoma, lateral view (C) Head, anterior view (D) Propodeum, dorsal view (E) Wings (inset: data labels) (F) Metasoma, lateral view.

Head. Smooth, impunctate. Frons unarmed. Setae on head and clypeus short and sparse. Flagellum tapered to a slender apex. Clypeus profile distinctly convex and bulbous. Clypeus edge convex. Upper tooth of mandible longer than the lower. Tentorial pits large and distinct. Eye in lateral view 0.74-0.76 times as broad as long, maximum width in anterior view 0.6-0.63 times shortest inter-ocular distance.

Mesosoma. Abdomen not compressed. Mesosocutum moderately punctate. Scuto-scutellar groove broad. Epicnemial carinae present ventrally and dorsally, dorsally converging toward anterior edge of mesopleuron. Propodeum with anterior margin medially straight, but may have a blunt medial projection; carination include pleural carinae and a well-defined posterior transverse carina. Wings hyaline. Fore wing with two bullae closely situated appearing as one or separated; vein 2m-cu straight; areolet anteriorly truncate-shaped. Hind wing with one or two basal hamuli and six to seven distal hamuli.

Metasoma. Depressed; tergum 1 with dorsolateral carinae substituted with longitudinal wrinkles, impunctate, posterior margin weakly convex; second tergum 0.96-1 times as long as wide, spiracle situated at basal 0.21-0.23 of tergum (measured in lateral view), gastrocoeli small to indistinct; tergum 6 half as wide as tergum 5; hypopygium moderately sclerotized. Ovipositor upcurved; sheath striations present.

CT 1.9-2.0; ML 1.2; IO 2.0; OO 1.3; Fl_1 5.1-6.1; OT 0.5-0.7; body length 4.2-5.6 mm; antenna length 6.3-6.5 mm; fore wing length 4.6-5.1 mm.

Differential diagnosis. *Cryptopimpla kogelbergensis* is immediately distinguishable from all other Afrotropical *Cryptopimpla* species by the distinctive colour combination of the mesopleuron, which is three-banded in brown, white and black; possession of a smooth head; and vein 2m-cu is straight on the fore wing. The maximum width of the eye in anterior view 0.6-0.63 times the shortest inter-ocular distance; the length of the first flagellomere 6.1-6.8 times longer than wide; the metasomal tergum 1 with dorsolateral carinae substituted with longitudinal wrinkles; and the metasomal tergum 2 as long as wide with small and distinct gastrocoeli distinguishes *C. kogelbergensis* from *C. goci*

where the maximum width of the eye in the anterior view is much narrower at 0.38 times the shortest inter-ocular distance; distinct dorsolateral carinae are presented as a short carina leading from a single carina ventrad of the spiracle; the length of the first flagellomere is 3.9 times longer than wide; vein 2m-cu on the fore wing is sinuate; and the second tergum is 1.21 times longer than wide with the gastrocoeli elongate.

Etymology. Named after the type locality. Noun in apposition.

Distribution. South Africa (Western Cape & Northern Cape).

***Cryptopimpla neili* Reynolds Berry & van Noort, 2016** (Fig. 3.6)

Type material. HOLOTYPE ♂: South Africa, Western Cape, Kogelberg Nature Reserve, 34°16.481'S, 19°01.033'E, 16 March 1999 - 16 April 1999, S. van Noort, KO98-M18, Malaise trap, Mesic Mountain Fynbos, last burnt c. 1988, SAM-HYMP047436 (SAMC).

Description. Body subpolished. Colour. Head black, clypeus and mandibles white to brown; white markings on either side of toruli. Body mostly fulvous with dark markings on metanotum and metasomal terga 5-8, pronotal collar white.

Head. Densely punctate. Frons unarmed. Setae on head and clypeus short and sparse. Eye in lateral view 0.74 times as wide as long. Shortest inter-ocular distance 1.94 times maximum eye width in anterior view. Flagellum tapered to a slender apex. Clypeus profile weakly convex with a curved lip on the ventral margin. Clypeus edge convex. Upper tooth of mandible longer than the lower. Tentorial pits small or indistinct.

Mesosoma. Abdomen not compressed. Mesosocutum moderately punctate. Shallow excavation separates mesoscutum from scutellum. Epicnemial carinae present ventrally and dorsally, dorsally converging toward anterior edge of mesopleuron. Anterior propodeal margin with a blunt median projection; carination absent. Wings hyaline. Fore wing with two bullae closely situated appearing as one; vein 2m-cu sinuate; areolet anteriorly truncate-shaped. Hind wing with two basal hamuli and six distal hamuli.

Figure 3.6: *Cryptopimpla neili* Holotype (A) Habitus, lateral view (inset: data labels) (B) Head and mesosoma, lateral view (C) Head, anterior view (D) Propodeum, dorsal view (E) Metasoma, lateral view (F) Metasomal terga 1 and 2, dorsal view.

Metasoma. Tergum 1 densely punctate, lacking dorsolateral carinae, posterior margin medially tapered to a point; second tergum 1.07 times longer than broad, spiracle situated

at basal 0.28 of tergum (measured in lateral view), gastrocoeli small and elliptic; terga 4-8 strongly compressed.

CT 2.0; ML 1.0; IO 2.3; OO 1.6; Fl_1 5.0; body length 7.5 mm; antenna length 8.5 mm; fore wing 6.9 mm.

Differential diagnosis. *Cryptopimpla neili* is closely-related to *C. hantami* because both species exclusively possess a shallow excavation separating the mesosocutum from the scutellum and the presence of small elliptic gastrocoeli on the second tergum, whereas a groove is present and the shape of the gastrocoeli is large or elongate in the other species in the *rubrithorax* species-group. *Cryptopimpla neili* is immediately distinguishable from all other Afrotropical *Cryptopimpla* species, including *C. hantami*, by having a unique colour combination of a fulvous body, white pronotal collar and a clypeus distinguished by two colours; and the metasomal tergum 1 lacking dorsolateral carinae with the posterior margin medially tapered to a point.

Etymology. Named after the first author's father. Noun in genitive case.

Distribution. South Africa (Western Cape).

Comments. A rare species known only from one specimen. Intensive sampling in other areas of the Cape Floral Kingdom produced no further specimens. The metasomal terga 4-8 of the male are strongly compressed and this separates the species from the closely-related species *C. fernkloofensis*, *C. hantami*, *C. parslactis C. rubrithorax* and *C. onyxi*. However, no male specimens are available for the remaining species *C. elongatus* and *C. zwarti* within the *rubrithorax* species-group. Thus, no comparisons could be made with those species.

***Cryptopimpla onyxi* Reynolds Berry & van Noort, 2016** (Fig. 3.7)

Type material. HOLOTYPE ♀: South Africa, Western Cape, Walker Bay Nature Reserve, 34°27.414'S, 19°21.393'E, 57m, 14 May –14 June 1997, S. van Noort, WB97-M01, Malaise trap, South coast Strandveld, SAM-HYM-P047460 (SAMC). **Paratypes**

7♂: South Africa, Western Cape, Walker Bay Nature Reserve, 34°27.414'S, 19°21.393'E, 57m, 6 September – 4 October 1997, S. van Noort, WB97-M09, Malaise trap, South coast Strandveld, SAM-HYM-P044545, SAM-HYM-P047478, SAM-HYM-P047479, SAM-HYM-P047481 (SAMC, BMNH); ♂: South Africa, Western Cape, Walker Bay Nature Reserve, 34°27.414'S, 19°21.393'E, 57m, 18 Apr – 16 May 1998, S. van Noort, WB97-M30, Malaise trap, South coast Strandveld, SAM-HYM-P048105 (SAMC); ♂: South Africa, Western Cape, Kogelberg Nature Reserve, 34°16.481'S, 19°01.033'E, 16 Mar – 16 Apr 1999, S. van Noort, KO98- M17, Malaise trap, Mesic Mountain Fynbos last burnt c. 1988, SAM-HYM- P47482 (SAMC).

Description. Body subpolished. Body black. Pronotal collar white.

Head. Densely punctate. Frons unarmed. Clypeus profile weakly convex with a curved lip on the ventral margin. Clypeus edge convex. Upper tooth of mandible longer than lower. Setae on head and clypeus short and sparse. Flagellum tapered to a slender apex. Tentorial pits small or indistinct. Eye in lateral view 0.7-0.72 times as long as wide, maximum width in anterior view 0.4-0.56 times shortest inter-ocular distance.

Mesosoma. Abdomen not compressed. Mesosocutum moderately punctate. Scuto-scutellar groove broad with deep lateral indentations. Epicnemial carinae present ventrally and dorsally, dorsally converging toward anterior edge of mesopleuron. Propodeum with carination reduced to medial area or absent, its anterior margin with a blunt median projection. Wings hyaline. Fore wing with two bullae closely situated appearing as one; vein 2m-cu sinuate; areolet truncate-shaped. Hind wing with one or two basal hamuli and six to seven distal hamuli.

Metasoma. Tergum 1 punctate with dorsolateral carinae substituted with longitudinal wrinkles, posterior margin weakly convex; second tergum 1.09-1.25 times longer than wide, spiracle situated at basal 0.25-0.26 of tergum (measured in lateral view), gastrocoeli elongate; terga 4-8 moderately compressed in females, no dorsolateral compression in males; female metasomal tergum 5 as wide as tergum 6; hypopygium strongly sclerotized.

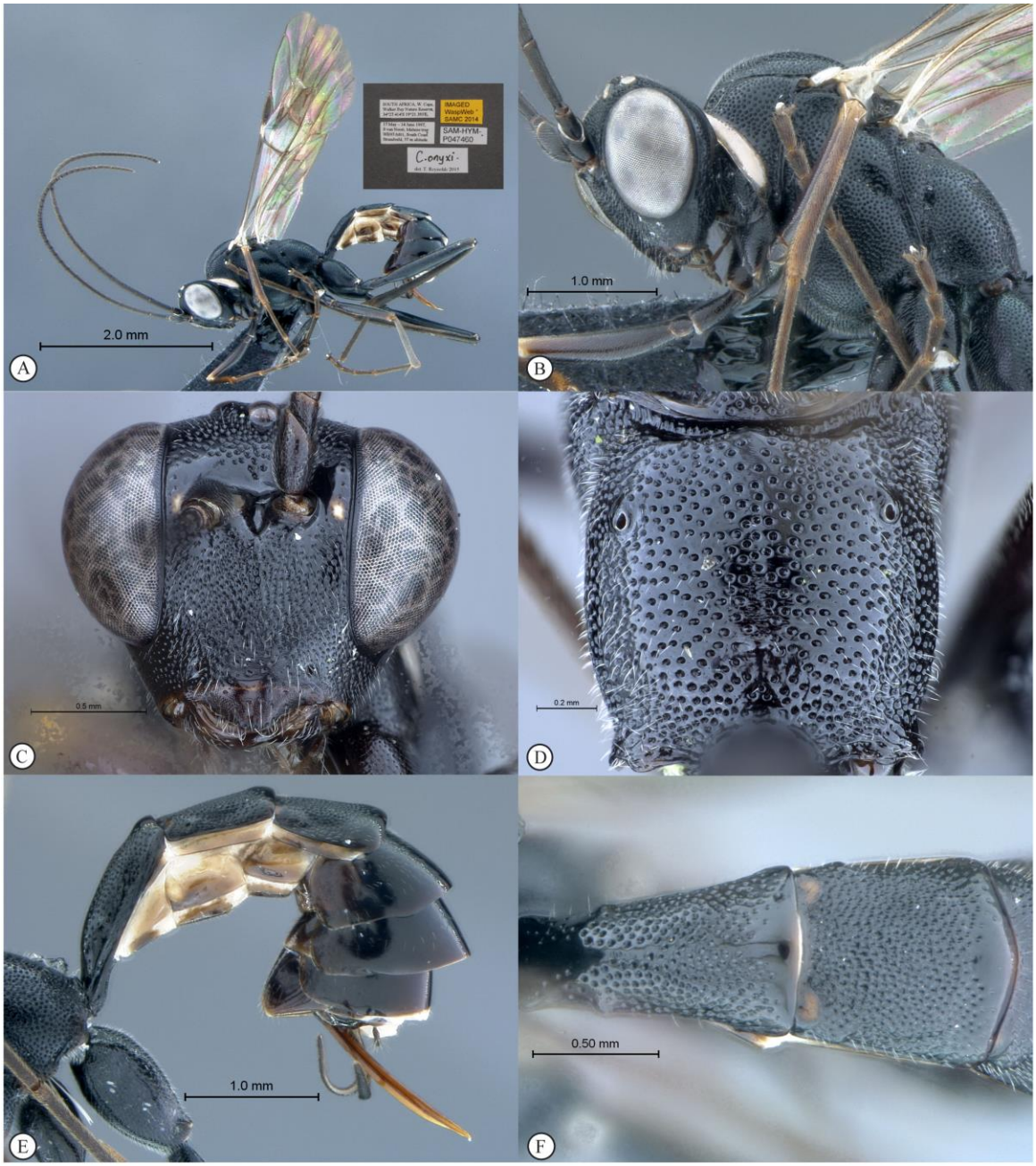

Figure 3.7: *Cryptopimpla onyxi* Holotype (A) Habitus, lateral view (inset: data labels) (B) Head and mesosoma, lateral view (C) Head, anterior view (D) Propodeum, dorsal view (E) Metasoma, lateral view (F) Metasomal terga 1 and 2, dorsal view.

CT 1.6-1.8; ML 0.9-0.96; IO 2.1; OO 1.9; Fl_1 4.2; OT 0.5 (SAM-HYM-P047460); body length 6-8.4 mm; antenna length 8.1-9.0 mm; fore wing length 6.1-6.8 mm.

Differential diagnosis. *Cryptopimpla onyxi* is immediately distinguishable from all other Afrotropical *Cryptopimpla* species by having a unique colour combination of a black body and a white pronotal collar. The clypeus is 1.6-1.8 times broader than high, distinguishing *C. onyxi* from all other species in the *rubrithorax* species-group where the clypeus is more than 1.8 times broader than high. The scuto-scutellar groove in *C. onyxi* is broad with deep lateral indentations, distinguishing the species from closely-related species *C. fernkloofensis*, *C. parslactis*, *C. hantami* and *C. neili*. The metasomal tergum 1 with dorsolateral carinae substituted with longitudinal wrinkles distinguishes the species from *C. fernkloofensis* and *C. neili*. Gastrocoeli on tergum 2 are elongate, separating *C. onyxi* from closely-related species *C. fernkloofensis*, *C. elongatus*, *C. neili* and *C. hantami*.

Etymology. So named because of the black colour of the species. Noun in apposition.

Distribution. Occurs in Strandveld and Mountain Fynbos vegetation types in South Africa (Western Cape).

Comments.The female metasomal tergum 5 as wide as tergum 6 separates the species from closely-related species *C. hantami*, *C. zwarti*, *C. elongatus* and *C. rubrithorax* where tergum 5 is half as wide as high. However, no female specimens are available for *C. fernkloofensis*, *C. parslactis* and *C. neili*. Thus, no comparisons could be made with those closely-related species.

***Cryptopimpla parslactis* Reynolds Berry & van Noort, 2016** (Fig. 3.8)

Type material. HOLOTYPE ♂: South Africa, Northern Cape, Hantam National Botanical Garden, 31°23.802'S, 19°08.799'E, 752m, 23 July–23 Aug 2008, S. van Noort, GL07-REN1-M43, Malaise trap, Nieuwoudtville Shale Renosterveld, SAMHYM-P044547 (SAMC).

Description. Body subpolished. Colour. Head and mesosoma mostly black, with the exception of the medial region of the mesopleuron and the propodeum that is orange. Legs with fore and mid coxae, trochanters and trochantellus black. Terga 2-8 mostly

black, tergum 2 medially orange and terga 7-8 white posteriorly. Femora 1-2 black to light orange. Tibia and tarsus of front leg light orange. Tibia 2 light orange, tarsus 2 brown. Femora 3 orange, tibia and tarsus of hind leg brown.

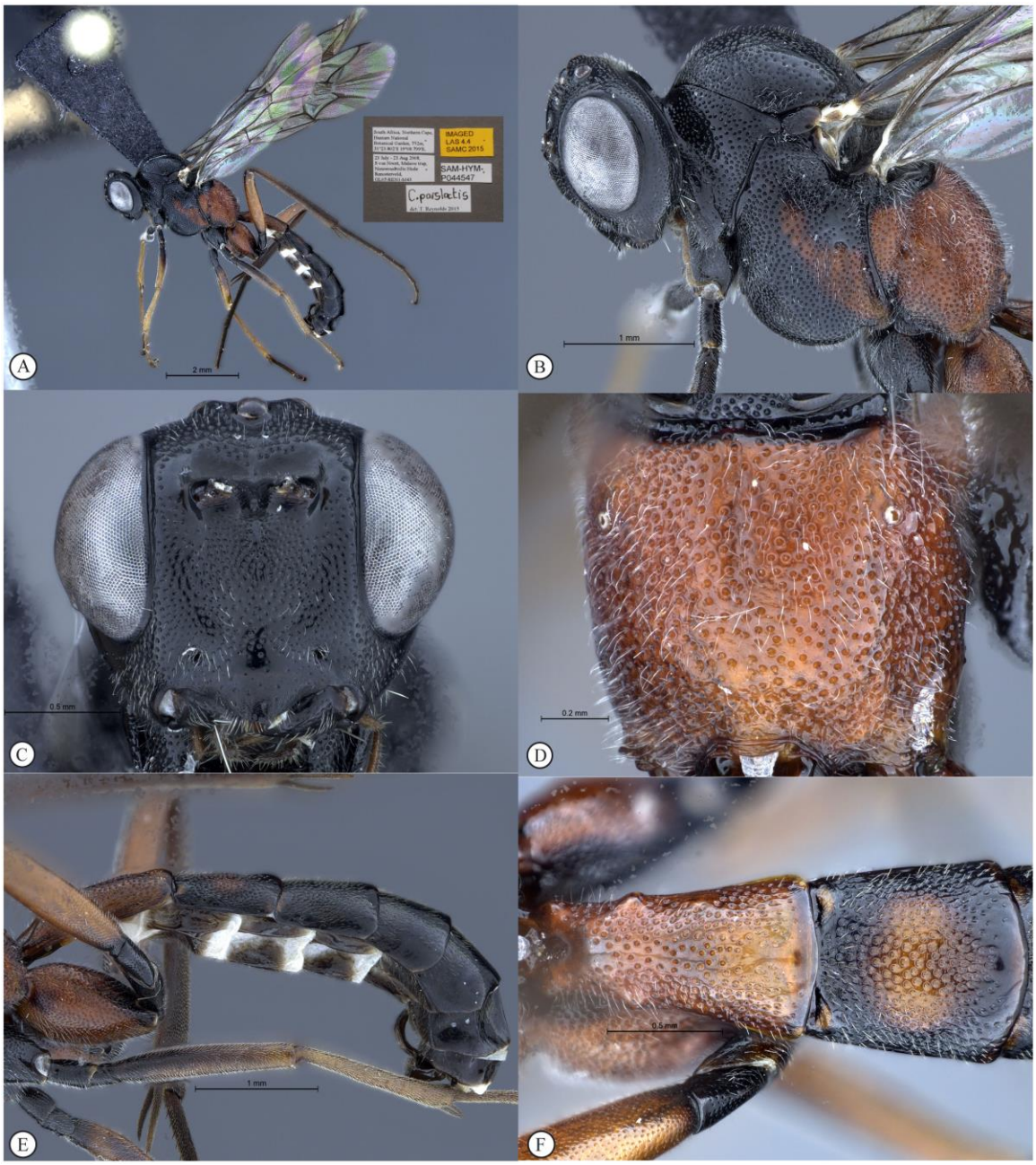

Figure 3.8: *Cryptopimpla parslactis* Holotype (A) Habitus, lateral view (inset: data labels) (B) Head and mesosoma, lateral view (C) Head, anterior view (D) Propodeum, dorsal view (E) Metasoma, lateral view (F) Metasomal terga 1 and 2, dorsal view.

Head. Densely punctate. Frons unarmed. Clypeus profile weakly convex with a curved lip on the ventral margin. Clypeus edge convex. Upper tooth of mandible longer than lower. Setae on head and clypeus short and sparse. Tentorial pits small and indistinct. Flagellum tapered to a slender apex. Eye in lateral view 0.7 times as long as wide, maximum width in anterior view 0.46 times shortest inter-ocular distance.

Mesosoma. Abdomen not compressed. Scuto-scutellar groove broad. Mesoscutum with fewer punctures inward of wing base. Epicnemial carinae present ventrally and dorsally, dorsally converging toward anterior edge of mesopleuron. Propodeum without carinae, its anterior margin with a weak and blunt medial projection. Wings slightly infuscate, venation dark. Fore wing with two bullae close together appearing as one; vein 2m-cu sinuate; areolet truncate-shaped. Hind wing with one basal hamulus and six distal hamuli.

Metasoma. Depressed. Tergum 1 with dorsolateral carinae substituted with longitudinal wrinkles, densely punctate, with posterior margin weakly convex; tergum 2 of metasoma 1.09 times as long as wide posteriorly, spiracle situated at basal 0.28 of tergum (measured in lateral view), gastrocoeli elongate; tergum 6 as wide as tergum 5.

CT 2.3; ML 0.92; IO 2.6; OO 2.0; body length 7.4 mm; fore wing length 7.0 mm.

Differential diagnosis. *Cryptopimpla parslactis* is immediately diagnosable from other Afrotropical *Cryptopimpla* by being the only species to have slightly infuscate wings with darker venation. *Cryptopimpla parslactis* is distinguishable from closely-related species in the *rubrithorax* species-group that have a rufous and black colour combination, by having a completely black mesoscutum and a combination of a mostly black metasoma with tergum 1 completely rufescent. In addition, while punctuation on the mesoscutum in the dorsal view is common amongst all the species, fewer punctures on mesoscutum exist inward of the wings bases of *C. parslactis*. The metasomal tergum 1 with dorsolateral carinae substituted with longitudinal wrinkles distinguishes *C. parslactis* from *C. fernkloofensis* and *C. neili.* Gastrocoeli on tergum 2 are elongate separating *C. parslactis* from closely-related species *C. fernkloofensis, C. elongatus* and *C. hantami*.

Etymology. So named because the wings are not quite hyaline, but rather slightly infuscate with a creamy-brown colour, “pars” meaning wing and “lactis” meaning cream.

Distribution. South Africa (Northern Cape).

Comments. A rare species known only from one specimen. Intensive sampling in other areas of the Cape region produced no further specimens.

***Cryptopimpla rubrithorax* Morley, 1916** (Fig. 3.9).

Type material. HOLOTYPE ♀: South Africa, Western Cape, Elsenberg, 11 October 1914, Mally and Petty, SAM-HYM-P000874 (SAMC). **Additional material**: ♀ South Africa, Western Cape, Kogelberg Nature Reserve, 34°16.481'S, 19°01.033"E, 16 September 1999, S. van Noort, KO98-M40, Malaise trap, Mesic mountain fynbos last burnt c. 1988, SAM-HYM-P044558 (SAMC). 2♀, 3♂ South Africa, Western Cape, Koeberg Nature Reserve, 33°37.622'S, 18°24.259'E, 8 August – 5 September 1997, S. van Noort, KO97-M07, KO97-M08, Malaise trap, West Coast Strandveld, SAM-HYM-P047461 (SAMC, BMNH). 1♀ South Africa, Western Cape, Koeberg Nature Reserve, 33°37.622'S, 18°24.259'E, 5 September – 3 October 1997, S. van Noort, KO97-M09, Malaise trap, West Coast Strandveld, SAM-HYM-P047477 ♀, ♂ South Africa, Northern Cape, Hantam National Botanical Garden, 31°23.802'S, 19°08.799'E, 752m, 23 July 2008 - 23 August 2008, S. van Noort, GL07-REN1- M43, Malaise trap, Nieuwoudtville Renosterveld Shale, SAM-HYM-P044547 (SAMC, BMNH).

Description (updated from Morley, 1916). Body subpolished. Colour. Head and metasoma black, posterior margins of terga 6-8 white. Clypeus rarely distinguished by colour to the rest of the face. Mesosoma rufescent, black ventrally; mesonotum black at the wing bases.

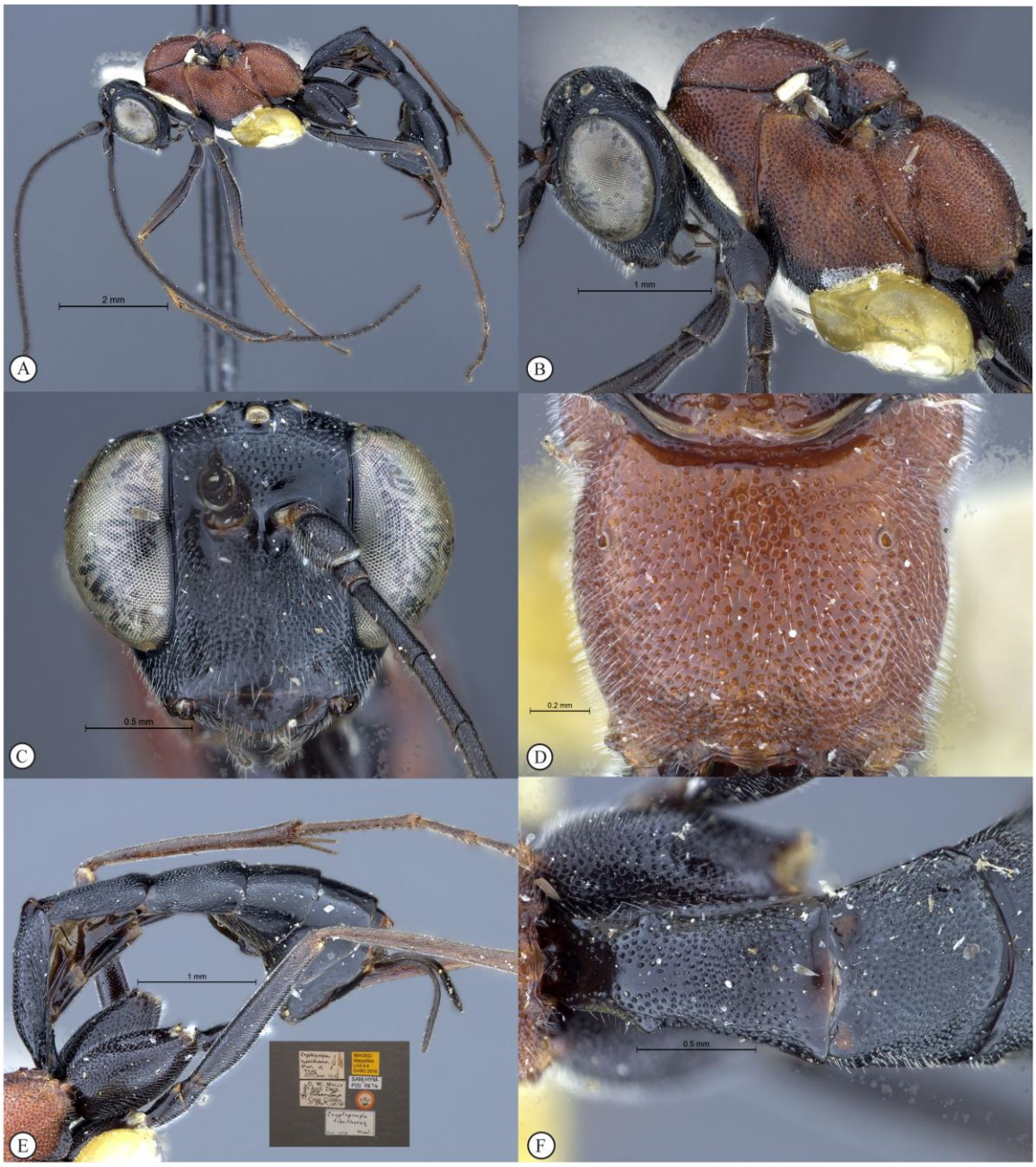

Figure 3.9: *Cryptopimpla rubrithorax* Holotype (A) Habitus, lateral view (B) Head and mesosoma, lateral view (C) Head, anterior view (D) Propodeum, dorsal view (E) Metasoma, lateral view (inset: data labels) (F) Metasomal terga 1 and 2, dorsal view.

Head. Densely punctate. Frons unarmed. Setae on head and clypeus short and sparse. Clypeus profile weakly convex with a curved lip on the ventral margin. Clypeus edge convex. Upper tooth of mandible longer than the lower. Flagellum tapered to a slender

apex. Tentorial pits small or indistinct. Maximum eye width in anterior view 0.6-0.66 shortest inter-ocular distance, eye large in lateral view with maximum width 0.7-0.75 times maximum length.

Mesosoma. Abdomen not compressed. Mesosocutum moderately punctate. Scuto-scutellar groove broad with deep lateral indentations. Epicnemial carinae present ventrally and dorsally, dorsally converging toward anterior edge of mesopleuron. Propodeum lacking carinae, its anterior margin medially straight but may have a blunt medial projection. Wings hyaline. Fore wing with two bullae closely situated appearing as one; vein 2m-cu sinuate; areolet truncate-shaped. Hind wing with one basal hamulus and six distal hamuli.

Metasoma. Tergum 1 densely punctate with dorsolateral carinae substituted with longitudinal wrinkles, posterior margin weakly convex; second tergum 0.8-1.09 times as broad as long, spiracle situated at basal 0.25-0.32 of spiracle (measured in lateral view), gastrocoeli elongate; terga 4-8 slightly compressed; female metasomal tergum 6 half as wide as tergum 5; hypopygium strongly sclerotized.

CT 1.9-2.2; ML 0.9-1.3; IO 1.9-2.4; OO 1.4-2.1; Fl_1 4.3-5.4; OT 0.6; body length 7-8.6 mm; antenna length 7.9-9.7 mm; fore wing length 6.3-6.9 mm.

Differential diagnosis. Reduction of the dorsolateral carinae to longitudinal wrinkles on the metasomal tergum 1 distinguishes this species from the closely-related species *C. fernkloofensis* and *C. neili*. Elongate gastrocoeli on tergum 2 separate the species from *C. fernkloofensis*, *C. elongatus*, *C. hantami* and *C. neili*. The malar space and basal mandibular width are more or less equal in length with the malar space 0.91-1.3 times as long as the basal mandibular width, as opposed to the malar length index being much shorter in the closest related species *C. zwarti*, where the malar space is 0.6 times as long as the basal mandibular width. The shortened malar space in *C. zwarti* produces a more globular head shape, compared to a more lenticular head shape in *C. rubrithorax* due to the longer malar space. *Cryptopimpla rubrithorax* can be further separated from *C. zwarti*

by the length of tergum 2 relative to its width. In *C. rubrithorax* tergum 2 is 0.8-1.09 times broader than long compared to 1.25 times as broad as long in *C. zwarti*.

Etymology. The species epithet is likely to refer to the rufescent colour of the metasoma of this species (Morley 1916).

Distribution. South Africa (Northern and Western Cape).

Comments. This species occurs in three vegetation types, Strandveld, Mesic Mountain Fynbos and Renosterveld, and exhibits corresponding intra-specific variation in terms of colouration. The specimen sampled from mesic mountain fynbos, which has a white pronotal collar and tegula as per Morley's original description, whereas the specimens from the Renosterveld have a black pronotal collar and tegula. Molecular sequencing demonstrated that there is no genetic divergence between specimens associated with the two different habitats (0% sequence divergence for COI, 28S, and 18S), with two site changes on the COI gene sequence. Strandveld specimens also have black pronotal collars and tegulae, but are slightly darker in colour and are blacker ventrally on the mesosoma.

***Cryptopimpla zwarti* Reynolds Berry & van Noort, 2016** (Fig. 3.10)

Type material. HOLOTYPE ♀: South Africa, Eastern Cape, Grahamstown, Faraway Farm 33.19′S 19°26.31′E, April 1990, I. Crampton, Malaise trap, SAM-HYM-P005220 (SAMC).

Description. Body subpolished. Colour. Head black, clypeus and mouthparts brown. Mesosoma rufescent, small black spot on underside; mesotum black only at the wing bases. Front legs: mostly light brown; coxa, trochanter and trochantellus black. Middle & hind legs: coxa to femora mostly black with shades of light brown on the coxa; remaining leg light brown. Metasoma black, terga 6-8 posteriorly white.

Head. Densely punctate. Frons unarmed. Clypeus profile weakly convex with a curved lip on the ventral margin. Clypeus edge convex. Upper tooth of mandible longer than

lower. Setae on head and clypeus short. Tentorial pits small and indistinct. Eye in lateral view 0.71 times as wide as long, maximum width in anterior view 0.66 times shortest inter-ocular distance. Flagellum tapered to a slender apex.

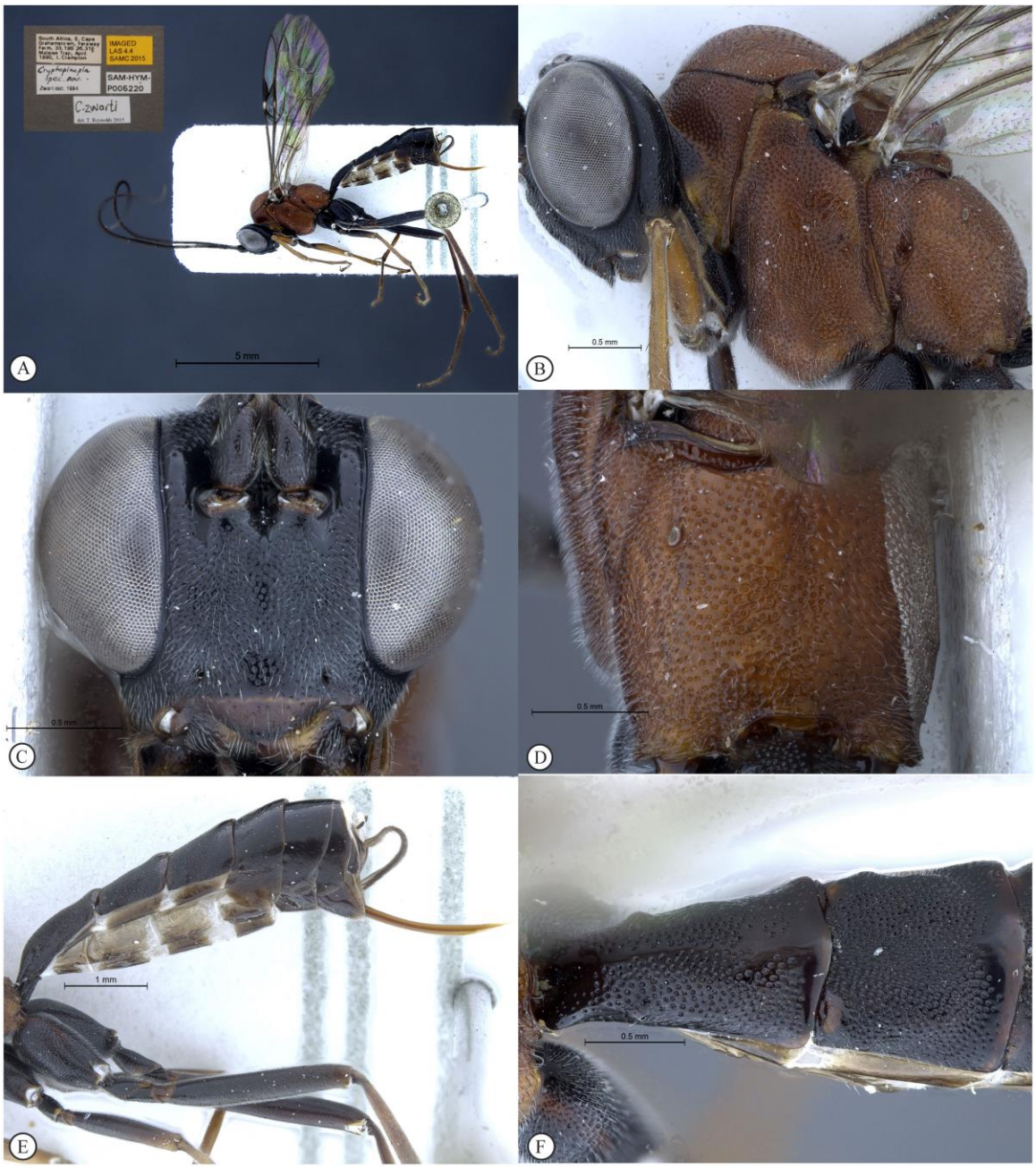

Figure 3.10: *Cryptopimpla zwarti* Holotype (A) Habitus, lateral view (inset: data labels) (B) Head and mesosoma, lateral view (C) Head, anterior view (D) Propodeum, dorsal view (E) Metasoma, lateral view (F) Metasomal terga 1 and 2, dorsal view.

Mesosoma. Abdomen not compressed. Mesosocutum moderately punctate. Broad scuto-scutellar groove with deep lateral indentations. Epicnemial carinae present ventrally and dorsally, dorsally converging toward anterior edge of mesopleuron. Propodeum without carinae, its anterior margin with a blunt median projection. Wings hyaline. Fore wing with two bullae close together appearing as one; vein 2m-cu sinuate; areolet truncate-shaped. Hind wing with one basal hamulus and six distal hamuli.

Metasoma. Slightly compressed. Tergum 1 with dorsolateral carinae substituted with longitudinal wrinkles, densely punctate with posterior margin weakly convex; second tergum 1.25 times broader than long, spiracle situated at basal 0.3 of tergum, gastrocoeli elongate; tergum 6 half as wide as tergum 5; hypopygium strongly sclerotized.

CT 2; ML 0.6; IO 2.2; OO 1.6 OT 0.6; Fl_1 4.9; body length 8.3 mm; antenna length 9.4 mm; fore wing length 6.9 mm.

Differential diagnosis. *Cryptopimpla zwarti* is distinguishable from other Afrotropical *Cryptopimpla* species by having a malar space 0.6 times as long as the basal mandibular width, whereas all the other Afrotropical *Cryptopimpla* species have a ML index of 0.8 or more. A broad scuto-scutellar groove with deep lateral indentations distinguishes *C. zwarti* from closely-related species *C. fernkloofensis, C. neili, C. hantami* and *C. parslactis*. The metasomal tergum 1 with dorsolateral carinae substituted with longitudinal wrinkles distinguishes *C. zwarti* from closely-related species *C. fernkloofensis* and *C. neili*. Gastrocoeli on tergum 2 are elongate separating the species from *C. fernkloofensis, C. elongatus* and *C. hantami*.

Etymology. Named after the retired agricultural entomologist, K. W. Robert Zwart (Wageningen Agricultural University) who first recognized it as a potentially new species in 1994. Noun in genitive case.

Distribution. South Africa (Eastern Cape).

Comments. By having a malar space much shorter than the basal mandibular width (malar index of 0.6), the shape of the head is more globular, which in combination with a

second tergum that is broader than long, separates *C. zwarti* from its closely-related species *C. rubrithorax*, which have a malar space 0.91-1.3 times as long as the basal mandibular width, creating a more lenticular-shaped head, and a second tergum that is 0.92-1.2 times as long as broad (i.e. no more than 1.09 times broader than long).

3.4 Discussion

The review of *Cryptopimpla* in the Afrotropical region allowed for a comparative morphological assessment of these species with *Cryptopimpla* species from other biogeographical regions, highlighting differences in regional suites of character states. The presence of a posterior transverse carina on the propodeum is common in world *Cryptopimpla* species (Townes 1969, Sheng 2011), but usually absent in Afrotropical species, only being present in two of the ten known species. Among the few *Cryptopimpla* species outside of the Afrotropical region that do not possess pleural carinae or a posterior transverse carina are *C. labralis* and *C. escarinata* from North America (Townes & Townes 1978). *Cryptopimpla labralis*, like species within the *rubrithorax* species-group, possesses a weakly convex clypeus. *Cryptopimpla labralis* is distinctly different from species within the *rubrithorax* species-group by having an areolet that is petiolate, the fore wing lengths are 4.3–4.7 mm long and the OO index is 0.42, compared to the *rubrithorax* species-group where the areolet is truncate-shaped, forewing lengths are 5.8–7.2 mm long and the OO index is 0.5–0.6. Unfortunately, the character state for absence/presence of the posterior transverse carinae on the propodeum is not detailed in all of the historical species descriptions and we have not been able to obtain the types to confirm the state of this condition for most of the global species. It is clear, however, that the lack of carinae on the propodeum and a weakly convex clypeus, are character states that are not restricted to African *Cryptopimpla* species assemblages. This should not compromise the taxonomic results since almost all species of *Cryptopimpla* are exclusive of a single biogeographical region (Yu et al. 2018).

Our morphological species-group delimitation is supported by molecular results based on the mitochondrial COI gene (~23% sequences divergence) and the nuclear 28S gene (~4% sequence divergence). Strong support for monophyly of the genus was

obtained from a combined data analysis using both molecular (18S, 28S, COI) and morphological data (Chapter 2).

The species *C. fernkloofensis*, *C. goci*, *C. neili* and *C. parslactis* are described based on a single male specimen. Without the presence of the diagnostic female character of a shortened ovipositor sheath, male *Cryptopimpla* are sometimes confused and incorrectly described as the cosmopolitan banchine genus *Lissonota* (e.g. Gravenhorst 1829, Holmgren 1860). There are, however, a number of morphological characters that can differentiate *Cryptopimpla* from *Lissonota* when only males are available. The apical 0.3–0.4 portion of the flagellum is tapered to a slender apex in *Cryptopimpla* (Townes 1969, Takasuka et al. 2011) whereas the flagellum is not tapered or may be only weakly tapered at the apex in *Lissonota* (Townes 1969). The first metasomal tergum is only moderately narrowed toward the base in *Lissonota* species as opposed to being evenly and rather strongly narrowed toward the base in *Cryptopimpla* species. Lastly, in all *Cryptopimpla* species the upper tooth is distinctly longer than the lower (Townes 1969, Sheng 2011, Takasuka et al. 2011), whereas it is not a consistent character state for *Lissonota*. While these three character states are useful in distinguishing *Cryptopimpla* from *Lissonota*, our placement of *C. fernkloofensis*, *C. goci*, *C. neili* and *C. parslactis* in the genus *Cryptopimpla* is further supported by their overall morphological resemblance to females of their respective species-groups.

Cryptopimpla is only known from South Africa in the Afrotropical region. The genus was previously represented by a single species in the region and the present study has yielded an additional nine species endemic to temperate areas of South Africa. This is unlikely to be a sampling artifact, given the numerous sampling inventories carried out in other African countries, and the absence of additional specimens in international museum collections. *Cryptopimpla* is a predominately northern hemisphere genus, with highest species richness in the temperate regions (Sheng & Zheng 2005, Kuslitzky 2007, Sheng 2011, Takasuka et al. 2011, Yu et al. 2018). This may explain its apparent exclusion from the tropical regions of Africa. Although the winter rainfall Cape region of South Africa has been fairly extensively sampled over the past 25 years, with deployment of numerous long-term (spanning 1 to 5 years) inventory surveys, ensuring that seasonal variation in species assemblages is encompassed, in effect this effort has only just started scratching

the surface with regard to documenting the ichneumonid diversity present in the area. In reality these inventory sites are relatively few and widely spaced, with the implication that the vast majority of the 440 vegetation types (Mucina & Rutherford 2006) in South Africa, Lesotho and Swaziland are still not comprehensively sampled. This fact in combination with the rarity of the genus (only 33 specimens known for the 9 species), with species often represented by a single specimen, suggests that there are still numerous *Cryptopimpla* species to be discovered in South Africa. The current revision has increased the knowledge of African species ninefold and that of the global fauna by ~16%. Further comprehensive sampling will undoubtedly elevate *Cryptopimpla* species richness for the Afrotropical region.

Chapter 4

Identification key to genera of Banchinae (Hymenoptera; Ichneumonidae) occurring in the Afrotropical region with a review of the endemic genus *Tetractenion*

4.1. Introduction

Banchinae is a cosmopolitan group of moderately small to large-sized parasitoid wasps (Gauld et al. 2002). The group is usually well represented in all faunas and amongst the most commonly collected of all ichneumonids (Gauld et al. 2002, Broad et al. 2011). There are roughly 1800 described species and 66 genera of Banchinae currently recognized (Watanabe & Maeto 2012, 2014, Broad 2014, Choi et al. 2015, Reynolds Berry & van Noort 2016, Herrera-Florez 2017, Vas 2017, Watanabe 2017, 2018, Yu et al. 2018, Kasparyan & Kulitzky 2018, Li et al. 2018, Sheng 2018). With the banchine fauna of many areas of the world poorly known and a number of undescribed genera from tropical regions in museum collections, the number of species is certainly far greater (Broad et al. 2011). Within the Afrotropical region, the subfamily is comprised of the tribes Banchini (*Exetastes* group), Glyptini, and Atrophini, and a dichotomous identification key to banchine genera within the Afrotropical region was last produced by Townes and Townes (1973), who provided the most comprehensive taxonomic treatment to date. Nevertheless the generic key is outdated and not supported with applicable illustrations. Subsequently, the genus *Glyptopimpla* Morley was removed from synonymy with *Teleutaea* Förster and considered a valid genus and a senior synonym of *Zygoglypta* Momoi, 1965 and *Orientoglypta* Kuslitzky (Gupta 2002) (i.e. *Glyptopimpla* is now the accepted name). The Afrotropical Banchinae (Hymenoptera: Ichneumonidae) currently comprises 12 genera and 187 described species: *Apophua* Morley, *Atropha* Kriechbaumer, *Cryptopimpla* Taschenberg, *Exetastes* Gravenhorst, *Glyptopimpla* Morley, *Himertosoma* Schmiedeknecht, *Lissonota* Gravenhorst, *Sjostedtiella* Szépligeti, *Syzeuctus* Förster, *Spilopimpla* Cameron, *Tetractenion* Seyrig, 1932 and *Tossinola* Viktorov.

Tetractenion Seyrig belonging to the tribe Banchini is a very rare genus restricted to the Afrotropical region. The genus comprised of only two species, *T. luteum* recorded from continental Africa (Democratic Republic of Congo and Kenya) and *T. acaule* recorded from Madagascar. The purpose of this chapter is to provide an updated generic key to Banchinae in the Afrotropical region, with a revision of the genus *Tetractenion* wherein four new species are described.

4.2. Material and methods

4.2.1. Photographs

Specimens were either pinned or point mounted on black, acid-free cards for examination (using a Leica M205C stereomicroscope with LED light source), photography and long-term preservation. Images were taken using the Leica LAS 4.4 system which comprised a Leica® Z16 microscope with a Leica DFC450 Camera with a 0.63× video objective attached. Leica Application Suite V 4.4 software was installed on a desk top computer. The imaging process, using an automated Z-stepper, was managed using the Leica Application Suite V 4.4 software installed on a desktop computer. Diffused lighting was achieved using a Leica Dome. Images of the types held in Musée Royal de l'Afrique Centrale, Tervuren (RMCA) were kindly made available by Stéphane Hanot and Arnaud Henrard and those in the Muséum national d'Historie naturelle, Paris (MNHN) were kindly made available by Agnièle Touret-Alby. All images presented in this chapter are available at http: //www.waspweb.org (van Noort 2018).

4.2.2 Depositories

Codens follow Arnett et al. (1993)

NHMUK: The Natural History Museum, London, England (Gavin Broad).
MNHN: Muséum national d'Historie naturelle, Paris (Agnièle Touret-Alby)
RMCA: Musée Royal de l'Afrique Centrale, Tervuren (Stéphane Hanot)
SAMC: Iziko South African Museum, Cape Town, South Africa (Simon van Noort).
CASC: California Academy of Sciences, San Francisco, United States of America (Robert Zuparko).

4.2.3 Nomenclature and abbreviations

The morphological terminology follows Wahl and Sharkey (Wahl & Sharkey 1993), but the wing venation nomenclature follows Gauld (1991). Most morphological terms are also defined on the HymAToL website (http://www.hymatol.org) and HAO website (http://portal.hymao.org/projects/32/public/ontology/). The following morphometric abbreviations are used (in order of appearance in the descriptions):

B: body length, from toruli to metasomal apex (mm).
A: antenna length, from base of scape to flagellar apex (mm).
F: front wing length, from tegula to wing apex (mm).
CT (clypeus transversality index): maximum width of clypeus: median height.
ML (malar line index): malar line: basal mandibular width.
IO (inter-ocellar index): shortest distance between posterior ocelli: ocellus diameter.
OO (oculo-ocellar index): shortest distance between eye and posterior ocellus: ocellus diameter.
Fl_n (length index of flagellomere n): length: width of flagellomere n.
OT (ovipositor sheath-tibia index): length of ovipositor sheath: length of hind tibia.

The first three measurements (absolute measures) were measured on all specimens in the type series, with measurements from the primary type reported separately in brackets if necessary.

4.3. Results

4.3.1. Key to Banchinae genera of the Afrotropical region

1. Genal carina with strong sinuation before junction with oral carina (A). Propodeum with complete carination (B). Areolet open (C) ...***Apophua***

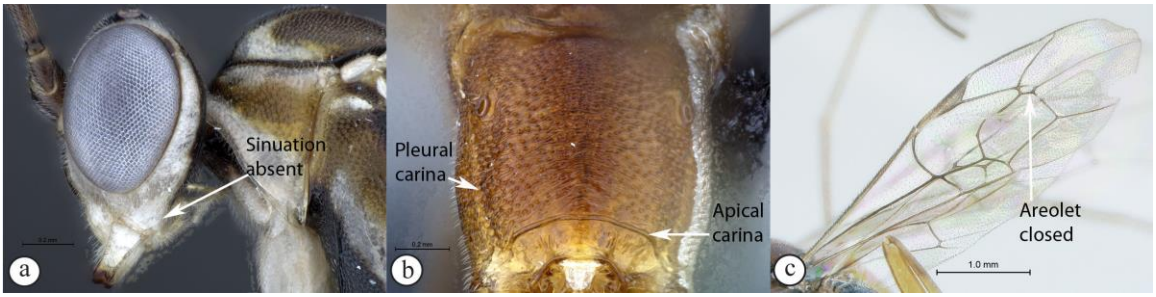

– Genal carina without a strong sinuation (a). Propodeum with apical and pleural carinae present (but rarely complete) or lacking (if apical and pleural carinae are complete then always combined with open areolet (b) Areolet open or closed (c)...**2**

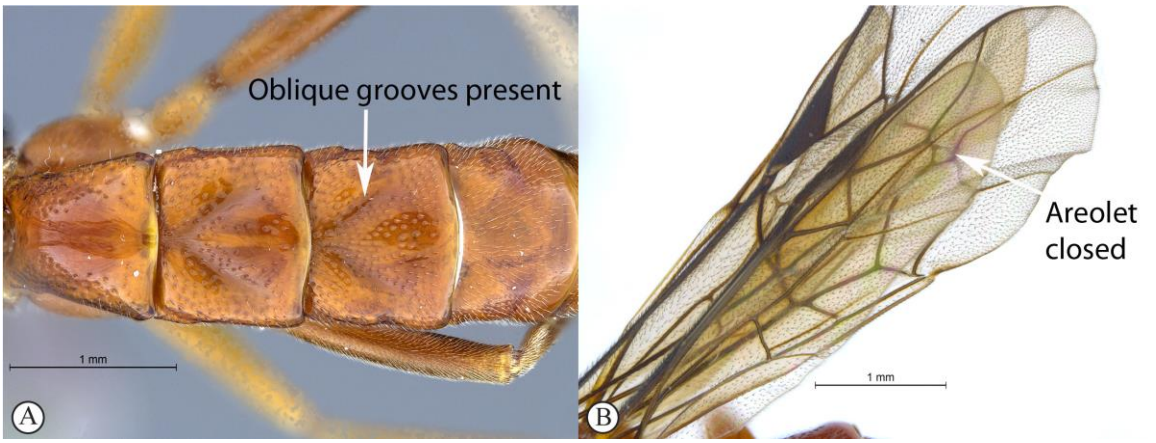

2. Tergites 2-4 with a median pair of (usually) deep oblique grooves that converge anteriorly and diverge posteriorly (A). Areolet closed (B) …**3**

– Tergites 2-4 without a median pair of oblique grooves (a). Areolet open or closed (b) …**4**

3. Cheek 0.5 to 0.8 as long as basal width of mandible (A). Epomia long and strong (B) ...***Glyptopimpla***

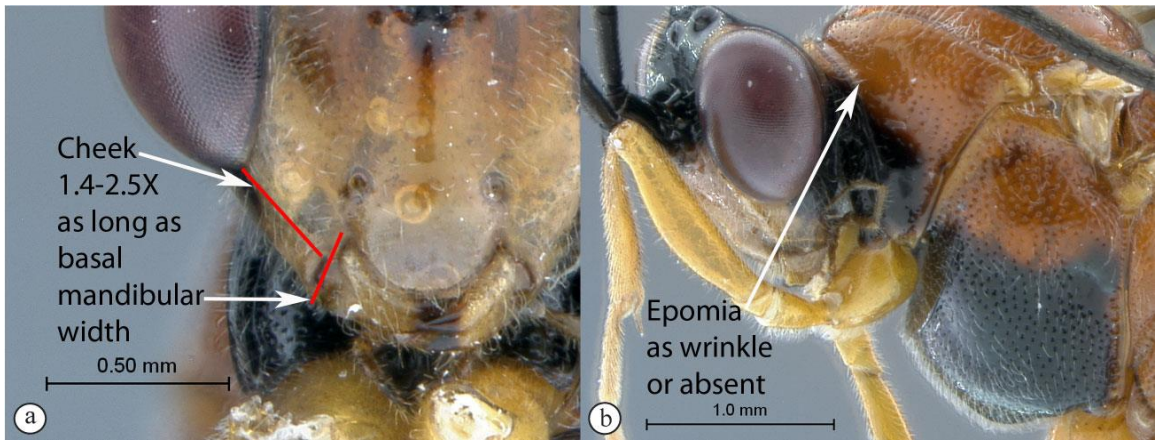

– Cheek 1.4 to 2.5 as long as basal width of mandible (a). Epomia usually absent or indistinct represented by a short wrinkle (b) ...***Sjostedtiella***

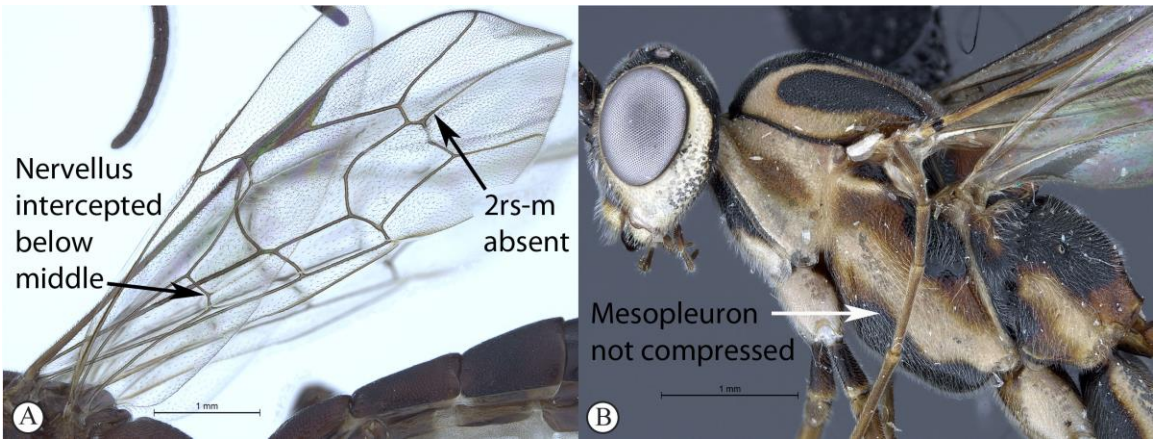

4. Hind wing with nervellus intercepted below the middle, rarely not intercepted; fore wing with second intercubitus (2rs-m) sometimes lacking, shape of areolet when present various (A). Mesopleuron not compressed (B) ...**5**

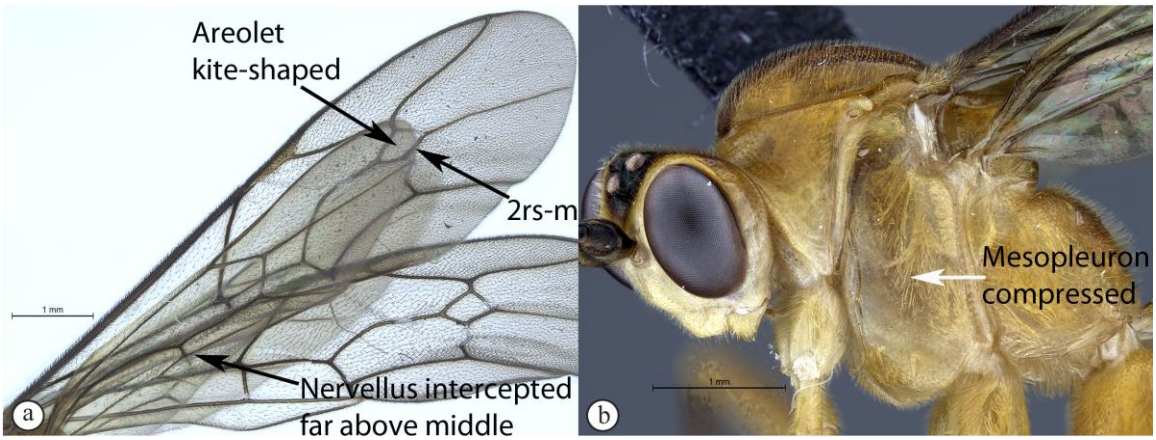

– Hind wing with nervellus intercepted far above the middle; fore wing with second intercubitus (2rs-m) always present, kite-shaped areolet (a). Mesopleuron usually compressed (b) ...**11**

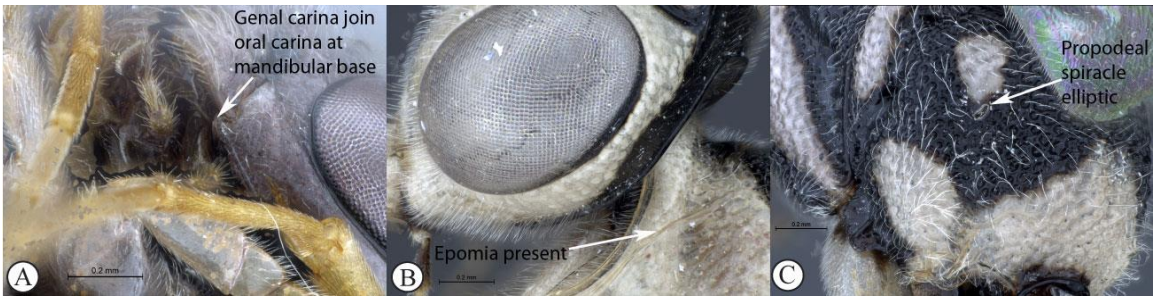

5. Genal carina joining oral carina at base of mandible (A). Epomia usually present (B). Propodeal spiracle elliptic (C) ...***Syzeuctus***

– Genal carina joining oral carina distant from base of mandible (a). Epomia usually absent (b) Propodeal spiracle circular to elongate (c) ...**6**

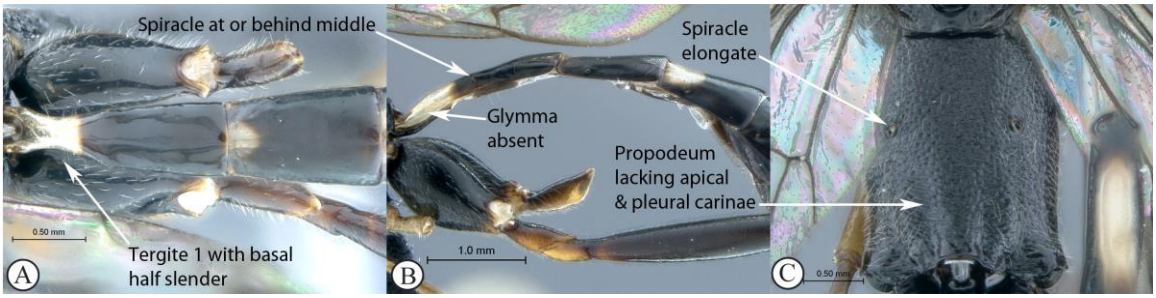

6. Tergite 1 with basal half slender (A), glymma absent (B) and its spiracle at or behind middle (A, B). Propodeum lacking apical and pleural carinae (C). Propodeal spiracle elongate (C) ...***Atropha***

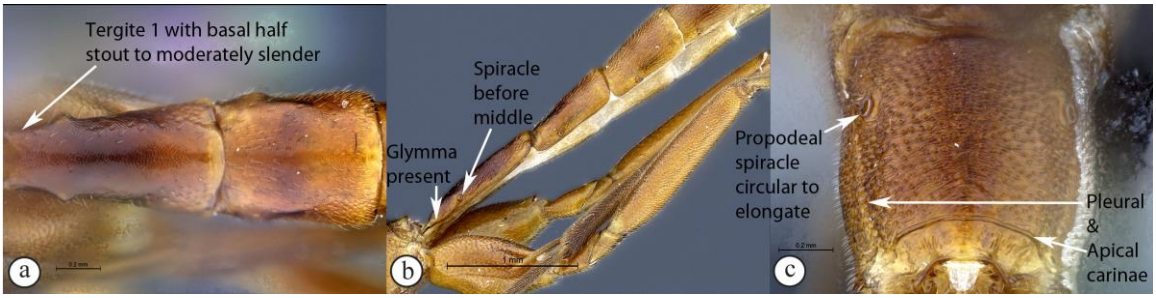

– Tergite 1 with basal half stout to moderately slender, glymma present (a), with spiracle in front of middle (a, b). Propodeum usually with either apical carina or pleural carina, or both (c). Propodeal spiracle circular to elongate (c) ...**7**

7. Occipital carina broadly interrupted above, apex of submetapleural lobe tooth-like (A). Tarsal claws simple with a single basal tooth above (B). Areolet open (C) ...***Tossinola***

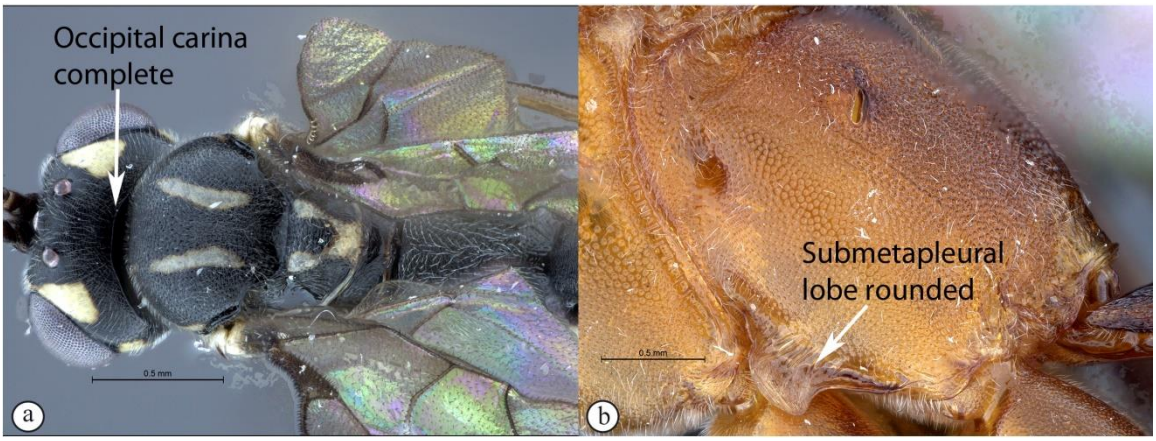

– Occipital carina complete (a). Apex of submetapleural lobe rounded (b). Tarsal claws simple or pectinate. Areolet open or closed ...**8**

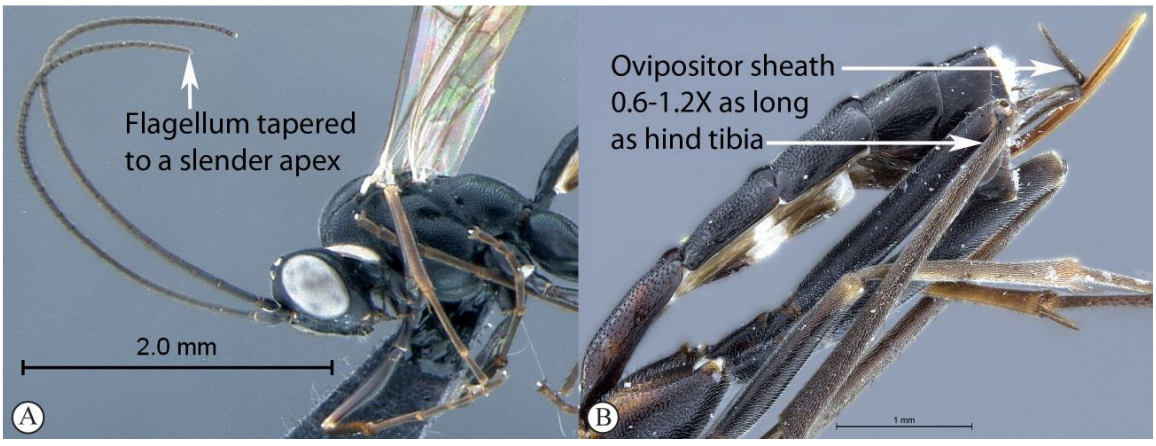

8. Apical 0.3-0.4 of flagellum tapered to a slender apex (A). Ovipositor sheath 0.6-1.2 X as long as hind tibia (B) ...**9**

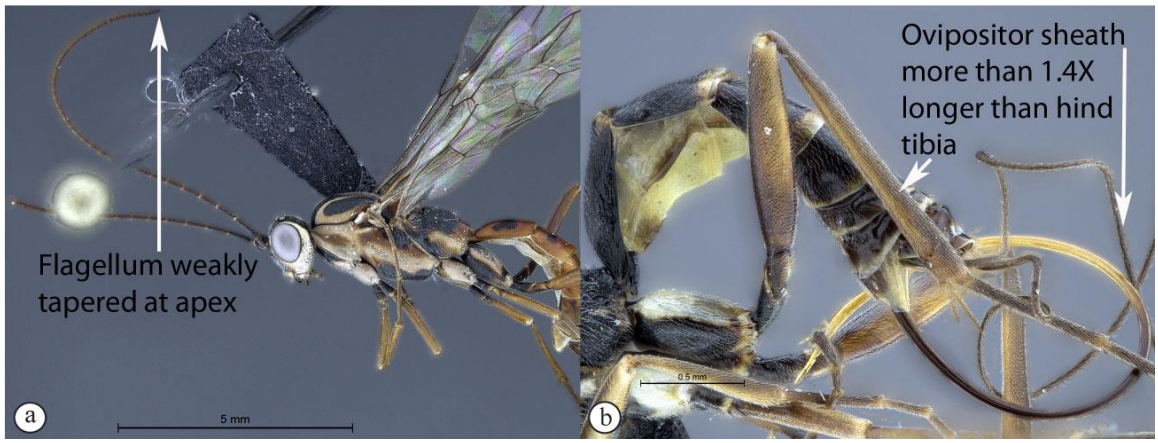

– Flagellum not tapered or may be weakly tapered at the apex (a). Ovipositor usually more than 1.4X as long as hind tibia (b) ...**10**

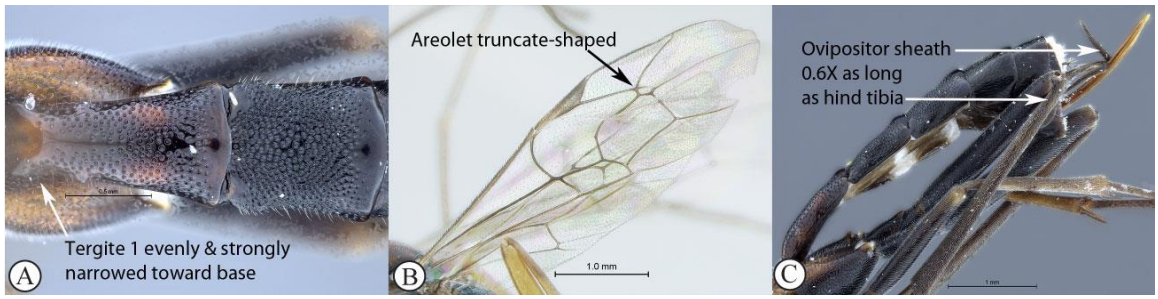

9. First tergite usually evenly and rather strongly narrowed toward base (A). Areolet always truncate-shaped (B). Ovipositor 0.6X as long as hind tibia (C) ...***Cryptopimpla***

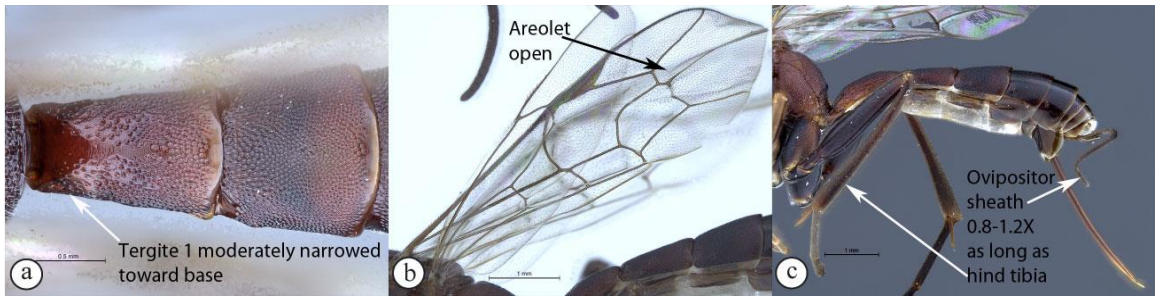

– First tergite only moderately narrowed toward base (a). Areolet always absent (b). Ovipositor 0.8-1.2X as long as hind tibia (c) ....***Spilopimpla***

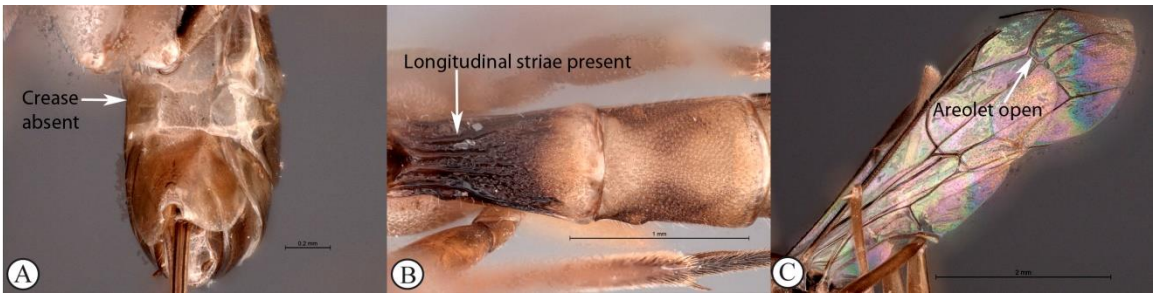

10. Crease separating laterotergite 5 usually absent (A). First tergite nearly always with longitudinal striae (B). Areolet open (C) ...***Himertosoma***

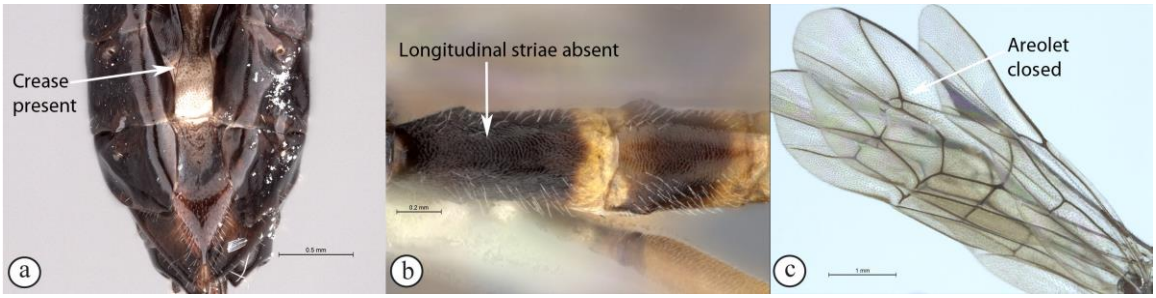

– Crease separating laterotergite 5 present (a). First tergite rarely covered with longitudinal striae (b). Areolet present or sometimes lacking (c) ...***Lissonota***

11. Genal carina joining oral carina above base of mandible (A). Ovipositor sheath short to long (0.14 to 1.8X) as long as hind tibia (B). Length of lower mandibular lower tooth usually equal to upper (C). Clypeal edge not swollen and not connected to the tentorial pits (D) ...***Exetastes***

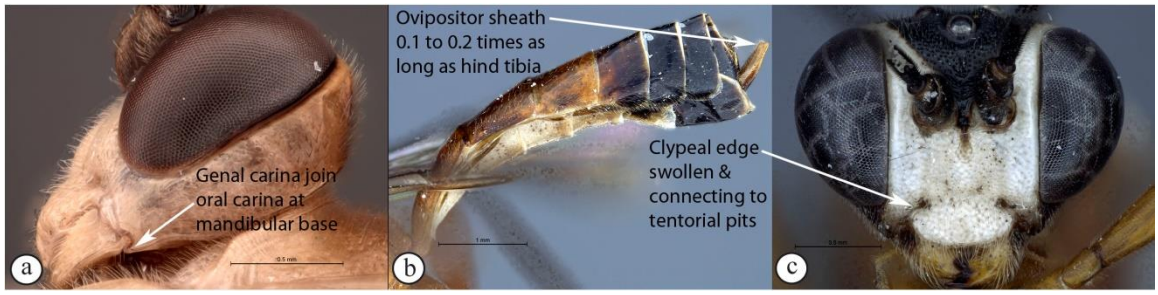

– Genal carina joining oral carina at base of mandible (a). Ovipositor sheath always short 0.1 to 0.2X as long as hind tibia (b). Lower tooth of mandible always longer than upper (c). Clypeal edge swollen and connecting to the tentorial pits (d) ...***Tetractenion***

4.3.2 *Tetractenion* Seyrig, 1932

http://species-id.net/wiki/Tetractenion

Tetractenion Seyrig, 1932, Mém. Acad. Malgache 11: 167. Type: *Tetractenion acaule* Seyrig. Monobasic.

Diagnosis (updated from Townes 1969) Front wing 6.4 to 10 mm, long. Body of moderate proportions, the hind legs long. Frons unarmed. Head with three lobes, tentorial pits deep, clypeus small, convex with declivity and apically turned inside on itself, with clypeus edge straight and swollen ending at the tentorial pits. Antennae long and slender, apically tapered. Teeth of mandible both triangular, the lower tooth longer than the upper tooth. Labium not elongate. Occipital carinae joining genal carinae at the base of mandible. Epicnemial carina present and ending at anterior edge of mesopleuron. Apex of scutellum rounded, notaulus present but faint. Propodeum weakly convex, often with transverse wrinkling and with a posterior transverse carina and lateral longitudinal carinae present but faint or reduced Tarsal claws 1-2 pectinate to apex, tarsal claws 3 pectinate or simple. Areolet is often large and quadrate with a short stalk, receiving second recurrent vein at center. Fore-wing with nervulus opposite basal vein or a little distad, ramellus present or absent on 1m-cu. Hind wing with nervellus intercepted above the middle. Metasomal tergite 1 without dorsolateral carinae. Epipleura of tergite 2 and 3

about 0.15X as wide as long. Apical third of abdomen moderately compressed. Ovipositor sheath about 0.1-0.2 times as long as hind tibia.

4.3.3 Key to Afrotropical species of the genus *Tetractenion*

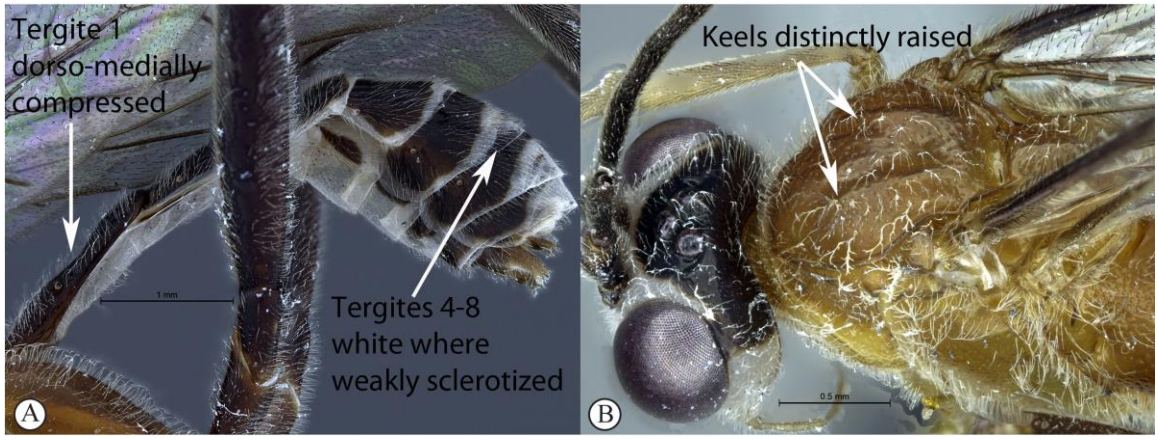

1. Metasomal tergite 1 distinctly dorso-medially compressed, tergites 4-8 white where weakly sclerotized (A). Keels distinctly raised on mesoscutal lobes, notauli do not end at the edge of the scutellum (B) ***...T. acaule***

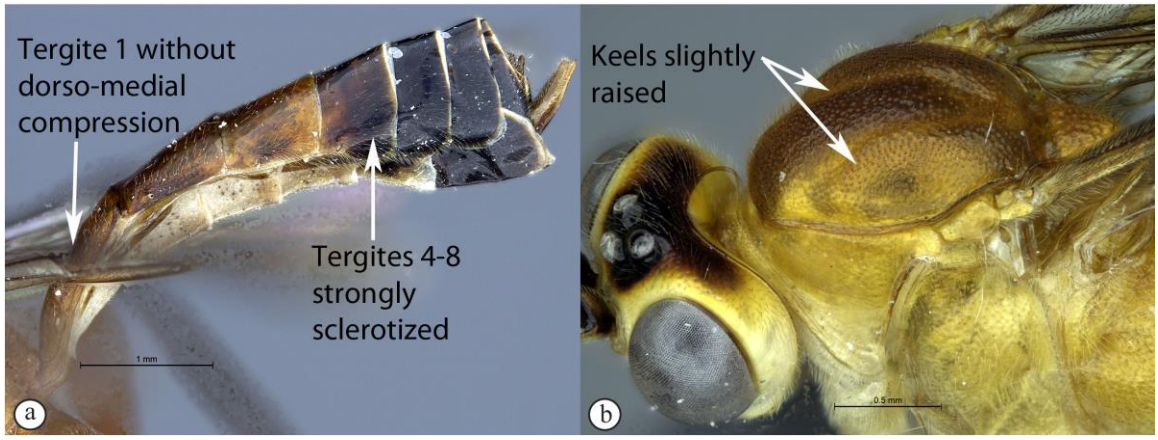

– Metasomal tergite 1 with dorso-medial compression weak or absent, tergites 4-8 strongly sclerotized (a). Keels only slightly raised on mesoscutal lobes, notauli present, but faint, meeting at the edge of the scutellum (b) ...**2**

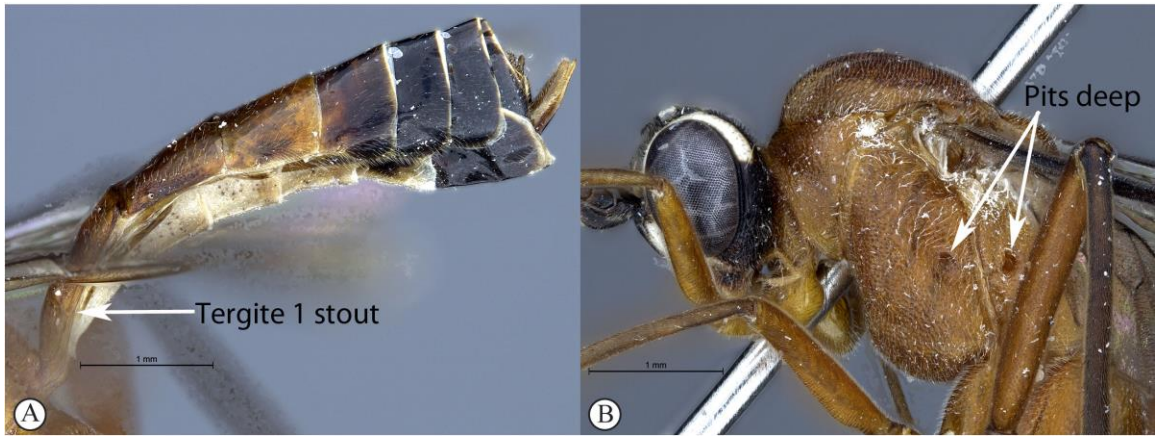

2. Metasomal tergite 1 stout, about as long as wide (A). Pits on the mesopleuron and propodeum are large and deep (B) …***T. ibayaensis* sp. nov.**

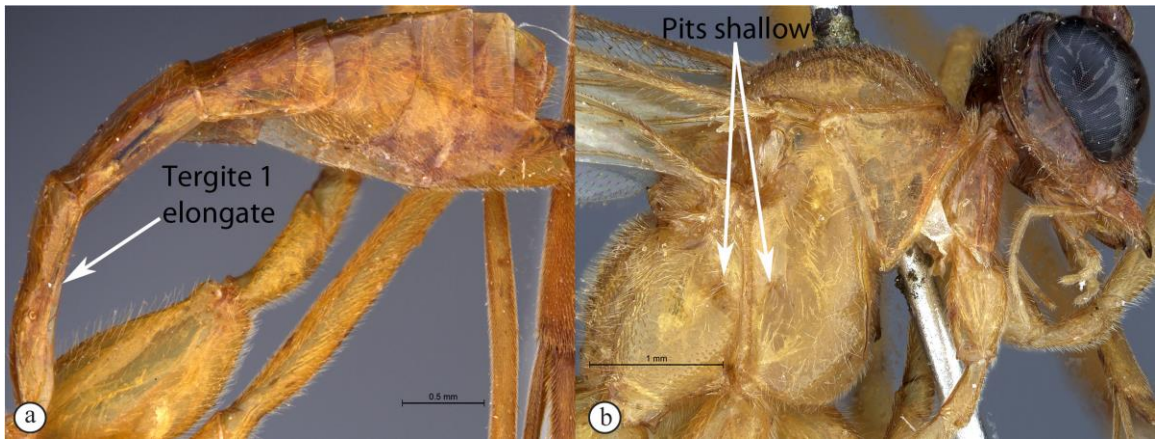

– Metasomal tergite 1 elongated, about twice as long as wide (a). Pits on the mesopleuron and propodeum shallow (b) …**3**

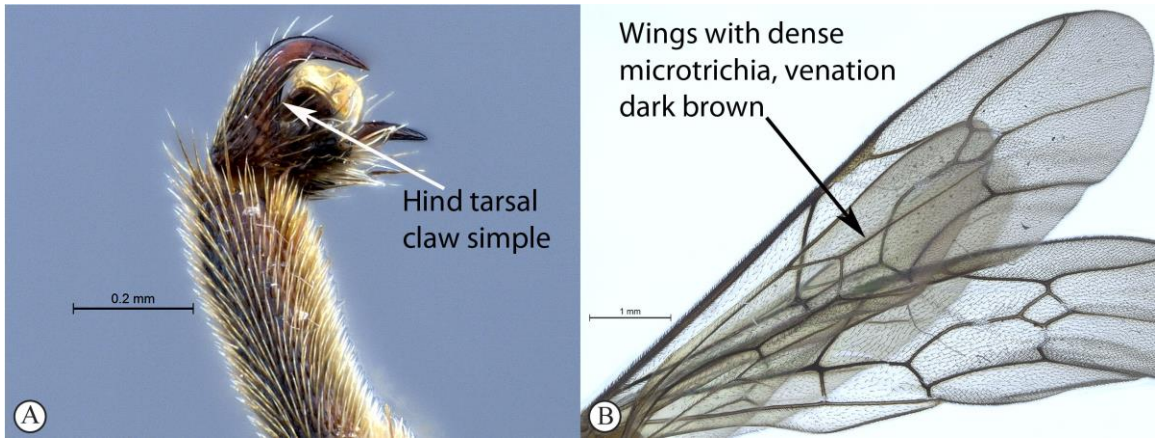

4. Hind tarsal claw simple (A). Wings with dense microtrichia, venation dark (B) ...***T. luteum***

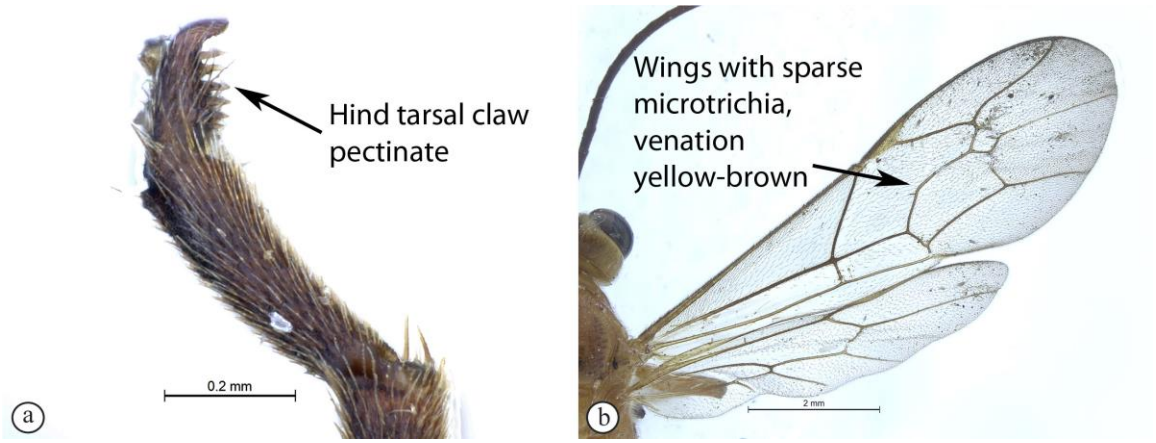

– Hind tarsal claw pectinate (a). Wings with more sparse microtrichia, venation yellowish-brown (b) ...**4**

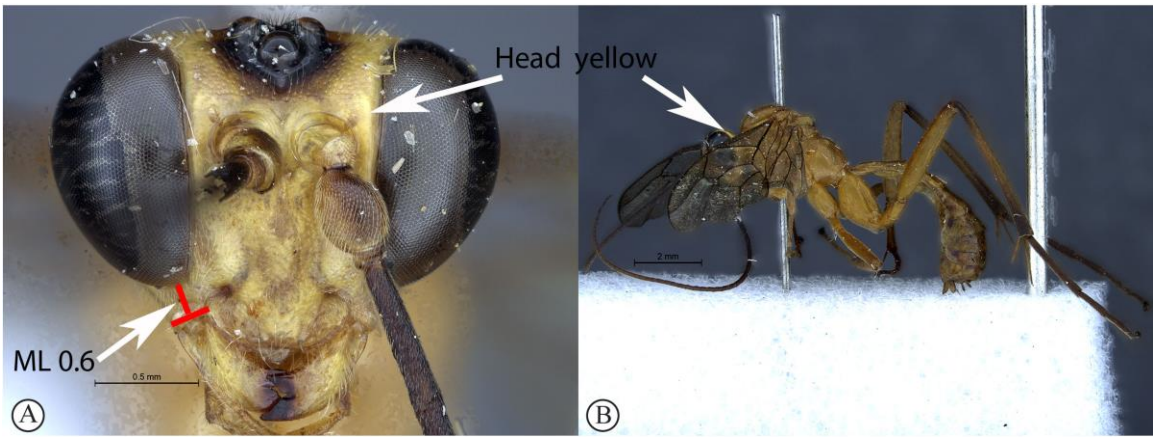

4. ML 0.6 (A). Head yellow, congruent with yellow body (B) ...***T. brucoenesis* sp. nov.**

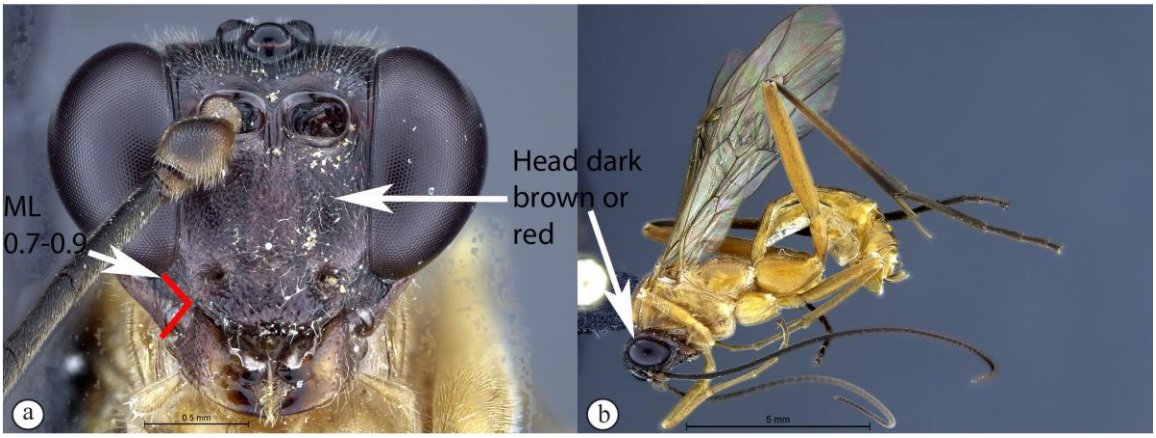

– ML 0.7-0.9 (a). Head dark brown or red, contrasting with yellow body (b) ...**5**

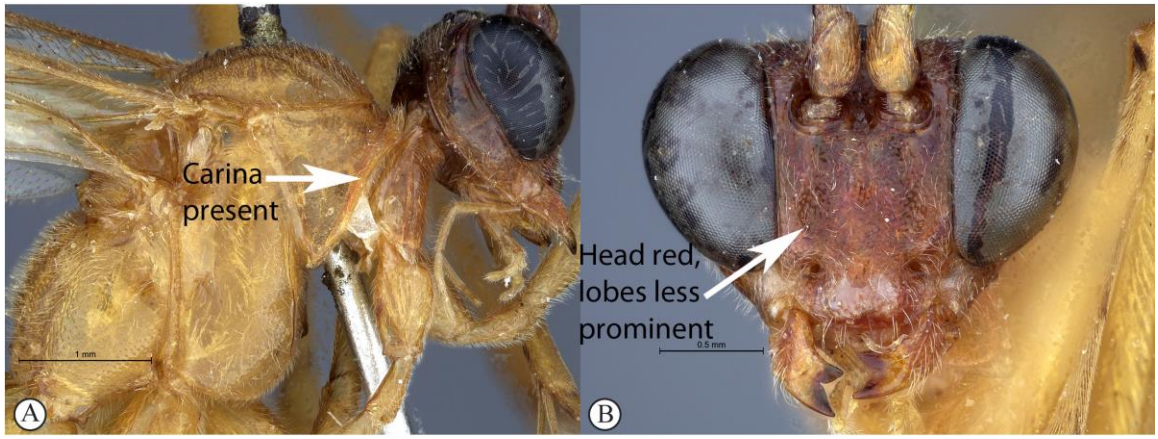

5. Pronotal collar with strong carina present (A). Head red and less robust, face weakly three lobed (B) ...***T. rosei* sp. nov.**

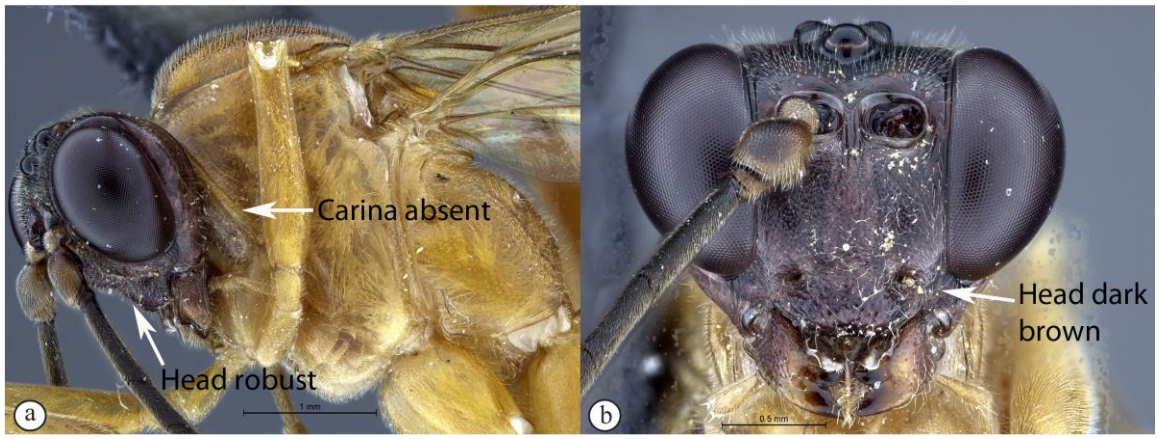

– Pronotal collar weakly wrinkled (a). Head dark brown and more robust, face strongly three-lobed ...***T. pascali* sp. nov.**

4.3.4 Species descriptions

Tetractenion acaule **Seyrig 1932** (Fig. 4.1)

Type material. Lectotype ♂, ♀: Madagascar, Bekily, Reg. Sud. de L'ile, Feb 1930 and Jan-Feb 1931, P.L.G. Benoit, Coll. Mus. Congo (MNHN) (photos of Lectotype examined: http://coldb.mnhn.fr/catalognumber/mnhn/ey/ey9333. **Additional material**. ♀: MADAGASCAR: Majunga Prov. , Besalampy District, Marofototra dry forest, 17 km W of Besalampy, 4-11 February 2008, 16° 43.30′S 44° 25.42′E, Calif. Acad. of Sciences, coll: M.Irwin, R.Harin'Hala, malaise, dry wash in forest, elev 170 ft MG-42A-20 (CASC).

Description (updated from Seyrig 1932). Size 9-11 mm. Head white with a large black central area on occiput, reaching eyes on vertex and pointed on frons; antenna black, without pale ring; mesosoma red; metasomal tergites 1 and 2 red, though tergite 2 sometimes brownish, following tergites black with large membranous white areas from tergite 4; legs red, hind leg femur, tibia and tarsus infuscate; wings with sparse microtrichia, venation brown, stigma brown and centrally translucent reddish.

Head narrow, straight behind eyes; occiput deeply and angularly excavated, occipital carina strong, extending to lower gena at the base of mandible; eyes very large; malar line almost half as long as mandibular basal width; face and clypeus finely, evenly and rather sparsely punctate on a shiny background; face with three lobes, tentorial pits deep, clypeus small, convex with declivity and apically turned inside on itself, with clypeus edge straight and swollen ending at the tentorial pits; mandibular teeth triangular, the lower tooth longer than the upper tooth; antenna long, slender and apically tapered.

Mesosoma stout; mesonotum often compressed on lateral surface, deeply punctate, inter-punctuate spaces about as wide as punctures, rather matt, but not coriaceous; keels are distinctly raised on outer mesoscutal lobes of the mesoscutum, notauli not ending at the scutellum; apex of scutellum rounded; pronotum shining with a distinct thickened carina on the collar, sparsely and very finely punctate; mesopleuron as sparsely but more deeply punctate, speculum similarly punctate, background hardly shining, epicnemial carina ending at anterior edge of mesopleuron; shallow pits on the mesopleuron and propodeum; metapleuron matt and deeply punctate; propodeum weakly convex, dorsally roughly punctate, punctate posteriorly confluently grading into transverse wrinkles, posterior transverse carina reduced, lateral longitudinal carinae present but faint; propodeal spiracle roundish-elliptic, small.

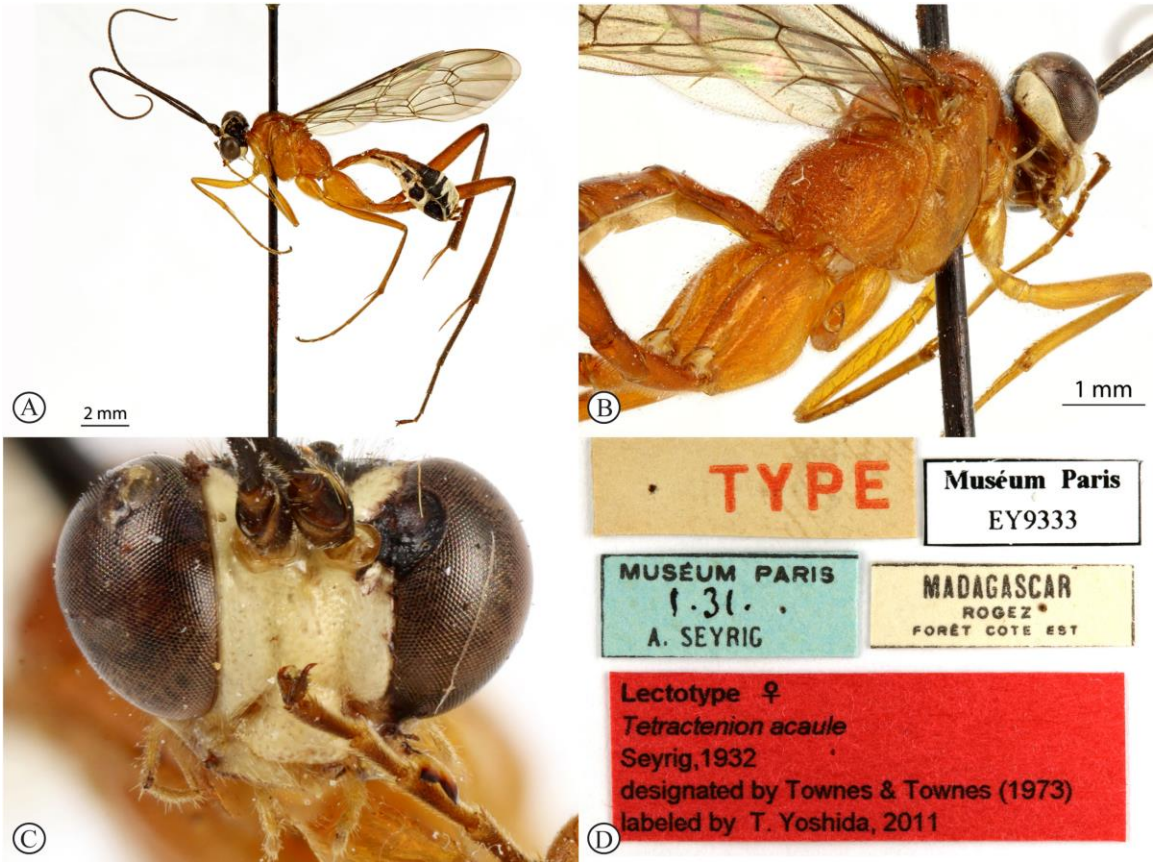

Figure 4.1: *Tetractenion acaule* Lectotype (A) Habitus, lateral view (B) Habitus, dorsal view (C) Head, anterior view (D) and data labels. Photographs of Lectotype © RECOLNAT (ANR-11-INBS-0004) - Christophe Hervé - 2014. http://coldb.mnhn.fr/catalognumber/mnhn/ey/ey9333 (used with permission of Agnièle Touret-Alby – Curator of Hymenoptera MNHN).

Metasoma hardly punctate at base of tergite 2 and indistinctly punctate beyond base; tergite 1 elongate, more than twice as long as wide, basally tapered, glymma present, spiracle positioned slightly in front of middle and protruding, especially dorsally, with a distinct medial depression dorso-ventrally; tergite 2 longer than wide or subquadrate with gastrocoelli distinct; tergite 3 quadrate to transverse; metasomal tergites 4-8 moderately laterally compressed; ovipositor sheath concealed or hardly protruding.

Fore wing without ramellus on rs-m vein; Rs hardly sinuate; areolet large and quadrate with a short stalk, receiving second recurrent vein at center; Hind wing with nervellus

intercepted above the middle. Legs very long, hind femur reaching beyond metasomal apex, length of tibia 3 plus tarsus 3 as long as body; spurs of tibia 3 longer than half metatarsal length.

Male hardly different: temples a bit less narrowed behind eyes, metasomal tergite 2 entirely black.

Differential diagnosis. *Tetractenion acaule* is immediately distinguishable from all other *Tetractenion* species by its unique colour combination of a red mesosoma and a mostly black metasoma; distinct keels present on outer mesoscutal lobes, notauli not reaching the edge of the scutellum; metasomal tergite 1 with distinct medial compression in dorso-ventral view, tergite 2 with gastrocoelli distinct, and tergites 4-8 dorso-posteriorly weakly sclerotized, appearing as large membranous white areas on dorsal surface.

Tetractenion acaule closely resembles *T. ibayaensis* as both species are similar in colour, having largely fulvous bodies with a white face and the hind femur infuscate, whereas the remaining *Tetractenion* species are largely yellow in colour with yellow hind femurs. *Tetractenion acaule* can easily be distinguished from *T. ibayaensis* by having a white cheek and weakly sclerotized metasomal tergites 4-8; head narrow, straight behind the eyes; pronotal collar with a distinct carina present; distinct keels present on outer mesoscutal lobes, notauli not reaching the edge of the scutellum; pits on the mesopleuron and propodeum are shallow; the metasomal tergite 1 distinctly dorso-medially compressed; gastrocoelli on tergite 2 distinct; tergite 4-8 postero-dorsally weakly sclerotized and white; and tarsal claws on the hind leg are simple; whereas in *T. ibayaensis* the cheek is brown and only tergites 4-8 are strongly sclerotized; head is rounded behind the eyes; the pronotal collar with no more than a wrinkle present; mesoscutal lobes hardly present, notauli reaching the edge of the scutellum; pits on the mesopleuron and propodeum are deep; the metasomal tergite 1 stout, indistinctly dorso-ventrally compressed in the medial region ; gastrocoelli on tergite 2 indistinct; and tarsal claws on the hind legs are pectinate.

Distribution. Madagascar.

Tetractenion ibayaensis **Reynolds & van Noort sp. nov.** (Fig. 4.2).

Type material. Holotype ♀:Tanzania, Mkomazi Game Reserve, Ibaya Camp , north west side, 3°57.91'S 37°48.09'E, 22 – 24 April 1996, S. van Noort, *Acacia/Commiphora/Combretum* bushland, Yellow P. Trap, SAM-HYM-P019172 (SAMC).

Description. Mostly fulvous body; tibia and tarsus 3 brown; metasomal tergites 4-8 brown to nearly black; head with face and area around eyes white; frons and occiput dark brown to near black; mandibles yellow with base and tips brown. Sparse microtrichia on the wings, venation and stigma brown.

Head is rounded behind the eyes; occiput deeply and angularly excavated, occipital carina strong, extending to lower gena at mandibular base; malar line half as long as mandibular basal width; eyes very large; face and clypeus finely and evenly punctate on a shiny background; face with three lobes, tentorial pits deep; clypeus small, convex with declivity and apically turned inside on itself, clypeus edge straight and swollen ending at the tentorial pits; mandibular teeth triangular, the lower tooth longer than the upper tooth; clypeal and mandibular hairs long; antenna long, slender and apically tapered.

Mesosoma stout and deeply punctate on a shiny background; mesonotum compressed on lateral surface; epicnemial carina present and ending at anterior edge of mesopleuron; deep pits on the mesopleuron and propodeum; pronotum moderately punctate on a shiny background with no more than a wrinkle on the collar; mesososcutal lobes hardly present on mesoscutum, notauli faint and ending at the edge of the speculum; propodeum weakly convex, posteriorly confluently grading into weak transverse wrinkles, posterior transverse carina indistinct, lateral longitudinal carinae reduced, spiracle small and circular.

Metasoma with tergite 1 stout, basally tapered, not distinctly dorso-ventrally compressed in the medial region, glymma present, spiracle positioned in front of middle and protruding, especially dorsally, hardly punctate dorso-laterally, metasoma indistinctly

punctate beyond and shining; gastrocoelli on tergite 2 indistinct; tergites 2 and 3 quadrate, tergites 4-8 only slightly laterally compressed.

Fore wing without ramellus on rs-m vein; areolet large and quadrate with a short stalk, receiving second recurrent vein at center. Hind wing with nervellus intercepted above the middle. Legs very long; hind femur reaching beyond metasomal apex, length of tibia 3 plus tarsus 3 as long as body; spurs of tibia 3 longer than half metatarsal length; tarsal claws pectinate.

CT 2.1; ML 0.5; IO 1.6; OO 1.6; Fl_1 4.3; OT 0.2; B 8.1mm; A 8.1; F 6.4mm.

Differential diagnosis. *Tetractenion ibayaensis* is immediately distinguishable from other *Tetractenion* species by having a largely fulvous body and a white face, with the occiput, cheeks and metasomal tergites 4-8 dark brown to black, and the hind leg tibia and tarsus infuscate. The clypeal and mandibular hairs are long. The metasoma is hardly laterally compressed with metasomal tergite 1 stout, being about as long as wide. Pits on the mesopleuron and propodeum are visibly large and deep. In addition, the clypeus edge, although swollen, is hardly apically turned inside and the propodeal spiracle is distinctly circular and not circular-elliptic as in the other species.

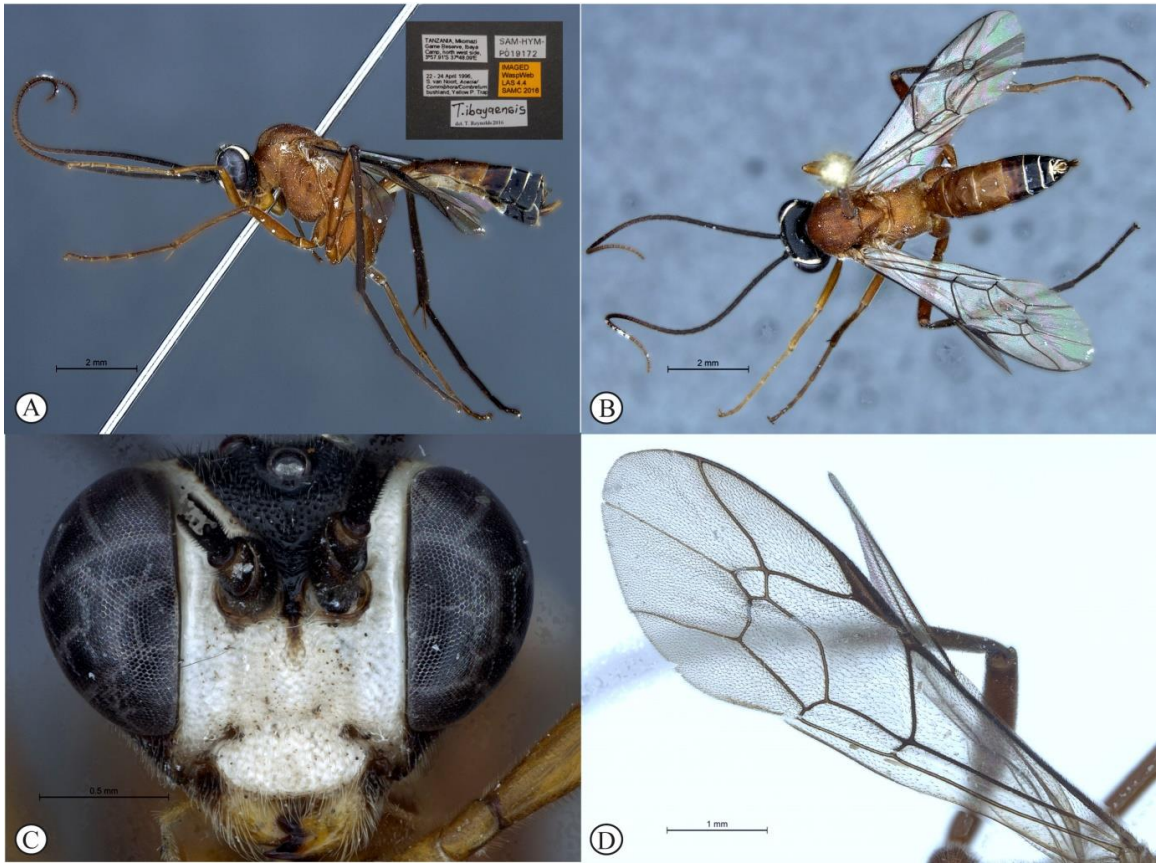

Figure 4.2: *Tetractenion ibayaensis* sp. nov. (A) Habitus, lateral view (insert: data labels) (B) Habitus, dorsal view (C) Head, anterior view (D) and wings.

Head rounded behind the eyes distinguishes the species from *T. acaule* and *T. pascali*. The pronotal collar is no more than a wrinkle, separating the species from *T. acaule* and *T. rosei*. Tarsal claws of the hind legs are pectinate, separating the species from *T. acaule* and *T. luteum*. The wings with sparse microtrichia distinguish *T. ibayaensis* from *T. luteum* and *T. pascali*, and the stigma is brown separating the species from *T. luteum, T. pascali, T. rosei* and *T. pseudolutea*. Metasomal tergites 2 and 3 quadrate separates the species from all other *Tetractenion* species except *T. acaule* where tergite 2 is sometimes subquadrate; and *T. pascali*, and *T. rosei*, respectively. Sparse microtrichia on the wings separates *T. ibayaensis* from *T. pascali* and *T. luteum*.

Etymology. Named after the type locality. Noun in apposition.

Distribution. Tanzania.

Tetractenion luteum Seyrig 1935 (Fig. 4.3)

Type material. Holotype ♂: Mt Kenya, Kenya, June 1932, Muséum National d'Historie Naturelle, Paris. **Paratype** ♀: Elizabethville, Democratic Republic of Congo, 4 January 1921, M. Bequaert, Musée Royal de l'Afrique Centrale, Tervuren. Det. PLG Benoit, 1952. **Additional material**. ♀: South Africa, Eastern Cape, Pearston, Plains of Camdeboo Game Reserve, 32°32.033'S 25°14.267'E, 969m, 30.x.2009- 22.ii.2010, S. van Noort, Malaise Trap, Camdeboo Escarpment Thicket, PCD09-ACA1-M02, SAM-HYM-P047483 (SAMC). ♂, ♀: South Africa, Eastern Cape, Asante Sana Game Reserve, 32°16.762'S 24°57.309'E, 1186m, 6.x.2010- 17.i.2011, S. van Noort, Malaise Trap, Southern Karoo Riviere Riverine Woodland, ASA09-WOO1-M18, SAM-HYM-P047487 (SAMC, NHMUK). ♂: South Africa, Eastern Cape, Asante Sana Game Reserve, 32°16.762'S 24°57.309'E, 1186m, 7 Apr- 28 July 2010, S. van Noort, Malaise Trap, Southern Karoo Riviere Riverine Woodland, ASA09-WOO1-M10, SAM-HYM-P047484 (SAMC). ♂: South Africa, Eastern Cape, Asante Sana Game Reserve, 32°15.841'S 24°57.091'E, 1354m, 6.x.2010- 17.i.2011, S. van Noort, Malaise Trap, Camdeboo Escarpment Thicket, ASA09-BUS1-M17, SAM-HYM-P047485 (SAMC). Namibia, near Windhoek: a bush between kleine Kuppe and Aus Born Mountains, A. Gumovsky, 23-25.xii.2011, SAM-HYM-P047488 (SAMC). ♂: *Exetastes* sp. indet. In B.M. G.J. Kerrich det. 1958. Pres by Com Inst Ent BM 1960-3. U.C. Ibadan, 9.9.1953, Coll. G.H. Caswell, P49.

Description (updated from Seyrig 1935). Size 7.6-10.4mm. Head yellow with black marking on occiput to middle of frons, no contact with eyes on vertex; meso- and metasoma uniformly yellow, as are the legs, but hind tibia with shades of infuscation and hind tarsus infuscate; wings with dense microtrichia, venation brown, stigma yellow.

Head with temple short, rounded behind the eyes; occiput deeply and angularly excavated, occipital carina strong, extending to lower gena at the base of the mandible; eyes very large, malar line a bit shorter than width of mandibular base; face and clypeus finely and evenly and rather sparsely punctate on a matt background; face with three lobes, tentorial pits deep, clypeus small, convex with declivity and apically turned inside

on itself, with clypeus edge straight and swollen ending at the tentorial pits; mandibular teeth triangular, the lower tooth longer than the upper tooth; antenna about as long as body, slender and apically tapered.

Mesosoma stout, matt to subpolished; pronotum finely punctate on a subpolished background with no more than a wrinkle present on the pronotal collar; mesoscutum moderately punctate, mesoscutal lobes hardly present, notauli faint and reaching edge of scutellum; mesonotum and mesopleuron finely punctate; mesonotum compressed on lateral surface, epicnemial carina ending at anterior edge of mesopleuron; shallow pits on the mesopleuron and propodeum; propodeum weakly convex, matt to subpolished, moderately punctate posteriorly confluently grading into transverse wrinkles posterior transverse carina reduced, lateral longitudinal carinae present but faint; spiracle small and circular-elliptic.

Metasoma with a subpolished background, tergite 1 twice as long as wide, glymma present, basally tapered and weak to indistinctly dorso-ventrally depressed in the medial region, spiracle positioned in front of middle and protruding, especially dorsally; tergite 2 longer than wide, gastrocoelli indistinct; tergite 3 quadrate; basal half of tergite 1 and dorso-lateral region of tergite 2 hardly punctate, indistinctly punctate beyond base.

Fore-wing with ramellus absent on rs-m vein; areolet large and quadrate with a short stalk, receiving second recurrent vein at the center. Hind wing with nervellus intercepted above the middle. Legs very long; hind femur reaching beyond metasomal apex, length of tibia 3 plus tarsus 3 as long as body, spurs of tibia 3 longer than half metatarsal length; fore and mid tarsal claws pectinate, hind tarsal claws simple.

Differential diagnosis. *Tetractenion luteum* is immediately distinguishable from the other species in the genus as this species is the only yellow-coloured *Tetractenion* species to possess simple hind tarsal claws and this character is consistent in both sexes.

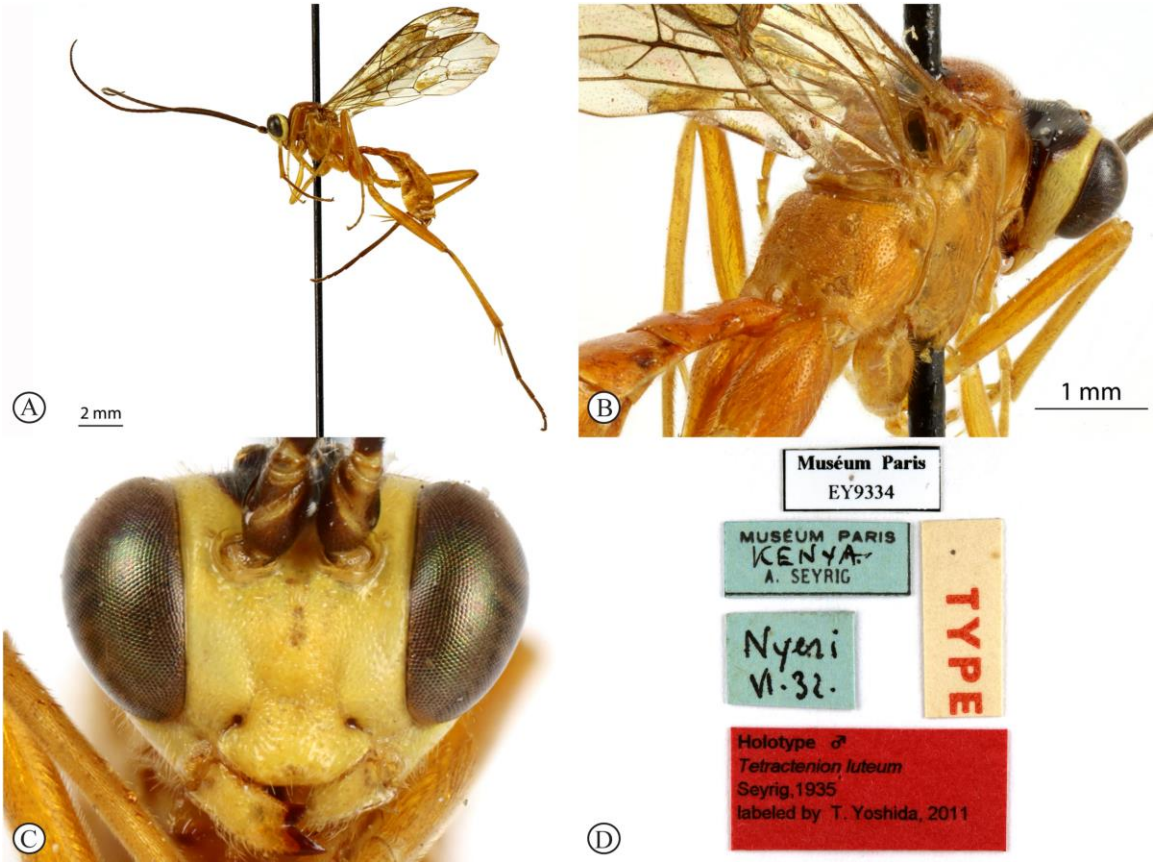

Figure 4.3: *Tetractenion luteum* (A) Habitus, lateral view (B) Habitus, dorsal view (C) Head, anterior view (D) and data labels.

The head rounded behind the eyes distinguishes the species from *T. acaule* and *T. pascali*. Malar line nearly as long as wide as base of mandible separates *T. luteum* from *T. acaule*, *T. pseudolutea* and *T. ibayaensis*. The pronotal collar is weakly wrinkled, separating the species from *T. acaule* and *T. rosei*. The metasomal tergite 2 is longer than wide and distinguishes the species from *T. ibayaensis*; tergite 3 quadrate separates *T. luteum* from *T. pseudolutea*, *T. pascali* and *T. rosei*. *Tetractenion pascali* is the only other species that possess dense microtrichia on the wings.

Distribution. Democratic Republic of Congo, Kenya, Namibia and South Africa.

Tetractenion pascali **Reynolds & van Noort sp. nov.** (Fig. 4.4).

Type material. Holotype ♀: Namibia, near Windhoek, between Mandume Ndemufayo Avenue and Western Bypass, 23.xii.2011, SAM-HYM-P047471 (SAMC). ♂: South Africa, Eastern Cape, Asante Sana Game Reserve, 32°16.762'S 24°57.309'E, 1186m, 23 Feb – 7 April 2010, S. van Noort, Malaise Trap, Southern Karoo Riviere, Riverine Woodland, ASA09-WOO1-M06, SAM-HYM-P044553 (SAMC). ♀: Namibia, near Windhoek: a bush between kleine Kuppe and Aus Born Mountains, A. Gumovsky, 23-25.xii.2011 (NHMUK).

Description. Head brown, mandibles yellow from base to brown at apex. Antennae brown. Body is yellow with red-brown areass on metanotum, tibia 3 with shades of infuscation and tarsus 3 infuscate. Wings with dense microtrichia, stigma yellow, venation brown.

Head narrowed straight behind eyes; occiput deeply and angularly excavated, occipital carina strong, extending to lower gena at mandibular base; malar line nearly as long as basal mandibular width; eyes very large; face and clypeus features robust, mandibles large; face three-lobed and punctate on a shiny background, punctures on the second lobe and clypeus deeper than the punctures on the lobes flanking the eyes; tentorial pits deep; clypeus small, convex with declivity and apically turned inside on itself, with clypeus edge straight and swollen ending at the tentorial pits; mandibular teeth triangular, the lower tooth longer than the upper tooth; antenna long, slender and apically tapered.

Mesosoma stout and moderately punctate on a shiny background; pronotum with no more than a wrinkle on the collar; mesoscutal lobes present on mesoscutum, notauli ending at edge of speculum; epicnemial carina present at ending at anterior edge of mesopleuron; shallow pits on the mseopleuron and propodeum; mesonotum depressed on lateral surface. Propodeum weakly convex, punctate and posteriorly confluently grading into transverse wrinkles with posterior transverse carina present and distinct, lateral longitudinal carinae present but faint and, spiracle small circular-elliptic.

Metasoma indistinctly punctate on a shiny background; tergite 1 elongate, twice as long as wide, basall tapered, dorso-ventrally compressed in the medial region, glymma present, spiracle positioned in front of middle and hardly protruding; tergite 2 longer than wide, gastrocoelli indistinct; tergite 3 longer than wide; tergite 4-8 laterally compressed.

Fore wing without ramellus on rs-m vein; areolet large and quadrate with a short stalk, receiving second recurrent vein at center; hind wing with nervellus intercepted above the middle. Legs very long, hind femur reaching beyond metasomal apex, length of tibia 3 plus tarsus 3 as long as body; spurs of tibia 3 longer than half metatarsal length; tarsal claws pectinate.

Males: similar to females; ramellus present.

CT 2-2.4; ML 0.7-0.9; IO 1.2-1.3; OO 1.6-2.1; Fl_1 4.5-4.8; OT 0.2; B 7.7-11.5mm; A 11-14mm; F 9.2-10mm.

Differential diagnosis. *Tetractenion pascali* is immediately distinguishable from all other *Tetractenion* species by having a colour combination of a largely yellow body and a darkly coloured head. The facial features are more robust compared to the other species, with the 3 lobes on the face prominent and the mandibles larger, and the spiracle on the second tergite of the metasoma is hardly protruding. In addition, though the posterior transverse carina may be reduced or faint in the other species, it is distinct in *T. pascali*.

The malar line nearly as long as wide as base of mandible separates *T. pascali* from *T. acaule, T. pseudolutea* and *T. ibayaensis*. Pectinate hind tarsal claws distinguish *T. pascali* from *T. luteum* and *T. acaule*, and a weakly wrinkled pronotal collar separates the species from *T. acaule* and *T. rosei*. The metasomal tergites 2 and 3 longer than wide separates the species from *T. ibayaensis*; and *T. acaule*, *T. luteum* and *T. ibayaensis*, respectively. *Tetractenion luteum* is the only other species besides *T. pascali* that possess dense microtrichia on the wings.

Etymology. Named after our colleague, Pascal Rousse, who first noted this to be a new species.

Distribution. Namibia and South Africa.

Comments. In males, the ramellus on the fore-wing is present, distiguishing the species *from T. acaule* and *T. luteum*. The wings of *T. rosei* are inter-locked and this character could not be compared.

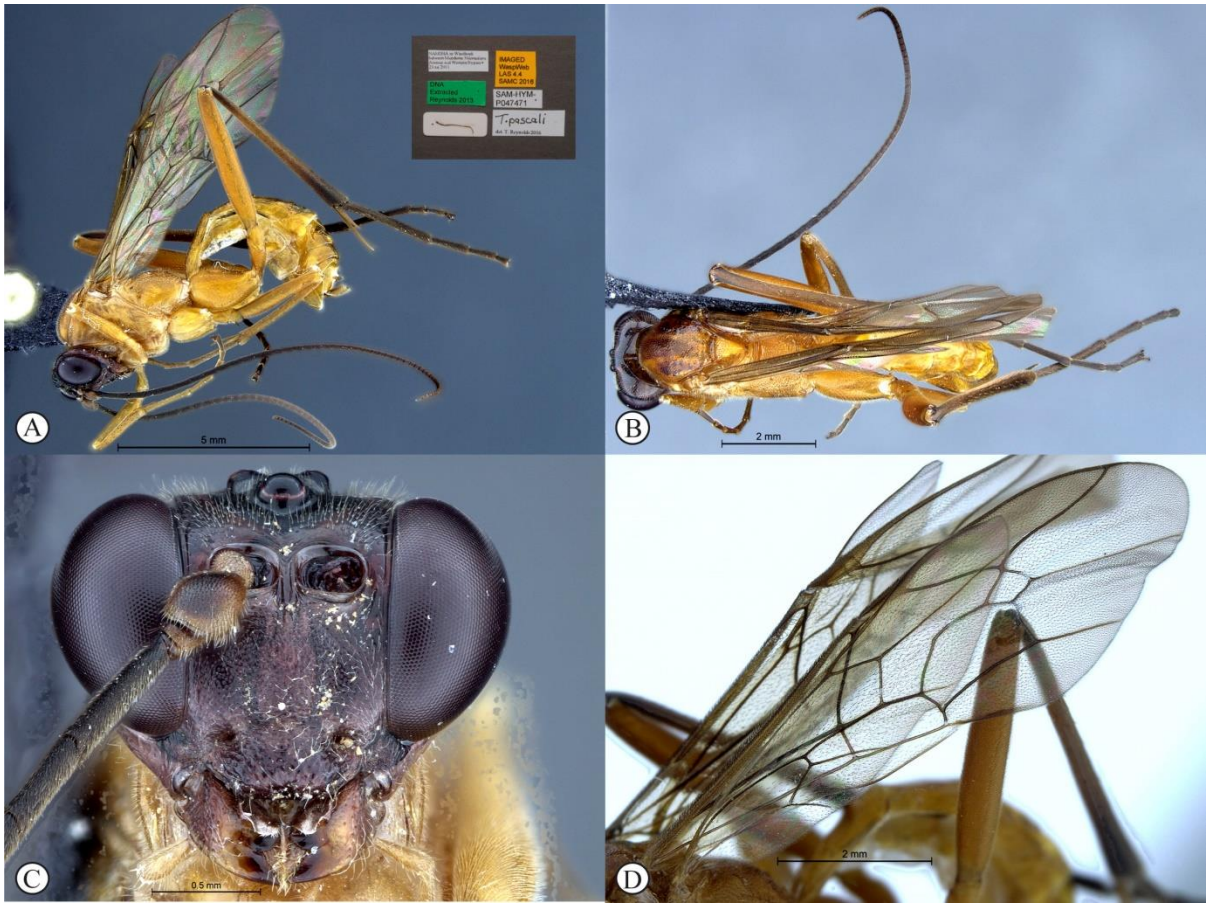

Figure 4.4: *Tetractenion pascali* sp. nov. (A) Habitus, lateral view (insert: data labels) (B) Habitus, dorsal view (C) Head, anterior view (D) and wings.

Tetractenion pseudolutea **Reynolds & van Noort sp. nov.** (Fig. 4.5).

Type material. Holotype ♀: ANGOLA (A11), Bruco, 26.ii – 2.iii.1972, Southern African Exp. B.M. 1972-1 (NHMUK). **Additional material**. 2♀: ANGOLA (A11), Bruco, 26.ii – 2.iii.1972, Southern African Exp. B.M. 1972-1 (NHMUK). ♀: Umbilo, Durban, Natal, 26.10.19, A.L. Bevis, Imp.Inst.Ent.Brit.Mus., 1933-190 (NHMUK). ♂:

Cameroon, Ahal, 28.ix.1953. C.I.E. Coll. 15098. Pres. by Com. Inst. Ent. B.M. 1962-1. *Exetastes* sp. det. J.F. Perkins (NHMUK). ♀: Namibia, near Windhoek, between Mandume Ndemufayo Avenue and Western Bypass, 23.xii.2011, [collector not named] (SAMC).

Description. The colour of the body is the same as *Tetractenion luteum*, except for the density of the microtrichia on the wings. *Tetractenion pseudolutea* has sparse microtrichia on the wings with yellow-brown venation, stigma is yellow.

Head is rounded behind the eyes, occiput deeply and angularly excavated, occipital carina strong, extending to lower gena at the base of the mandible; eyes very large, malar line more than half as long as wide as base of mandible; face and clypeus finely and evenly punctate, background hardly shining; face with three lobes, tentorial pits deep, clypeus small, convex with declivity and apically turned inside on itself, clypeus edge straight and swollen ending at the tentorial pits; mandibular teeth triangular, the lower tooth longer than the upper tooth; antennae long, slender and apically tapered.

Mesosoma stout; mesoscutum deeply punctate, mesoscutal lobes hardly present, notauli faint and ending at the edge of the scutellum; pronotum finely punctate on a shiny background with no more than a wrinkle on the collar; mesopleuron and mesonotum finely punctate; mesonotum compressed on lateral surface, epicnemial carina ending at anterior edge of mesopleuron; shallow pits on the mesopleuron and propodeum; propodeum weakly convex, finely punctate and posteriorly confluently grading into transverse wrinkles, posterior transverse carina reduced, lateral longitudinal carinae present but faint, spiracle small and circular-elliptic.

Metasoma indistinctly punctate on a shiny background; tergite 1 twice as long as wide, glymma present, basally tapered, sometimes weakly dorso-ventrally depressed in the medial region, spiracle positioned in front of middle and protruding, especially dorsally; tergite 2 longer than wide, gastrocoelli indistinct; tergite 3 longer than wide;Tergites 4-8 moderately laterally compressed.

Fore-wing with ramellus rarely present on rs-m vein; areolet large and quadrate with a short stalk, second recurrent vein at the center. Hind wing with nervellus intercepted above the middle. Legs very long, hind femur reaching beyond metasomal apex, length of tibia 3 plus tarsus 3 as long as body, spurs of tibia 3 longer than half metatarsal length; tarsal claws pectinate.

CT 2.3; ML 0.6; IO 0.9-1.0; OO 1.7; Fl_1 4.6-5.6; OT 0.1; B 9.1-10.7mm; A 11.3-11.8mm; F 8.6-9.8mm.

Differential diagnosis. While the colour combinations of *Tetractenion pseudolutea* are identical to *T. luteum,* it is distinguishable from *T. luteum* by by having pectinate tarsal claw on the hind leg.

The head is rounded behind the eyes, separating the species from *T. acaule* and *T. pascali.* The pronotal collar with no more than a wrinkle present distinguishes the species from *T. acaule* and *T. rosei*. The hind leg with tarsal claws pectinate distinguishes *T. pseudolutea* from *T. acaule* and *T. luteum*. The wings with sparse microtrichia, separates the species from *T. luteum* and *T. pascali*; with yellowish-brown venation separating the species from *T. acaule, T. luteum, T. ibayaensis* and *T. pascali;* and a yellow stigma distingushes the species from *T. acaule* and *T. ibayaensis*. Metasomal tergites 2 and 3 longer than wide distinguishes *T. pseudolutea* from *T. ibayaensis*, and *T. acaule, T. luteum* and *T. ibayaensis*, respectively. Sparse microtrichia on the wings separates the species from *T. pascali* and *T. luteum.*

Etymology. This species appears at first glance to be identical in colouration to *T. luteum,* but has morphological differences.

Distribution. Angola, Namibia and South Africa.

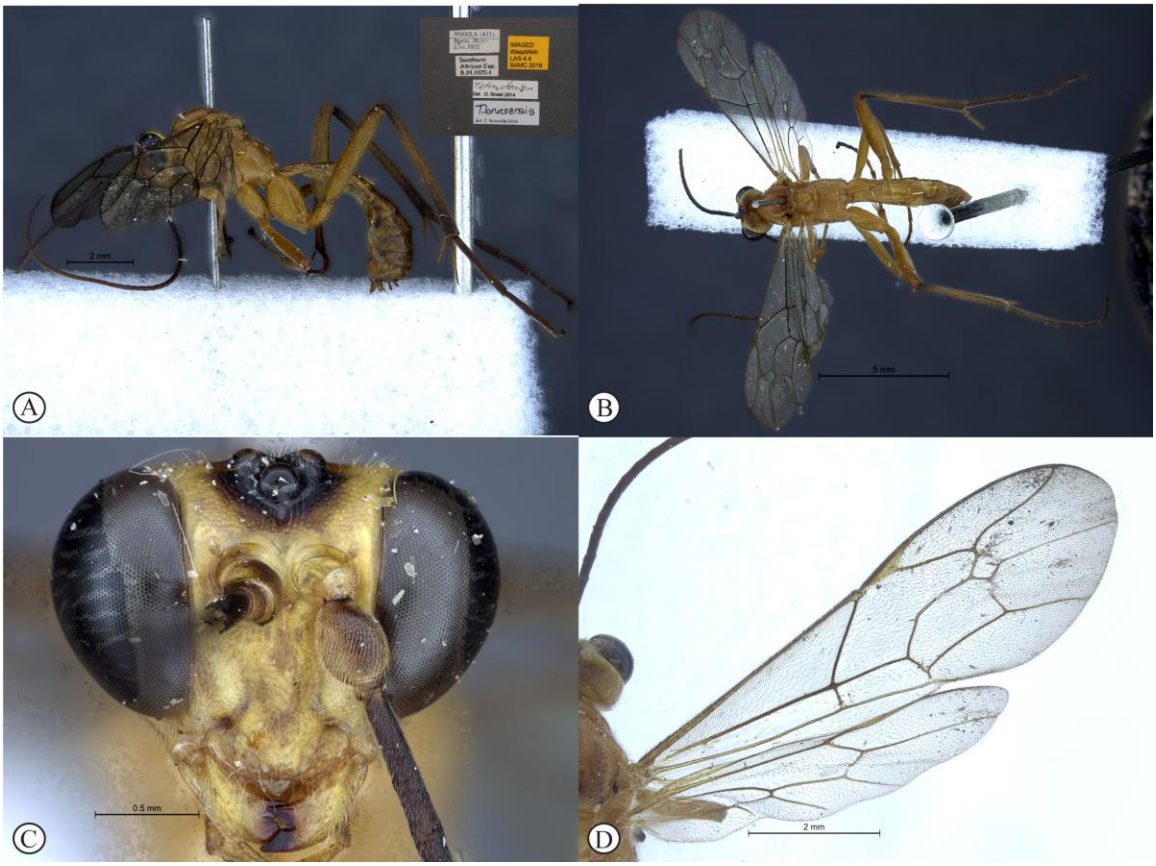

Figure 4.5: *Tetractenion pseudolutea sp.nov.* (A) Habitus, lateral view (insert: data labels) (B) Habitus, dorsal view (C) Head, anterior view (D) and wings.

Tetractenion rosei **Reynolds & van Noort sp. nov.** (Fig. 4.6).

Type material. Holotype ♂Cameroon, Yaoundé, 1953. Pres. by Com. Inst. Ent., B. M. 1962-1. Det. as *Exetastes* sp. by J. F. Perkins, C. I. E. Coll. 15098 (NHMUK).

Description. Head and pronotum reddish, black area restricted to the region of the ocelli. Body, legs, antennae yellow. Wings with sparse microtrichia, venation yellow, stigma yellow.

Head is rounded behind the eyes; occiput deeply and angularly excavated, occipital carina strong, extending to lower gena at mandibular base; malar nearly as long as basal mandibular width; eyes very large; face and clypeus moderately and evenly punctate on a shiny background; face with three lobes, tentorial pits deep; clypeus small, convex with

declivity and apically turned inside on itself, with clypeus edge straight and swollen ending at the tentorial pits; mandibular teeth triangular, the lower tooth longer than the upper tooth; antenna long, slender and apically tapered.

Mesosoma stout with a shiny background; mesopleuron moderately punctate, epicnemial carina present and ending at anterior edge of mesopleuron; shallow pits on the mesopleuron and propodeum; mesonotum moderately punctate, depressed on lateral surface; pronotum sparsely and finely punctate on a shiny background with a well-defined carina on the collar; mesoscutum deeply punctate, mesoscutal lobes hardly present, notauli faint, ending at edge of speculum; propodeum weakly convex, deeply punctate posteriorly confluently grading into transverse wrinkles, posterior transverse carina indistinct; lateral longitudinal carinae present, spiracle small and round.

Metasoma indistinctly punctate on a shiny background; tergite 1 more than twice as long as wide, basally tapered, glymma present, with a slight dorso-ventral depression in the medial region, spiracle in front of middle and protruding; tergites 2 and 3 longer than wide; gastrocoelli on tergite 2 indistinct. Tergite 4-8 laterally compressed.

Hind wing with nervellus intercepted above the middle. Legs very long, hind femur reaching beyond metasomal apex, length of tibia 3 plus tarsus 3 as long as body; spurs of tibia 3 longer than half metatarsal length; tarsal claws pectinate.

CT 1.6; ML 0.9; IO 1.4; OO 2.2; Fl_1 3.5; B 9.3mm; F 8.6mm.

Differential diagnosis. *Tetractenion rosei* is immediately distinguishable from other *Tetractenion* by the reddish colour of the head and pronotum in combination with a yellow body, legs completely yellow and venation on the wings also yellow.

The head not narrowed straight behind the eyes but rather rounded distinguishes the species from *T. acaule* and *T. pascali*. The malar line nearly as long as wide as base of mandible separates *T. rosei* from *T. acaule, T. pseudolutea* and *T. ibayaensis*. *Tetractenion acaule* is the only other species besides *T. rosei* possessing a thickened and well-defined carina on the pronotal collar.

Pectinate hind tarsal claws, separates the species from *T. acaule* and *T. luteum*. The wings with sparse microtrichia separates the species from *T. luteum* and T. *pascali*, and the stigma is yellow distinguishing the species from *T. acaule* and *T. ibayaensis*. The metasomal tergites 2 and 3 longer than wide separates *T. rosei* from *T. ibayaensis*; and *T. acaule*, *T. luteum* and *T. ibayaensis*, respectively.

Figure 4.6: *Tetractenion rosei* sp. nov. (A) Habitus, lateral view (B) Habitus, dorsal view (B) Head, anterior view (D) and wings (insert: data labels).

Etymology. So named because of the reddish colour of the head and pronotal collar. Noun in apposition.

Distribution. Cameroon.

Comments. This is a rare species known only from one female specimen. Sampling in other areas of the Afrotropical region has so far not produced any further specimens. The

wings are inter-locked in such a way that a useful diagnostic character of the wings cannot be seen, i.e. whether the ramellus is present or not.

4.4 Discussion

Since publication of the first key to genera of Banchinae in the Afrotropical region (Townes & Townes 1973), new knowledge on the subfamily has been acquired and there have been recent technological advances allowing for production of good quality images to illustrate relevant characters. The updated key is now more user-friendly.

The morphological characters that were used to update the key to Banchinae genera in the Afrotropical region include:

1. A reduced hypostoma was suggested to be a derived trait in the tribe Atrophini (Wahl 1988).
2. Occipital carina with strong sinuation that curves out onto cheek (Townes 1969). This character, although noted in the global generic key by Townes (1969), was not included in the previously published generic key to Afrotropical Banchinae (Townes & Townes 1973). This is a strong and reliable character distinguishing *Apophua* from the remaining Glyptini genera, *Sjostedtiella* and *Glyptopimpla*.
3. Areolet in Atrophini small when present. The shape of the areolet has been found to be a useful character to separate the genera. For example, it is always truncate in *Cryptopimpla*, generally petiolate when present in *Lissonota* and triangular with a long stalk in *Syzeuctus* and *Atropha*. Thus, when distinguishing the tribes Atrophini and Banchini, the areolet in *Exetastes* and *Tetractenion* is always large and rhombic with a very short stalk, whereas in those Atrophini that possess an areolet it is always small, but variably shaped.
4. A truncate-shaped areolet present in many *Cryptopimpla* species has been reported (Townes 1969, Sheng 2011, Takasuka et al. 2011) to be a character state that is constant for all Afrotropical *Cryptopimpla* species (Reynolds Berry & van Noort 2016). Similarly, in *Lissonota* the shape of the areolet, when present, is nearly always petiolate (i.e. dorsal aspect pointed) (Townes 1969).

5. In the global description of the genus *Exetastes* by Townes (1969), he noted that the length of the lower mandibular tooth relative to the upper could be either equal or slightly longer/shorter. “Slightly” is a poor character, especially concerning mandibular teeth, which wear out throughout the wasp’s life. In the description of the genus, based on Costa Rican species, by Gauld et al. (2002), all species had equal mandibular teeth. Relative length of the mandibular teeth is a more reliable character, if one of the teeth is markedly longer or short. For example, in most Afrotropical *Cryptopimpla* the upper tooth is distinctly longer than the lower (Reynolds Berry & van Noort 2016). Similarly, it has been previously noted (Townes 1969) and further corroborated during this revision of *Tetractenion*, that the upper mandibular tooth is distinctly shorter in all species, making it a diagnostic feature for the genus. While most Afrotropical *Exetastes* have equal mandibular teeth, two undescribed species in SAMC and NHMUK have mandibles with the lower tooth distinctly longer than the upper. This warrants further investigation, because these two genera are closely-related as they form part of the *Exetastes* group. This character may represent a transition between the two genera.
6. The swollen clypeal edge ending at the tentorial pits is a diagnostic feature of *Tetractenion*, while in Afrotropical *Exetastes* the clypeal edge is neither swollen nor connected to the tentorial pits as has been observed in other species (Gauld et al. 2002).
7. The length of the ovipositor sheath relative to the hind tibia has previously been used as an additional character to separate *Tossinola* from the other Afrotropical genera in the tribe Atrophini lacking an areolet (Townes & Townes 1973). However, the relative lengths overlap across *Lissonota*, *Cryptopimpla* and *Tossinola* species, making it an unreliable character to separate these genera. While a medially broadly interrupted occipital carina is still the most diagnostic character for the genus *Tossinola*, another useful character is the state of the apex of the submetapleural carinae: tooth-like in *Tossinola* (Townes 1969), but rounded in the other Afrotropical banchine genera.

8. With the exception of the newly described species *Cryptopimpla pilosus*, where the first tergite is only moderately tapered toward the base, all other Afrotropical *Cryptopimpla* possess a first tergite that is evenly and rather strongly narrowed toward the base (Reynolds Berry & van Noort 2016).
9. The habitus of *Spilopimpla* females is diagnostic with the combination of an open areolet, moderately short ovipositor, and a strongly arched metasoma providing a distinct overall appearance. Given that the areolet can also sometimes be absent in *Lissonota* species, assessment of the sculpturing of the first metasomal tergite is required to separate *Lissonota, Himertosoma* and *Spilopimpla*. In *Spilopimpla,* the first tergite has strong coarse punctures, without longitudinal wrinkles; *Himertosoma* species nearly always have longitudinal striae present and *Lissonota* species rarely possess either strong punctures or longitudinal striae (Townes 1969). The absence of a crease separating the laterotergite of the fifth metasomal tergite has been suggested as the single defining character that separates *Himertosoma* from *Lissonota* (Watanabe & Maeto 2012). This is true for most Afrotropical *Himertosoma*, and therefore a useful character to include in the generic key.

The genus *Tetractenion* was previously represented by two species and the present study has yielded an additional four species restricted to the Afrotropical region. Apart from the *T. rosei* and *T. pseudolutea* specimens that are housed at the Natural History Museum in London, to our knowledge, there are no additional historical specimens present in world collections.

The general habitus and colouration of *Tetractenion* species suggest that this is possibly a nocturnal genus. A list of characters associated with being nocturnal or crepuscular includes a general brown-yellow colour; long antennae; large eyes and large ocelli (Gauld & Huddleston 1976, Warrant et al. 2004, Greiner 2006). In addition, most species with this suite of characters are koinobionts (Quicke 2015). The benefit of being a koinobiont nocturnal species is that these parasitoid wasps are able to access hosts that are hidden during the day; many caterpillars conceal themselves during the day and come out to feed at night (Quicke 2015). Diurnal wasps, on the other hand, are faced with the

pressures of predation and competition for limited resources (Warrant 2008). Where known, all Banchinae are koinobiont endoparasitoids of Lepidopteran caterpillars (Gauld & Mitchell 1978, Gauld et al. 2002, Fernandes et al. 2010, Broad et al. 2011, Tschopp et al. 2013). *Tetractenion* species possess very large eyes and long antennae relative to body size (A = 8.1-14mm, B = 7.6-11.5mm). However, the ocelli were not found to be particularly large (IO = 0.9-1.6, OO = 1.6-2.2); i.e. an ocellus with a large diameter would result in IO and OO indices with values less than one. Like other members of the Banchinae tribe Banchini, *Tetractenion* have very short ovipositors to allow for attack on exposed caterpillars (Fitton 1985, 1987). Members of the tribes Glyptini and Atrophini have ovipositors about as long or longer than the metasoma and exploit semi-to-concealed hosts in leaf rolls, tunnels, buds, etc. (Townes 1969, Quicke 2015). This provides further support that the genus may have evolved to utilize resources not available during the day. With the rarity of this genus and endemicity to the Afrotropical region, *Tetractenion* is also predicted to be a more derived genus within the subfamily Banchinae within the Afrotropical region. Phylogenetic analyses of Banchinae within the Afrotropical region established the tribe Banchini (only the *Exetastes* group is present in the Afrotropical region), represented by *Tetractenion* (only *T. pascali* represented) and two *Exetastes* species, to be the most derived of the three tribes present in the region (Chapter 2). Dating of the genus *Tetractenion* could not be determined based on a single species, but given that *Exetastes* has a cosmopolitan distribution and *Tetractenion* is an African endemic it is likely that *Tetractenion* is the more derived of the two genera.

In reality, sampling of Ichneumonidae across the Afrotropical region has been relatively limited, and in combination with the rarity and endemicity of the genus, and with at least one species represented by only a single specimen, suggests that there are still numerous *Tetractenion* species to be discovered in the region. The current revision has increased the knowledge of the genus threefold. Further comprehensive sampling will undoubtedly elevate *Tetractenion* species richness for the Afrotropical region.

Chapter 5

Conclusions and future directions

As the family Ichneumonidae is of enormous size, encompassing a great variety of parasitoid life history strategies and all lineages have distinct evolutionary histories, it seemed best to investigate the evolution of parasitoid wasps using a small clade within the family. Such a group would be the koinobiont lepidopteran parasitoids of the subfamily Banchinae, with a specific focus on the Afrotropical region, which has been poorly studied. This study has achieved a better understanding of the large-scale diversity patterns of ichneumonid wasps within the subfamily, providing novel data supporting the underlying evolutionary factors driving and maintaining these. The study has embraced multiple biogeographical regions, vegetation types, years, seasons, collecting methods, and identification techniques.

The fossil history of Ichneumonidae in Africa (99-145 mya) and the divergence estimate of Banchinae in the Afrotropical region, including the 95% confidence interval (60-109 mya), coincides with the vicariance event of the Gondwana separation of Southern America from Africa which occurred 95-110 mya (Sanmartín & Ronquist 2004, Kopylov et al. 2010). It's most likely that this vicariance event played a key role in shaping the evolution of Banchinae. All splits within genera are less than 62 mya, long after major continents split up. Thus the cosmopolitan distribution of the subfamily is likely the result of extensive dispersal over time as good dispersal abilities are reported in other ichneumonid subfamilies (Ophioninae, Quicke 2015; Labeninae, Spasojevic et al. 2018). Results suggest that the well-supported Afrotropical banchine clades of *Apophua*, *Cryptopimpla* and *Syzeuctus* diverged during the Eocene epoch, ranging between ~49-35 mya, in line with the age of the oldest known fossil for Banchinae (albeit extant) as well as several other ichneumonid genera (Evanoff et al. 2001, Menier et al. 2004, Spasojevic et al. 2017, 2018).

Divergence estimation for the family Ichneumonidae dates back to 140-190 my (Whitfield 2002, Quicke et al. 2009, Peters et al. 2017), following the diversification of

their lepidopteran major hosts during the Cretaceous era (Grimaldi & Engel 2005). However, ichneumonids were not the group of focus in these studies and therefore the divergence estimate should be treated with circumspection. Previous studies have highlighted the need for a dated phylogeny of the family with age estimates for the subfamilies to better understand the evolution of parasitoid wasps (Spasojevic et al. 2017, 2018). The estimated date of divergence for the subfamily Banchinae in the Afrotropical region provide some insight into ichneumonid wasp evolution, particularly within the Ophioniformes group. It is hypothesized that the subfamily Ophioninae, who like Banchinae belong to the Ophioniformes group, diversified ~65-70 mya (LeGall et al. 2010). In the past, members of Ophioninae have been confused with the subfamily Banchinae. For example, the genus *Skiapus* was first described as a banchine wasp (Morley 1917) and then later recognized as belonging to the Ophioninae based on molecular and additional morphological data (Rousse et al. 2016). While the placement of the *Banchus* group (excluding *Agathilla bradleyi*) with members of the Ophioninae (used as outgroup), based on the available molecular data for the group included in the global total evidence tree, could be as a result of long-branch attraction, the divergence estimate for Ophioninae (LeGall et al. 2010) at least 5 my younger than Afrotropical Banchinae, suggests that the *Banchus* group may be more derived and potentially represents a transition lineage between the two subfamilies.

Divergence estimation support the hypothesis that forest-associated lineages are more basally positioned as the genus *Sjostedtiella*, endemic to the Afrotropical region, dates back to the Paleocene and was most strongly represented in forested regions. The dating of the temperate-associated genus *Cryptopimpla* to the early Eocene refutes the hypothesis that lineages found within the Cape region are more derived. This is probably owing to the worldwide distribution of the genus and also, within a global context, is found to be paraphyletic.

This dissertation has shown that additional research in Afrotropical environments can dramatically increase the knowledge pertaining to banchine species richness. A focus on two of the smaller genera (previously represented by one or two species per genus in the Afrotropical region) in the subfamily has yielded 13 new species. However, the

revision of all genera was beyond the scope of the thesis. The phylogenetic framework has proved most useful in making interpretations and comparisons among and within species. The use of mitochondrial and nuclear DNA combined with the scoring of new and existing morphological characters has contributed to the growing field of evolutionary research within the massive clade of ichneumonid parasitoid wasps.

The taxonomy of parasitoid wasps has great potential to feed into biological control processes because the diversification of organisms with a parasitic lifestyle is often closely linked to the evolution of their host associations (Tschopp et al. 2013). “If a tight host association exists, closely related species tend to attack closely related hosts” (Tschopp et al. 2013). Host records are vital for exposing the level of specialisation and food web dynamics (Veijalainen 2012, thesis). Vice versa, taxonomic data are irrelevant if host records are lacking. In addition, ichneumonids display high levels of host-related morphological homoplasy (Spasojevic et al. 2017). It has been found though, that three species of Glyptini, (two *Glypta* species and *Apophua simplicipes*) and one species of Atrophini, *Lissonota sp.* (Stoltz & Whitfield 1992, Lapointe et al. 2005, 2007) are now known to possess polydnaviruses (PDVs). Polydnaviruses are insect viruses that are injected into the host during oviposition to supress immune physiological responses of the host and enhance parasitoid survival (Strand & Burke 2012, Zhu et al. 2018). This symbiotic relationship also benefits these organisms in the utilization of new niches (Zhu et al. 2018). These PDVs differ considerably in morphology from those present in Campopleginae (also member of the Ophioniformes group), the only other ichneumonid subfamily known to have them (Quicke 2015). In fact, each wasp species has a genetically unique PDV, that does not replicate inside the host and which are replicate-defective outside of the wasp (Burke & Strand 2012). Combined with increasing knowledge on PDVs, the evolutionary opportunity for symbiotic associations is large (Dupuy et al. 2006, Burke & Strand 2012). Furthermore there is also evidence for parasitoid-host coevolution between wasps and fruitflies (Hamerlinck et al. 2016).

What still remains to be done with the taxa used here is to widen sampling, particularly in the Oriental region, and both West and East Africa. The results presented

here illustrate the need for a rigorous evaluation of the diversity of the *Banchus* group which do not seem to form part of the subfamily Banchinae.

References

Althoff DM (2003) Does parasitoid attack strategy influence host specificity? A test with New World braconids. *Ecological Entomology*, 28, 500–502.

Anderson A, McCormack S, Helden A, Sheridan H, Kinsella A, Purvis G (2011) The potential of parasitoid Hymenoptera as bioindicators of arthropod diversity in agricultural grasslands. *Journal of Applied Ecology*, 48, 382–390.

Arnett RH, GA Samuelson, GM Nishida (1993) *The insect and spider collections of the world*. Sandhill Crane Press, Gainsville, Florida.

Aubert JF (1978) Les ichneumonides ouest-palaearctiques et leurs hôtes 2. Banchinae et Suppl. aux Pimplinae. Laboratoire d'Evolution des Etres Organises, Paris & EDIFAT-OPIDA, Echauffour; Paris.

Belshaw R, Fitton MG, Herniou E, Gimeno C, Quicke DLJ (1998) A phylogenetic reconstruction of the Ichneumonoidea (Hymenoptera) based on the D2 variable region of 28S ribosomal RNA. *Systematic Entomology*, 23, 109–123.

Belshaw R, Quicke DLJ (1997) A molecular phylogeny of the aphidiinae (Hymenoptera: Braconidae). *Molecular Phylogenetics and Evolution*, 7, 281-293.

Belshaw R, Quicke DLJ (2002) Robustness of ancestral state estimates: evolution of life history strategy in ichneumonid parasitoids. *Systematic Biology*, 51, 450-477.

Benoit PLG (1959) Hymenoptera: Ichneumonidae (Banchinae, Bassinae, Pimplinae et Tryphoninae). *South Africa Animal Life*, 6, 441-482.

Bossert S, Murray EA, Blaimer BB, Danforth BN (2017) The impact of GC bias on phylogenetic accuracy using targeted enrichment phylogenomic data. *Molecular Phylogenetics and Evolution*, 111, 149-157.

Broad GR (2010) A review of the genus *Geraldus* Fitton (Hymenoptera: Ichneumonidae: Banchinae), with description of a new species. *Journal of Natural History*, 44, 1419–1425.

Broad GR (2014) A revision of *Sachtlebenia* Townes, with notes on the species of

Townesion Kasparyan (Hymeoptera: Ichneumonidae: Banchinae). *Proceedings of the Russian Entomological Society*, 85, 63-76.

Broad GR, Sääksjärvi IE, Veijalainen A, Notton DG (2011) Three new genera of Banchinae (Hymenoptera: Ichneumonidae) from Central and South America. *Journal of Natural History*, 45, 1311–1329.

Brock JP (2017) The banchine wasps (Ichneumonidae: Banchinae) of the British Isles .*Handbooks for identification of British insects, 7*. Royal Entomological Society, London, UK.

Brown JW, Janzen DH, Hallwachs W (2013) A food plant specialist in Sparganothini: a new genus and species from Costa Rica (Lepidoptera, Tortricidae). *ZooKeys*, 303, 53–63.

Burgess N, Clarke GP, Rodgers WA (1998) Coastal forests of eastern Africa: status, endemism patterns and their potential causes. *Biological Journal of the Linnean Society*, 64, 337–367.

Burke GR, Strand MR (2012) Polydnaviruses of parasitic wasps: domestication of viruses to act as gene delivery vectors. *Insects*, 3, 91-119.

Buffington ML, Burks R, McNeil L (2005) Advanced techniques for imaging microhymenoptera. *American Entomologist*, 51, 50–54.

Buffington ML, Gates M (2009) Advanced imaging techniques II: using a compound microscope for photographing point-mount specimens. *American Entomologist*, 54, 222–224.

Butcher BA, Smith MA, Sharkey MJ, Quicke DLJ (2011) A new derived species group of *Aleiodes* parasitoid wasps (Hymenoptera, Braconidae, Rogadinae) from Asia with descriptions of three new species. *Journal of Hymenoptera Research*, 23, 35–42.

Campbell V, Legendre P, Lapointe F-J (2011) The performance of the Congruence Among Distance Matrices (CADM) test in phylogenetic analysis. *BMC Evolutionary Biology*, 11:64.

Chandra G, Gupta VK (1977) Ichneumonologia Orientalis, 7. The tribes Lissonotini and Banchini (Hymenoptera: Ichneumonidae: Banchinae). *Oriental Insects Monograph*, 7, 1-290.

Choi JK, Kang GW, Lee JW (2015) Two new species of *Leptopatopsis* Ashmead (Hymenoptera: Ichneumonidae: Banchinae) from South Korea and gynandromorphy in *L. nigricapitis*. *Zootaxa*, 3964, 275-287.

Clausnitzer V (2003) Dragonfly communities in coastal habitats of Kenya: indication of biotope quality and the need of conservation measures. *Biodiversity and Conservation*, 12, 333–356.

Couvreur TLP, Chatrou LW, Sosef MSM, Richardson JE (2008) Molecular phylogenetics reveal multiple tertiary vicariance origins of the African rain forest trees. *BMC Biology*, 6:54

Cowling SA, Cox PM, Jones CD, Maslin MA, Peros M, Spall SA (2008) Simulated glacial and interglacial vegetation across Africa: implications for species phylogenies and trans-African migration of plants and animals. *Global Change Biology*, 14, 827–840.

Crisci JV (2001) The voice of historical biogeography. *Journal of Biogeography*, 28, 157–168.

Cronk QC (2009) Evolution in reverse gear: the molecular basis of loss and reversal. *Cold Spring Harbor Symposia on Quantitative Biology*, 74, 259-266.

Crosskey RW, White GB (1977) The Afrotropical region. *Journal of Natural History*, 11, 541–544.

Daniels SR, Cumberlidge N, Pérez-Losada M, Marijnissen SA, Crandall KA (2006) Evolution of Afrotropical freshwater crab lineages obscured by morphological convergence. *Molecular Phylogenetics and Evolution*, 40, 227–235.

Darriba D, Taboada GL, Doallo R, Posada D (2012) jModelTest 2: more models, new heuristics and parallel computing. *Nature Methods*, 9:772.

Datson PM, Murray BG, Steiner KE (2008) Climate and the evolution of annual/perennial life-histories in *Nemesia* (Scrophulariaceae). *Plant Systematics and Evolution*, 270, 39-57.

Dupont L (2011) Orbital scale vegetation change in Africa. *Quaternary Science Reviews*, 30, 3589–3602.

Dupuy C, Huguet E, Drezen JM (2006) Unfolding the evolutionary story of polydnaviruses. *Virus Research*, 117, 81-89.

du Toit N, Jansen van Vuuren B, Matthee S, Mathee CA (2012) Biome specificity of distinct lineages within the four-striped mouse *Rhabdomys pumilio* (Rodentia: Muridae) from southern Africa with implications for taxonomy. *Molecular Phylogenetics and Evolution*, 65, 75-86.

Eernisse DJ, Kluge AG (1993) Taxonomic congruence versus total evidence, and amniote phylogeny inferred from fossils, molecules, and morphology. *Molecular Biology and Evolution*, 10, 1170–1195.

Engelbrecht HM, Mouton PLN, Daniels SR (2011) Are melanistic populations of the Karoo girdled lizard, *Karusasuarus polyzonas*, relics or ecotypes? A molecular investigation. *African Zoology*, 46, 146-155.

Evanoff E, McIntosh WC, Murphey PC (2001) Stratigraphic summary and 40Ar/39Ar geochronology of the Florissant Formation, Colorado. In: Evanoff E, Gregory-Wodzicki KM, Johnson KR (eds.). Fossil flora and stratigraphy of the Florissant Formation, Colorado. *Proceedings of the Denver Museum of Nature and Science, Series* 4, no. 1, pp. 1-16.

Fang F, Sun H, Zhao Q, Lin C, Sun Y, Gao W, Xu J, Zhou J, Ge F, Liu N (2013) Patterns of diversity, areas of endemism, and multiple glacial refuges for freshwater crabs of the genus *Sinopotamon* in China (Decapoda: Brachyura: Potamidae). *PLoS ONE*, 8:e53143.

Feakins SJ, Peter B, Eglinton TI (2005) Biomarker records of late Neogene changes in northeast African vegetation. *Geology*, 33, 977–980.

Fernandes LBDR, Dias Filho MM, Fernandes MA, Penteado-Dias AM (2010)

Ichneumonidae (Hymenoptera) parasitoids of Lepidoptera caterpillars feeding on *Croton floribundus* Spreng (Euphorbiaceae). *Revista Brasileira de Entomologia*, 54, 263–269.

Fisher BL (1996) Origins and affinities of the ant fauna of Madagascar. *Biogeographie de Madagascar*, 1996, 457–465.

Fitton MG (1985) The ichneumon-fly genus *Banchus* (Hymenoptera) in the Old World. *Bulletin of the British Museum (Natural History)*, 51, 1–60.

Fitton MG (1987) A review of the *Banchus* group of ichneumon-flies, with a revision of the Australian genus *Philogalleria* (Hymenoptera: Ichneumonidae). *Systematic Entomology*, 12, 33–45.

Folmer O, Black M, Hoeh W, Lutz R, Vrijenhoek R (1994) DNA primers for amplification of mitochondrial cytochrome c oxidase subunit I from diverse metazoan invertebrates. *Molecular Marine Biology and Biotechology*, 3, 294-299.

Gauld ID (1985) the phylogeny, classification and evolution of parasitic wasps of the subfamily Ophioninae (ichneumonidae). *Bulletin of the British Museum (Natural History)*, 51, 1-185.

Gauld ID (1988) Evolutionary patterns of host utilization by ichneumonid parasitoids (Hymenoptera: Ichneumonidae and Braconidae). *Biological Journal of the Linnean Society*, 35, 351-377.

Gauld ID (1991) The Ichneumonidae of Costa Rica 1. *Memoirs of the American Entomological Institute*, 47, 1-589.

Gauld ID, Fitton MG (1984) An introduction to the Ichneumonidae of Australia. British Museum (Natural History), London.

Gauld ID, Huddleston T (1976) The nocturnal Ichneumonoidea of the British Isles. Including a key to the genera. *Entomologist's Gazette*, 27, 35-49.

Gauld ID, Gomez J, Godoy C (2002) Subfamily Banchinae. In: Gauld ID (ed.). The Ichneumonidae of Costa Rica, 4. *Memoirs of the American Entomological Institute*, 66, 263–746.

Gauld ID, Mitchell P (1978) The taxonomy, distribution and host preferences of African parasitic wasps of the subfamily Ophioninae (Hymenoptera: Ichneumonidae). Commonwealth Agricultural Bureau, Slough.

Gauld ID, Wahl DB (2000a) The Townesioninae: a distinct subfamily of Ichneumonidae (Hymenoptera) or a clade of the Banchinae? *Transactions of the American Entomological Society*, 126, 279–292.

Gauld ID, Wahl DB (2000b) The Labeninae (Hymenoptera: Ichneumonidae): a study in phylogenetic reconntruction and evolutionary biology. *Zoological Journal of the Linnean Society*, 129, 271-347.

Gillespie JJ, Munro JB, Heraty JM, Yoder MJ, Owen AK, Carmichael AE (2005) A secondary structural model of the 28S rRNA expansion segments D2 and D3 for chalcidoid wasps (Hymenoptera: Chalcidoidea). *Molecular Biology and Evolution*, 22, 1593–1608.

Gravenhorst JLC (1829) Ichneumonologia Europaea. Pars III. Vratislaviae. 1097 pp.

Grimaldi D, Engel MS (2005) *Evolution of Insects*. Cambridge University Press, New York.

Gupta V (2002) *Glyptopimpla* Morley (Hymenoptera: Ichneumonidae: Banchinae) — a valid genus with descriptions of new species from the Orient. *Oriental Insects*, 36, 221–237.

Greiner B (2006) Visual adaptations in the night active wasp *Apoica pallens*. *Journal of Comparative Neurology*, 495, 255-262.

Hafner MS, Sudman PD, Villablanca FX, Spradling TA, Demastes JW, Nadler SA (1994) Disparate rates of molecular evolution in cospeciating hosts and parasites. *Science*, 265, 1087-1090.

Hall T (1999) BioEdit: a user-friendly biological sequence alignment editor and analysis program for Windows 95/98/NT. *Nucleic Acids Symposium Series*, 41, 95–98.

Hamerlinck G, Hulbert D, Hood GR, Smith JJ, Forbes AA (2016) Histories of host shifts and cospeciation among free-living parasitoids of *Rhagoletis* flies. *Journal of*

Evolutionary Biology, 29, 1766-1779.

Hebert PDN, Ratnasingham S, Zakharov EV, Telfer AC, Levesque-Beaudin V, Milton MA, Pedersen S, Jannetta P, deWaard JR (2016) Counting animal species with DNA barcodes: Canadian insects. *Philosophical Transaction of the Royal Society B*, 371: 20150333.

Heinrich S, Zonneveld KAF, Bickert T, Willems H (2011) The Benguela upwelling related to the Miocene cooling events and the development of the Antarctic Circumpolar Current: evidence from calcareous dinoflagellate cysts. *Paleoceanography*, 26, PA3209, doi:10.1029/2010PA002065

Heraty J, Hawks D, Kostecki JS, Carmichael A (2004) Phylogeny and behaviour of the Gollumiellinae, a new subfamily of the ant-parasitic Eucharitidae (Hymenoptera: Chalcidoidea). *Systematic Entomology*, 29, 544-559.

Herrera AF, Penteado-Dias AM (2011) Five new species of the genus *Sphelodon* (Hymenoptera: Ichneumonidae) from Brazil with a key to the Neotropical species. *Revista de Biologia Tropical*, 59, 1621–1636.

Herrera-Florez AF (2017) A new species of *Sphelodon* Townes (Hymenoptera: Ichneumonidae: Banchinae) from Colombia. *Zootaxa*, 4277, 289-294.

Hewitt GM (1996) Some genetic consequences of ice ages, and their role, in divergence and speciation. *Biological Journal of the Linnean Society*, 58, 247-276.

Hrcek J, Miller SE, Quicke DLJ, Smith MA (2011) Molecular detection of trophic links in a complex insect host-parasitoid food web. *Molecular Ecology Resources*, 11, 786-794.

Holmgren AE (1860) Forsok till uppstallning och beskrifning af Sveriges Ichneumonider. Tredje Serien. Fam. Pimplariae. (Monographia Pimplariarum Sueciae). *Kongliga Svenska Vetenskapsakademiens Handlingar*, 3, 1-76.

Hopkins T, Roininen H, Sääksjärvi IE (2018) Assessing the species richness of Afrotropical ichneumonid wasps with randomly placed traps provides ecologically informative data. *African Entomology*, 26, 350-358.

Jacobs BF (2004) Palaeobotanical studies from tropical Africa: relevance to the evolution of forest, woodland and savannah biomes. *Philosophical Transactions of the Royal Society, London, Series B: Biological Sciences*, 359, 1573–1583.

Kamilar JM, Cooper N (2013) Phylogenetic signal in primate behaviour, ecology and life history. *Philosophical Transactions of the Royal Society B Biological Sciences*, 368: 20120341.

Kang GW, Choi JK, Lee JW (2018) Three new records of the genus *Glyptopimpla* (Hymenoptera: Ichneumonidae: Banchinae) from South Korea. *Journal of Asia-Pacific Biodiversity*, 11, 367-370.

Kang GW, Kolarov J, Lee JW (2019) Four new species of the genus *Lissonota* (Ichneumonidae: Banchinae) from South Korea. *Entomological Research*, 49, 239-257.

Karanth KP (2006) Out-of-India Gondwanan origin of some tropical Asian biota. *Current Science*, 90, 789–792.

Kasparyan DR (1993) Townesioninae, a new ichneumonid subfamily from the Eastern Palaearctic (Hymenoptera: Ichneumonidae). *Zoosystemica Rossica*, 2, 155-159.

Kasparyan DR, Kuslitzky WS (2018) Contribution to the fauna of the ichneumon-wasp genus *Rhynchobanchus* Kriechbauer, 1894 (Hymenoptera, Ichneumonidae: Banchinae) in the Russian Far East. *Entomological Review*, 98, 748-752.

Kerr PH, Fischer EM, Buffington ML (2008) Dome lighting for insect imaging under a microscope. *American Entomologist*, 54, 198–200.

Khalaim AI (2011) First record of the subfamilies Banchinae and Stilbopinae (Hymenoptera: Ichneumonidae) from the Late Eocene Rovno amber (Ukraine). *Russian Entomological Journal*, 20, 295–298.

Khalaim AI, Ruíz-Cancino E (2008) A new species of *Alloplasta* Förster from Mexico (Hymenoptera: Ichneumonidae: Banchinae). *Zoosystematica Rossica*, 17, 81–82.

Khalaim AI, Ruíz-Cancino E (2012) Mexican species of *Exetastes* (Hymenoptera: Ichneumonidae: Banchinae), with description of three new species. *Revista Mexicana de Biodiversidad*, 83, 370–379.

Klopfstein S, Quicke DLJ, Kropf C, Frick H (2011) Molecular and morphological phylogeny of Diplazontinae (Hymenoptera, Ichneumonidae). *Zoologica Scripta*, 40, 379–402.

Kopylov DS (2010) A new subfamily of ichneumon wasps (Insecta, Hymenoptera, Ichneumonidae) from the Upper Cretaceous (Cenomanian) of the Russian Far East. *Paleontological Journal*, 44, 422–433.

Kopylov DS (2011) Ichneumon wasps of the Khasurty locality in Transbaikalia (Insecta, Hymenoptera, Ichneumonidae). *Paleontological Journal*, 45: 406.

Kopylov DS, Brothers DJ, Rasnitsyn AP (2010) Two new labenopimpline ichneumonids (Hymenoptera: Ichneumonidae) from the Upper Cretaceous of southern Africa. *African Invertebrates*, 51, 423–430.

Kuslitzky WS (2007) 12. Subfamily Banchinae. In: Lelej AS (ed.). *A key to the insects of Russian Far East. Vol. 4. Neuropteroidea, Mecoptera, Hymenoptera. Part 5*.: Dal'nauka, Vladivostok. pp. 433–472. (in Russian)

Lapointe R, Tanaka K, Barney WE, Whitfield JB, Banks JC, Béliveau C, Stoltz D, Webb BA, Cusson M (2007) Genomic and morphological features of a banchine ploydnavirus: comparison with bracoviruses and ichnoviruses. *Journal of Virology*, 81, 6491-6501.

Lapointe R, Wilson R, Vilaplana L, O'Reilly DR, Falabella P, Douris V, Bernier-Cardou M, Pennacchio F, Iatrou K, Malva C, Olszewski JA (2005) Expression of a *Toxoneuron nigriceps* polydnavirus-encoded protein causes apoptosis-like programmed cell death in lepidopteran insect cells. *Journal of General Virology*, 86, 963-971.

Laurenne NM, Broad GR, Quicke DLJ (2003) Preliminary molecular phylogenetic analysis of Cryptinae and related taxa based on 28S D2+D3 rDNA analysed using POY. In: Melika G, Thuróczy C (eds.). *Parasitic wasps: evolution, systematics, biodiversity and biological control*. Budapest, Hungary: Agroinform Kiadó, Budapest, Hungary, pp.

229-233.

Laurenne NM, Broad GR, Quicke DLJ (2006) Direct optimization and multiple alignment of 28S D2-D3 rDNA sequences: problems with indels on the way to a molecular phylogeny of the cryptine ichneumon wasps (Insecta: Hymenoptera). *Cladistics*, 22, 442–473.

Lawes M (1990) The distribution of the samango monkey (*Cercopithecus mitis erythrarchus* Peters, 1852 and *Cercopithecus mitis labiatus* I. Geoffrey, 1843) and forest history in southern Africa. *Journal of Biogeography*, 17, 669–680.

LeGall P, Silvain JF, Nel A, Lachaise D (2010) Les insectes actuels témoins des passés de l'Afrique:essai sur l'origine et la singularité de l'entomofaune de la région afrotropicale. *Annales de la Société Entomologique de France*, 46, 297-343.

Legendre P, Lapointe F-J (2004) Assessing congruence among distance matrices: single-malt scotch whiskies revisited. *Australian and New Zealand Journal of Statistics*, 46, 615–629.

Li ZJ, Li T, Yan J, Sheng ML (2018) The genus *Rhynchobanchus* Kriechbaumer in China, with descriptions of a new species and first record of the genus from Oriental region (Hymenoptera, Ichneumonidae, Banchinae). *Zookeys*, 752, 125-136.

Linder HP (2003) The radiation of the Cape flora, southern Africa. *Biological Reviews*, 78, 597-638.

Linder HP (2008) Plant species radiations: where, when, why? *Philosophical Transactions of the Royal Society of London. Series B*, 363, 3097-3105.

Liu H, Wang W, Song G, Qu Y, Li S-H, Fjeldså J, Lei F (2012) Interpreting the process behind endemism in China by integrating the phylogeography and ecological niche models of the *Stachyridopsis ruficeps*. *PLoS OnNE*, 7:e46761.

Longrich NR, Bhuller BS, Tokaryk T, Field DJ (2011) Mass extinction of birds at the Cretaceous-Paleogene (K-Pg) boundary. *Proceedings of the National Academy of Sciences*, 108, 15253-15257.

Lorenzen ED, Heller R, Siegismund HR (2012) Comparative phylogeography of African

savannah ungulates. *Molecular Ecology*, 21, 3656–3670.

Losey JE, Vaughan M (2006) The economic value of ecological services provided by insects. *BioScience*, 56, 311–323.

Matthee CA, Burzlaff JD, Taylor JF, Davis SK (2001) Mining the mammalian genome for artiodactyl systematics. *Molecular Biology and Evolution*, 50, 367–390.

Mausfield-Lafdhiya P, Schmitz A, Ineich I, Chirio L (2004) Genetic variation in two african *Euprepis* species (Reptilia, Scincidae), based on maximum-likelihood and bayesian analyses: taxonomic and biogeographic conclusions. *Bonner zoologische Beitrage*, 52, 159–177.

McLennan DA (2010) How to read a phylogenetic tree. *Evolution: Education and Outreach*, 3:273.

Menier JJ, Nel A, Waller A, de Ploëg G (2004) A new fossil ichneumon wasp from the Lowermost Eocene amber of Paris Basin (France), with a checklist of fossil Ichneumonoidea s.l. (Insecta: Hymenoptera: Ichneumonidae: Metopiinae). *Geologica Acta*, 2, 83–94.

Miyamoto MM, Fitch WM (1995) Testing species phylogenies and phylogenetic methods with congruence. *Systematic Biology*, 44, 64–76.

Momoi S, Sugawara H, Honma K (1975) Ichneumonid and Braconid parasites of Lepidopterous leaf-rollers of economic importance in horticulture and teaculture. In: Yasumatsu K, Mori H, (eds.). *Approaches to Biological Control*, 7, pp. 47-60.

Morley C (1916) On some South African Ichneumonidae in the collection of the South African Museum. *Annals of the South African Museum*, 15, 353-400.

Morley C (1917) On some South African Ichneumonidae in the collection of the South African Museum. *Annals of the South African Museum*, 17, 191–229.

Morrone JJ, Crisci JV (1995) Historical biogeography: introduction to methods. *Annual Review of Ecology and Systematics*, 26, 373-401.

Mucina L, Rutherford MC (2006). *The vegetation of South Africa, Lesotho and Swaziland*. *Strelitzia* 19. South African National Biodiversity Institute, Pretoria.

Nichols DJ, Johnson KR (2008) *Plants and the K-T boundary*. Cambridge University Press, Cambridge, UK.

Nylander JA, Ronquist F, Huelsenbeck JP, Nieves-Aldrey JL (2004) Bayesian phylogenetic analysis of combined data. *Systematic Biology*, 53, 47–67.

Padial JM, Miralles A, De la Riva I, Vences M (2010) The integrative future of taxonomy. *Frontiers in Zoology*, 7:16.

Pampel W (1913) Die weiblichen Geschlechtsorgane der Ichneumoniden. *Zeitschrift fuer wissenschaftlichliche Zoologie*, 108, 290–357.

Peters RS, Krogmann L, Mayar C, Donath A, Gunkel S, Meusemann K, Kozlov A, Podsiadlowski L, Petersen M, Lanfear R, Diez PA, Heraty J, Kjer KM, Klopfstein S, Meier R, Polidon C, Schmitt T, Liu S, Niehuis (2017) Evolutionary history of the Hymenoptera. *Current Biology*, 27, 1013-1018.

Quicke DLJ (2012) We know too little about parasitoid wasp distributions to draw any conclusions about latitudinal trends in species richness, body size and biology. *PLoS ONE*, 7:e32101.

Quicke DLJ (2015) *The braconid and ichneumonid parasitoid wasps. Biology, systematics, evolution and ecology*. Wiley Blackwell, Oxford, UK.

Quicke DLJ, Laurenne NM, Fitton MG, Broad GR (2009) A thousand and one wasps: a 28S rDNA and morphological phylogeny of the Ichneumonidae (Insecta: Hymenoptera) with an investigation into alignment parameter space and elision. *Journal of Natural History*, 43,1305–1421.

Quicke DLJ, Smith MA, Janzen DH, Hallwachs W, Fernandez-Triana J, Laurenne NM, Zaldívar-Riverón A, Shaw MR, Broad GR, Klopfstein S, Shaw SR, Hrcek J, Hebert PDN, Miller SE, Rodriguez JJ, Whitfield JB, Sharkey MJ, Sharanowski BJ, Jussila R, Gauld ID, Chesters D, Vogler AP (2012) Utility of the DNA barcoding gene fragment for parasitic wasp phylogeny (Hymenoptera: Ichneumonoidea): data release and new

measure of taxonomic congruence. *Molecular Ecology Resources*, 12, 676–85.

Rannala B, Huelsenbeck JP, Yang Z, Nielsen R (1998). Taxon sampling and the accuracy of large phylogenies. *Systematic Biology*, 47, 702-710.

Rehan SM, Leys R, SchwarzMP (2013) First evidence for a massive extinction event affecting bees close to the K-T boundary. *PLoS ONE*, 8:e76683

Renne PR, Deino AL, Hilgen FJ, Kuiper KF, Mark DF, Mitchell WS, Morgan LE, Mundil R, Smit J (2013) Time scales of critical events around the Cretaceous-Paleogene boundary. *Science*, 339, 684-687.

Reynolds Berry T, van Noort S (2016) Review of Afrotropical *Cryptopimpla* Taschenberg (Hymenoptera, Ichneumonidae, Banchinae), with description of nine new species. *Zookeys*, 640, 103-137.

Ronquist F, Teslenko M, van der Mark P, Ayres D, Darling A, Höhna S, Larget B, Liu L, Suchard MA, Huelsenbeck JP (2012) MrBayes 3.2: efficient bayesian phylogenetic inference and model choice across a large model space. *Systematic Biology*, 61, 539-542.

Rousse P, Quicke DLJ, Matthee CA, Lefeuvre P, van Noort S (2016) A molecular and morphological reassessment of the phylogeny of the subfamily Ophioninae (Hymenoptera: Ichneumonidae). *Zoological Journal of the Linnean Society*, 178, 128-148.

Rousse P, van Noort S (2014) Afrotropical Ophioninae (Hymenoptera, Ichneumonidae): an update of Gauld and Mitchell's revision, including two new species and an interactive matrix identification key. *Zookeys*, 456, 59-73.

Rousse P, Villemant C (2012) Ichneumons in Reunion Island: a catalogue of the local Ichneumonidae (Hymenoptera) species, including 15 new taxa and a key to species. *Zootaxa*, 57, 1–57.

Sääksjärvi IE, Gauld ID, Salo J (2004) Phylogenetic evaluation of the tropcial *Camptotypus* genus-group (Hymenoptera: Ichneumonidae), with a key to the world genera. *Journal of Natural History*, 38, 2759–2778.

Saghai-Maroof MA, Soliman KM, Jorgensen RA, Allard RW (1984) Ribosomal DNA

spacer-length polymorphisms in barley: mendelian inheritance, chromosomal location, and population dynamics. *Proceedings of the National Academy of Sciences of the United States of America*, 81, 8014–8018.

Sands AF, Apanaskevich DA, Matthee S, Horak IG, Matthee CA (2017) The effect of host vicariance and parasite life history on the dispersal of multi-host ectoparasite, *Hyalomma truncatum*. *Journal of Biogeography*, 44, 1124-1136.

Sanmartín I, Ronquist F (2004) Southern hemisphere biogeography inferred by event-based models: plant versus animal patterns. *Systematic Biology*, 53, 216-243.

Santos BF (2017) Phylogeny and reclassificaton of Cryptini (Hymenoptera, Ichneumonidae, Cryptinae), with implications for ichneumonid higher-level classification. *Systematic Entomology*, 42, 650-676.

Santos BF, Aguiar AP (2013) Phylogeny and revision of *Messatoporus* Cushman (Hymenoptera, Ichneumonidae, Cryptinae), with descriptions of sixty five new species. *Zootaxa*, 3634, 1-284.

Santos AMC, Quicke DLJ (2011) Large-scale diversity patterns of parasitoid insects. *Entomological Science*, 14, 371–382.

Seyrig A (1932) *Les Ichneumonides de Madagascar*. I Ichneumonidae Pimplinae. *Mémoires de l'Académie Malgache*. Fascicule 11: 183pp.

Seyrig A (1935) Mission scientifique de l'Omo. Tome III. Fascicule 18. Hymenoptera, II. Ichneumonidae: Cryptinae, Pimplinae, Tryphoninae et Ophioninae. *Mémoires du Muséum National d'Histoire Naturelle*, 4, 1–100.

Sharanowski BJ, Dowling APG, Sharkey MJ (2011) Molecular phylogenetics of Braconidae (Hymenoptera: Ichneumonoidea), based on multiple nuclear genes, and implications for classification. *Systematic Entomology*, 36, 549–572.

Sharkey MJ (2007) Phylogeny and classification of Hymenoptera. *Zootaxa*, 548, 521–548.

Shaw MR (1999) Gregarious development in endoparasitic koinobiont Ichneumonidae (Hymenoptera). *Entomologist's Gazette*, 50, 55–56.

Shaw MR, Hochberg ME (2001) The neglect of parasitic Hymenoptera in insect conservation strategies: the British fauna as a prime example. *Journal of Insect Conservation*, 5, 53–263.

Sheng ML (2011) Five new species of the genus *Cryptopimpla* Taschenberg (Hymenoptera, Ichneumonidae) with a key to species known from China. *ZooKeys*, 117, 9–49.

Sheng ML, Sun SP, Wang XN, Wu HW (2018) A new genus and species of subfamily Banchinae (Hymenoptera, Ichneumonidae) from China. *Zootaxa*, 441, 541-550.

Sheng ML, Zheng H (2005) The genus *Cryptopimpla* from China (Hymenoptera, Ichneumonidae). *Acta Zootaxonomica Sinica*, 30, 415-418.

Simon C, Frati F, Beckenbach A, Crespi B, Liu H, Flook P (1994) Evolution, weighting, and phylogenetic utility of mitochondrial gene sequences and a compilation of conserved polymerase reaction primers. *Annals of the Entomological Society of America*, 87, 651-701.

Smith MA, Eveleigh ES, McCann KS (2011) Barcoding a quantified food web: crypsis, concepts, ecology and hypotheses. *PLoS ONE*, 6: E14424.

Smith MA, Fernandez JT, Roughley R, Hebert PDN (2009) DNA barcode accumulation curves for understudied taxa and areas. *Molecular Ecology Resources*, 9, 208-216.

Spasojevic T, Broad GR, Bennett AMR (2017) Ichneumonid parasitoid wasps from the Early Eocene Green River Formation: five new species and a revision of the known fauna (Hymenoptera, Ichneumonidae). *PalZ*, 92, 35-63.

Spasojevic T, Wedmann S, Klopfstein S (2018) Seven remarkable new fossil species of parasitoid wasps (Hymenoptera, Ichneumonidae) from the Eocene Messel Pit. *PLoS ONE*, 13: e0197477.

Stoltz DB, Whitfield JB (1992) Viruses and virus-like entities in the parasitic Hymenoptera. *Journal of Hymenoptera Research*, 1, 125-139.

Strand MR, Burke GR (2012) Polydnaviruses as symbionts and gene delivery systems. *PLoS Pathologens*, 8:e1002757.

Sudheer K, Narendran T, Saji A (2007) Taxonomy of a new ichneumonid genus from the Middle East (Insect, Hymenoptera, Ichneumonidae). *Senckenbergiana Biologica*, 87, 85–188.

Swofford D (2002) PAUP: *Phylogenetic Analysis Using Parsimony (and other methods)*. Sinauer Associates, Sunderland, Massachusetts.

Szöllősi GJ, Tannier E, Daubin V, Boussau B (2015) The inference of gene trees with species trees. *Systematic Biology*, 64, 42-62.

Takasuka K, Watanabe K, Konishi K (2011) Genus *Cryptopimpla* Taschenberg new to Sulawesi, Indonesia, with description of a new species (Hymenoptera, Ichneumonidae, Banchinae). *Journal of Hymenoptera Research*, 23, 65–75.

Taschenberg EL (1863) Die Schlupfwespenfamilie Pimplariae der deutschen Fauna, mit besonderer Rücksicht auf die Umgegend von Halle. *Zeitschrift für die Gesammten Naturwissenschaften*, 21, 245–305.

Tedesco A, Aguiar A (2013) Phylogeny and revision of *Toechorychus* Townes (Hymenoptera, Ichneumoniae, Cryptinae), with descriptions of thirty-five new species. *Zootaxa*, 3633, 1-138.

Tolley KA, Tilbury CR, Measey GJ, Menegon M, Branch WR, Matthee CA (2011) Ancient forest fragmentation or recent radiation? Testing refugial speciation models in chameleons within an African biodiversity hotspot. *Journal of Biogeography*, 38, 1748-1760.

Townes HK (1969) Genera of Ichneumonidae, Part 3 (Lycorininae, Banchinae, Scolobatinae, Porizontinae). *Memoirs of the American Entomological Institute*, 13, 1–307.

Townes HK, Townes M (1973) A catalogue and reclassification of the Ethiopian Ichneumonidae. *Memoirs of the American Entomological Institute*, 19, 1–416.

Townes HK, Townes M (1978) Ichneumon-flies of America north of Mexico: 7. Subfamily Banchinae, tribes Lissonotini and Banchini. *Memoirs of the American Entomological Institute*, 26, 1-614.

Tschopp S, Riedel A, Kropf C, Nentwig W, Klopfstein (2013) The evolution of host associations in the parasitic wasp genus *Ichneumon* (Hymenoptera: Ichneumonidae): convergent adaptations to host pupation sites. *BMC Evolutionary Biology*, 13:74.

van Noort S (2004) Ichneumonid (Hymenoptera: Ichneumonidea) diversity across an elevational gradient on Monts Doudou in southwestern Gabon. *California Academy of Science Memoir*, 28, 187–216.

van Noort (2018) WaspWeb: Hymenoptera of the Afrotropical region. URL: www.waspweb.org (accessed on 30/11/2018).

van Zinderen Bakker EM (1975) The origin and palaeoenvironment of the Namib Desert Biome. *Journal of Biogeography*, 2, 65-73.

Vas Z (2017) Data to the Vietnamese ichneumon wasp fauna with description of a new *Teleutaea* species (Hymenoptera: Ichneumonidae). *Folio Entomologica Hungarica*, 78, 101-110.

Veijalainen A, Broad GR, Wahlberg N, Longino JT, Sääksjärvi IE (2011) DNA barcoding and morphology reveal two common species in one: *Pimpla molesta* stat. rev. separated from *P. croceipes* (Hymenoptera, Ichneumonidae). *ZooKeys*, 124, 59–70.

Veijalainen A (2012) Species richness of Neotropical parasitoid wasps (Hymenoptera: Ichneumonidae) revisited, PhD thesis, University of Turku, Finland.

Veijalainen A, Sääksjärvi IE, Erwin TL, Gómez IC, Longino JT (2012a) Subfamily composition of Ichneumonidae (Hymenoptera) from western Amazonia: insights into diversity of tropical parasitoid wasps. *Insect Conservation and Diversity*, 6, 28–37.

Veijalainen A, Wahlberg N, Broad GR, Erwin TL, Longino JT, Sääksjärvi IE (2012b). Unprecedented ichneumonid parasitoid wasp diversity in tropical forests. *Proceedings of the Royal Society B: Biological Sciences*, 279, 4694–4698.

Verboom GA, Archibald JK, Bakker FT, Bellstedt DU, Conrad F, Dreyer LL, Forest F, Galley C, Goldblatt P, Henning JF, Mummenhoff K, Linder HP, Muasya AM, Oberlander KC, Savolainen V, Snijman DA, van der Niet T, Nowell TL (2009) Origin

and diversification of the Greater Cape flora: ancient species repository, hot-bed of recent radiation or both? *Molecular Phylogenetics and Evolution*, 51, 44-53.

Wagener B, Reineke A, Löhr B, Zebitz CPW (2006) Phylogenetic study of *Diadegma* species (Hymenoptera: Ichneumonidae) inferred from analysis of mitochondrial and nuclear DNA sequences. *Biological Control*, 37, 131–140.

Wahl DB (1985) A revision of the genus *Agathilla* (Hymenoptera: Ichneumonidae). *Transactions of the American Entomological Society*, 111, 265-277.

Wahl DB (1988) A review of the mature larvae of the Banchini and their phylogenetic significance, with comments on the Stilbopinae (Hymenoptera: Ichneumonidae). In: Gupta VK (ed.). *Advances in Parasitic Hymenoptera Research*, Brill, Leiden, pp. 147–161.

Wahl DB (1991) The status of *Rhimphoctona*, with special reference to the higher categories within Campopleginae and the relationships of the subfamily (Hymenoptera: Ichneumonidae). *Society*, 117, 193–213.

Wahl DB (1993) Cladistics of the genera of Mesochorinae (Hymenoptera: Ichneumonidae). *Systematic Entomology*, 18, 371–387.

Wahl DB, Sharkey MJ (1993) Chapter 10. Superfamily Ichneumonoidea. In: Goulet H, Huber JT (eds.), *Hymenoptera of the World: An Identification Guide to Families*. Agriculture Canada, Ottawa, Canada, pp. 358–509.

Wahlberg N (2006) That awkward age for butterflies: insights from the age of the butterfly subfamily Nymphalinae. *Systematic Biology*, 55, 703-714.

Wahlberg N, Brower AVZ, Nylin S (2005) Phylogenetic relationships and historical biogeography of tribes and genera in the subfamily Nymphalinae (Lepidoptera: Nymphalidae). *Biological Journal of the Linnean Society*, 86, 227–251.

Warrant EJ (2008) Seeing in the dark: vision and visual behaviour in nocturnal bees and wasps. *Journal of Experimental Biology*, 211, 1737-1746.

Warrant EJ, Kelber A, Gislén A, Greiner B, Ribi W, Wcislo WT (2004) Nocturnal vision and landmark orientation in a tropical halicid bee. *Current Biology*, 14, 1309-1318.

Watanabe K (2017) Revision of the genus *Amphirhachis* Townes, 1970 (Hymenoptera, Ichneumonidae, Banchinae) from Japan. *Zookeys*, 685, 49-64.

Watanabe K (2018) Taxonomic on *Exetastes fukuchiyamanus* Uchida, 1928 (Hymenoptera, Ichneumonidae, Banchinae), with description of a new species from Japan and China. *Zootaxa*, 4399, 281-288.

Watanabe K, Maeto K (2012) A new species of the genus *Himertosoma* from the Ryukyus, Japan, with a key to species from the Palaearctic and Oriental regions (Hymenoptera, Ichneumonidae, Banchinae). *ZooKeys*, 234, 59–66.

Watanabe K, Maeto K (2014) Revision of the genus *Apophua* Morley, 1913, from Japan (Hymenoptera, Ichneumonidae, Banchinae). *Zootaxa*, 3784, 501-527.

White F (1981) The history of the Afromontane archipelago and the scientific need for its conservation. *African Journal of Ecology*, 19, 33–54.

Whitfield JB (2002) Estimating the age of the polydnavirus/braconid wasp symbiosis. *Proceedings of the Natural Academy of Sciences of the United States of America*, 99, 7508-7513.

Wiens JJ, Donoghue MJ (2004) Historical biogeography, ecology and species richness. *Trends in Ecology and Evolution*, 19, 639–644.

Yoder AD, Nowak MD (2006) Has vicariance or dispersal been the predominant force in biogeographic Madagascar? Only time will tell. *Annual Review of Ecology, Evolution, and Systematics*, 37, 405–431.

Yu D, Acterberg C, van Hortsmann K (2018) Taxapad 2012, Icneumonoidea 2011. URL: www.taxapad.com (accessed on 30/11/2018).

Zaldívar-Riverón A, Belokoblylskij SA, León-Règagnon V, Quicke DLJ (2008a) Molecular phylogeny and historical biogeography of the cosmopolitan parasitic wasp subfamily Doryctinae (Hymenoptera: Braconidae). *Invertebrate Systematics*, 22, 345-363.

Zaldívar-Riverón A, Shaw MR, Sáez AG, Mori M, Belokoblylskij SA, Shaw SR, Quicke DLJ (2008b) Evolution of the parasitic wasp subfamily Rogadinae (Braconidae):

phylogeny and evolution of lepidopteran host ranges and mummy characteristics. *BMC Evolutionary Biology*, 8:329.

Zhang JF (1989) *Fossil insects from Shanwang, Shandong, China*. Shandong Science and Technology Publishing House, Shandong, China.

Zhu F, Cusumano A, Bloem J, Weldegergis BT, Villela A, Fatouros NE, van Loon JJA, Dicke M, Harvey JA, Vogel H, Poelman EH (2018) Symbiotic polydnavirus and venom reveal parasitoid to its hyperparasitoids. *PNAS*, 115, 5205-5210.

Zong S, Sheng M, Luo Y, Lu C (2012) *Lissonota holcocerica* Sheng sp.n (Hymenoptera: Ichneumonidae) parasitizing *Holcocerus hippophaecolus* (Lepidoptera: Cossidae) from China. *Journal of Insect Science*, 12, 1–7.